Molecular characterization of CNS interneurons:
subtype diversity and fate determinants

I n a u g u r a l – D i s s e r t a t i o n

zur

Erlangung des Doktorgrades

der Mathematisch-Naturwissenschaftlichen Fakultät

der Universität zu Köln

vorgelegt von

Olaf Thorsten Hardt

aus Köln

2008

Berichterstatter/in: Prof. Dr. Dagmar Knebel-Mörsdorf

                            Prof. Dr. Sigrun Korsching

                            Prof. Dr. Keith Dudley

Tag der mündlichen Prüfung: 14.10.2008

Zusammenfassung

Im Rahmen dieser Arbeit wurden zwei Ansätze genutzt, um neue Einblicke bezüglich der Identität und molekularen Regulation inhibitorischer Interneurone im Gehirn zu erlangen. Zum einen wurde eine generelle molekulare Charakterisierung GABAerger Interneuron-Subpopulationen durchgeführt, zum anderen wurden neue Regulatoren der *Bulbus Olfaktorius* Interneuron-Differenzierung identifiziert und funktionell analysiert.

GABAerge Neurone, die häufigsten inhibitorischen Nervenzellen im Gehirn, sind essentiell für die korrekte Informationsverarbeitung im zentralen Nervensystem. Während die große Mehrheit dieser Zellen lokal projizierende Interneurone sind, findet man in einigen Arealen wie dem Striatum auch GABAerge Projektionsneurone. Bisher wurden GABAerge Neurone anhand einiger biochemischer, morphologischer und elektrophysiologischer Eigenschaften charakterisiert. Da aber keine strikte Korrelation zwischen diesen Faktoren existiert, gelang es bisher nicht, Subpopulationen GABAerger Zellen systematisch zu unterteilen.

Im ersten Teil dieser Arbeit wurden die generellen molekularen Eigenschaften GABAerger Neurone analysiert und Unterschiede zwischen verschiedenen Hirnarealen definiert. Dazu wurden fluoreszent markierte GABAerge Neurone aus transgenen GAD67-GFP Mäusen mit Hilfe der FACS Technologie aus dem gesamten Hirn sowie den definierten Arealen *Bulbus Olfaktorius*, *Cortex*, *Striatum* und *Cerebellum* isoliert. Anschließend wurden Proteom- sowie Genexpressions-Analysen durchgeführt, die mit Hilfe von *in situ* Hybridisierungen und qPCRs validiert wurden. Neue intrazelluläre und Zelloberflächen-Marker sowie Gene, die vermutlich wichtig für die Entwicklung und Funktionalität GABAerger Neurone sind, wurden identifiziert. Korrelations- und Clusteranalysen zeigten insbesondere Unterschiede zwischen Zellen des Vorder- und Hinterhirns auf. Während GABAerge Neurone des Vorderhirns hauptsächlich durch drei Familien von Transkriptionsfaktoren, der *Distal-less*-Familie, der POU-Familie und der ETS/FOX-Familie, charakterisiert waren, definierten spezifische Transkriptionsfaktoren der ZIC- und LHX-Familien inhibitorische Hinterhirn-Neurone.

Interneurone des *Bulbus Olfaktorius* werden zeitlebens durch adulte neuronale Stammzellen in der Subventrikulär-Zone generiert. Die molekularen Mechanismen der terminalen Differenzierung dieser Zellen sind bisher allerdings nur ansatzweise verstanden. Definierte Differenzierungsstadien dieser Interneurone sowie ihrer Vorläuferzellen wurden mit Hilfe magnetischer Zellisolierung nach Mikrodissektion von periglomerulärem beziehungsweise subventrikulärem Gewebe isoliert. Durch Genexpressions-Analysen wurde eine Reihe von Kandidaten identifiziert, die vermutlich an der Differenzierung olfaktorischer Interneurone beteiligt sind. Zwei dieser Gene, NeuroD1 und NeuroD2, wurden auf ihre funktionelle Relevanz *in vivo* hin untersucht. Mit Hilfe der *in vivo* Elektroporation wurde die Überexpression dieser Transkriptionsfaktoren in Stamm-, Vorläufer- sowie ausdifferenzierten Zellen induziert. Dabei konnte gezeigt werden, dass die starke Expression von NeuroD2 eine verzögerte Differenzierung GABAerger Interneurone des *Bulbus Olfaktorius* bewirkt. Im Gegensatz dazu war die Überexpression von NeuroD1 ausreichend, um eine vorzeitige und ektopische Differenzierung von Vorläuferzellen entlang ihrer tangentialen Migrationsroute sowie im Striatum auszulösen. Diese Überexpression führte weiterhin hochspezifisch zur Ausbildung eines Dopaminergen Neurotransmitter-Phänotyps, woraus eine zentrale Rolle von NeuroD1 für die Spezifizierung bifunktionaler GABA/Dopamin-positiver Interneurone hervorgeht.

Im Rahmen dieser Studie wurde eine umfassende molekulare Basis für das Verständnis räumlich und zeitlich definierter GABAerger Neurone bereitgestellt. Weiterhin wurden Gene identifiziert, die zentrale Funktionen während der Differenzierung inhibitorischer Interneuron-Subpopulationen übernehmen.

Abstract

In this project two approaches have been used to gain insights into the identity and molecular regulation of interneurons in the brain. First, a general molecular characterization of GABAergic neuron subtypes has been performed and second, novel fate determinants specifically for olfactory bulb interneurons have been identified and investigated in detail.

GABAergic neurons, the largest population of inhibitory neurons in the brain, play crucial roles in information processing. While most of these neurons are interneurons, some, for example in the striatum, represent projection neurons. So far, biochemical, morphological, and electrophysiological properties served as exclusive criteria for the classification of GABAergic neurons. Although these parameters allow for a partial description of subpopulations, a systematic dichotomy is not available.

Therefore, the general molecular characteristics of GABAergic neurons were analyzed and differences among distinct brain regions were defined. Transgenic GAD67-GFP mice in concert with flow cytometric cell sorting were used to isolate GABAergic neurons from defined regions of the postnatal mouse brain, namely olfactory bulb, cortex, striatum and cerebellum. Subsequently, gene expression profiling as well as cell surface proteome analysis were carried out and identified genes were validated by *in situ* hybridization and qPCR. Potential new marker genes for GABAergic neurons and candidate factors necessary for their differentiation and general functionality were determined. Clustering of gene expression data revealed major differences between hind- and forebrain GABAergic neurons indicating a correlation between their development and localization. For example, while GABAergic neurons of the forebrain are characterized mainly by three groups of transcription factors, namely the Distal-less-family, the POU-family and the ETS/FOX-family; specific members of the ZIC- and LHX-family define hindbrain inhibitory neurons.

Olfactory bulb interneurons are generated throughout live by adult neuronal stem cells localized in the subventricular zone. While considerable information is available concerning the generation and migration of these cells, the molecular mechanisms regulating their terminal differentiation are barely understood.

Therefore, mature interneurons from the periglomerular layer and their specific precursors were isolated by microdissection and magnetic cell sorting. Gene expression analysis was performed by microarray analysis. Several candidate factors to be involved in the differentiation of olfactory bulb interneurons were identified. The bHLH transcription factors NeuroD1 and NeuroD2 were analyzed for their functional relevance *in vivo*. Using *in vivo* electroporation, overexpression of these transcription factors was induced in postnatal forebrain stem cell populations as well as their progeny, namely neuronal precursors and mature neurons of the olfactory system. It was shown that high expression of NeuroD2 delayed the differentiation of Type A neuronal precursor cells into granule- and periglomerular neurons. In contrast, overexpression of NeuroD1 induced the premature and ectopic differentiation of precursor cells. Furthermore, NeuroD1 induced specifically a dopaminergic phenotype, indicating that it represents a novel key fate determinant for the specification of periglomerular interneurons, possibly with a GABA/dopamine bifunctional neurotransmitter phenotype.

In conclusion, this study represents a comprehensive molecular basis for the understanding of spatially as well as temporally defined GABAergic neuron subpopulations and led to the identification of novel fate determinants for the differentiation of inhibitory interneuron subpopulations.

Abbreviations

bp	Base pair(s)
BrdU	5-Bromo-2-deoxyuridine
BSA	Bovine serum albumin
cDNA	Copy DNA
CNS	Central nervous system
dATP	Deoxyadenosine triphosphate
dCTP	Deoxycytosine triphosphate
dGTP	Deoxyguanosine triphosphate
DMEM	Dulbecco's modified Eagle's medium
DNA	Deoxyribonucleic acid
dNTP	Deoxyribonucleotid triphosphate
dTTP	Deoxythymidine triphosphate
E	Embryonic day
ECM	Extracellular matrix
EPL	External plexiform layer
FACS	Fluorescence-activated cell sorting
FCS	Fetal calf serum
GABA	γ-aminobutyric acid
GCL	Granule cell layer
GO	Gene Ontology
h	Hour(s)
HBSS	Hank's Balanced Salt Solution
IPL	Internal plexiform layer
LV	Lateral ventricle
MACS	Magnetic cell separation
MCL	Mitral cell layer
min	Minute(s)
mRNA	Messenger RNA
NSC	Neural stem cell(s)
OB	Olfactory bulb
P	Postnatal day
PBS	Phosphate-buffered saline
PCR	Polymerase chain reaction
PGL	Periglomerular layer
qPCR	Quantitative real-time PCR
RMS	Rostral migratory stream
RNA	Ribonucleic acid
RT	Room temperature
SAM	Serial analysis of microarrays
sec	Second(s)
SGZ	Subgranular zone
SVZ	Subventricular zone
U	Unit(s)
VZ	Ventricular zone

Table of contents

1 Introduction

1.1 GABAergic neurons: function and diversity

Gamma-aminobutyric acid (GABA) represents the main inhibitory neurotransmitter in the adult mammalian brain (Owens and Kriegstein, 2002b). It was identified over half a century ago (Awapara *et al.*, 1950). In vertebrates, GABA is synthesized from glutamate (Roberts and Frankel, 1950), which is the main excitatory neurotransmitter in the central nervous system. Two glutamic acid decarboxylase (GAD) enzymes, GAD65 and GAD67, catalyze this step (Erlander *et al.*, 1991; Erlander and Tobin, 1991). Whereas GAD67 is more generally distributed among GABAergic neurons, GAD65 predominates in the visual and the neuroendocrine systems (Feldblum *et al.*, 1993). Subsequent to its synthesis, GABA is transported into synaptic vesicles by the vesicular neurotransmitter transporter VGAT (Fon and Edwards, 2001). Upon activation of the cell, GABA is released into the synaptic cleft where it can bind to pre- or postsynaptically localized $GABA_A$, $GABA_B$ or $GABA_C$ receptors (Fig. 1.1). While $GABA_A$ and $GABA_B$ receptors are found throughout the brain, $GABA_C$ receptors are predominantly expressed in the vertebrate retina (Bormann and Feigenspan, 1995). $GABA_A$ and $GABA_C$ receptors are ionotropic, meaning that upon binding of GABA a chloride specific ion pore is opened, which results in a direct hyperpolarization of the target cell (Bormann, 2000). In contrast, $GABA_B$ receptors are metabotropic, mediating their downstream effect by activating a heterotrimeric G-protein coupled signaling cascade and therefore induce a slower but more persistent inhibition by modulation of either presynaptic calcium or postsynaptic potassium currents (Bormann, 1988). Subsequently, a reuptake of GABA by GABA transporters (GATs), localized in the plasma membrane of surrounding glial and neuronal cells, terminates the signaling (Cherubini and Conti, 2001). After transamination of GABA, catalyzed by the enzyme GABA-T, it is metabolized in the tricarboxylic acid cycle (Madsen *et al.*, 2008; Palmada and Centelles, 1998).

As nearly all organisms from bacteria to humans synthesize GABA, multiple functions of this amino acid have evolved (Elliott and Hobbiger, 1959; Morse *et al.*, 1980; Owens and Kriegstein, 2002a), including the regulation of key developmental steps, like cell proliferation and circuit refinement (Owens and Kriegstein, 2002b).

However, the most important role of GABA is its function as a neurotransmitter. Interestingly, while GABA acts exclusively as an inhibitory neurotransmitter in the adult brain, it can function also as an excitatory neurotransmitter during development. In

developing neurons, the intracellular chloride concentration is much higher than in mature neurons (Ben-Ari *et al.*, 1989). Therefore, activation of $GABA_A$ receptors induces an efflux of chloride resulting in membrane depolarization that can directly evoke an action potential discharge in some cases (Chen *et al.*, 1996). During cortical development, $GABA_A$, $GABA_B$ and $GABA_C$ mediated signaling induces the modulation of proliferation, migration as well as differentiation (Owens and Kriegstein, 2002b). In addition, nonsynaptic GABA signaling from neuroblasts towards GFAP expressing neuronal stem cells during adult neurogenesis in the subventricular zone inhibits proliferation of these stem cells (Liu *et al.*, 2005).
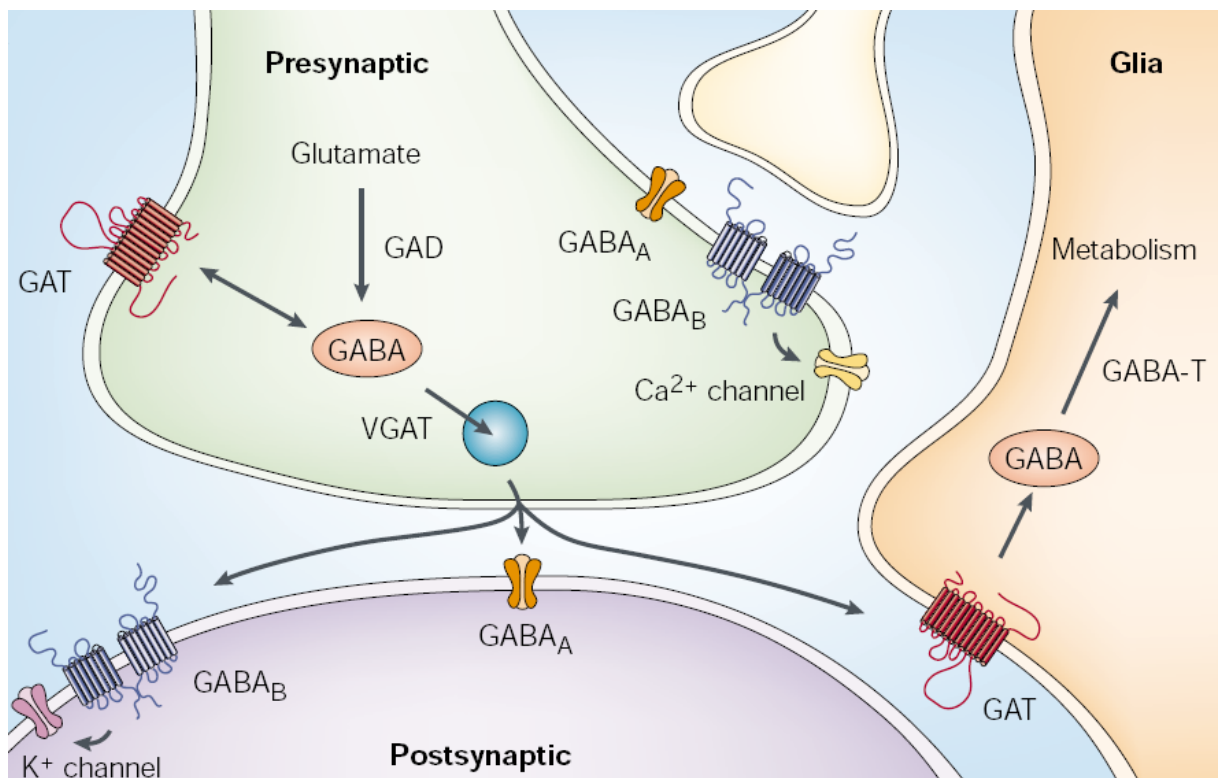
Figure 1.1: GABA signaling and metabolism

Schematic diagram of GABA metabolism and synaptic signaling. GABA is synthesized from glutamate via decarboxylation catalyzed by the enzymes GAD65 or GAD67and transported into synaptic vesicles by the vesicular neurotransmitter transporter VGAT. Upon activation of the cell, GABA is released into the synaptic cleft where it can bind to pre- or postsynaptically localized $GABA_A$, $GABA_B$ or $GABA_C$ receptors. $GABA_A$ and $GABA_C$ receptors are ionotropic, whereas $GABA_B$ receptors are metabotropic. GATs (GABA transporters), localized in the plasma membrane of surrounding glial and neuronal cells, are responsible for the reuptake of GABA. After transamination of GABA, catalyzed by the enzyme GABA-T, it is metabolized in the tricarboxylic acid cycle. Modified from Owens and Kriegstein (Owens and Kriegstein, 2002b).

GABAergic neurons (Tab. 1.1) are defined as group of neurons using GABA as their primary neurotransmitter. Functioning mainly as inhibitory neurons, they play a crucial role in information processing by regulating the activity of other neurons. Their essential role for correct brain function becomes apparent as the loss or malfunction of these neurons results in the development of neurological diseases like Huntington's disease or Schizophrenia (Bossy-Wetzel *et al.*, 2004a; Hashimoto *et al.*, 2003). GABAergic neurons show a high degree of anatomical, electrophysiological and synaptic diversity (Blatow *et al.*, 2005; Markram *et al.*, 2004). Historically defined, GABAergic neuron subtypes were classified and named according to their morphology and localization (Tab. 1.1). Whereas GABAergic cells represent local projecting interneurons in most brain regions, there are also GABAergic projection neurons in the striatum, which build up long range axonal innervations of the globus pallidus externa and substantia nigra (Flames and Marin, 2005; Lobo *et al.*, 2006). Research over the past decades lead to further classification of these cells with respect to the expression of marker genes as well as their electrophysical properties. The calcium binding proteins Calbindin (CB), Parvalbumin (PV) and Calretinin (CR) as well as the neuropeptides Vasoactive intestinal peptide (VIP), Somatostatin (SST), Cholecystokinin (CCK) and NeuropeptideY (NPY) are differentially expressed among GABAergic neuron subtypes (Markram *et al.*, 2004). Furthermore, a remarkable variety of receptors, especially AMPA-, NMDA-, Metabotropic glutamate-, GABA$_A$, 5-HT$_3$- and nicotinic receptors, complexes their diversity (Blatow *et al.*, 2005). The interaction of these proteins as well as so far unidentified factors allow for a broad pattern of electrophysiological properties. Non-accommodating, accommodating, stuttering, bursting and irregular spiking are the five major electrophysiological classes among neocortical interneurons (Markram *et al.*, 2004). Although all these parameter allow for a valuable, detailed and partly functional description of different GABAergic neurons, there is no clear correlation among these characteristics and a systematic dichotomy of defined subclasses is still lacking.

Table 1.1: Major GABAergic neuron subtypes

Olfactory bulb	Cortex	Striatum	Cerebellum
Periglomerular neuron	Chandelier neuron	Striatopallidal medium spiny neuron	Purkinje neuron
Granule neuron	Large basket neuron		Stellate neuron
	Nest basket neuron	Striatonigral medium spiny neuron	Basket neuron
	Small basket neuron		Golgi neuron
	Double bouquet neuron		
	Bipolar neuron		
	Bitufted neuron		
	Martinotti neuron		
	Cajal Retzius neuron		
	Neurogliaform neuron		

1.1.1 GABAergic neurons of the olfactory bulb

Two main subtypes of GABAergic neurons are found in the olfactory bulb. Both subpopulations, namely periglomerular layer interneurons and granule neurons, are named according to their localization in the periglomerular- or granule layer of the olfactory bulb (see also Fig. 1.4). The periglomerular layer contains glomeruli, which are build up of globular tangles of axons and represent the region where axons from olfactory receptor neurons, localized in the olfactory epithelium, and dendrites from mitral and tufted neurons, projecting to the olfactory cortex, are connected (Ache and Young, 2005). Each glomerulus contains the axons of olfactory receptor neurons that express the same odorant receptor (Treloar *et al.*, 2002). Therefore, it has been hypothesized that each odor is spatially mapped in the glomerular layer (Lledo *et al.*, 2005).

In contrast to previous data, which claimed that only a subpopulation of periglomerular layer interneurons are GABAergic, recent studies have shown that all of these cells indeed use GABA as neurotransmitter (Panzanelli *et al.*, 2007). However, about 16% of periglomerular layer interneurons show a bifunctional GABAergic/dopaminergic neurotransmitter phenotype (Panzanelli *et al.*, 2007; Parrish-Aungst *et al.*, 2007). Further non overlapping subpopulations of these cells express either the calcium binding proteins Calbindin (14%) or Calretinin

(44%). Periglomerular interneurons establish intra- as well as interglomerular connections and therefore play a key role during the first step of olfactory processing (Lledo *et al.*, 2005). Complex neuronal interactions via chemical synapses as well as gap junctions between periglomerular interneurons and mitral-, tufted- and olfactory receptor neurons are found (Kosaka and Kosaka, 2005). In general, upon activation of an interneuron by one of these cells, it triggers feedback- as well as lateral inhibition to the surrounding neurons via a rare bi-directionality, dendro-dendritic class of synapses (Kosaka and Kosaka, 2005).

Granule cells of the olfactory bulb connect to mitral and tufted cells via bi-directional, dendro-dendritic synapses (Arevian *et al.*, 2008). Upon release of the excitatory neurotransmitter glutamate by mitral or tufted cells, the granule cell is activated and releases GABA, thereby inhibiting the initial as well as neighboring mitral and tufted cells (Ache and Young, 2005; Schoppa and Urban, 2003).

In conclusion, both systems trigger feedback- as well as lateral inhibition to mitral- and tufted neurons. The general function of lateral inhibition is to enhance contrast, facilitate discrimination of similar stimuli, and mediate competitive interactions between active neurons (Hirsch and Gilbert, 1991). This probably increases the discrimination of similar odors and advantage strong versus intermediate and weak signals (Urban, 2002).

One special feature of granule as well as periglomerular layer interneurons is the generation and replacement of these cells throughout live by adult neurogenesis (Lledo and Saghatelyan, 2005), which is described in detail in chapter 1.2.

1.1.2 GABAergic neurons of the cortex

The cortex forms up to 80% of the mammalian brain and is essential for higher brain functions like memory, attention, perceptual awareness, thought, language and consciousness. This area harbors a huge amount of diverse GABAergic interneuron subtypes. More than 10 morphological defined classes are localized in this area. However, the overall amount of GABAergic interneurons is outnumbered by pyramidal cells in cortical regions by approximately 10-fold (Peters *et al.*, 1985). Despite their huge variety, cortical interneurons also have common features that distinguish them from pyramidal neurons. The majority of mature interneurons has aspiny dendrites and can receive excitatory as well as inhibitory synapses onto their somata. Furthermore, the axons of inhibitory neurons usually arborize within a cortical column and can project laterally across columns, but do not typically project down into the white matter to contact distant brain regions (Markram *et al.*, 2004).

The major subclasses, which are listed in table 1.1, can be grouped according to their axonal aborization as interneurons seem to be particularly specialized to target different domains of neurons, different layers of a column and different columns (Markram *et al.*, 2004). Thereby, they can be functionally divided into axon-targeting (Chandelier neuron), soma- and proximal dendrite-targeting (Nest basket-, Large basket- and Small basket neuron), dendrite-targeting (Double bouquet-, Bipolar-, Neurogliaform- and Bitufted neuron), and dendrite and tuft-targeting (Cajal Retzius- and Martinotti neuron) interneurons (DeFelipe, 1997). Expression of the calcium binding proteins Calbindin, Parvalbumin and Calretinin as well as the neuropeptides Vasoactive intestinal peptide, Somatostatin, Cholecystokinin and NeuropeptideY further divides these anatomically defined classes into subpopulations. Most anatomical classes express several of these markers, but there are also excluded combinations. For example, Large basked cells never express Vasoactive intestinal peptide, whereas Double bouquet cells do not express Parvalbumin, Somatostatin or NeuropeptideY (Markram *et al.*, 2004). The observation of at least 15 distinct electrophysiological patterns further complexes the situation for an appropriate sorting of these cells into groups, especially, as no strict correlation among these characteristics exists (Markram *et al.*, 2004; Monyer and Markram, 2004).

As the cortex processes many different higher brain functions, the huge diversity of inhibitory interneurons in this area may be necessary to provide sufficient sensitivity, complexity and dynamic range to match excitation regardless of the intensity and complexity of the stimulus. The synaptic diversity might be further crucial to secure the dynamic range and to choreograph moments of imbalance between excitation and inhibition in the context of any background (Silberberg *et al.*, 2004). Subtypes with diverse electrophysiological properties could be driven by the need of interneurons to monitor and respond to many sources of excitatory input, like those from the same layer, the adjacent layer, neighboring columns, other neocortical regions, the opposite hemisphere as well as subcortical input (Markram *et al.*, 2004).

The developmental mechanisms underlying this wide range of interneuron diversity are still barely understood (Fig. 1.2). One factor is the existence of several origins for these neurons (Parnavelas *et al.*, 2002; Parnavelas *et al.*, 2000). Although initial studies focused on the lateral ganglionic eminence as source for cortical interneurons (Anderson *et al.*, 1997), recent data claims that the medial ganglionic eminence is the primary source of these cells (Wonders and Anderson, 2005). Several observations also support the hypothesis that a minor population of cortical GABAergic neurons originates from the lateral ganglionic eminence

and, like cortical projection neurons, from the cortex itself (Wonders and Anderson, 2005). There is a number of correlations among the origin and later subtype of these interneurons. Whereas Parvalbumin expressing interneurons exclusively and Somatostatin expressing interneurons mainly originate from the medial ganglionic eminence, Calretinin positive cells are largely derived from the lateral ganglionic eminence (Wonders and Anderson, 2006). Furthermore, it was shown that the combinatory expression of DLX1, DLX2, DLX5, DLX6, NKX2.1, LHX6 and ER81 in combination with general position inputs can define the fate of cortical interneuron subtypes during embryonic development (Wonders and Anderson, 2006).
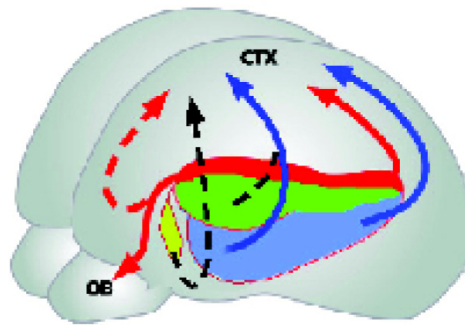
Figure 1.2: Origins of cortical interneuron subpopulations
Parvalbumin expressing cortical interneurons exclusively and Somatostatin expressing interneurons mainly originate from the medial ganglionic eminence (blue). Calretinin positive cells are largely derived from the lateral ganglionic eminence (green and red). In addition, also olfactory bulb interneurons are generated by stem cells localized in the dorsal part of the lateral ganglionic eminence (red) during development. The arrows indicate the migration path of newly generated interneuron precursors. Modified from Wonders and Anderson (Wonders and Anderson, 2005). Abbreviations: OB = olfactory bulb; CTX = cortex

1.1.3 GABAergic neurons of the striatum

The striatum, the largest component of the basal ganglia, is a key regulator for planning and modulation of movement. In contrast to other brain areas, where GABAergic neurons represent mainly local projecting interneurons, those of the striatum are GABAergic projection neurons innervating distant areas of the brain. However, there is also a minor fraction ($< 2\%$) of GABAergic interneurons in the striatum, expressing either Parvalbumin, Somatostatin or Calretinin (Marin *et al.*, 2000). Two morphologically indistinguishable and mosaically distributed subpopulations of GABAergic projection neurons are found in this area and defined by their target region (Lobo *et al.*, 2006). The Striatopallidal medium spiny

neuron innervates the globus pallidus externa, whereas the Striatonigral medium spiny neuron innervates the substantia nigra (Gerfen, 1992).

Current models of striatal function suggest that these two pathways provide balanced but antagonistic influences on the basal ganglia output. The Striatonigral (direct) pathway promotes movement, whereas the Striatopallidal (indirect) pathway inhibits movement (Graybiel, 2000). The functional imbalance of these pathways leads to a variety of movement disorders, like Huntington's disease, Parkinson's disease, Tourette syndrome and dystonia (DeLong, 1990). The specific loss of striatal GABAergic projection neurons probably represents the initial reason for the development of Huntington's disease (Beal and Ferrante, 2004). Therefore, the *in vitro* differentiation and subsequent transplantation of GABAergic neurons from multipotent neural stem cells is one promising approach for cell replacement therapies of this disease (Bosch *et al.*, 2004).

There is considerable agreement that the lateral ganglionic eminence is the origin of striatal projection neurons (Deacon *et al.*, 1994), whereas less is known about the origin of striatal interneurons. The actual model proposes that both cell types originate from the lateral ganglionic eminence, with radially migrating cells generally become projection neurons, whereas tangentially migrating cells mainly form interneurons of the striatum and cerebral cortex (Marin *et al.*, 2000).

1.1.4 GABAergic neurons of the cerebellum

The cerebellum is part of the hindbrain and plays a crucial role in integration of sensory perception and motor control. However, recent studies have demonstrated that the cerebellum influences also cognitive functions such as planning, verbal fluency, abstract reasoning, prosody and use of correct grammar in humans (Fine *et al.*, 2002). The by far most frequent neurons in the cerebellum are glutamatergic granule cells, the overall most abundant cell type of the mammalian central nervous system constituting up to 80% of all brain cells (Fine *et al.*, 2002). However, this area harbors several subtypes of GABAergic neurons in distinct layers. Purkinje cells, like GABAergic projection neurons of the striatum, build long range axons to innervate the deep cerebellar- and vestibular nuclei in the brainstem (Huang *et al.*, 2007). These cells receive excitatory input from cerebellar glutamatergic granule neurons via parallel fibers and from the inferior olivary nucleus via climbing fibers (Huang *et al.*, 2007). A single Purkinje cell can receive input from 100,000 to 200,000 parallel fibers. Stellate- and basket cells are GABAergic interneurons localized in the molecular layer of the cerebellum. The stellate cell axons selectively innervate Purkinje cell dendrites, whereas basket cells project

exuberant axon terminals to the axon initial segments to form pinceau synapses (Sotelo, 1990). Finally, golgi cells that are localized in the granule cell layer locally project to surrounding granule cells (Eccles *et al.*, 1966; Schulman and Bloom, 1981).

The function of GABAergic neurons in the cerebellum is mainly to regulate synaptic integration, probability and timing of action potential generation, and plasticity in principal neurons in order to refine sensory perception and motor control (Huang *et al.*, 2007).

Despite their variety, different types of cerebellar GABAergic neurons all derive from a subset of ventricular zone cells, which migrate in the white matter and proliferate up to the postnatal life span (Leto *et al.*, 2006).

1.2 Adult neurogenesis

In contrast to the historical view that the brain is a static organ and existing neurons can not be replaced by new cells after birth (Ramon, 1952), post-developmental neurogenesis has been shown across species from crustaceans, birds and mammals up to humans (Lledo *et al.*, 2006). Interestingly, the degree of postnatal neurogenesis decreases with increasing brain complexity. Adult neurogenesis in lower vertebrates, such as lizards, provides an additional supply of neurons capable of regenerating entire brain parts, whereas in mammals adult neurogenesis is restricted to only a few regions, where it provides neuronal replacement (Lledo *et al.*, 2006). This may be due to the problems of more difficult integration for newborn neurons in highly complex systems (Kempermann *et al.*, 2004). It is widely accepted that two areas in the mammalian brain, namely the subgranular zone (SGZ) of the hippocampal dentate gyrus and the subventricular zone (SVZ), show adult neurogenesis (Fig. 1.3). The existence of constitutive neurogenesis in other brain areas, such as the substantia nigra, is discussed controversially (Frielingsdorf *et al.*, 2004; Zhao *et al.*, 2003).

Granule cells of the dentate gyrus are generated throughout live by neuronal stem cells of the SGZ (Ming and Song, 2005). These cells are excitatory glutamatergic microneurons, projecting to the CA3 area of the Hippocampus. In contrast, inhibitory GABAergic interneurons of the olfactory bulb are generated by adult neuronal stem cells localized in the SVZ (Lledo and Saghatelyan, 2005). This system of adult neurogenesis was found in many mammalian species, including mice, rats and apes (Curtis *et al.*, 2007a). However, whereas the existence of adult neuronal stem cells in the human SVZ is widely accepted, there is an ongoing discussion based on controversial data about the existence of adult neurogenesis in the human olfactory bulb (Curtis *et al.*, 2007b; Sanai *et al.*, 2004).

The function of neurogenesis during adulthood is not fully understood. It was suggested that the cellular function of adult born neurons might differ from that of their older counterparts (Lledo *et al.*, 2004). For example, young granule cells in the adult dentate gyrus show a greater propensity for synaptic plasticity compared to older granule cells (Snyder *et al.*, 2001). Newborn granule and periglomerular cells in the olfactory bulb show markedly different active membrane properties and greater plasticity in response to sensory deprivation compared with the existing neurons around them (Carleton *et al.*, 2003; Saghatelyan *et al.*, 2005). However, it is not known, if adult-born cells only replace each other or if they also replace much older neurons (Lledo *et al.*, 2006). The ongoing neurogenesis in the olfactory bulb probably enlarges the possibility of this system for building up new neuronal circuits in order to allow an increased adaptation to changing environmental influences (Lledo *et al.*, 2006). This is in concordance to data showing that an increase in neurogenesis could be initiated by olfactory discrimination learning (Alonso *et al.*, 2006) and that reduction of progenitor proliferation leads to impaired odor discrimination in rodents (Gheusi *et al.*, 2000). However, oppositional data exists regarding the modulation of neurogenesis in the dentate gyrus upon spatial learning (Lledo *et al.*, 2006).
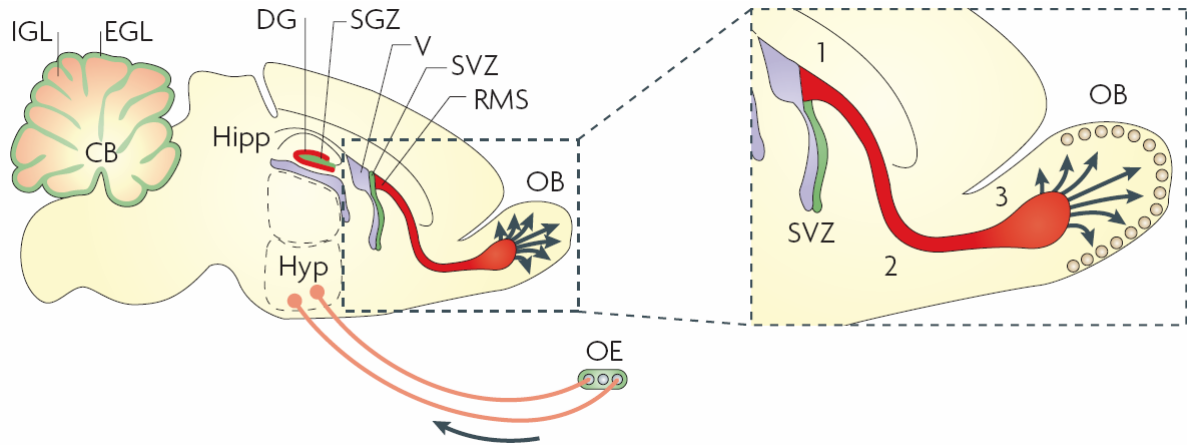
Figure 1.3: Regions of postnatal neurogenesis

In the mammalian brain mainly two areas, namely the subgranular zone of the hippocampal dentate gyrus and the subventricular zone, show adult neurogenesis. Glutamatergic granule cells of the dentate gyrus are generated throughout live by neuronal stem cells of the SGZ. Furthermore, adult neuronal stem cells localized in the SVZ (1) generate precursors that migrate along the rostral migratory stream (2) and differentiate into inhibitory GABAergic interneurons of the olfactory bulb (3). In addition, there is also restricted early postnatal neurogenesis and migration in the cerebellum and the hypothalamus. Germinal zones (green) and adjacent target zones (red) are indicated by color. Modified from Ghashghaei *et al.* (Ghashghaei *et al.*, 2007). Abbreviations: IGL = internal granule cell layer; EGL = external granule cell layer; CB = cerebellum; Hipp = hippocampus; DG = dentate gyrus; SGZ = subgranular zone; V = ventricle; SVZ = subventricular zone; RMS = rostral migratory stream; OB = olfactory bulb; Hyp = hypothalamus; OE = olfactory epithelium

1.2.1 Stem cells in the subventricular zone

The neuronal stem cells that give rise to GABAergic interneurons of the olfactory bulb throughout live are localized in the subventricular zone between the lateral ventricle and the striatum. Before and during approximately two weeks after birth, radial glia cells in the ventricular zone, directly contacting the lateral ventricle, represent the stem cells in this system (Merkle and Alvarez-Buylla, 2006). In several species, like birds, lizards, turtles and fish, radial glia remain neurogenic throughout live, whereas in mammals their role as neuronal stem cells is adopted by GFAP expressing astrocyte-like cells later on (Merkle and Alvarez-Buylla, 2006). During the first weeks, the remaining radial glia give rise to neurons, oligodendrocytes, ependymal cells and parenchymal astrocytes as well as the mentioned neurogenic astrocytes in the SVZ of the mammalian brain (Merkle *et al.*, 2004). However, some data indicate an intermediate role for Prominin-1 (CD133) expressing ependymal cells

as early, slow dividing stem cells which generate SVZ neurogenic astrocytes instead of their generation directly by radial glia (Coskun *et al.*, 2008).

Despite their different morphology and localization, radial glia and neurogenic astrocytes share common features as both equally give rise to neuronal precursors and mature neuronal cell types in the olfactory bulb. Both stem cell populations divide asymmetrically, resulting in the generation of one stem cell and one Type C transiently amplifying neuronal progenitor cell (Gotz and Barde, 2005). Upon arrival of these intermediate precursors in the SVZ, they send out numerous processes and start to divide symmetrically (Noctor *et al.*, 2004). These divisions amplify the number of precursors originating from a single stem cell division (Gotz and Huttner, 2005). The molecular mechanisms underlying these processes are barely understood. However, it was shown that GABA is released by the precursor cells and inhibits the stem cell proliferation via nonsynaptic, SNARE-independent GABA$_A$ receptor signaling (Liu *et al.*, 2005). This feedback loop thereby negatively regulates the amount of newly generated precursors, avoiding an overproduction of these cells (Liu *et al.*, 2005), whereas synaptically released dopamine enhances the Type C cell proliferation via activation of D2 receptors (Hoglinger *et al.*, 2004). Upon amplification, the Type C cells can differentiate into astrocytes, oligodendrocytes or Type A neuronal progenitors, which start their migration towards the olfactory bulb via the rostral migratory stream (Marshall *et al.*, 2005).

Recent studies have shown that the neuronal stem- and progenitor cells represent a heterogeneous population regarding both their origin and fate. Young *et al.* (Young *et al.*, 2007) determined the embryonic origins of adult forebrain SVZ stem cells. It was shown that all parts of the telencephalic neuroepithelium, including the medial ganglionic eminence, the lateral ganglionic eminence and the cerebral cortex, contribute multipotent, self-renewing stem cells to the adult SVZ (Young *et al.*, 2007). The embryonic origin thereby determines the localization of generated adult neuronal stem cells. Whereas descendants of the medial ganglionic eminence localize to the ventral parts of the SVZ, those of the lateral ganglionic eminence are present in the lateral SVZ during adulthood (Young *et al.*, 2007). Adult neuronal stem cells originating from the embryonic cerebral cortex localize to the dorsal parts of the SVZ (Young *et al.*, 2007). In addition, recent data also indicates a heterogeneous fate of newly generated precursors which depends on the localization of the initial stem cell (Merkle *et al.*, 2007). It was shown that adult neuronal stem cells of a given localization generate only a specific subset of GABAergic interneurons. For example, whereas Calretinin expressing periglomerular layer interneurons originate from stem cells in the lateral parts of the anterior SVZ, Calbindin expressing cells are generated by stem cells in the ventral parts of the more

posterior SVZ (Merkle *et al.*, 2007). Also the localization of mature granule cells is dependent on their origin, as deep granule cells are generated by stem cells in the ventral SVZ, whereas superficial granule cells are descendants of dorsal SVZ stem cells (Merkle *et al.*, 2007). However, heterotopical grafting of respective SVZ stem cells does not change the cell types they generate, indicating that these features are intrinsically determined and not dependent on local signals (Merkle *et al.*, 2007). In conclusion, the further identity of newborn neurons in the olfactory bulb seems to be already determined by their originating SVZ stem cells.

Whereas a correlation among stem cell localization and neuron subpopulations derived thereof was nicely shown, there is a lack of knowledge concerning molecular factors determining these fate decisions. At the level of Type C intermediate precursors, some respective genes have been identified. For example, a subset of these cells, expressing the basic helix-loop-helix transcription factor OLIG2, differentiates into astrocytes and oligodendrocytes (Hack *et al.*, 2005; Marshall *et al.*, 2005). In contrast, only three genes, DLX2, PAX6 and SP8, are so far known to be important for the specification of the numerous neuronal subtypes, namely dopamine/GABA double positive periglomerular interneurons in the case of DLX2 as well as PAX6 and non-dopaminergic Calretinin positive cells in the case of SP8 (Hack *et al.*, 2005; Kohwi *et al.*, 2005; Waclaw *et al.*, 2006).

1.2.2 Migration in the rostral migratory stream

Upon the differentiation of a Type C intermediate precursor into a Type A neuronal precursor, this cell migrates along the rostral migratory stream towards the olfactory bulb. The mode of migration in the RMS is unique, as the Type A neuronal precursors migrate as chains, sliding along each other in the RMS (Lois and Alvarez-Buylla, 1994). This chain migration is different to the glial- or axonal-guided modes of neuronal migration in the developing brain, because the substrate for motility is provided by the migrating cells themselves (Ghashghaei *et al.*, 2007). The existence of astrocytes, which encapsulate the migrating cells by forming a glial tube, raises the possibility that migrating neurons might use them as an additional substrate for oriented migration (Lois *et al.*, 1996). However, as isolated RMS cells can also migrate as chains *in vitro* in the absence of glial cells, they do not seem to be essential (Wichterle *et al.*, 1997). Several molecules have been identified which are probably involved in this migratory process (Ghashghaei *et al.*, 2007; Pennartz *et al.*, 2004).

The initiation of migration is probably regulated by a dynamic balance of chemorepulsive and chemoattractive signals. However, it has been shown that the existence of an olfactory bulb is not essential for correct migration of Type A precursors, therefore it seems that

chemorepulsion is the main force in this case (Kirschenbaum *et al.*, 1999). The chemorepulsive Slit-Robo pathway represents one key signal important for the initiation of migration. In SLIT1-deficient mice, clusters of Type A precursors migrate caudally into the corpus callosum, instead of into the RMS (Nguyen-Ba-Charvet *et al.*, 2004). SLIT1 and SLIT2 are secreted by cells surrounding the SVZ and both proteins have been shown to repulse the ROBO1, ROBO2 and ROBO3-receptor expressing Type A neuronal precursors (Wu *et al.*, 1999). Besides its initial role, Slit-Robo signaling may modulate the polarity of SVZ neuroblasts during migration by regulation of the cell-polarity factors glycogen synthase kinase-3β and protein kinase Cζ, which are needed for centrosome reorientation and process stabilization (Higginbotham *et al.*, 2006). Although long-distance chemoattractive signals appear to be not necessary for the initiation of migration (Kirschenbaum *et al.*, 1999), local chemoattraction may be involved. Netrin1-DCC signaling can attract migrating Type A cells *in vitro* and therefore represents one candidate pathway for this process (Mason *et al.*, 2001). In addition, the start of migration may be partially supported by the highly polarized processes of radial glia or neurogenic astrocytes, which could direct the neuronal precursors towards the RMS (Ghashghaei *et al.*, 2006).

Once the cells left the SVZ and joined the RMS, their polarity and migratory speed have to be regulated continuously in order to direct them towards the olfactory bulb. A migration speed of up to 120 μm/h has been observed in wild type Type A cells *in vitro* (Wichterle *et al.*, 1997). A complex interaction of extracellular matrix signals, secreted guidance- or motogenic signals, cell adhesion molecules, and cell-surface tyrosine kinase- or integrin signaling is necessary for correct maintenance of migration (Juliano, 2002). One key factor for the chain organization of Type A cells is the polysialated form of the neuronal cell adhesion molecule (PSA-NCAM). NCAM-knockout mice show an enlarged RMS and smaller olfactory bulb containing fewer newly generated neurons (Cremer *et al.*, 1994; Rutishauser, 1996; Tomasiewicz *et al.*, 1993). The tyrosine kinase receptor ERBB4 and its ligands, neuregulin1 and neuregulin2, are expressed by the migrating cells themselves. It has been shown that these molecules are involved in the regulation of orientated migration in the RMS and dysfunction of this pathway leads to a lack of oriented processes (Anton *et al.*, 2004). Besides ErbB4, also the Eph tyrosine kinase receptors and their ephrin ligands have been identified as indirect modifiers of neuroblast migration in the RMS (Ghashghaei *et al.*, 2007). Blocking of integrin α1, α5, α6, β1 or β4 function modulates neuronal migration in the RMS, probably by interrupting the transmission of extracellular matrix signals into the cells (Emsley and Hagg, 2003; Schmid *et al.*, 2005). These integrins are differently expressed by migrating Type A

precursors dependent on the age of mice. Whereas the α1, β1 and β8 subunits are expressed mainly during early postnatal periods, β3 and β6 integrin expression persists in until adulthood (Ghashghaei *et al.*, 2007). Putative ligands for these receptors are the laminin subunits α5 and γ1, which have been identified in the RMS as well as tenascin-C, which is expressed by the astroglial tube (Murase and Horwitz, 2002). As for the initiation of migration, again the microtubule associated proteins GSK3β and PKCζ are essential for the ability of migrating cells to reorient their centrosomes and stabilize their processes (Higginbotham *et al.*, 2006). Furthermore, the protein Doublecortin (DCX), which localizes to the microtubule cage around the nucleus as well as the leading processes, was shown to be important for regulating the velocity of migration, branching of leading processes and nuclear translocation towards the centrosome in the direction of migration (Koizumi *et al.*, 2006a; Koizumi *et al.*, 2006b).

In conclusion, the coordinated actions of several signaling pathways allow the migrating Type A neuronal precursors to arrive in the olfactory bulb, where they stop the tangential migration phase.

1.2.3 Migration and differentiation within the olfactory bulb

Upon arrival in the center of the olfactory bulb, Type A neuronal precursors change their migration mode from tangential chain migration into a radially, individual and glial-independent migration towards their final positions in the granule and periglomerular layers (Ghashghaei *et al.*, 2007). The transcription factor ARX (aristaless-related homeobox gene) is essential for the entry of cells into the olfactory bulb, as mutations in ARX lead to the accumulation of Type A cells at the junction between the end of the RMS and the olfactory bulb (Yoshihara *et al.*, 2005). However, the molecular mechanism of this process is not known. One factor, the extracellular matrix protein Reelin, was shown to be critical for the change from tangential chain- to radial individual migration as it acts as a detachment signal for the migrating neuronal precursors (Hack *et al.*, 2002). Whereas Reelin is expressed and secreted by the mitral cells of the olfactory bulb, its receptor apolipoprotein-E receptor 2 and its downstream signaling target, the adaptor protein disabled-1 are present in the migrating neuroblasts (Ghashghaei *et al.*, 2007). In addition to Reelin, the extracellular matrix protein tenascin-R seems to modulate the initiation of detachment and radial migration of precursor cells (Saghatelyan *et al.*, 2004). Interestingly, the expression of tenascin-R is olfactory sensory-activity dependent, suggesting that tenascin-R might be important for the recruitment

of new neurons to regions of the olfactory bulb where network activity demands incorporation and input from new neurons (Saghatelyan *et al.*, 2004).

About 80% to 90% of the Type A neuronal precursor cells stop their radial migration in the deep- or superficial granule layer and become granule neurons (Kohwi *et al.*, 2005). The remaining precursors migrate further to periglomerular layer, where they become post-migratory, late precursors and differentiate into periglomerular interneurons (Fig. 1.4). Granule neurons as well as periglomerular neurons can be further divided into several subpopulations based on the expression of marker genes (see also 1.1.1). The three main subtypes of periglomerular layer interneurons are bifunctional GABAergic/dopaminergic cells (16%), and either Calbindin- (14%) or Calretinin- (44%) expressing populations (Panzanelli *et al.*, 2007; Parrish-Aungst *et al.*, 2007). The granule cell population is further divided concerning the localization into deep- and superficial granule neurons, with a subpopulation of superficial granule neurons also being dopaminergic and GABAergic (Saino-Saito *et al.*, 2004). During the differentiation of granule neurons as well as periglomerular neurons, a typical expression pattern of known marker genes, correlating with the differentiation status of many neuronal cell types, can be observed. Whereas the expression of PSA-NCAM, DCX, TUJ1 (β-III-tubulin) and TUC4 is downregulated, that of NeuN in general and of Calbindin, Calretinin or TH in the respective subpopulations is upregulated (Lledo *et al.*, 2006). The first functional sodium current spikes in newborn granule and periglomerular neurons appear about 14 days after the initial generation of their progenitors in the SVZ (Belluzzi *et al.*, 2003; Mizrahi, 2007). In contrast to these markers, which correlate with the differentiation status, only three genes, namely DLX2, PAX6 and SP8, have been identified to regulate the differentiation of olfactory bulb interneuron subpopulations. Expression of PAX6 was shown to be necessary for the differentiation of periglomerular interneurons with a GABA/dopamine bifunctional neurotransmitter phenotype (Hack *et al.*, 2005; Kohwi *et al.*, 2005). Recent data indicates that this function of PAX6 is dependent on a direct interaction with the transcription factor DLX2 (Brill *et al.*, 2008). In contrast, expression of SP8 is required for the development of non-dopaminergic Calretinin positive cells in the periglomerular layer (Waclaw *et al.*, 2006).

However, all these genes act during earlier time windows, whereas almost nothing is known about the factors that regulate the final differentiation of newly generated olfactory bulb interneurons.
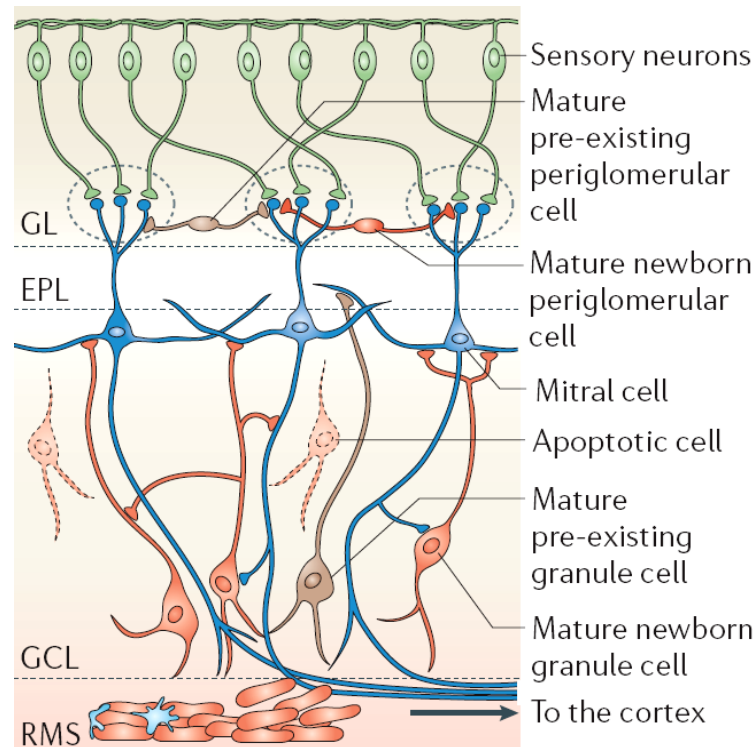
Figure 1.4: Differentiation of newly generated olfactory bulb interneurons

Upon arrival in the center of the olfactory bulb, Type A neuronal precursors (red in RMS) change their migration mode from tangential chain migration into a radially, individual migration towards their final positions in the granule and periglomerular layers. The majority of Type A neuronal precursor cells stop their radial migration in the granule layer and differentiate into granule neurons (red in GCL), whereas the remaining precursors migrate further to periglomerular layer, become post-migratory and differentiate into periglomerular interneurons (red in GL). However, it is not known if adult-born cells only replace each other or if they fulfill a more general role by replacing the functions of much older neurons (brown). Modified from Lledo *et al.* (Lledo *et al.*, 2006). Abbreviations: GL = periglomerular layer; EPL = external plexiform layer; GCL = granule cell layer; RMS = rostral migratory stream

1.2.4 Neurodegenerative diseases affecting the subventricular zone

The human subventricular zone is specifically affected in several neurological diseases, like Huntington's disease, Alzheimer's disease, Parkinson's disease, epilepsy and stroke. In response to neurodegeneration in Huntington's disease, epilepsy and stroke, there is an upregulation of progenitor cell production, cytokine levels and migratory proteins in the SVZ, leading to an increase in the number of adult-born neurons (Curtis *et al.*, 2007a). In contrast, in Alzheimer's disease and Parkinson's disease fewer proliferating cells are found in the SVZ (Curtis *et al.*, 2007a).

Huntington's disease, an autosomal dominant disorder caused by expanded CAG repeats in the huntingtin gene, results in a loss of GABAergic projection neurons of the striatum (Vonsattel *et al.*, 1985). The loss of neurons next to the localization of adult neuronal stem cells induces an increased progenitor cell production in the SVZ (Phillips *et al.*, 2005). It was suggested that enriched expression of NPY and NOS upon the development of Huntington's disease are possible mechanisms initiating increased mitosis in the SVZ (Hansel *et al.*, 2001; Reif *et al.*, 2004).

Parkinson's disease is characterized by a degeneration of dopaminergic neurons in the substantia nigra pars compacta, which is part of the basal ganglia circuitry that projects to the striatum and synapses on GABAergic projection neurons in this region (Curtis *et al.*, 2007a). Progenitor proliferation in the SVZ was shown to be reduced in animal models as well as human patients with Parkinson's disease which leads to impaired odor discrimination in rodents and is also a common and early sign of this disease in humans (Lledo *et al.*, 2006). The molecular mechanisms are not fully understood yet. However, it was shown that synaptically released dopamine enhances Type C cell proliferation via activation of D2 receptors and a lack of this signaling may therefore reduce the amount of new cells (Hoglinger *et al.*, 2004).

During Alzheimer's disease, an accumulation of neurofibrillary tangles and amyloid plaques, composing of β-amyloid peptides, is observed. This probably causes the massive cell death of mature neurons (Mattson, 2000). Animal studies that were based on presenilin 1 transgenes as well as intraventricular infusion of β-amyloid peptides were found to result in an impairment of adult neurogenesis (Donovan *et al.*, 2006; Haughey *et al.*, 2002a). Besides the reduction of adult stem cell proliferation, β-amyloid peptides can directly promote apoptosis in neuron restricted neural progenitor cells (Haughey *et al.*, 2002b). In addition, an immunotherapy against the N-terminus of the β-amyloid peptide in a transgenic mouse model of Alzheimer's disease was shown to stimulate endogenous neurogenesis (Becker *et al.*, 2007).

The involvement of the SVZ in major neurodegenerative diseases and its modulation by defined factors may offer new opportunities for specific therapies. However, the molecular basis underlying adult neurogenesis has to be understood in order to identify possible targets and mechanisms for subsequent approaches.

1.3 Aim of this study

Several attempts have been made to categorize subpopulations of GABAergic neurons at different developmental stages. This included, amongst others, the analyses of their major functional role, spatiotemporal placement, plasticity, morphology, discharge properties, connectivity pattern, neurochemistry, as well as protein, sugar, and lipid markers. However, while all these parameter allow for a valuable, detailed and partly functional description of different GABAergic neurons they have not led to a systematic dichotomy so far. Therefore, new marker genes as well as factors important for the differentiation and general functionality of GABAergic neurons have to be identified. Furthermore, the molecular analysis of GABAergic neurons from different brain regions is a promising approach to classify these cells and define region specific characteristics. However, due to the lack of a specific surface marker for GABAergic neurons it is not possible to purify these cells, which is a prerequisite for a subsequent molecular characterization.

Therefore, the first aim was to establish a protocol for the isolation of GABAergic neurons in general as well as from defined brain regions. Subsequently, these cells had to be analyzed on a molecular level by comprehensive whole genome expression profiling. This method has emerged as a reliable tool for the description of cells. Based on the expression of thousands of genes, each cell type or cell stage is assigned an unambiguous and specific pattern. Furthermore, bioinformatic analyses offer the opportunity to quantify the relationship of individual cell populations by calculating correlation matrices. Moreover, by assessing prominent transcription pathways, functional explanation of the observed differences can be given and new single gene markers identified. Analyzing the transcriptomes of GABAergic neurons in general as well as subpopulations of these cells should give new insights into the topics mentioned above.

In a parallel approach, the focus was to identify novel factors that regulate interneuron differentiation. The postnatal generation of olfactory bulb GABAergic interneurons offers a promising model system to study the development of these cells in detail. As this system is affected in major neurodegenerative diseases, a detailed understanding of the molecular mechanisms regulating defined steps during the differentiation process is essential for the development of cell- or drug based therapeutic approaches. In addition, the identification of novel fate determinants, important for the differentiation of specific neuronal subtypes, may offer new possibilities for the *in vitro* generation of these cells from neuronal- or even embryonic stem cells in order to replace lost neurons after neurodegeneration caused by injury

or disease. Several factors that regulate the proliferation of adult stem cells in the SVZ as well as the migration of progenitor cell towards the olfactory bulb have been identified. However, there is a striking lack of known factors that are involved in the further differentiation of these progenitors.

Therefore, novel genes that are important for the differentiation of olfactory bulb GABAergic neurons had to be identified. Again, whole genome expression profiling was the most promising approach to address this point. To identify genes that are significantly regulated during differentiation, a protocol for the isolation of mature olfactory bulb interneurons as well as their progenitor cells had to be established in order to analyze and compare the transcriptomes of these subpopulations. In addition, promising candidates had to be examined for their functional relevance *in vivo* to distinguish marker genes, which are regulated as a consequence of the differentiation state, from those which are fate determinants and are important for the regulation of this process.

2 Material and Methods

2.1 Enzymes and Reagents

ABI Prism Big Dye Terminator Cycle Sequencing Kit	Applied Biosystems / Perkin Elmer
SUPERSCRIPT II RT-Kit	Invitrogen
RNA 6000 Pico Assay	Agilent Technologies
Total RNA Isolation NucleoSpin®RNAII	Macherey Nagel
Gel extraction NucleoSpin®ExtractII	Macherey Nagel
RNA Clean-up NucleoSpin®RNA Clean-up	Macherey Nagel
Rediprime DNA labeling system	GE Healthcare
BCATM Protein Assay Kit	Pierce
ECL$^+$-Kit	GE Healthcare
Terminal deoxynucleotidyl transferase	GE Healthcare
Taq-Polymerase	Invitrogen
Elongase-Enzyme-Mix	Invitrogen
DNaseI	Ambion, Roche
Proteinase K	Roche
RNaseA	Roche
RNaseH	Invitrogen
Alkaline Phosphatase	Roche
DNA Polymerase I, large (Klenow) fragment	NEB
T4-DNA-Ligase	Promega
Allophycocyanine (APC)	Cyanotech
Papain	Worthington
Trypsin	Gibco

2.2 Antibodies and MicroBeads

Mouse IgG anti-NeuN	Invitrogen
Mouse IgM anti-A2B5	G. Rougon
Mouse IgG1 anti-Calb2	Sigma
Mouse IgG2a anti-PSA 735	R. Gerardy-Schahn
Rabbit anti-GAD65/67	Sigma
Rabbit anti-NeuroD1	Abcam
Rabbit anti-NeuroD2	Abcam
Rabbit anti-GAPDH	Assay Designs
Rabbit anti-TUJ1	Covance
Rabbit anti-GFAP	Sigma-Aldrich
Guinea pig IgG anti-DCX	Chemicon
Swine anti-rabbit HRP	Dako Cytomation
Goat anti-mouse IgM Alexa 488	Molecular Probes/Invitrogen
Goat anti-rabbit IgG Cy5	Cambridgeshire
Goat anti-guinea pig IgG Cy5	Abcam
Goat anti-mouse IgG Alexa 633	Molecular Probes
Goat anti-mouse IgM Alexa 633	Molecular Probes
Goat anti-mouse IgG Fc Cy3	Jackson
Goat anti mouse IgM Texas Red	Abcam
Donkey anti-mouse IgG Cy3	Jackson
Donkey anti-rabbit Cy3	Jackson
AffiniPure Goat-anti-rabbit IgG (H+L)	Dianova
R-PE-goat-anti-rabbit	Molecular Probes
full length A. v. EGFP Polyclonal AB	Clontech
Goat-anti-rabbit-FITC, F2765	Molecular Probes
anti-Dig. fab fragments phosphatase	Roche
anti-rabbit IgG MicroBeads	Miltenyi Biotec
anti-mouse IgM MicroBeads	Miltenyi Biotec
anti-mouse IgG MicroBeads	Miltenyi Biotec
anti-PE MicroBeads	Miltenyi Biotec

2.3 Chemicals and expendable items

All chemicals, unless otherwise specified in the text, were purchased at Merck. All buffers and media for cell culture were purchased at Invitrogen. NanoPURE Diamont^{TM} ultrapure water (Barnstead) was used for experiments.

10-20% Tris/Glycine-gel	Anamed
1 kb-PLUS-DNA-Ladder^{TM}	Invitrogen
GeneRuler^{TM} 100bp DNALadder Plus	NanoDrop Technologies
MagicMark^{TM} Western Protein Standard	Invitrogen
PAGE-Ruler^{TM} Prestained Protein Ladder	Fermentas
Extra thick Blot Paper (Mini Blot size)	BioRad
Hybond-P PVDF-Membrane	GE Healthcare
Hybond-XL Nylon-Membrane	GE Healthcare
Electroporation Cuvette (Type 165-2107)	BioRad
NAP-10-Column	GE Healthcare
PD-10-Column	GE Healthcare
Superdex 200 16/60- Column	GE Healthcare
Microcons Type YM-10	Millipore
Neubauer chamber	Brand
μ-MACS$^{®}$ Separation column	Miltenyi Biotec
Pre-Separation filter	Miltenyi Biotec
Syringe needle 26G ½", short	Braun
SuperFrost$^{®}$ Plus microscope slides	Menzel
Sigma Fast BCIP/NBT	Sigma
CpG ODNs 1668	Metabion
PHA-Lectin	Sigma
Azaserine	Sigma
Freunds Adjuvant incomplete	Sigma
Polyethylenglycol	Roche

2.4 Instruments

NanoDrop	NanoDrop Technologies
Agilent 2100 Bioanalyzer	Agilent Technologies
Trans-Blot SD SemiDry Transfer Cell	BioRad
LSM 510	Carl Zeiss
Axioskop 2$^+$	Carl Zeiss
Axioplan 2 equipped with ApoTome	Carl Zeiss
Cryo 1°C-freezing container	Nalgene
Gene Pulser II	BioRad
Electroporator CUY21 edit device	Nepagene
Electrodes CUY650P10	Nepagene
Flow cytometer FACScalibur^{TM}	BD Biosciences
Flow cytometer FACSvantageSE^{TM}	BD Biosciences
µ-MACS-Separator	Miltenyi Biotec
Cell culture hood: Hera Safe	Heraeus
Incubator: Hera Cell	Heraeus
Scale APX-200	Denver Instruments
Scale SPB61	Scaltec
Heating block BT 1301	HLC
Bacteria incubator	WTB Binder
Water bath	Julabo
Centrifuge Eppendorf 5415D	Eppendorf
Centrifuge Megafuge 1.0	Heraeus
Cyclone Storage Phosphor System	Packard
Thermocycler: PTC-225	MJ Research
Multiplate reader Genios	Tecan
Cell culture incubator Labotec Gasboy C40	Labotec
Vibratome microtome	Microm
Cryostat CM3050	Leica
Binocular MZFLIII	Leica
Peristaltic pump Lamda Preciflow	Lambda Laboratory Instruments
Stereotaxic rig	Kopff

2.5 *E. coli* strains

Table 2.1 *E. coli* strains

E. coli strain	Genotype	Reference
DH5α[TM]	*F- φ80lacZΔM15 Δ(lacZYA-argF)U169 recA1 endA1 hsdR17(rk-, mk+) phoA supE44 thi-1 gyrA96 relA1 λ-*	Invitrogen

2.6 Molecular biological methods

Unless otherwise specified, standard molecular biological methods were carried out according to Sambrook and Russell (Sambrook and Russell, 2001).

2.6.1 Isolation of RNA

RNA was isolated using the NucleoSpin® RNA Clean-up Kit (Macherey Nagel) according to the manufacture's instructions. RNA quality was confirmed using Agilent Bioanalyzer Pico chip gel electrophoresis (Agilent). RINs (RNA Integrity Numbers) and ratios of 28S/18S rRNA served as quality controls.

2.6.2 Isolation of DNA

2.6.2.1 Plasmid preparation from *E. coli*

Preparation of plasmid DNA from *E. coli* was done using alkaline lysis followed by column purification (Birnboim and Doly, 1979). For small scale preparations the NucleoSpin® Plasmid Kit (Macherey Nagel) and for large scale preparations the EndoFree Plasmid Kit (Qiagen) was used according to the manufacture's instructions. DNA was dissolved either in elution buffer (10 mM Tris/HCl, pH 8.5) or PBS (pH 7.2, Invitrogen) and stored at -20°C.

2.6.2.2 DNA preparation from agarose gels

DNA was isolated from agarose gels using the NucleoSpin® Extract II Kit (Macherey Nagel) according to the manufacture's instructions. DNA was dissolved either in elution buffer (10 mM Tris/HCl, pH 8.5) or distilled water and stored at -20°C.

2.6.2.3 DNA preparation from mouse tails

Tail biopsies of four to six week old mice were incubated in 700 µl lysis buffer (50 mM Tris/HCl pH 8.0, 100 mM EDTA pH 8.0, 100 mM NaCl, 1% SDS) containing 35 µl Proteinase K (10 mg/ml) over night at 55°C. After centrifugation (10 min, 14000 g), the supernatant was transferred into a new tube and DNA was precipitated using isopropyl alcohol at a final concentration of 60%. After centrifugation (10 min, 14000 g), the DNA was desalted using 1 ml 70% ethanol (centrifugation for 10 min, 14000 g) and dissolved in 300 µl TE buffer.

2.6.3 Polymerase chain reaction (PCR)

The polymerase chain reaction (PCR) allows the amplification of precise parts from a DNA template by using primers specific for both ends of the sequence (Mullis *et al.*, 1986; Saiki *et al.*, 1988). The target sequence is amplified by the factor 2^n, where n is the number of cycles. For standard PCRs the *Taq*-Polymerase (Invitrogen) and for cloning approaches the *Elongase*-Enzyme-Mix (Invitrogen) was used.

Table 2.2 Constitution of standard PCRs

	Taq-Polymerase	*Elongase*-Enzyme-Mix
DNA template	1-100 ng	1-100 ng
1. primer	200 nM	200 nM
2. primer	200 nM	200 nM
dNTP-mix (10 mM)	200 µM	200 µM
10 x PCR-Buffer	1 x	1 x
$MgCl_2$	1,5 - 2,8 mM	1,5 - 2,0 mM
DNA-Polymerase	1 U	1 µl**
Distilled H_2O	up to 30-50 µl	up to 30-50 µl

** Activity (U/µl) not known

Table 2.3 PCR programs

Step	Taq-Polymerase		Elongase-Enzyme-Mix	
1. Denaturing	95°C	4 min	95°C	4 min
2. Annealing	57 - 63°C	30 s	50-68°C	30 s
3. Primer extension	72°C	60 s	68°C	2 min
4. Denaturing	94°C	30 s	94°C	30 s
5. Cycles (step 2.-4.)		20-34 x		34 x
6. Annealing	57 - 63°C	30 s	50-68°C	30 s
7. Final extension	72°C	5 min	68°C	5 min
8. Cooling	10°C	stop	10°C	stop

The Thermocycler PTC-225 (MJ Research) was used for all PCRs. Size determination and purification of the PCR products was done using agarose gel electrophoresis (Loeb and Chauveau, 1969; Takahashi *et al.*, 1969).

2.6.4 DNA sequencing

The method of chain termination was used for DNA sequencing (Sanger *et al.*, 1977). During this method (also called "cycle sequencing") cyclic, PCR-based DNA amplification is combined with base specific chain termination (Carothers *et al.*, 1989; Murray, 1989). For all sequencing reactions, the ABI Prism Big Dye Terminator Cycle Sequencing Kit (PE Applied Biosystems) was used. Amplified fragments were purified using 96-well-G50-Superfine plates (GE Healthcare). Subsequently, the purified fragments were separated and analyzed in an ABI Prism™ 377 DNA Sequencer (PE Applied Biosystems).

Raw data was processed with Sequence Analysis 3.0 software (PE Applied Biosystems). Sequence data was analyzed with Lasergene (DNASTAR, London, UK).

2.6.5 Restriction hydrolysis

Sequence specific hydrolysis of DNA was achieved by incubation for at least 1 h with restriction enzymes at a concentration of 1 Unit/μg DNA template. Buffers and incubation temperatures were chosen referring to the manufacture's instructions. Subsequently, the DNA fragments were separated in an agarose gel electrophoresis and purified with the NucleoSpin® Extract II Kit (Macherey Nagel, see 2.6.2.2).

2.6.6 DNA dephosphorylation

Prior to ligation of insert fragments with vector-DNA, the vector-DNA was dephosphorylated to prevent internal ligation. The target DNA was incubated with alkaline Phosphatase (Roche, 1 Unit/µg DNA) in dephosphorylation buffer (Roche) for 30 min at 37°C. For removal of the enzyme, DNA was precipitated with isopropyl alcohol (see 2.6.2.3) and resolved in distilled water.

2.6.7 DNA ligation

DNA fragments were ligated by incubation with 10 Units *T4*-DNA-Ligase (Promega) per µg of DNA in Ligation Buffer (Promega) at 16°C over night. To obtain highest ligation efficiency, vector- to insert-DNA ratios from 1:1 to 1:5 were tested.

2.6.8 Transformation of *E. coli*

For amplification, plasmids were transformed into DH5α-cells (Invitrogen) using the "heat shock"-transformation protocol of the manufacturer.

2.6.9 Cloning of expression vectors

2.6.9.1 Generation of an expression vector for NeuroD1

The coding sequence for Neurogenic Differentiation 1 (NeuroD1, GeneID: 18012) was obtained from the SwissProt Database (http://www.expasy.ch/sprot/). As the complete open reading frame is spanning only one exon of the gene, the coding sequence was amplified from genomic DNA using the following primers:

Forward primer:

5' GGGGGAAGCTTCACCATGACCAAATCATACAGCGAGAG 3'

(red: *Hin*dIII recognition site, blue: Start-codon)

Reverse primer:

5' GGGGGGGATCCGAAACTGACGTGCCTCTAATCGTG 3'

(red: *Bam*HI recognition site)

After amplification (see 2.6.3) and purification (see 2.6.2.2), the PCR fragment was incubated with the restriction enzymes *Bam*HI (NEB) and *Hin*dIII (Fermentas) in SureCut B restriction buffer (Roche) followed by purification (see 2.6.5). A eukaryotic expression vector based on the chicken β-actin promoter and the CMV enhancer, pCX-MCS2 (see Fig. 2.1), a gift from Xavier Morin (Morin *et al.*, 2007), was treated the same way. After dephosphorylation of the vector DNA, the NeuroD1 PCR fragment was ligated with pCX-MCS2 (see 2.6.7) and transformed into DH5α-cells (see 2.6.8). The final construct, pCX-ND1, was verified by sequencing (see 2.6.4 and 6.1).
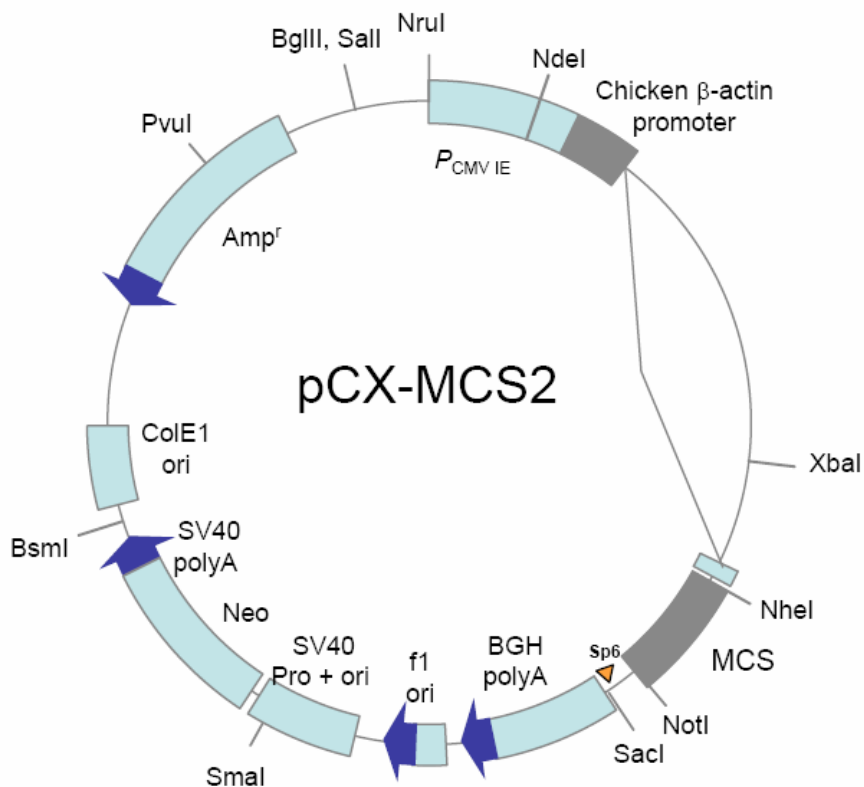
Figure 2.1: The expression vector pCX-MCS2

Map showing the main modules and restriction endonuclease binding sites of the pCX-MCS2 expression vector.

2.6.9.2 Generation of an expression vector for NeuroD2

The coding sequence for Neurogenic Differentiation 2 (NeuroD2, GeneID: 18013) was obtained from the SwissProt Database (http://www.expasy.ch/sprot/) and amplified from whole brain cDNA (a gift from Sonja Gemmel), using the following primers:

Forward primer:

5' GGGGGAAGCTTCTCTCTGAGGCACCATGCTGAC 3'

(red: *Hin*dIII recognition site, blue: Start-codon)

Reverse primer:

5' GGGGGGGATCCGTCGGCGCGAGGTCTCAGTTATG 3'

(red: *Bam*HI recognition site)

Cloning of the PCR fragment into pCX-MCS2 was equal to NeuroD1 (see 2.6.9.1). The final construct, pCX-ND2, was verified by sequencing (see 2.6.4 and 6.1).

2.6.10 Microarray analysis

2.6.10.1 Amplification of RNA

For the generation of amplified cDNA after MACS- (see 2.8.4) or FACS-purification (see 2.8.5), the SuperAmp Protocol (Miltenyi Biotec) was applied. Briefly, 5000-10000 cells per approach were collected in 6.4 µl SuperAmp Lysis Buffer, the mRNA was extracted using magnetic beads and transcribed into cDNA using tagged random and oligo(dT) primers. First strand cDNA was 5' tagged by incubation with 21.5 Units terminal deoxynucleotidyl transferase (GE Healthcare) for 60 min at 37°C. The enzyme was inactivated at 70°C for 5 min. Tagged cDNA was globally amplified using primer complementary to the tag sequence using the PCR program in Table 2.4. The PCR Products were purified using the NucleoSpin® Extract II Kit (Macherey Nagel, see 2.6.2.2) and cDNA yield was quantified by OD measurement (NanoDrop, NanoDrop Technologies). Length distribution of amplified cDNA was analyzed by capillary electrophoresis (Bioanalyzer, Agilent).

Table 2.4 PCR program for SuperAmp amplification of cDNA

Step	Parameters	
1. Sample prewarming	78°C	30 s
2. Denaturing	95°C	15 s
3. Annealing	65°C	30 s
4. Primer extension	68°C	2 min
5. Cycles (step 2.-4.)		20 x
6. Denaturing	94°C	15 s
7. Annealing	65°C	30 s
8. Primer extension	68°C	2 min + 10 s/cycle
5. Cycles (step 6.-8.)		21 x
6. Annealing	65°C	30 s
7. Final extension	68°C	10 min
8. Cooling	10°C	stop

2.6.10.2 Fluorescent labeling of RNA

To detect hybridized cDNA after microarray hybridization, 250 ng of the purified PCR product (see 2.6.10.1) was labeled with either Cy5- or Cy3-dCTP (GE Healthcare) in a Klenow Fragment (10 Units per sample) reaction for 2 h at 37°C before heat inactivation at 70°C for 5 min. Labeled cDNA was purified using the CyScribe GFX Purification Kit (GE Healthcare) and quantified by OD measurement (NanoDrop, NanoDrop Technologies).

2.6.10.3 Microarray hybridization

Agilent whole mouse genome 44k microarrays were hybridized according to the manufacture's instructions (http://www.chem.agilent.com/scripts). Briefly, 2.5 µg of combined Cy3-/Cy5-labeled and purified cDNAs (see 2.6.10.2) were adjusted with dH$_2$O to a volume of 200 µl and denatured for 5 min at 95°C. After adding 50 µl control targets (Agilent) and 250 µl 2x Hybridization Buffer (Agilent), samples were incubated on the microarrays at 65°C for >16 h. Afterwards, microarrays were washed with Wash Buffer I (Agilent) for 1 min at 37°C, with Wash Buffer II (Agilent) for 1 min at 25°C and dried after 30 s incubation in acetonitrile. Scanning was performed using the Agilent DNA-Microarray Scanner.

2.6.10.4 Microarray data analysis

Scanned images were analyzed using the Agilent Feature Extraction software (Version 9.1) by which the local background was subtracted and a rank consistency based probe selection for Lowess normalization was done. After filtering the data with respect to signal significance a two-tailed t test was used to determine signal versus background significance. Spots with a P-value of >0.01 were omitted. Exported raw data were further processed by the Luminator software (Agilent) yielding expression values. Subsequently, only expression ratios of genes with a P-value of <0.001 were used. After log2-transformation of the ratios, data were imported in TIGR MeV Version TM4 (Saeed *et al.*, 2003). Average linkage clustering of genes was done using Euclidean Distance (Eisen *et al.*, 1998). Significantly different expressed genes among the analyzed brain areas were identified by SAM (Serial Analysis of Microarrays) using the Tusher *et al.* method (Tusher *et al.*, 2001) with at least 100 permutations per analysis. Gene Ontology (GO) analysis was carried out using TreeRanker (Schacherer, F., unpublished) at a significance level of 0.005. Interactions between genes and pathway analysis were computed with PathwayArchitect software (Stratagene) interpreting only verified interactions.

2.6.11 Quantitative real-time PCR

Transcript levels were measured by quantitative real-time PCR using PerkinElmer Applied Biosystems prism model 7000 sequence detection system (PE ABI 7000 SDS). Forward and reverse primer sequences are listed in table 2.5. GAPDH was used to normalize the expression data. Four ng of globally amplified cDNA libraries (see 2.6.10.1) were used as template for each PCR analysis, all assays were performed with four replicates. Threshold cycle, Ct, was measured as the cycle number at which the SYBR green emission increases above threshold level. The following cycle conditions were used: 95°C for 10 min followed by 50 cycles of 95°C for 15 s, 60°C for 1 min. For each amplified product, melting curves were determined according to the supplier's guidelines ensuring specific amplification. For each run, negative controls were performed by omitting the template.

Table 2.5 Primers for qPCR

Strain	Forward primer	Reverse primer
DLX1	CCACCGAGTCCTGGACCAC	CCCTCCCTCTGATTTCCCC
DLX2	TATTGGAAGTGGCGACCAGG	TGGCACTAAAGGATCCCACG
DLX5	TCAATCAATTCCCACCTGCC	AAACTGAGCAAGAGAAAGTAGCCC
FOXG1	CGATGTATGTGGTCACTAACAGGTC	GCGCAACACAGGTTACATATTTG
ZIC1	TGCAAACATTTCGTCCCAAAG	TGACACGTAGATCCAGGCTCG
ZIC2	CCACGGTGATTTTAACGGCT	AAGGGAAATGGGAGAAAGGC
LHX5	AAGAGGTTGCTATGGCCACG	TCCTCATCTTTGTCTGGCCG
GAPDH	GACCTGACCTGCCGTCTAGAA	TCAGTGTAGCCCAGGATGCC

2.7 Protein biochemical methods

2.7.1 Isolation of proteins

Cells or tissues were lysed by sonification in RIPA buffer (150 mM NaCl, 1%NP-40, 0.5% Sodiumdeoxycholate, 0.1% SDS, 1 mM EDTA, 50 mM Tris pH 8.0) and subsequent incubation for 1-2 h at 4°C. Concentration of the protein solutions was determined in a Bradford assay (Bradford *et al.*, 1970).

2.7.2 Polyacrylamide gel electrophoresis (PAGE)

Proteins were separated according to their mass by sodium dodecyl sulfate polyacrylamide gel electrophoresis (SDS-PAGE) (Laemmli, 1970). Samples (5-20 μg) were diluted in loading buffer (2% SDS; 60 mM Tris/HCl, pH 6.8; 10% glycine; 5% β-mercaptoethanole; 0.02% bromophenol blue) and loaded onto 10-20% Tris/Glycine-gels (Anamed). Gel electrophoresis was performed using an X-cell Sure Lock Novex Mini cell System (Invitrogen) in running buffer (50 mM Tris/HCl pH 8.3; 380 mM glycine; 0.1% SDS). Protein sizes were determined by referring to the PAGE-Ruler™ Prestained Protein Ladder (Fermentas).

2.7.3 Western-blotting

After separation by SDS-PAGE (see 2.7.2), Proteins were blotted onto PVDF membranes (Hybond-P, Amersham Biosciences), which were activated with methanol for 30 s and equilibrated with transfer buffer for 5 min. Before blotting, protein gels were equilibrated with distilled water for 5 min. Proteins were transferred onto the PVDF membrane via a Trans-Blot SD SemiDry Transfer Cell (BioRad).

2.7.4 Immunodetection of proteins

Detection of proteins on PVDF membranes was carried out by binding of specific antibodies. To block unspecific binding-sites, membranes were incubated in 5% BSA in TBST (0.9% NaCl; 10 mM Tris/HCl, pH 7.4, 0.05% Triton TX100). Subsequently, membranes were incubated with the primary antibody in blocking buffer for 2 h at room temperature. Membranes were washed 3 times for 10 min in TBST and incubated with a secondary antibody, coupled to horseradish peroxidase, in blocking buffer for at least 1 h. The ECL^{+}-Kit (GE Healthcare) was used for visualization of bound antibodies.

2.8 Cell biological methods

2.8.1 Dissociation of brain tissue

Brain tissue was enzymatically dissociated to obtain a single-cell suspension by using the Neuronal Tissue Dissociation Kit (Papain or Trypsin, Miltenyi Biotec). For some applications, the concentration of Papain or Trypsin was varied to prevent loss of cell surface epitopes. In this case, the protease concentration is specified in the respective section.

2.8.2 Cultivation of eukaryotic cells

2.8.2.1 Cell lines

All cell lines were cultured in 25-175 cm^2 flasks or 6-96 well flat- or round-bottom culture plates (BD Falcon). Murine 1881 cells (Promochem) were cultured in Dulbecco's modified Eagles medium (DMEM; Miltenyi Biotec or Invitrogen) supplemented with 10% FCS (Biochrom), 15 mM HEPES (Invitrogen) and 2 mM L-Glutamine (Invitrogen) in a humidified incubator with a 5% CO_2 atmosphere at 37°C. SP2/0 cells (Promochem) were cultured in DMEM containing 20% FCS (PAA Laboratories), 20 mM HEPES and 2 mM L-Glutamine in a humidified incubator with a 9% CO_2 atmosphere at 37°C.

2.8.2.2 Primary brain cells

Dissociated brain cells (see 2.8.1) were cultured in DMEM/Ham's F12 medium (3/1) containing 2 mM Glutamax, 1% N2 supplement, 1% B27 and 1% penicillin/streptomycin (all from GIBCO) in poly-l-lysine-coated (0.01%, Sigma) 24-96 well flat-bottom culture plates (BD Falcon). For immunocytochemistry, 50.000 cells per well were seeded on poly-l-lysine-coated (0.01%, Sigma) glass coverslips in 4-well plates containing 500 µl culture medium.

2.8.3 Transfection of cell lines

Cell lines were transfected by electroporation. During the exponential proliferation phase, suspension cells were harvested by centrifugation (150-300 g, 10 min) and resuspended in fresh medium without FCS. After transfer into a sterile electroporation cuvette (Type 165-2107, BioRad), 0.5-1x10^7 cells were mixed with 15-50 µg pre-diluted DNA and incubated on ice for 15 min. Electroporation was performed using the Bio-Rad Gene Pulser II instrument with the following settings:

210-270 V
0.975 µF
Time constant 15-25 ms

After the pulse, cells were kept at 37°C for 10 min before subsequent culturing (see 2.8.2.1).

2.8.4 Magnetic cell separation (MACS®)

The MACS® technology allows the separation of cells according to specific cell surface markers (Abts *et al.*, 1989; Miltenyi *et al.*, 1990; Radbruch *et al.*, 1994). In principle, monoclonal antibodies which are covalently linked to superparamagnetic microbeads are incubated with single cell suspensions. These antibodies bind to cell surface markers directly or indirectly (via specific primary antibodies) and thereby magnetically label the target cell. After extensive washing, cell suspensions are separated with high gradient magnetic columns. Cells labeled with the microbeads retain in the column, whereas unlabeled cells pass through and can be collected as untouched fraction. Subsequently, the labeled cells can be eluted by displacing the column from the magnetic field. In general, this technology can be used in two ways: either depletion of unwanted cells by collection of the eluted, unlabeled fraction, or direct enrichment of labeled cells. After magnetic separation, purity of isolated cell subsets can be analyzed by flow cytometry or immunostaining.

The MACS® technology was used for the purification of glomerular layer precursors and interneurons. Coronal sections (300 μm) of olfactory bulbs from 20 postnatal day 2 mouse brains were serially cut using a vibratome (Leica, see 2.9.1). The glomerular layers of these slices were dissected and dissociated (see 2.8.1). Afterwards, the cells were centrifuged at 300 g for 7 min and the pellet (about $1.1x10^6$ cells) was resuspended in 200 μl HBSS-BSA (Miltenyi Biotec) containing 0.6 μl c-ganglioside-specific mouse IgM A2B5 ascites (ATCC CRL-1520, kindly provided by G. Rougon, Marseille) and incubated on a gently rocking rotator for 30 min at 4°C. Subsequently, the cells were washed in 10 ml HBSS-BSA and centrifuged for 7 min at 300 g. The same incubation and washing conditions were applied for all further antibodies. The pellet was resuspended in 20% (v/v) anti-mouse IgM MicroBeads (Miltenyi Biotec) in 200 μl and, after incubation and washing, resuspended in 1 ml HBSS-BSA. Cells were separated using an MS Column and a MiniMACS™ Separator (Miltenyi Biotec) according to the manufacture's instruction. The A2B5⁺ fraction, retained in the column, was eluted and kept on ice, while the flow-through was incubated with 5 μg/ml PSA-specific mouse IgG2a 735 antibody (kindly provided by R. Gerardy-Schahn, Hannover). Using 20% (v/v) anti-mouse IgG MicroBeads (Miltenyi Biotec) in 100 μl HBSS-BSA as secondary antibody directed against 735, the marked PSA⁺ cells were selected by retention in a column placed in a MiniMACS™ Separator, whereas the PSA⁻ cells were collected from the flow-through. Type A early precursor cells were purified similar, by using SVZ- instead of glomerular layer-tissue as starting material.

2.8.5 Flow cytometry

The flow cytometric analysis of cells or particles allows the analysis of physical- (cell size, cell granularity) and fluorescent-properties (after immunostaining with antibodies coupled to fluorescent dyes or internal expression of fluorescent markers). Therefore, singularized labeled cells are excited in a fluid stream by Argon- (488 nm) and diode-lasers (633nm). Depending on their label, the cells emit light which can be detected. The combination of scattered and fluorescent light emissions is detected and analyzed to define information about the physical structure and expression pattern of different molecules for each single cell. The flow cytometric analysis was done using a FACSCalibur^{TM} combined with the CellQuest software version 3.1 or version 3.3 (Becton Dickinson).

Table 2.6 Fluorochromes used for FACS

Fluorochrome	Absorption maximum (nm)	Emission maximum (nm)
EGFP	488	509
FITC	495	517
Phycoerythrin (PE)	565	576
Propidium-Iodid (PI)	538	617
Allophyconcyanin (APC)	651	660

Besides the analysis of cells, the FACS-technology also allows the separation of a heterogeneous cell population (Cantor *et al.*, 1975). This fluorescence-activated cell sorting is based on the same flow cytometric principle as mentioned before. In addition, the fluid stream is fractionated into single drops containing a maximum of one cell per drop. The drops which contain target cells, defined by their scattered and fluorescent light emissions, are electrically charged and deflected into reaction tubes based upon their charge.

For the isolation of GFP$^+$ GABAergic cells from whole brains, 4 transgenic GAD67-GFP mice at postnatal day 1 were sacrificed and their brains recovered. For the isolation of cells from different brain areas, the brains of 6 postnatal day 1 old GAD67-GFP mice were dissected into olfactory bulb, cortex, striatum, and cerebellum. GFP$^+$ GABAergic cells for immunization were isolated from brains of 8 to 12 postnatal day 1 old GAD67-GFP mice. The tissues were then dissociated to a single cell suspension (see 2.8.1). Cells were resuspended in PBS (Gibco) and sorted on a FACSVantage SE^{TM} cell sorter (Becton Dickinson) for their FSC (forward scatter), SSC (side scatter) and FL-1 (EGFP) signals. Background signals were

set using dissociated brain cells from wild-type mice (C57Bl/6 / 6NCrl). Dead cells were excluded using PI (Sigma, 20 µg/ml), which intercalates into the DNA of dead cells.

2.8.6 *In vivo* electroporation

The technology of postnatal electroporation was initially established by Camille Boutin (Boutin *et al.*, 2008). This method allows the targeted transfection of radial glia cells in the postnatal ventricular zone. At that stage, radial glia cells still represent the stem cell population of the SVZ/RMS/olfactory bulb system. Transfection of these cells induces strong expression of transgenes in the stem cell population as well as their progeny, neuronal precursors and mature neurons of the olfactory system.

Animals were treated according to guidelines approved by the French ethical committee. Postnatal day 1 old mice (CD1 strain, Charles-River) were anesthetized by hypothermia (4 min) and fixed to a support using band-aid. The skin and the skull covering the lateral ventricle were opened for about 2 mm using an ophthalmic scalpel. As a general positional marker, a virtual line connecting the right eye with lambda (visualized by a strong cold light source) was used and the incision was positioned 1 mm caudal to the midpoint of this line. Subsequently, the animal was placed in a stereotaxic rig (Kopff) under a Hamilton syringe connected to a glass capillary (diameter 200 µm, pulled out manually, GC100-15, Clark) containing 2 µl of plasmid solution (5 µg/µl, in PBS containing 1% Fast Green). The syringe was placed over the incision, positioned at the level of the skull, then lowered between 2.5 mm to 3.0 mm into the lumen of the right lateral ventricle and the stained DNA solution was injected. An injection was considered correct when the shape of the now slightly dark stained lateral ventricle was visible under the light source. Only successfully injected animals were subjected to five electrical pulses (100 V, 50 ms, separated by 950 ms intervals) using the CUY21 edit device (Nepagene) and 10 mm tweezer electrodes (CUY650P10, Nepagene) coated with conductive gel (Control Graphique Medical). Electroporated animals were reanimated for several minutes on a 37°C heating plate before being returned to the mother.

To transfect a different population of neuronal progenitor cells, cortical projection neuron precursors were electroporated at embryonic day 14 *in utero* (Saito and Nakatsuji, 2001; Shimogori and Ogawa, 2008).

Timed pregnant mice (with embryos at E14) were anesthetized with xylazin/ketamin (4.6 mg/kg body weight). After cleaning the abdomen with 70% ethanol, a midline lapratomy was performed and the uterus taken out. For DNA microinjection, a pulled out glass capillary

(diameter 200 µm, GC100-15, Clark) containing 1 µl of plasmid solution (3 µg/µl, in PBS containing 1% Fast Green) was used. The DNA was injected into the lateral ventricle using a mouth controlled pipette system. The correct injection site was visible through the uterine wall by illuminating with a fiber optics light source. Square electric pulses (50 ms, at 25 V, 5 pulses) were delivered to embryos through the uterus by using the CUY21 edit device (Nepagene) and 10 mm tweezer electrodes (CUY650P10, Nepagene). The uterus was kept wet by dropping saline. Subsequently, the uterine horns were repositioned in the abdominal cavity, filled with prewarmed saline at 37°C, and the abdominal wall and skin were sewed up with surgical sutures. The pregnant mice were sacrificed 4 days after electroporation and the embryos removed. The embryonic brains were dissected, fixed with 4% PFA over night at 4°C and cut using a vibratome at 50 µm (see 2.9.1).

2.8.7 Immunization

Contralateral footpad immunization was used to induce monoclonal antibody production in rats (Brooks *et al.*, 1993; Yin *et al.*, 1997). For all immunization approaches, GFP$^+$ GABAergic neurons were isolated from dissociated brain tissue (see 2.8.1) of 8 to 12 GAD67-GFP mice by FACS (see 2.8.5). Subsequently, about 0.8-1.3 x 10^7 purified cells were injected subcutaneously (s.c.) into the left hind footpad of Lewis rats (LEW/HanHsd, Harlan). To minimize the unspecific immunoresponse, in most cases a decoy was injected into the right hind footpad in parallel. Boosts were administrated at days -3, 0, 4, 7, 11 and 14, with only a decoy injection at day -3. In different immunization attempts, several different decoys and adjuvants were tested. Either the GFP$^-$ fraction after FACS (see 2.8.5), dissociated brain tissue of Actin-GFP mice (see 2.8.1) or EGFP protein (a gift from Gritt Günther) served as decoy. Detailed immunization schemes are listed in the results section.

2.8.8 Cell fusion

One day after the last immunization (see 2.8.7), cells from the popliteal lymph node of the one hind footpad were isolated and used for the fusion with a murine myeloma partner (Sp2/0 cells) based on the HAT system (Cotton and Milstein, 1973; Kohler and Milstein, 1975). After fusion, cells were seeded into 96 well flat-bottom culture plates (BD Falcon) in 150 µl DMEM containing 20% FCS (PAA Laboratories), 20 mM HEPES, 2 mM L-Glutamine, 0,1 mM Hypoxanthin (Sigma) and 2 µg/ml Azaserine (Sigma). Mouse peritoneal macrophages had been isolated 2 days before and cultured in the same wells to increase the

survival after fusion. The plates were incubated in a humidified incubator with a 9% CO_2 atmosphere at 37°C. After 5 to 7 days, 50 µl of culture medium was added to each well followed by subsequent incubation.

2.8.9 Screening of hybridoma supernatants

Screening of hybridoma supernatants was carried out by immunolabeling followed by flow cytometric analysis (see 2.8.5). Wells containing clones (see 2.8.8) of more than 1 mm diameter were marked and 50 µl supernatant was transferred into a new well of a 96 well round-bottom culture plate (BD Falcon). About 1×10^4 dissociated cells from brains of GAD67-GFP mice (see 2.8.1) were added to each supernatant. After 15 min at 4°C, the plates were centrifuged (200 g, 10 min) and washed with 150 µl PBS for three times. The cells were resuspended in 50 µl PBS containing mouse anti-rat (mar) kappa (κ) monoclonal antibody (1:700, clone 18.5, mouse IgG2a, Miltenyi Biotec) coupled to APC and incubated at 4°C for 10 min. After three washing steps (150 µl PBS, 200 g, 10 min), the cells were resuspended in 300 µl PBS containing PI (Sigma, 20 µg/ml) and analyzed by flow cytometry (see 2.8.5). If a hybridoma clone had produced an antibody which recognizes a cell surface antigen on GABAergic cells, the cells would be double positive for GFP and APC.

2.9 Histological methods

2.9.1 Preparation of brain tissue

For histological analysis, pups were deeply anaesthetized with an overdose of xylazin/ketamin (more than 10 mg/kg body weight). Perfusion was performed intracardiacally with a solution of 4% paraformaldehyde in PBS. The brain was removed and immersed overnight in the same fixative at 4°C. For vibratome sectioning, brains were washed three times for 10 min in PBS and stored at 4°C. Sections were cut at 50 µm using a microtome (Microm). For cryostat sectioning, brains were cryoprotected in 25% sucrose over night and frozen at -80°C. Afterwards, 10 µm sections were cut on a CM3050 cryostat (Leica), collected on Superfrost Plus slides (Menzel) and stored at -80°C.

2.9.2 *In situ* hybridization

Labeled antisense RNA probes were generated by T7 based *in vitro* transcription from EasyProbe[TM] templates (Miltenyi Biotec) using the Dig-RNA labeling kit (Roche) according to the manufacture's instructions. The EC10 EasyProbe[TM] template (Miltenyi Biotec) fragment, homologous to the bacterial ABC transporter YgaD, served as negative control. For hybridization, 10 μm cryostat sections were incubated in RIPA buffer (150 mM NaCl, 1% NP-40, 0.5% sodium deoxycholate, 0.1% SDS, 1 mM EDTA, 50 mM Tris pH 8.0) twice for 10 min and post-fixed in 4% paraformaldehyde in PBS for 10 min at room temperature. After washing in PBS for 5 min, the slides were hybridized using the a-Hyb[TM] hybridization station (Miltenyi Biotec) at a continuous pump rate of 1 ml/min. After washing with PBS for 1 min, the tissue was acetylated for 10 min with 0.25% acetic anhydride in 0.1 M triethanolamin/HCl (pH 8.0). After an additional incubation in PBS, the sections were prehybridized with hybridization solution (50% formamide, 4x SSC, 1x Denhardt's, 2 mM EDTA, 10% dextrane sulphate, 0.5 mg/ml yeast t-RNA, and 0.5 mg/ml salmon sperm DNA) for 30 min at 37°C. The labeled probe was dissolved in hybridization solution, denatured at 82°C and applied to the sections. Hybridization was carried out for 150 min at temperatures from 42°C to 65°C, depending on the probe. After washing twice for 1 min in 2x SSC/50% formamide at 25°C and twice for 1 min in 1x SSC, the a-Hyb[TM] was blocked using 0.1% BSA in 1x SSC for 5 min. Following a washing for 1 min in 2.5x SSC/0.2% Tween 20, the sections were blocked in detection solution (2% sheep serum in 2.5x SSC/0.2% Tween 20) for 15 min and incubated in detection solution containing phosphatase-conjugated anti-Dig fab fragments (Roche) for 30 min. Slides were then washed twice in 4x SSC/0.2% Tween 20 for 1 min and twice in AP buffer (100 mM Tris/HCl, 100 mM NaCl and 50 mM MgCl2) for 1 min. Visualization was performed using NBT/BCIP (Sigma) dissolved in AP buffer containing Levamisol (1 mM) until the staining became visible, whereas the negative control staid clear. The reaction was stopped by rinsing the slides in PBS for 5 minutes. Sections were mounted with Aquamount (DAKO). Microscopy was done using a Zeiss Axioskop 2[+] equipped with an AxioCam HRc digital camera and the AxioVison 3.1 software (all from Zeiss).

2.9.3 Immunocytochemistry

For immunocytochemistry, 50.000 cells were seeded per well on poly-l-lysine-coated (0.01%, Sigma) glass coverslips in 4-well plates containing 500 μl culture medium (see 2.8.2.2). A2B5

ascitic fluid was added 1:400 to the living cells for 20 min. The cells were fixed after 1 h to avoid in vitro differentiation. After fixation in 3.8% PFA in PB (0.5% BSA in PBS) for 20 min at room temperature, cells were washed and 3% BSA in PB was added as blocking buffer for 30 min. Primary antibodies (A2B5, Mouse IgM, kindly provided by G. Rougon, 1:400; Calb2, Mouse IgG1, Sigma, 1:1000; GAD65/67, Rabbit, Sigma, 1:400; Polysialic acid (PSA) 735, Mouse IgG2a, kindly provided by R. Gerardy-Schahn, 1:400; TUJ1, Rabbit IgG, Covance, 1:2000) were diluted in blocking buffer and applied for 2 h at room temperature. After washing, the cells were incubated 1 h with secondary antibodies (Goat anti-mouse IgM Alexa 488, Molecular Probes/Invitrogen, 1:2000; Goat anti-mouse IgG Fc Cy3, Jackson ImmunoResearch Laboratories, 1:1000; Goat anti-rabbit IgG Cy5, Cambridgeshire, 1:800; Donkey anti-mouse IgG Cy3, Jackson, 1:400; Donkey anti-rabbit Cy3, Jackson, 1:400; Goat anti-mouse IgG Alexa 633, Molecular Probes, 1:1000; Goat anti-mouse IgM Alexa 633, Molecular Probes, 1:800). After application of secondary antibodies, the cells were washed twice for 10 min in PB, one time for 10 min in distilled water, air-dried and mounted with Fluorescence Mounting Medium (DAKO). Fluorescence microscopy was performed using an Axioplan 2 equipped with an ApoTome imaging module, an AxioCam MRc digital camera and the AxioVison 4.2 software (all from Zeiss).

2.9.4 Immunohistochemistry

For immunohistochemistry, 50 μm vibratome sections (see 2.9.1) were used. Staining was done on floating sections as described previously (Hack *et al.*, 2002). Briefly, sections were first incubated overnight at 4°C with primary antibodies (MenB against PSA, 1:250, provided by G. Rougon, Marseille, France; DCX, 1:200, Chemicon; Mash1, 1:200, Upstate) before incubation with the corresponding fluorescently labeled secondary antibody (Goat anti-guinea pig IgG Cy5, Abcam, 1:200; Goat anti mouse IgM Texas Red, Abcam 1:800; Goat anti-mouse IgG Fc Cy5, Jackson, 1:1000). Cell nuclei were stained with Hoechst 33258 and the samples were mounted with Fluorescence Mounting Medium (DAKO). Optical images were taken either using an Axioplan 2 equipped with an ApoTome or a LSM510 laser confocal scanning microscope (all from Zeiss).

2.10 Mouse breeding

Animals were maintained at a 12 h light-dark circle in an SPF animal facility. All protocols were in accordance to the German "Tierschutzgesetz". Experiments were partially performed at the IBDML (Marseille, France) in accordance to protocols approved by local authority guidelines.

Table 2.7 Mouse strains

Name	Strain background	Reference
CD1	Crl:CD1 (ICR)	Charles River Laboratories
Bl6	C57Bl/6 / 6NCrl	Charles River Laboratories
Balb/c	BALB/cAnNCrl	Charles River Laboratories
GAD67-GFP	GAD67-GFP (Δneo), C57Bl/6 / 6NCrl	Tamamaki *et al*., 2003
TH-GFP	TH/EGFP, C57Bl/6 / 6NCrl	Matsushita *et al*., 2002
Actin-GFP	TgN(GFPU)5Nagy, C57Bl/6 / 6NCrl	Hadjantonakis *et al*., 1998

Genotyping was done by PCR (see 2.6.3) using strain specific primers (see Tab. 2.8).

Table 2.8 Primers for genotyping

Strain	Forward primer	Reverse primer
GAD67-GFP	GCTGTGAGCCTCACTCGGAGC	TGCTCAGGTAGTGGTTGTCG
TH-GFP	AAGTTCATCTGCACCACCG	TGCTCAGGTAGTGGTTGTCG
Actin-GFP	AAGTTCATCTGCACCACCG	TGCTCAGGTAGTGGTTGTCG

3 Results

Part I: Molecular analysis of region-specific fore- and hindbrain GABAergic neuron subpopulations

GABAergic neurons are a diverse group of inhibitory neurons. Different subpopulations are present in all brain regions and several attempts have been made to categorize these subpopulations (Markram *et al.*, 2004). While some of these results allow for a valuable, detailed and partly functional description of different GABAergic neurons, they have not led to a systematic dichotomy. Whole genome gene expression profiling has emerged as a method for the molecular description of cell populations. Based on the expression of genes, an unambiguous and specific pattern is assigned to each cell type or cell stage. Besides the pure categorization of cell types, the interpretation of their specific expression pattern may also help to get an understanding of functional properties and to identify novel markers which can be used for their isolation. To analyze GABAergic neuron subpopulations on a molecular level, first of all a method to isolate the respective cells had to be established.

3.1 Analysis and isolation of GABAergic neurons by flow cytometry

So far, no surface markers suitable for the isolation of GABAergic neurons by FACS or MACS® have been described. However, GAD67-GFP mice express GFP under the control of the endogenous glutamate decarboxylase 67 isoform-promotor (Tamamaki *et al.*, 2003). A specific expression of GFP in all GABAergic neurons throughout the brain of this mouse strain was shown (Tamamaki *et al.*, 2003). To check the suitability of this model system for flow cytometric analysis and purification of GABAergic neurons, an appropriate method for the dissociation of brain tissue to a single cell suspension was established.

3.1.1 Dissociation and flow cytometric analysis of GABAergic neurons

Different protocols for an optimal dissociation of brain tissue yielding high recovery rates of viable and singularized neural cells were tested. The total number of cells per brain, the efficiency for removal of tissue clumps and the percentage of dead cells, measured by propidiumiodide (PI) staining (see 2.8.5), served as criteria. Several Trypsin and Papain concentrations in combination with mechanical dissociation and filtration by cell strainers of

different mesh diameters (Miltenyi Biotec) were assayed. At postnatal day 1, the best results were obtained with a Papain based enzyme mix (NTDK Papain, Miltenyi Biotec) at standard concentration in combination with a 30 µm cell strainer (data not shown). No additional loss of GFP$^+$ GABAergic cells was observed compared to cell strainers with higher mesh sizes. However, the use of cell strainers with higher mesh sizes, e.g. 50 or 70 µm, was less compatible with flow sorting, due to frequent plugging of the microfluidic parts inside the cytometer. Subsequent to the dissociation of either wild-type or GAD67-GFP postnatal day 1 mouse brains, flow cytometric analysis was used to determine the GFP-fluorescence signals of single cells (Fig. 3.1). Whereas cells isolated from wild-type mice showed no GFP-fluorescence, about 15.8% ($\Delta = 2.1\%$, n = 6) of the cells originated from GAD67-GFP mice were strongly GFP positive. The rate of dead cells, as identified by PI staining, was 2-3%.
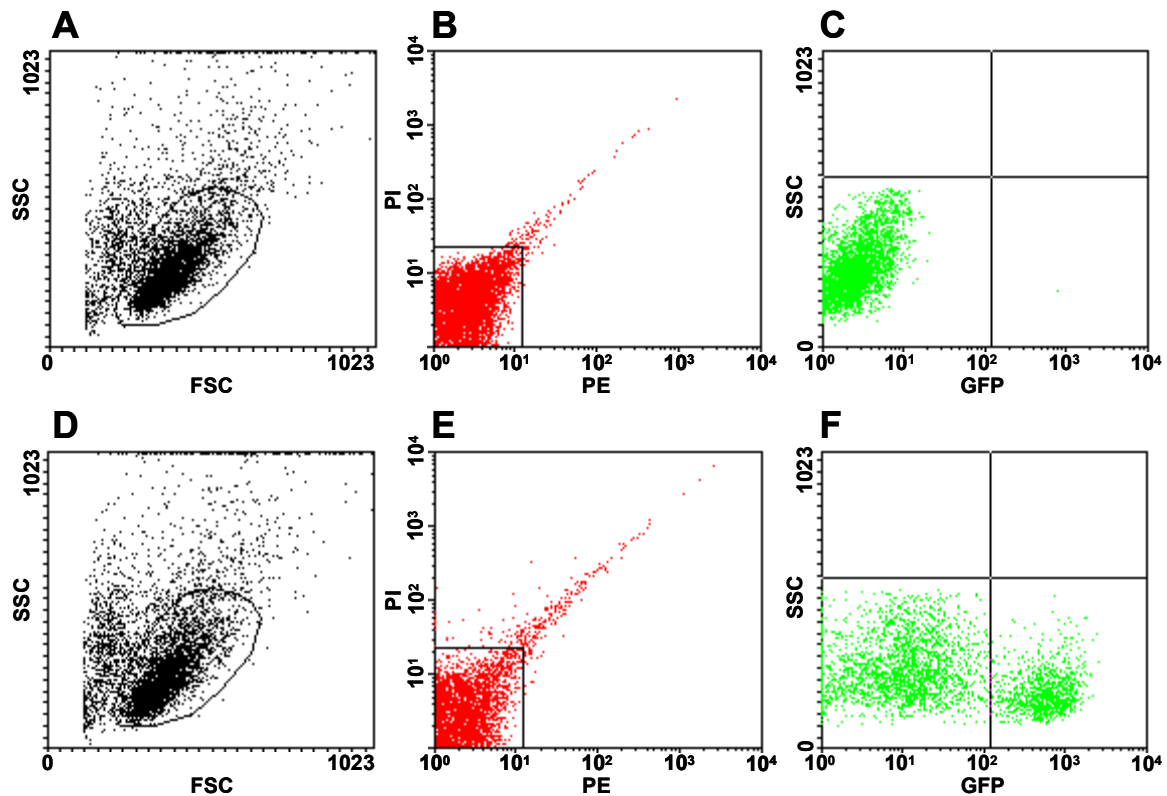
Figure 3.1: Flow cytometric analysis of dissociated brain tissue from GAD67-GFP mice

Brains of postnatal day 1 wild-type (A-C) or GAD67-GFP (D-F) mice were removed and dissociated to a single cell suspension. Flow cytometric analysis was used to determine the physical and fluorescent properties of each cell. Only events that were identified to have cell typical forward and side scatter properties (region in A and D) and showed low fluorescence in the PI channel (region in B and E) were considered as viable singularized cells and analyzed for their GFP expression (C and F). Cells isolated from wild-type mice showed no GFP fluorescence (C), whereas a subpopulation of cells (15.8%, $\Delta = 2.1\%$, n = 6) from GAD67-GFP mice was strongly GFP positive (G).

3.1.2 Quantification of GABAergic neurons from different brain regions

So far, the appearance of GABAergic neurons in distinct brain areas was analyzed mainly by immunohistochemistry (Kosaka and Kosaka, 2005). This method comprises several disadvantages like the time consuming staining procedures, inhomogeneous staining and the unequal distribution of marker proteins in distinct cell compartments, for example in the synaptic termini. It was reasoned that by using flow cytometry, it should be possible to investigate the regional distribution of GABAergic neurons at a much higher significance level, because higher cell numbers can be analyzed. To determine the proportion of GABAergic neurons in the major parts of the brain, tissue from olfactory bulb, cortex, striatum and cerebellum of twelve P1 old GAD67-GFP knock-in mice was dissected. Subsequently, tissues of two mice were pooled, dissociated enzymatically to a single cell suspension and analyzed by flow cytometry (Fig. 3.2). The number of EGFP-positive cells varied among different brain areas. The highest amount of positive cells was observed in the olfactory bulb with 58.8% ($\Delta = 3.2\%$, n = 6) reflecting that the largest population in the OB are inhibitory granule neurons. Striatal and cortical tissues contained 45.1% ($\Delta = 5.1\%$, n = 6) and 15.1% ($\Delta = 2.7\%$, n = 6) positive cells, respectively. The lowest number of GABAergic cells was found in the cerebellum (3.2%; $\Delta = 0.5\%$, n = 6).
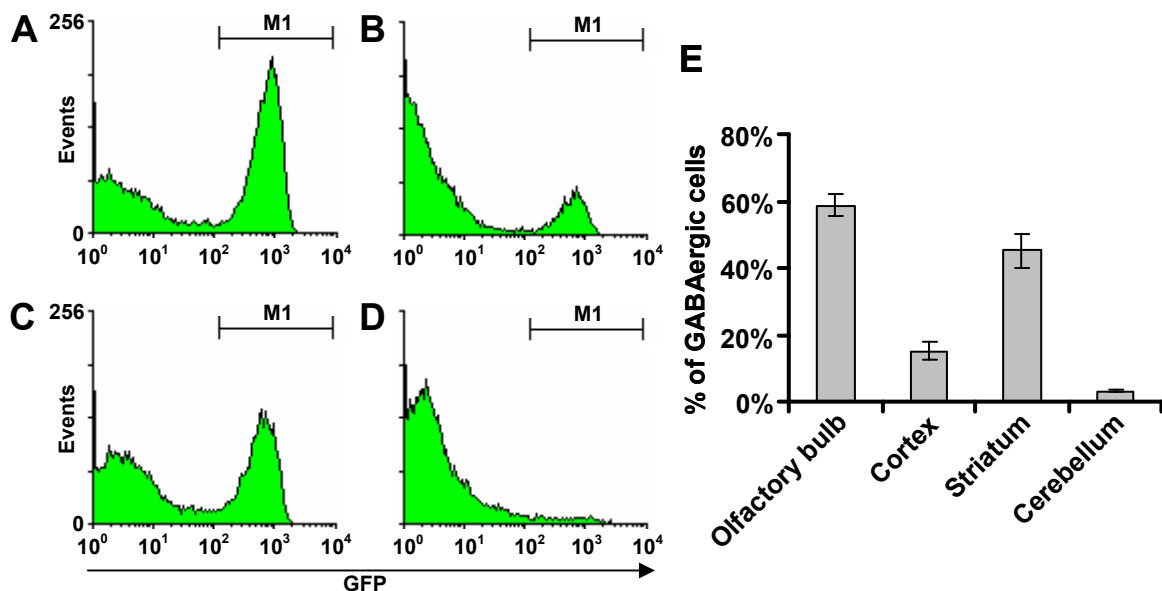
Figure 3.2: Quantification of GABAergic neurons among distinct brain areas
Flow cytometric analysis of GFP$^+$ cells in the olfactory bulb (A), the cortex (B), the striatum (C) the cerebellum (D) and subsequent quantification of positive cells (E). Error bars indicate the standard deviation of the mean value (n = 6 replicates from 12 mice).

3.1.3 Isolation of GABAergic neurons by FACS

Based on the results above, it was now tested whether it is also possible to purify GABAergic neurons by FACS (see 2.8.5). Cells of dissociated brains from postnatal day 1 old GAD67-GFP knock-in mice were sorted on a FACSVantage SE^{TM} cell sorter (Becton Dickinson) for their FSC (forward scatter), SSC (side scatter) and GFP (FL-1) signals. Background signals were defined by using dissociated brain cells from wild-type mice (C57Bl/6 / 6NCrl). Dead cells were excluded using PI. Each brain yielded around $1.0\text{-}1.2 \times 10^6$ GFP$^+$ GABAergic neurons with purity higher than 99% (Fig. 3.3). The rate of dead cells, as identified by PI staining, was again 2-3%. Aliquots of FACS purified cells were successfully cultivated for seven days. Neither extensive cell death nor loss of GFP fluorescence was observed, indicating that the procedure is not harmful to the cells (data not shown).
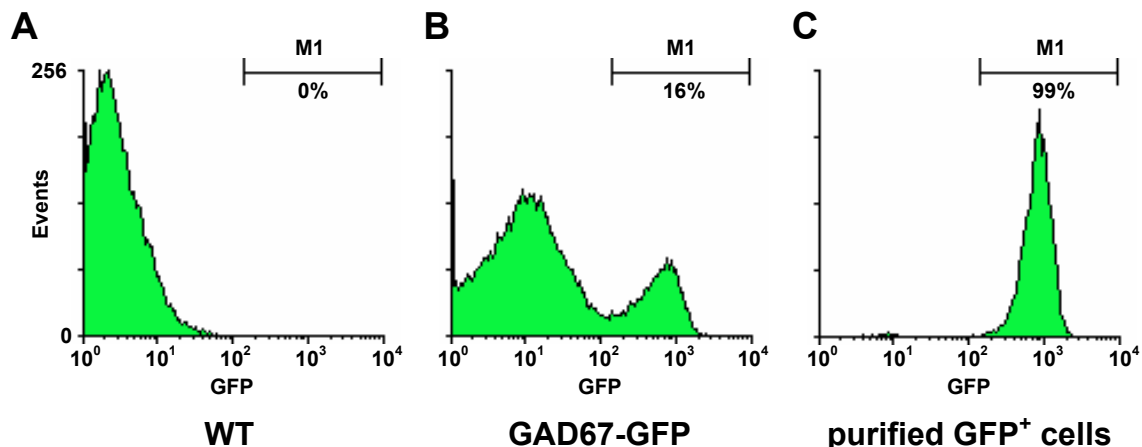
Figure 3.3: FACS purification of GABAergic neurons
Flow cytometric purification of GFP labeled GABAergic neurons. No background fluorescence was observed in cells from wild type mice (A), whereas in cells from GAD67-GFP mice a clear GFP$^+$ population could be identified (B). The purity of GFP$^+$ cells after sorting was above 99% (C).

3.2 Molecular analysis of GABAergic neurons

The possibility to obtain populations of highly pure GABAergic neurons allowed for the subsequent analysis of these cells on a molecular level. Whole genome gene expression profiling has emerged as a method for the description of cell types. The expression of thousands of genes allow for each cell type or cell stage to be assigned an unambiguous and specific pattern. Bioinformatic analyses offer the opportunity to quantify the relationship of individual cell populations by calculating correlation matrices. Moreover, by assessing

prominent transcription pathways, functional explanation of the observed differences can be given and new single gene markers can be identified. To analyze GABAergic neurons in general and the relationship of these cells among distinct brain regions, their gene expression profiles were assayed using Agilent whole mouse genome 44k microarrays (see 2.6.10 and Fig. 3.4).
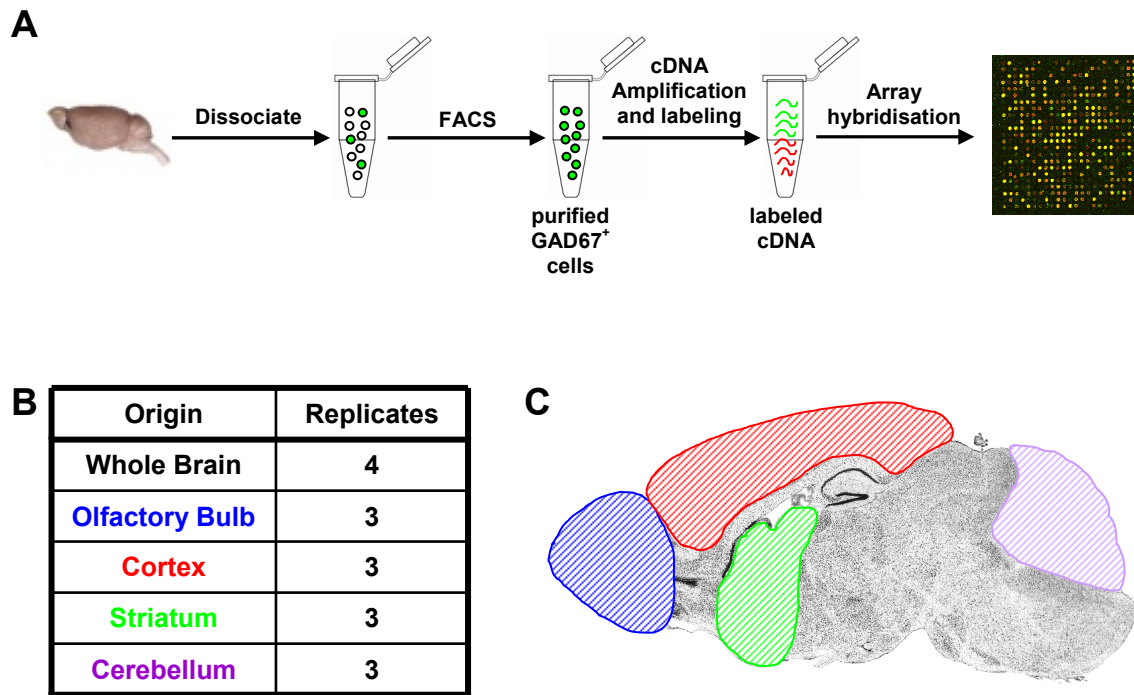
Figure 3.4: Experimental setup

(A) Scheme of the experimental setup for enzymatic dissociation of whole brains or brain areas from GAD67-GFP knock-in mice and purification of GFP^{+} cells by FACS. RNA of these cells was used to generate amplified cDNA, which was labeled with Cy5 in a Klenow reaction (red) and hybridized on Microarrays. Cy3 labeled cDNA (green) originated from whole brain mRNA served as a reference in all experiments. Furthermore, the number of replicates (B) and origin of the isolated cells (C) are indicated.

The yield of purified GABAergic neurons, especially of those isolated from the cerebellum, was too low for conventional RNA amplification techniques. To gain and compare results from all subpopulations, a method for rare cell gene expression profiling had to be established. Accordingly, a protocol for sensitive gene expression profiling, originally established for the analysis of blood cells (Appay *et al.*, 2007; Auffray *et al.*, 2007), was adapted for FACS purified neuronal cells (see 2.6.10). The protocol was validated by flow cytometric sorting and rare cell gene expression of 1881- and Jurkat cells (see 2.8.2.1). The

results matched with those of conventional gene expression profiling as well as those of cells which were not FACS purified (data not shown).

Directly after flow cytometric sorting, 10000 cells per experiment were lysed in SuperAmp Lysis Buffer and stored at -20°C until RNA extraction and amplification. For quality control, capillary chromatography of total RNA, isolated from FACS purified GABAergic neurons, was performed, revealing no signs of degradation (Fig. 3.5). Microarray analyses of GABAergic neurons isolated from either whole brain (n = 4), olfactory bulb (n = 3), cortex (n = 3), striatum (n = 3) or cerebellum (n = 3) was performed, amounting to a total of 16 array data sets (Fig. 3.4 B and C). Global PCR amplification of mRNA from 10000 flow sorted GFP positive cells yielded 2.5-3.5 µg cDNA. 250 ng of cDNA was labeled and hybridized on Agilent whole mouse genome 44k microarrays (see 2.6.10). RNA isolated from wild type mice whole brains (n = 4) at postnatal day 1 was amplified in the same way and served as a common reference for all hybridizations. Correlation coefficients of independent replicates ranged from 0.90 to 0.97, demonstrating high reproducibility. The Gene Expression Omnibus (GEO) series entry GSE8984 provides access to all data from this analysis (http://www.ncbi.nlm.nih.gov/projects/geo/). Furthermore, supplementary files are available for download by FTP (File Transfer Protocol) using the series accession number at ftp://ftp.ncbi.nih.gov/pub/geo/DATA/supplementary/series/.
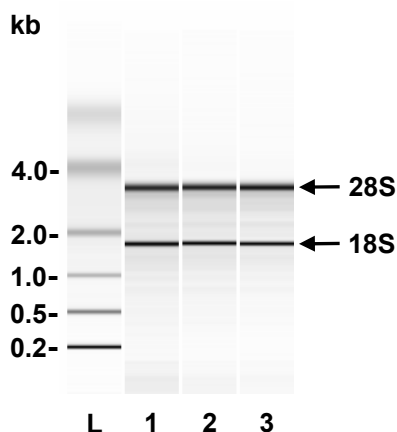
Figure 3.5: Quality control of isolated total RNA after FACS purification

For quality control, capillary chromatography of total RNA, isolated from FACS purified GABAergic neurons, was performed. No sign of degradation was observed. RINs (RNA Integrity Numbers) were between 7.8 and 8.7. Samples 1 to 3 show representative examples. The two major bands represent the 18S and 28S ribosomal RNA. The RNA ladder (L) spans 0.2-4.0 kb.

3.2.1 Global gene expression of GABAergic neurons

The primary goal was to analyze similarities in gene expression of all subpopulations and thereby define a general genomic signature of GABAergic neurons. Factors involved in the late differentiation and functionality of these cells as well as new marker genes, also with a focus on cell surface proteins, should be identified. The general approach was validated by assessing the gene expression results of known marker genes (Fig 3.6). As expected, mRNAs encoding the two key enzymes for GABA synthesis, GAD67 (GAD1) and GAD65 (GAD2), were strongly enriched in purified GABAergic neurons compared to the whole brain reference. Furthermore, the vesicular inhibitory amino acid transporter (VIAAT), responsible for the transport of GABA into synaptic vesicles, was enriched, whereas mRNA for the glutamate transporter SLC1A4 was not. TH, a marker for catecholaminergic neurons, showed decreased expression. Consistently, established markers of glial cells, like GFAP, GLT1 (SLC1A2), GLAST (SLC1A3), OLIG1, OLIG2, VIM, CD44 and PLP were decreased in GABAergic neurons.

Taken together, the expression of known neuronal and glial marker genes matched with the purification of GABAergic neurons.
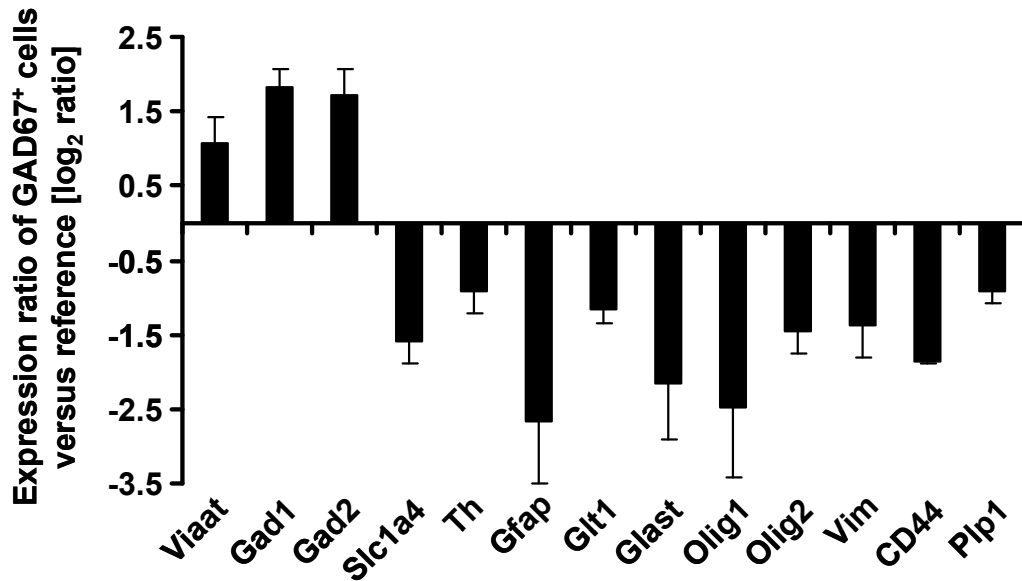
Figure 3.6: Expression analysis of known marker genes

The expression of known marker genes was analyzed to validate the microarray experiments. GAD1 (GAD67), GAD2 (GAD65) and VIAAT served as markers for GABAergic neurons and showed enriched expression. Markers for other neuronal cell types, like the glutamate transporter SLC1A4 and TH, a marker for catecholaminergic neurons, showed decreased expression. Also established markers of glial cells, like GFAP, GLT1 (SLC1A2), GLAST (SLC1A3), OLIG1, OLIG2, VIM, CD44 and PLP were decreased in GABAergic neurons. Expression values were calculated as normalized $\log_2$ ratios. Error bars indicate the standard deviation of the mean value (n = 16).

To analyze if there was a bias towards genes of specific functional classes in the fraction of transcripts showing increased or decreased expression, a Gene Ontology (GO) analysis was carried out. The 550 strongest enriched genes in GABAergic neurons of all origins or the whole brain reference were sorted according to their functional classes as defined by the Gene Ontology database (Fig. 3.7). The functional classes "Cell proliferation/differentiation" and "Cell adhesion/skeleton" were significantly over-represented in GABAergic neurons, indicating a lower developmental stage compared to other brain cells. In contrast, genes which are important for general metabolism were enriched in the whole brain reference. Additionally, genes coding for different receptors were predominantly found in the whole brain reference fraction, reflecting the larger receptor diversity among different cell types compared to GABAergic neurons.
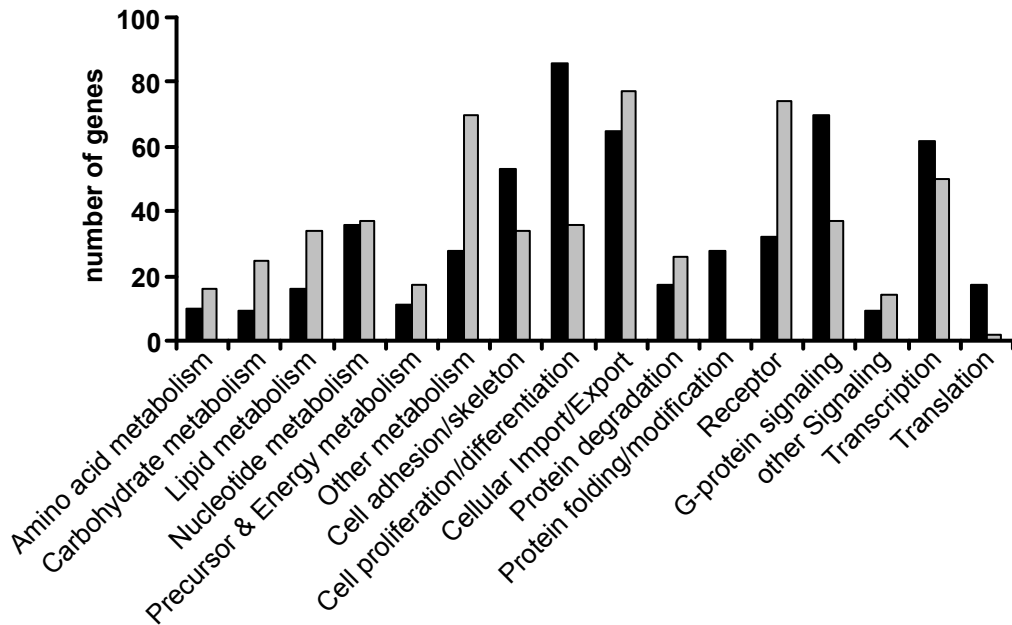
Figure 3.7: Grouping of genes according to Gene Ontology

Grouping of genes enriched in GABAergic neurons compared to whole brain enriched genes. The 550 strongest enriched genes in GABAergic neurons of all origins (black) or the whole brain reference (grey) were sorted according to their functional classes as defined by the Gene Ontology (GO) database. The absolute number of genes per GO class is depicted. The functional classes "Cell proliferation/differentiation" and "Cell adhesion/skeleton" were significantly over-represented in GABAergic neurons, whereas more genes which are important for general metabolism as well as genes coding for different receptors were found to be enriched in the whole brain reference.

To identify the transcripts most significantly expressed in all GABAergic neuron subtypes, the data was filtered for probes showing more than 3-fold higher signals in GABAergic cells than in the total brain reference in at least 14 of the 16 experiments. Using these criteria, an over-representation of genes expressed in the cortex and striatum, which are the regions containing the major part of GABAergic neurons in the brain, was avoided. The 55 targets which were identified and could be unambiguously annotated to characterized genes are listed in table 3.1.

Table 3.1: Genes enriched in GABAergic neurons

Gene name	GeneBank	ratio	SD	Gene Ontology annotation
Chd7	AK042727	**3.5**	0.2	
Fos	NM_010234	**5.7**	0.3	
Hoxa1	NM_010449	**4.2**	0.4	
LOC432637	NM_001004167	**6.4**	0.8	
Mkx	NM_177595	**3.5**	0.2	
Mll3	AY138582	**5.9**	0.7	Transcription
Myst4	AK129129	**13.8**	1.4	
Pcgf3	AK033609	**6.5**	0.5	
Phf21b	BC067021	**18.9**	1.6	
Sox7	NM_011446	**7.1**	1.0	
Zfpn1a2	NM_011770	**4.0**	0.5	
Angptl2	AK011976	**11.7**	1.2	
CD72	AF543214	**6.5**	1.0	
Cd84	NM_013489	**3.8**	0.2	
Eps15-rs	BC015259	**4.9**	0.5	
Ifitm5	NM_053088	**5.8**	1.2	Receptor signaling
Ncr1	NM_010746	**5.7**	0.4	
Prlpc2	NM_023332	**3.4**	0.4	
Tnfsf5	NM_011616	**6.1**	0.4	
Trip11	AK077954	**3.4**	0.2	
Wisp1	NM_018865	**5.3**	0.8	
Fpr-rs4	NM_008041	**5.1**	0.7	
Olfr1052	NM_147010	**4.1**	0.4	
Olfr1269	NM_146342	**6.3**	0.3	
Olfr560	NM_147113	**5.8**	1.4	
Olfr672	NM_146760	**13.2**	4.1	G-protein signaling
Olfr700	NM_146600	**4.8**	0.6	
Olfr849	NM_146527	**6.7**	0.3	
V1rc30	NM_134185	**7.8**	0.9	
Gria2	BC048248	**3.3**	1.0	
Slc34a1	NM_011392	**6.3**	0.8	Cellular import/export
Tnpo3	AK049446	**7.2**	0.3	
Klk9	NM_010116	**3.3**	0.1	
Kng2	NM_201375	**4.6**	0.4	Protein degradation
Usp49	AK019130	**8.6**	1.0	
2900006B13Rik	AK085984	**5.4**	0.6	
Fgb	NM_181849	**5.1**	0.4	Other metabolism
Saps2	AK083335	**3.5**	0.6	
Hamp	NM_032541	**11.9**	2.6	Metal ion homeostasis
Zswim6	BC021311	**3.7**	0.1	
Adipor2	AK046591	**5.8**	1.4	Lipid metabolism
Pla2g4b	BC042758	**6.4**	1.0	
C330018K18Rik	NM_177352	**7.1**	1.7	Carbohydrate metabolism
Gp1ba	NM_010326	**3.8**	0.3	Cell adhesion
Crkl	BC023080	**6.6**	1.1	Cell cycle
Eml5	AK047762	**3.4**	0.4	Cytoskeleton
Gad1	AK054554	**3.3**	1.1	Neurotransmitter metabolism
Adarb2	NM_052977	**4.4**	0.3	Nucleotide metabolism
Gpx5	NM_010343	**3.7**	0.3	Response to oxidative stress
Trspap1	BC055454	**4.4**	0.3	Translation

Table 3.1: continued

Gene name	GeneBank	ratio	SD	Gene Ontology annotation
1700081L11Rik	BC053389	**4.7**	0.4	
2810403A07Rik	AK038617	**3.8**	0.6	
2810407A14Rik	NM_175156	**12.1**	1.4	
5330439B14Rik	NM_177314	**5.1**	1.2	
6430706D22RIK	BC004768	**4.2**	0.1	
A430057M04Rik	NM_176925	**4.9**	0.7	
AK040702	AK040702	**5.1**	0.4	Unknown
B230325K18Rik	NM_176936	**4.4**	0.6	
C130023O10Rik	NM_177110	**14.5**	0.8	
LOC385154	AK041326	**3.5**	0.2	
LOC544848	AK032716	**5.1**	0.6	
Speer4f	NM_027609	**6.2**	0.2	
Sprrl9	NM_026335	**8.9**	0.5	

List of genes which were >3-fold enriched in GABAergic cells versus whole brain in at least 14 of 16 experiments. The mean expression ratios of 4 independent experiments using whole brain GABAergic cells are shown. The genes are sorted according to their Gene Ontology annotations. Abbreviations: SD = standard deviation of the mean value

The transcriptional regulator MYST4 (Qkf, Querkopf), which was shown to be required for the development of forebrain interneurons, was one of the strongest overrepresented genes (Thomas *et al.*, 2000). Furthermore, the homeobox transcription factor HOXA7, which has been implicated in neural tube formation in Xenopus (Wright *et al.*, 1989), was strongly represented, as were SOX7 and the signaling protein WISP1 which both interfere with WNT signaling (Takash *et al.*, 2001). High expression of RNA-editing molecules like ADARB2 and SECP43 was found. ADARB2 is a double-stranded RNA adenosine deaminase that has been suggested to edit defined brain-specific transcripts. It is considered to be a candidate for involvement in genetic forms of epilepsy (Melcher *et al.*, 1996; Mittaz *et al.*, 1997). Interestingly, the highly expressed cytoplasmatic protein CRKL complexes with the adaptor protein Dab1 (Chen *et al.*, 2004), pointing towards an activity of the reelin signaling pathway in interneurons. This suggests that several of the here isolated neurons are still migratory. In addition to the described genes, many uncharacterized genes and EST-sequences were found to be enriched.

In a second round of data filtering, less stringent criteria were applied by focusing on genes which were enriched in GABAergic neurons in at least 12 of the 16 experiments. In this approach, further genes belonging to the GO-groups "cytoskeleton" (e.g. MTAP4, EHD2, CAPZA2, PPFIA1, MOBKL1A, MTSS1), "RNA-processing" and "RNA-editing" (e.g. SFRS3, PDCD11, THOC1, THOC2, GLE1L, CSDE1, SRPK2), "neuron development" (e.g. PTCK3, MYT1, SOX11, LOXL2, SNAP91, POGZ) and "protein-glycosylation" (e.g. GALNT11, B3GALT2) were identified.

In conclusion, a specific genetic signature representative for all major populations of GABAergic neurons was generated and considerable amounts of candidate factors maybe involved in the generation and regulation of these cell populations were identified.

3.2.2 General differences among distinct brain regions

After defining the global transcriptome of GABAergic neurons, the gene expression profiles of cortical, striatal, olfactory bulb and cerebellar interneurons were compared by calculating Pearson correlation coefficients of pairwise comparisons. Unsupervised hierarchical clustering of correlation coefficients most strikingly grouped the regions of the forebrain, olfactory bulb, cortex and striatum, together but separated them from the cerebellum (Fig. 3.8 A). Furthermore, replicates for each brain area clustered together, indicating a specific expression profile, which differs from other parts of the brain. Within the forebrain regions, there was a subgrouping of striatal and cortical interneurons pointing towards a closer relationship among these populations compared to the olfactory bulb. This observation was supported by the fact that 31% of all genes which were at least 4-fold enriched in the olfactory bulb were found to be overexpressed in this area only. In contrast, in cortex (11%) and striatum (3%) considerably smaller amounts of genes showed an exclusive expression. In general, only 155 of 2104 (7%) enriched genes were present in all areas, indicating that each subgroup displays a unique expression pattern. (Fig. 3.8 B).

In summary, the approaches applied in this study identified minor differences among GABAergic neurons from distinct forebrain regions but major differences between fore- and hindbrain GABAergic neurons.
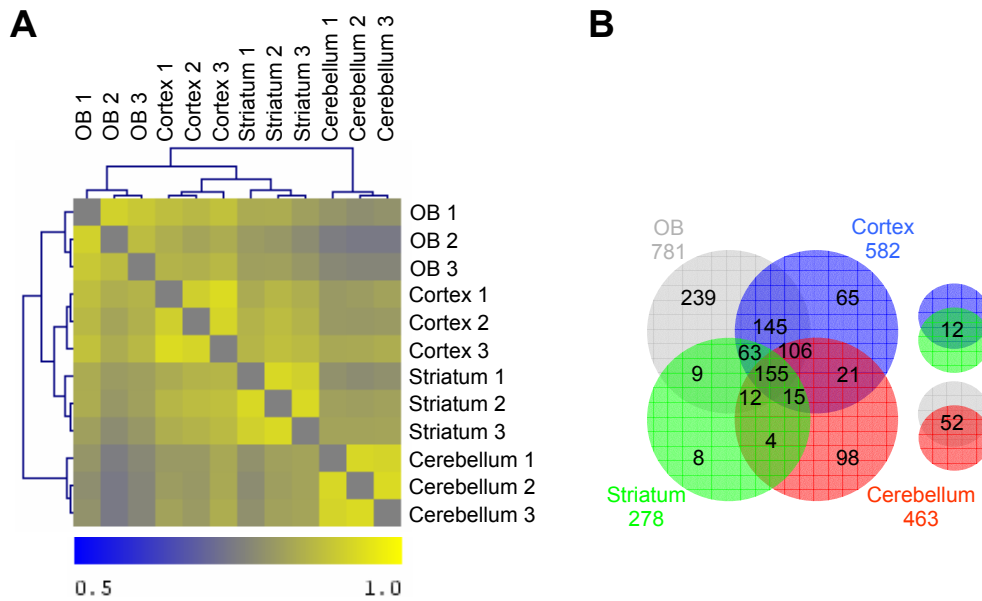
Figure 3.8: Correlation analysis

(A) Correlation matrix showing the relationship of gene expression profiles in all experiments. The matrix was generated by unsupervised hierarchical clustering of global expression data. Correlation coefficients are indicated by their color from blue (0.5) to yellow (1.0). Replicates for each brain area clustered together, indicating a specific expression profile, which differs from other parts of the brain. Groups belonging to the forebrain subclustered together and displayed the most significant differences compared to the cerebellum, which is part of the hindbrain. (B) Venn diagram showing shared and unique expression of genes enriched in GABAergic neurons from different brain areas. Focusing on the most important differentially expressed genes, only transcripts with at least 4-fold enrichment compared to whole-brain reference in any of the cell groups were selected. Only 155 of 2104 (7%) genes were enriched in all areas, indicating that each subgroup displays a unique expression pattern. Abbreviations: OB = olfactory bulb

3.2.3 Differential gene expression reflects distinct functions of GABAergic neurons in specific forebrain regions

After this general statistical classification of the global relationship between GABAergic cells from different brain areas, it was analyzed, which genes were specifically expressed in selected forebrain regions. To this end, discriminatory gene analysis using two class unpaired SAM (Serial Analysis of Microarrays) with at least 100 permutations per analysis (Tusher *et al.*, 2001) was performed. The brain region of interest was compared to the group of all remaining areas. Delta value was always chosen to result in 0% median number of false significant genes (see 2.6.10.4).

The first evaluation focused on genes specifically expressed in the cortex. Using the above criteria only 5 genes were found that were significantly higher represented in the cortex than in all other brain regions, while 62 were expressed at lower levels. Most of these genes were either functionally uncharacterized or not reported in relation to brain function (Fig. 3.9 A-C). The rather low number of cortex GABAergic neuron specific genes may reflect the high number of different interneuron subpopulations in this area, which maybe suppresses the identification of differently expressed genes in distinct subpopulations.

Next, SAM for olfactory bulb GABAergic neurons led to 272 genes with increased and 265 with decreased expression compared to other brain regions. Gene Ontology analysis of these genes using TreeRanker (Schacherer, F., unpublished) at a significance level of 0.005 identified enrichment of the GO groups "Development" and "Pattern". Within the genes showing strongest enrichment in this structure, FGF2 and FGF2-receptor as well as PIK3R1 and ROBO2 were found (Fig. 3.9 D and E). The high expression of these migration and differentiation associated genes, as well as the relatively low abundance of the differentiation correlated gene ATBF1 (Fig. 3.9 F), is in good agreement with the continuously ongoing neurogenesis in the olfactory bulb.

In striatal cells, the expression of 111 genes was increased compared to other brain regions, while not a single gene was found to be notably decreased. GO annotation identified a significant enrichment of genes belonging to the GO-groups "Extracellular region", "Extracellular space", "Signal", "Secreted", "Glycoprotein" and "Morphogenesis".

The significant enrichment of differently regulated genes (Fig. 3.9 G and H) with an impact on morphogenesis correlates with the specific connectivity and function of GABAergic neurons in the striatum. In contrast to other forebrain regions, where GABAergic neurons are generally found as local projecting interneurons, they represent almost exclusively projection neurons in the striatum. Factors regulating cell-cell and cell-matrix adhesion, like CSF1, LAMA1 and EDG1 (Matter and Laurie, 1994; Paik *et al.*, 2004; Yang *et al.*, 2006), were highly expressed. The same was true for transcription factors, either implicated in long-range axonogenesis in corticospinal motor neurons (BCL11B), in the regulation of cytoskeletal organization (FOXJ1) or in cell migration (TITF1) (Arlotta *et al.*, 2005; Gomperts *et al.*, 2004; Pan *et al.*, 2007).
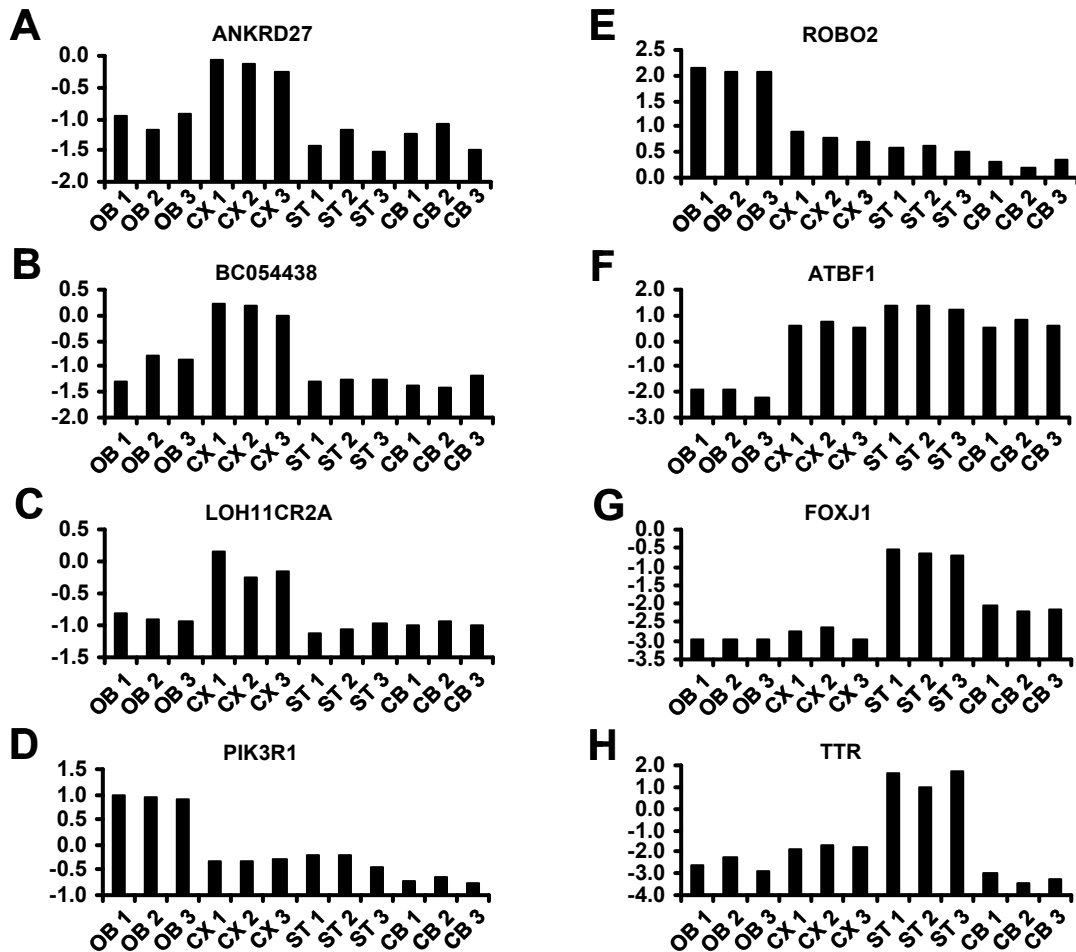
Figure 3.9: Expression ratios of selected genes identified by discriminatory gene analysis (DGA) for forebrain GABAergic neuron populations

The expression values of selected genes, identified by DGA to be differently enriched in a distinct brain region compared to all others, are depicted. ANKRD27 (A), BC054438 (B) and LOH11CR2A (C) were found to be differentially expressed in the cortex, PIK3R1 (D), ROBO2 (E) and ATBF1 (F) in the olfactory bulb, and FOXJ1 (G) as well as TTR (H) in the striatum. The columns represent the $\log_2$-transformed expression ratios for each replicate. Abbreviations: OB1-3 = olfactory bulb replicates 1-3; ST1-3 = striatum replicates 1-3; CX1-3 = cortex replicates 1-3; CB1-3 = cerebellum replicates 1-3

Finally, pathway analysis of genes enriched in the striatum and not related to morphogenesis led to the identification of a large number of genes interacting directly or indirectly with IGF2 (Fig. 3.10). This gene, as well as some of its interaction partners, has been implicated in the development of Huntington's disease, a neurodegenerative disorder that affects primarily striatal GABAergic neurons.
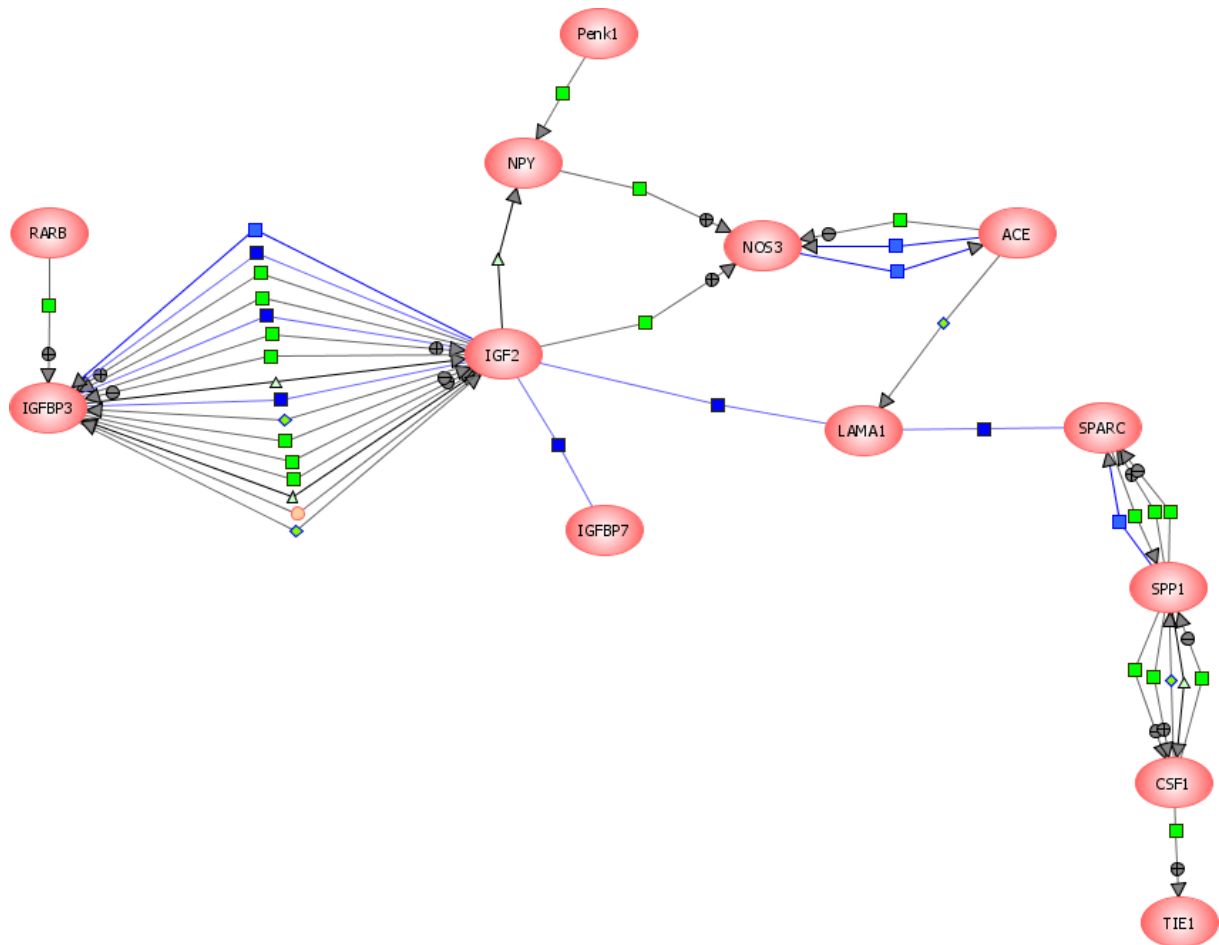
Figure 3.10: Pathway analysis for genes enriched in striatal GABAergic neurons

A network of genes, interacting directly or indirectly with IGF2, that where identified to be significantly enriched in striatal GABAergic neurons compared to populations of other brain regions, is depicted. The molecular network was generated using the PathwayArchitect software. Only manually validated interactions where taken into consideration. Interaction legend: light blue square = expression; dark blue square = binding; green square = regulation; rotated square = metabolism; circle = protein modification; triangle = transport

3.2.4 Comparison of fore and hindbrain GABAergic neurons

As mentioned above, hierarchical clustering demonstrated a grouping of forebrain versus hindbrain GABAergic neurons. The genes showing aberrant expression were analyzed in more detail. Differential gene analysis of GABAergic neurons from the cerebellum versus the three forebrain regions led to the identification of many transcripts showing increased or decreased expression levels compared to the other group. 241 genes were significantly enriched in forebrain GABAergic neurons. In contrast, 269 genes were expressed notably higher in the cerebellar population than in those of the forebrain. Subsequent GO analysis

revealed many candidates, involved in the development, migration and differentiation of neuronal cells. Expression patterns of these candidates are depicted in figure 3.11.
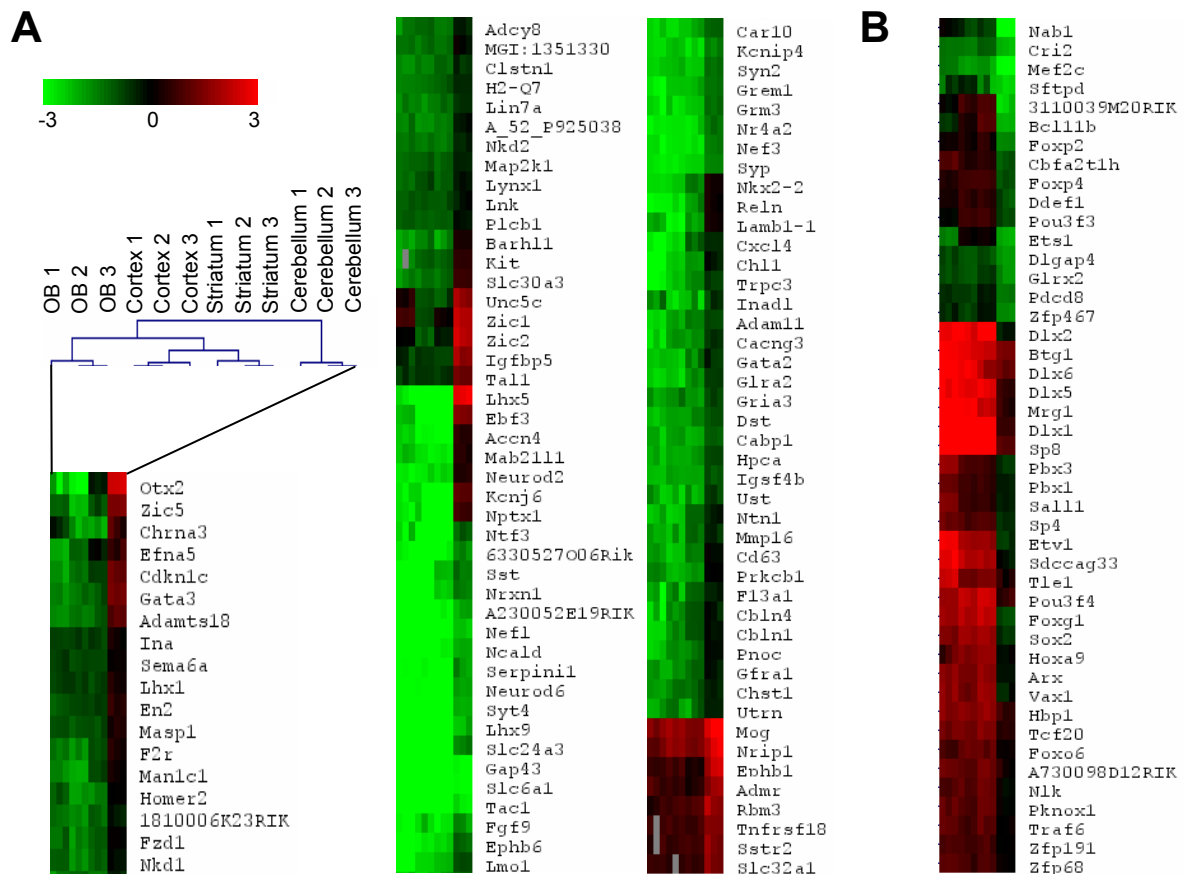
Figure 3.11: Cluster analysis

Cluster analysis of genes identified by discriminatory gene analysis of GABAergic neurons from the cerebellum compared to those of the forebrain. Discriminatory gene analysis (DGA) was done by the SAM (Serial Analysis of Microarrays) algorithm using the Tusher *et al.* method (Tusher *et al.*, 2001). Resulting genes and samples were grouped by similarities in gene expression patterns using two-dimensional hierarchical clustering (Pearson correlation, average linkage). Levels of log$_2$-transformed expression ratios are indicated from -3 (green) to 3 (red). (A) Genes identified by DGA show higher expression levels in GABAergic cells of the cerebellum compared to the forebrain. (B) Genes identified by DGA are highly expressed in GABAergic cells of the forebrain compared to the cerebellum. Abbreviations: OB = olfactory bulb

GO annotation of the 241 genes, enriched in forebrain GABAergic neurons, identified groups connected to the regulation of transcription with a strong bias towards homeobox transcription factors. Subsequent pathway analysis revealed three main groups. First, a group connected to the Distal-less-family (DLX) comprising DLX1, DLX2, DLX5 and DLX6, ARX, MSX3 and VAX1 (Fig. 3.12 A and B). Such genes are well known regulators of GABAergic

differentiation in the forebrain (He *et al.*, 2001). Second, transcripts linked to POU-transcription factors were identified which have been involved in the regulation of cortical neuron migration by interfering with Cdk5/Reelin signaling (McEvilly *et al.*, 2002). Third, the ETS and forkhead box-family members ETS1, ETV1, FOXG1, FOXO6, FOXP2 and FOXP4, as well as MRG1, PBX1 and PBX3 are connected to this group (Fig. 3.12 C and D). These transcriptional regulators play an important role in brain development from zebrafish to humans (Hoekman *et al.*, 2006; Shah *et al.*, 2006; Wijchers *et al.*, 2006).
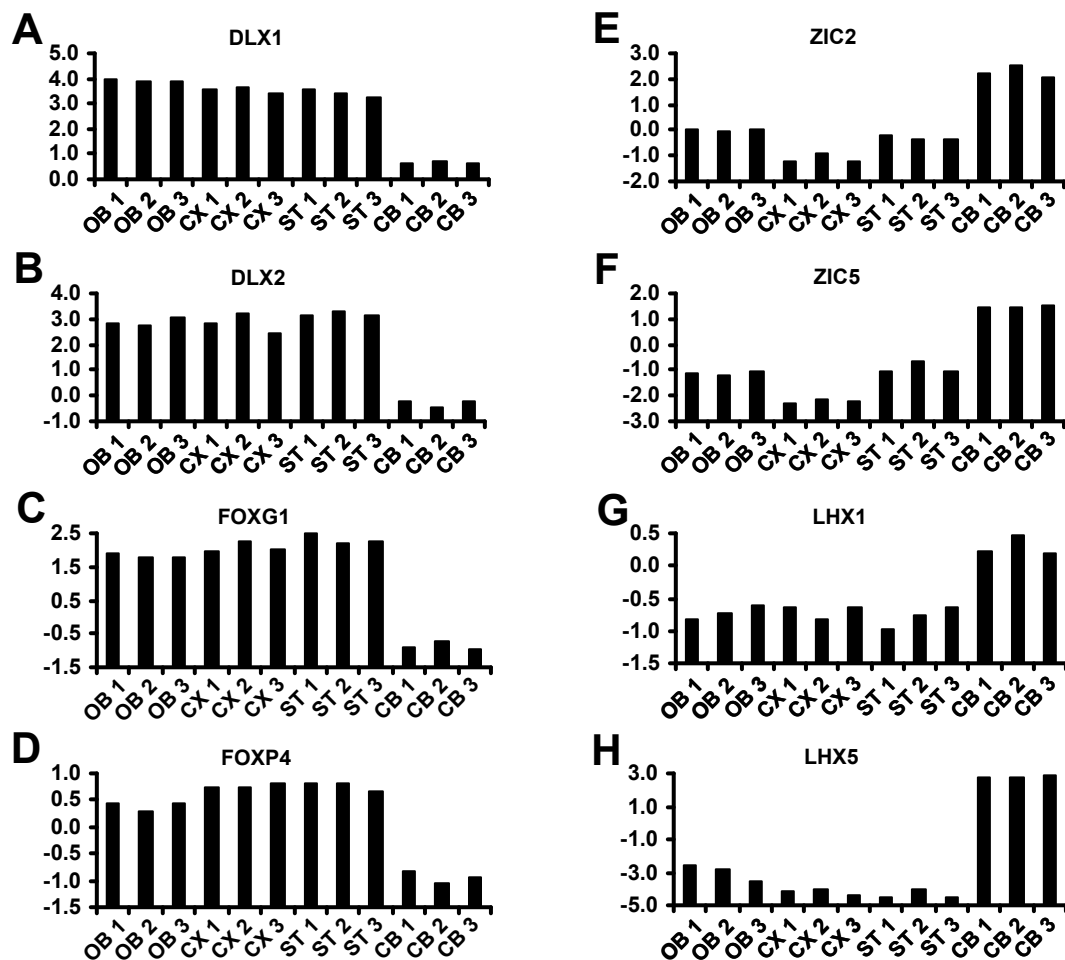
Figure 3.12: Expression ratios of selected genes identified by discriminatory gene analysis (DGA) for hindbrain GABAergic neuron populations

The expression values of selected genes, identified by DGA to be differently enriched specifically in either fore- or hindbrain populations are depicted. The expression of DLX1 (A), DLX2 (B), FOXG1 (C) and FOXP4 (D) was decreased in GABAergic neurons of the cerebellum compared to forebrain GABAergic neuron populations. In contrast, ZIC2 (E), ZIC5 (F), LHX1 (G) and LHX5 (H) were found to be differentially overrepresented in cerebellar GABAergic neurons. The columns represent the $\log_2$-transformed expression ratios for each replicate. Abbreviations: OB1-3 = olfactory bulb replicates 1-3; ST1-3 = striatum replicates 1-3; CX1-3 = cortex replicates 1-3; CB1-3 = cerebellum replicates 1-3

GO-annotation of the 269 genes, expressed notably higher in cerebellar cells than in cells of the forebrain, led to a significant higher representation of the groups "Nervous System Development", "Neuron Differentiation", "Cell Migration", "Cell-Cell Signaling", "Synaptic Transmission" and "Calcium Ion Binding". Pathway analysis displayed striking interactions either associated with homeobox transcription factors or with the Somatostatin (SST) pathway (Fig. 3.13). Expression of three transcription factors of the Zinc-finger protein of the cerebellum-family (ZIC1, ZIC2 and ZIC5), shown to be important for cerebellar development (Titomanlio *et al.*, 2005), was increased in the cerebellum but decreased in the forebrain (Fig. 3.12 E and F). Similarly, the LIM homeobox-family members LHX1, LHX5 and LHX9 were enriched (Fig. 3.12 G and H). The second group of strongly interacting genes found in the pathway analysis were SST receptors 1 and 2, as well as several related genes, including MATH-2 (NeuroD6), EPHB1, CDKN1C, NEF3 and NEFL (Fig. 3.13).

In conclusion, the comprehensive comparison of fore- and hindbrain GABAergic neurons suggests different transcriptional pathways used in these compartments to generate neurons with the same neurotransmitter phenotype.
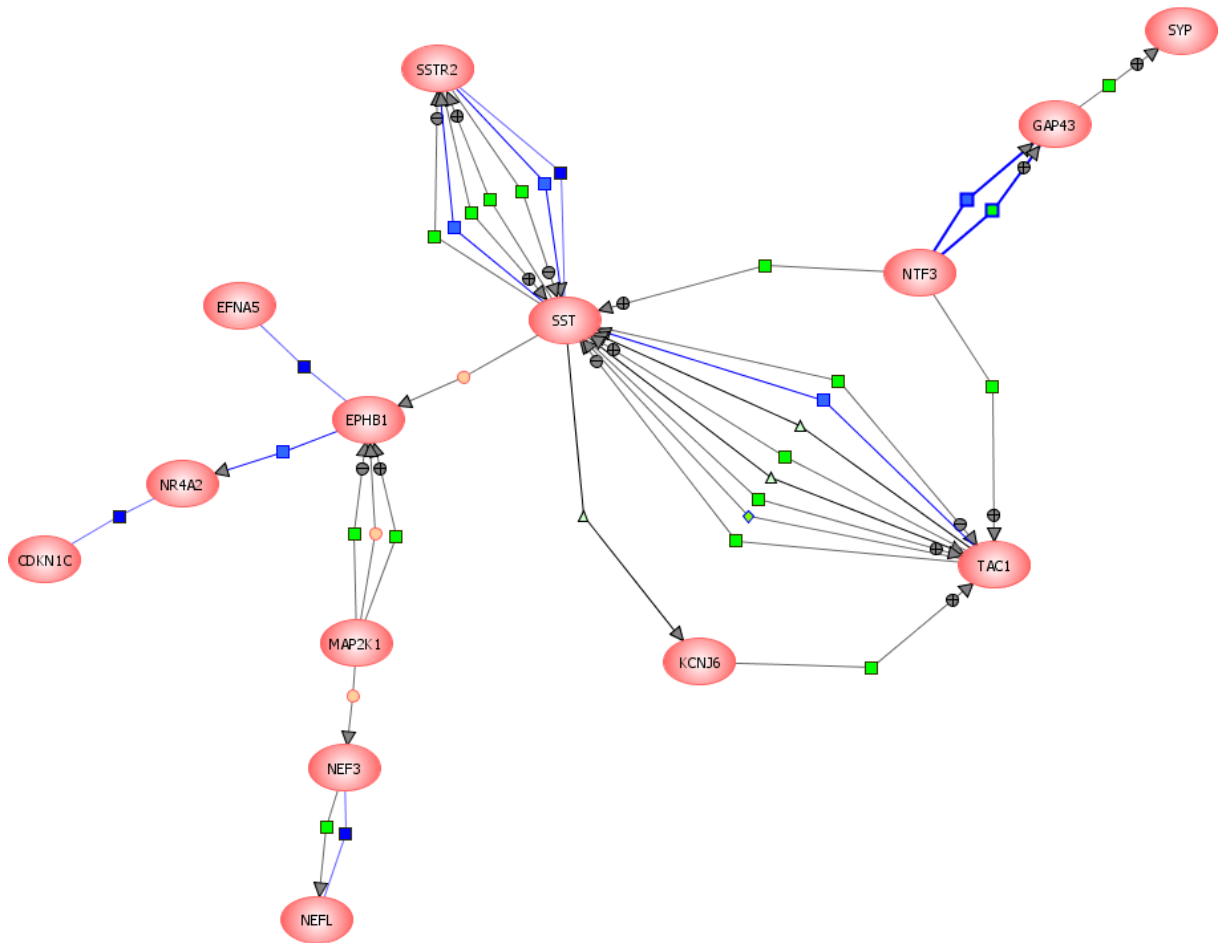
Figure 3.13: Pathway analysis for genes enriched in cerebellar GABAergic neurons

A network of genes, interacting directly or indirectly with the Somatostatin (SST) pathway that where identified to be significantly enriched in cerebellar GABAergic neurons compared to populations of the forebrain, is depicted. The molecular network was generated using the PathwayArchitect software. Only manually validated interactions where taken into consideration. Interaction legend: light blue square = expression; dark blue square = binding; green square = regulation; rotated square = metabolism; circle = protein modification; triangle = transport

3.2.5 Expression analysis of selected GABAergic neuron specific genes by *in situ* hybridization and quantitative real-time PCR

A general technical validation of the method used in this study, including flow cytometric sorting and rare cell gene expression profiling, e.g. by qPCR has been described before in detail (Appay *et al.*, 2007). As a biological validation of the results described above and for confirmation of newly identified marker genes of GABAergic neurons, *in situ* hybridization (see 2.9.2) was used as it represents an mRNA-amplification independent approach. The cell-type dependent expression patterns within functionally distinct regions for eleven selected

genes (GAD65, GAD67, K19, GATA4, FOS, GRIK3, WISP1, GPX5, ADARB2, CD72 and CD84) that showed enriched expression in GABAergic neurons were investigated. *In situ* hybridization patterns in postnatal day 1 old mice were compared to the GFP fluorescence of respective sections from GAD67-GFP knock-in mice. *In situ* hybridizations using a probe for GAD67 mRNA served as additional positive control (Fig. 3.14). Furthermore, we assessed the gene expression in adult mice by referring to the Allan Brain Atlas (Lein *et al.*, 2007).
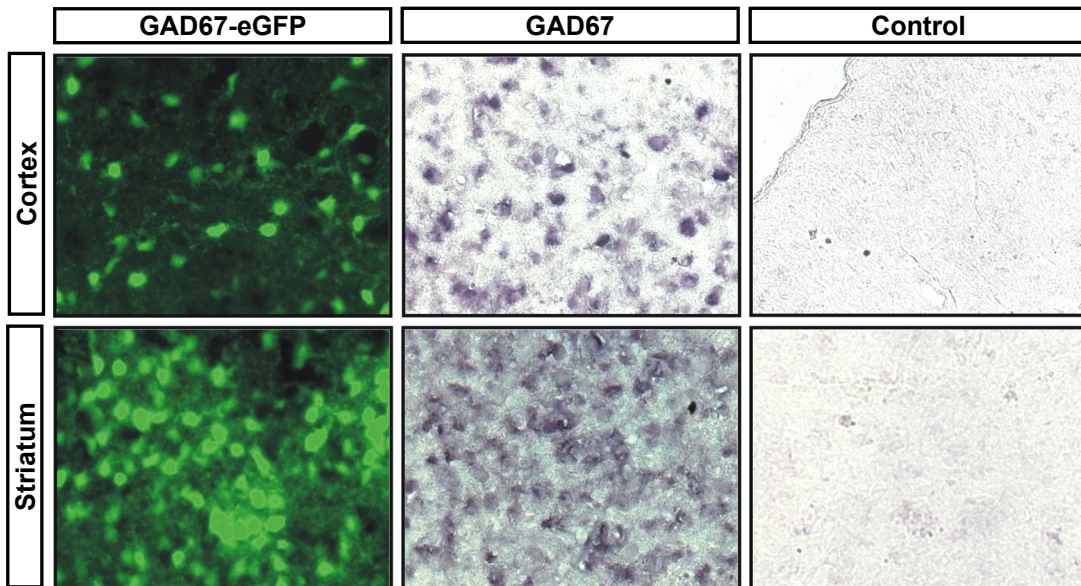
Figure 3.14: *In situ* hybridization for GAD67 and colocalization with GFP

As a further control, *in situ* hybridizations and colocalization studies using a probe for GAD67 were done. Examples of GAD67 *in situ* hybridization signals and colocalization with fluorescently labeled GABAergic neurons in serial brain sections of GAD67-GFP knock-in mice at postnatal day 1. No signal was observed in the negative control.

In general, *in situ* signals were in good agreement with the microarray results. All probes showed a colocalization of *in situ* hybridization signal and GFP-fluorescence, whereas no signal was observed in the negative control (Fig. 3.15). Exceptions were CD84 and GAD65, where no signal was detected.

One interesting observation was that the widespread expression of ADARB2 in GABAergic neurons of the early postnatal brain was strongly retained in the neurogenic regions of the adult nervous system, namely the olfactory bulb and the dentate gyrus of the hippocampus. This suggests that the gene may be more important during development/maturation of GABAergic neurons, than in their functional properties In contrast, many other genes, like GRIA2, USP49, CRKL, CD72 and ANGPTL2, maintained their specific expression in

GABAergic neurons also in the adult mouse brain. Although the transcript of CD72 was highly abundant in GABAergic neurons from early to adult stages, an antibody staining showed no labeling, even after dissociation with low protease concentrations (data not shown). This could be due to high protease sensitivity, post-transcriptional regulation or post-translational modification, as the antibody was tested only for CD72 expression on blood cells so far.

The region specific expression of many genes was maintained in 56-day old mice (Lein *et al.*, 2007). For example, *in situ* hybridization of DLX genes showed a strong signal in forebrain GABAergic neurons. On the other hand, factors like the ZIC-family members, LHX1, LHX5 and EN2 showed a highly specific expression in the cerebellum. In addition, the differential expression of seven genes (DLX1, DLX2, DLX5, FOXG1, LHX5, ZIC1 and ZIC2) among fore- and hindbrain GABAergic neurons, as observed in the discriminatory gene analysis, was validated by quantitative real-time PCR (see 2.6.11). In all cases, the expression pattern upon qPCR reproduced that of the microarray experiments (data not shown).
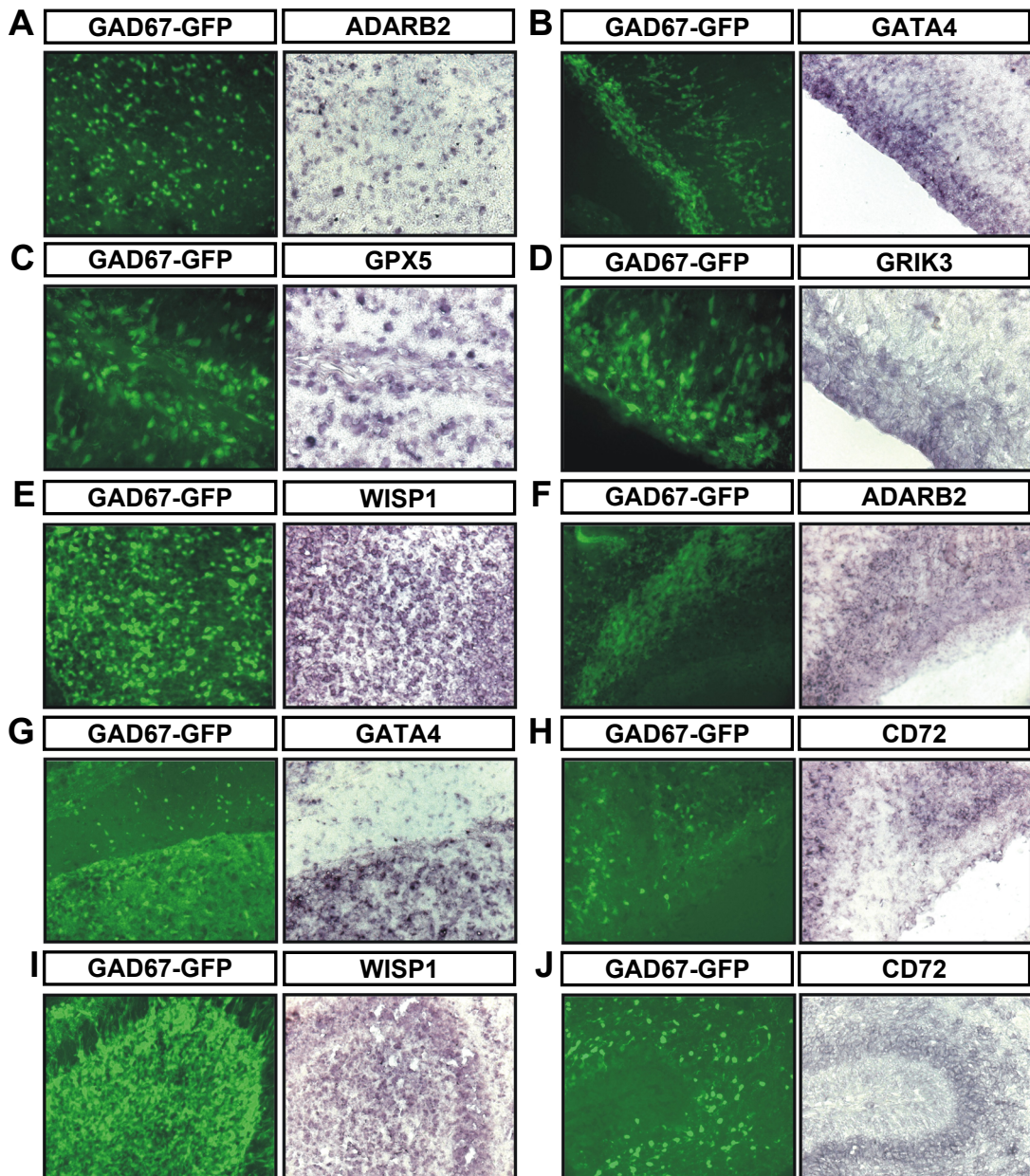
Figure 3.15: Independent validation of gene expression by *in situ* hybridization

Examples of tested candidates and colocalization of the signals with fluorescently labeled GABAergic neurons in serial brain sections of GAD67-GFP knock-in mice at postnatal day 1 are depicted. The slides represent the cortex (A to D), the striatum (E to H), the olfactory bulb (I) and the cerebellum (J). (A and F) *In situ* hybridization using a probe specific for ADARB2 mRNA. (B and G) *In situ* hybridization using a probe specific for GATA4 mRNA. (C) *In situ* hybridization using a probe specific for GPX5 mRNA. (D) *In situ* hybridization using a probe specific for GRIK3 mRNA. (E and I) *In situ* hybridization using a probe specific for WISP1 mRNA. (H and J) *In situ* hybridization using a probe specific for CD72 mRNA. All probes showed a colocalization of *in situ* hybridization signal and GFP-fluorescence.

3.3 Generation of monoclonal antibodies specific for GABAergic neuron cell surface markers

In parallel to the molecular analysis of purified GABAergic neuron subpopulations, alternative methods for the isolation of these cells or even subpopulations should be established. By using FACS, it is only possible to purify GABAergic neurons from genetically modified animals like the GAD67-GFP mouse strain. To overcome the need of a transgenic background, monoclonal antibodies that recognize cell surface molecules specific for these neurons would be very helpful. Such antibodies would allow the direct isolation of GABAergic neurons from different genetic backgrounds, e.g. disease models, by using magnetic or flow cytometric based cell sorting technologies. As GABAergic neurons could be isolated at high purities (see 3.1.3), it was decided to use the purified cells directly as immunogenic material.

Lewis rats were immunized (see 2.8.7) by contralateral footpad immunization to induce monoclonal antibody production (Brooks *et al.*, 1993; Yin *et al.*, 1997). About 0.8-1.3 x 10^7 purified GABAergic cells were injected subcutaneously into the left hind footpad of the rats. Several decoys, containing unspecific epitopes of the target- but also other cells, were injected into the right hind footpad in parallel to minimize the unspecific immunoresponse of the target lymph node. To increase the immunogenic potential of the injected cells, different adjuvants were tested. The immunization schemes are summarized in Table 3.2.

To screen specifically for antibodies that recognize cell surface molecules, brains of GAD67-GFP mice were dissociated and intact cells used for staining. By using living cells, the antibodies can not pass the membrane and therefore only stain epitopes outside the cell. An antibody which specifically binds to a cell surface molecule on GABAergic neurons should label all or at least a subgroup of the GFP$^+$ population but no cells from the GFP$^-$ fraction.

Table 3.2: Immunization schemes

	Protease	Decoy	Adjuvant	No. of clones
1	5 U/ml Papain	Actin-GFP brain / GFP⁻ fraction	FAI / PHA	15
2	5 U/ml Papain	Actin-GFP brain / GFP⁻ fraction	FAI / PHA	9
3	5 U/ml Papain	Actin-GFP brain / GFP⁻ fraction	FAI / PHA	57
4	5 U/ml Papain	Actin-GFP brain / GFP⁻ fraction	FAI / PHA	35
5	5 U/ml Papain	Actin-GFP brain / GFP⁻ fraction	FAI / PHA	48
6	5 U/ml Papain	50 µg recombinant GFP	FAI / PHA	74
7	5 U/ml Papain	Actin-GFP brain / GFP⁻ fraction	15 µg/µl CpG	>1000
8	5 U/ml Papain	Actin-GFP brain / no decoy	15 µg/µl CpG	>1000
9	0.5 U/ml Papain or 0.1% Trypsin	GFP⁻ fraction	15 µg/µl CpG	>1000
10	0.5 U/ml Papain or 0.1% Trypsin	50 µg recombinant GFP	15 µg/µl CpG	>1000

Actin-GFP brain and FAI were only used for the first boost. All further administrations were combined with the other decoys/adjuvants mentioned. Abbreviations: No. = number; FAI = Freunds Adjuvant incomplete; PHA = Leucoagglutinin PHA-L Lectin from *Phaseolus vulgaris* (red kidney bean); CpG = CpG ODNs 1668

The first 5 immunization approaches were carried out using a protease concentration of 5 U/ml Papain for brain tissue dissociation prior to FACS purification. As the purified GABAergic neurons are GFP⁺, and GFP has a high immunogenic potential, brain tissue of Actin-GFP transgenic mice served as decoy during the first boost to guide the unspecific anti-GFP immune response into the contralateral lymph node. For all further boosts, the GFP⁻ fraction from FACS purified GAD67-GFP brain cells was used as decoy to prevent the appearance of target cells in the decoy population. As Freunds Adjuvant incomplete (FAI) is a very potent stimulator of the immune system, it was co-injected the first day of immunization for generally activation of the host immune response. For subsequent boosts, instead of using FAI, the cells were coated with PHA-L, a lectin from *Phaseolus vulgaris*, to increase their immunogenic potential. Only very few hybridoma clones, less than 100 per fusion (see 2.8.8), were generated by using this strategy. None of the produced antibodies was specific for cell surface molecules of GABAergic neurons.

It was observed that the lymph node on the decoy injection site was always 3 to 5 times larger than that of the GABAergic fraction injection site. Probably, this is due to highly immunogenic epitopes in the GFP⁻ fraction. To prevent that the major immune response takes place only at the decoy side, the sixth immunization was carried out using recombinant GFP protein as decoy. Therefore, only the unspecific anti-GFP immune response should be guided into the contralateral lymph node. Again, the lymph node on the decoy injection site was approximately 3 times larger, less than 100 hybridoma clones were obtained, and no specific staining was observed. The conclusion was that the immunogenic potential of the GFP$^+$ fraction itself was rather low.

To increase the immune response at the GABAergic fraction injection site, CpG ODNs 1668, a synthetic pathogen DNA fragment, was co-injected in all further immunizations. Immunization approach no. 7 was, except for the different adjuvant, equal to immunizations no. 1 to 5. In approach no. 8 only the Actin-GFP decoy during the first boost was administrated without any further decoy injections. Both injections yielded in more than 1000 hybridoma clones per fusion, but again no specific antibody could be identified. During the last 2 approaches, the protease concentration of Papain was reduced to 0.5 U/ml and 50% of the brains were dissociated using 0.1% Trypsin. Thereby, more protease sensitive surface epitopes should be saved. The GFP⁻ fraction served as decoy during approach 9, while recombinant GFP protein was used during approach 10. Both injections resulted in more than 1000 hybridoma clones per fusion, but again no specific antibody could be identified.

In conclusion, none of the immunization approaches resulted in the generation of an antibody specific for GABAergic neurons. One explanation for this result could be that GABAergic neurons do not express highly immunogenic epitopes, at least those which are protease resistant, on their cell surface. An alternative to continue with further immunizations was to identify target proteins in these cells directly by proteome analysis.

3.4 Defining the surface proteome of GABAergic neurons

As a result of the gene expression analysis, many genes were identified which were highly and specifically expressed in GABAergic neurons and therefore may serve as new marker genes for these cells. However, only very few of these candidates were located in the plasma membrane and could serve as cell surface markers for the isolation of GABAergic neurons. To overcome this problem and focus directly on the identification of such markers, the cell surface proteome of GABAergic neurons was analyzed in collaboration with the group of

Dr. Bernd Wollscheid at the ETH in Zurich (Zhang *et al.*, 2003). Using this approach, proteins that contain N-linked carbohydrates and are localized in the plasma-membrane are labeled and identified by tandem mass spectrometry (MS/MS). The specificity is based on the conjugation of glycoproteins to a solid support using hydrazide chemistry on intact cells and the specific release of formerly N-linked glycosylated peptides via peptide-N-glycosidase F (PNGase F). Using this approach, the amount of identified membrane proteins is much higher than by conventional proteome analysis of whole membrane fractions. One limitation is the huge number of $1x10^8$ cells that is needed for optimal results.

The brains of 49 GAD67-GFP brains were resected. Half of the brains were dissociated with 0.5 U/ml Papain, the other half by using 0.1% Trypsin. Subsequently, the GFP$^+$ and GFP$^-$ fractions were isolated by FACS (see 2.8.5), yielding approximately $3x10^7$ positive and $7x10^7$ negative cells. The cells were labeled and the glycoproteins isolated using the "Cell Surface Glycopeptide Capture Protocol" (Tao *et al.*, 2005). Peptides from both populations were identified by tandem mass spectrometry.

As expected from the low cell numbers used, only 25 proteins were identified in the GFP$^+$ fraction, whereas 79 proteins were identified in the GFP$^-$ fraction. Seventeen proteins were found in both fractions. The 25 proteins that were specific for the GABAergic fraction are listed in table 3.3. Indeed, 22 (88%) of these proteins were GO annotated to the membrane fraction, whereas 3 of the proteins were fully uncharacterized. However, for some of the candidates the definitive membrane compartment was still not known, therefore a fraction may localize to intracellular membranes. Most of the identified candidates were sparsely characterized in general and no antibodies, or at least none suitable for flow cytometric analysis, are available. When compared to data from the transcriptome profiling, many correlations were observed. Several identified proteins, like Vcork1, 4732465J04Rik, Mpzl1, Siglece, Tmpo and Ndufa4, also displayed enrichment on the transcriptome level. In contrast, several candidates, like Atp1a3, P2ry1, Cxadr, Slc35c2 and Stx1b2, were not enriched in the microarray analysis. This was expected, as it is well known that due to post-transcriptional regulation many differences among the transcriptome and the proteome of a cell could be observed.

Taken together, a number of proteins were identified which are presumably expressed on the cell surface of GABAergic neurons. Besides new insights on the specific function for these proteins in inhibitory neurons, they may serve as target proteins for the generation of antibodies specific for extracellular epitopes. In addition, the proteins which were found only in the GFP⁻ fraction might represent novel surface markers for other populations of brain cells and may therefore be used for the purification or depletion of these cells.

Table 3.3: Proteins identified by mass spectrometry

Protein name	IPI link	Entrez accession	Number of Peptides	Score
Atp1a3	IPI00122048	232975	4	1.0000
Pgrmc1	IPI00319973	53328	3	0.9996
Armc10	IPI00137460	67211	2	0.9966
Stx1b2	IPI00113149	56216	2	0.9962
Acsl3	IPI00169772	74205	2	0.9955
Tmpo	IPI00320399	21917	2	0.9952
Tmed2	IPI00127983	56334	1	0.9942
Fkbp8	IPI00130833	14232	2	0.9942
Dcakd	IPI00221828	68087	1	0.9935
Slc25a5	IPI00127841	11740	1	0.9894
Vamp3	IPI00132276	22319	2	0.9844
Ndufa4	IPI00125929	17992	1	0.9827
Vkorc1	IPI00133579	27973	1	0.9737
Lrrc59	IPI00123281	98238	1	0.9645
EG639162	IPI00113394	639162	2	0.9325
4732465J04Rik	IPI00402943	414105	1	0.7431
Siglece	IPI00172333	83382	1	0.6712
Por	IPI00621548	18984	1	0.6425
P2ry1	IPI00116191	18441	1	0.6411
Syt13	IPI00111520	80976	1	0.6321
Cxadr	IPI00270376	13052	1	0.5571
AI464131	IPI00464256	329828	1	0.5398
Slc35c2	IPI00756392	228875	2	0.5395
Mpzl1	IPI00620858	68481	1	0.5347
Col24a1	IPI00551234	71355	1	0.5136

List of proteins which were identified by tandem mass spectrometry peptide fingerprinting. The number of peptides indicates how many peptides were identified matching to a respective protein. The score indicates the statistically probability of a unique identification.

Part II Molecular analysis of interneuron development

In the previous part, a molecular analysis of GABAergic neurons in general as well as the relationship among subpopulations of these cells from different brain regions was carried out. In a second part, the aim was to analyze the differentiation of progenitor cells into GABAergic neurons. As several neurodegenerative disorders, like Huntington's disease, show a loss of inhibitory neurons, a promising therapeutic approach is to replace these neurons to retain functionality. One possibility is to generate specific neuronal cell types *in vitro* before grafting, the other opportunity may be the activation and targeted differentiation of persistent, brain localized adult stem cells directly *in vivo*. For both approaches there is a prerequisite in deep understanding of the underlying mechanisms involved in neuronal differentiation. The goal was therefore to identify new candidate genes involved in the differentiation of GABAergic interneurons. Therefore, the transcriptome of mature GABAergic neurons as well as their progenitor cells was analyzed to identify genes which are differentially regulated during differentiation and may act as regulatory factors.

As a model system, the generation of inhibitory interneurons in the olfactory bulb was analyzed. These interneurons are generated from adult neuronal stem cells, localized in the subventricular zone (SVZ), throughout live (Lledo *et al.*, 2006). Interestingly, about 16% of these GABAergic interneurons show a bifunctional neurotransmitter phenotype as they are also dopaminergic (Panzanelli *et al.*, 2007). As the loss of dopaminergic neurons is the major phenotype at the onset of Parkinson's disease, understanding of their development is also of broad interest.

In this case, the use of dissociated brain tissue from GAD67-GFP mice in combination with flow cytometry sorting was not possible, as the precursor population already expresses GFP. The polysialylated form of NCAM (PSA-NCAM) serves as a marker for the differentiation status in this system as it is only present in precursor cells but absent in mature interneurons (Durbec and Cremer, 2001). Therefore, the expression profile of PSA$^-$ mature periglomerular layer interneurons was compared to that of late PSA$^+$ precursors localized also in the periglomerular layer (Fig 3.16 C and D). Furthermore, both cell populations were compared to their earlier progenitors, the Type A neuronal precursor cells, which migrate from the SVZ to the olfactory bulb via the rostral migratory stream and represent a mixed population that can give rise to granule as well as periglomerular interneurons (Fig 3.16 A and B).
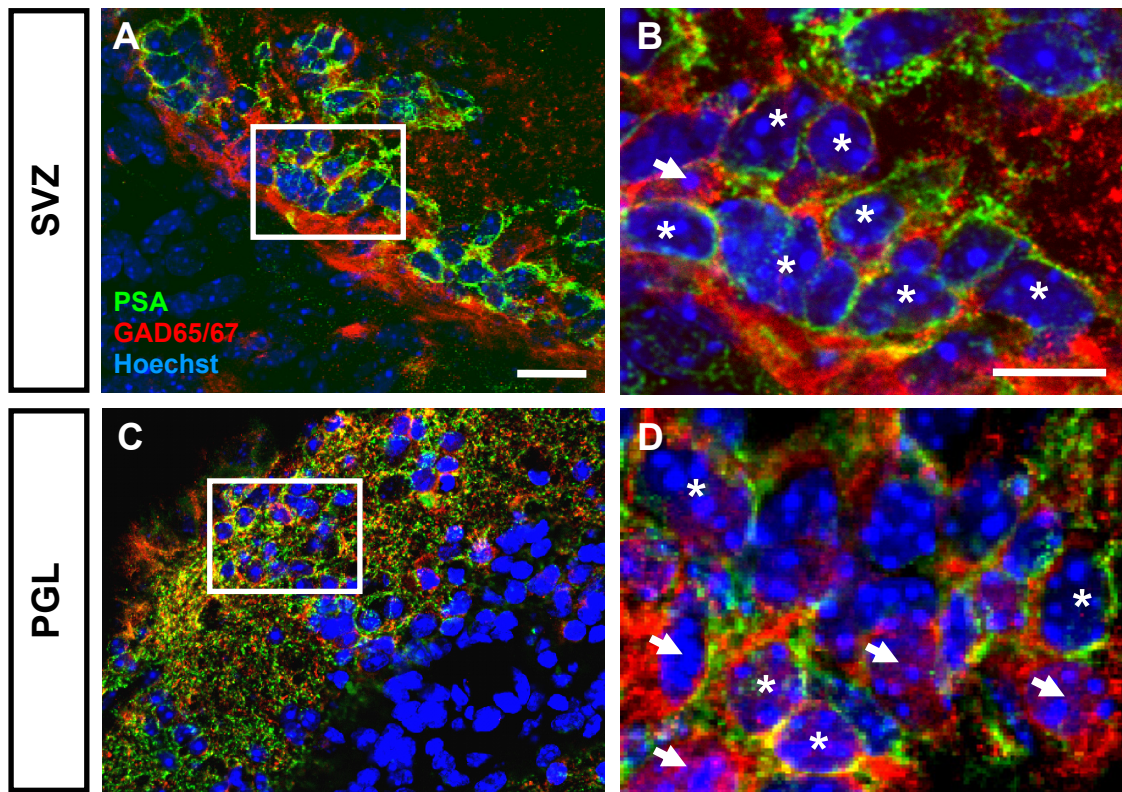
Figure 3.16: Immunohistochemistry of glomerular layer interneurons and their precursors

An immunostaining for the precursor marker PSA (green) and the GABAergic marker GAD65/67 (red) in the SVZ and the periglomerular layer is shown. Cell nuclei were stained with Hoechst (blue). In the SVZ, most of the cells were PSA$^+$/GAD65/67$^+$ Type A early neuronal precursor cells (stars), whereas only few mature PSA$^-$/GAD65/67$^+$ cells (arrows) were present (A and B). In contrast, a mixed population of PSA$^+$/GAD65/67$^+$ late precursor cells (stars) and mature PSA$^-$/GAD65/67$^+$ interneurons (arrows) were found in the PGL (C and D). Scale bar = 20 µm for A and C; 10 µm for B and D; Abbreviations: SVZ = subventricular zone; PSA = polysialic acid; PGL = periglomerular layer

3.5 Isolation of olfactory bulb interneurons and their precursors

As already mentioned, one major requirement for a molecular analysis of a cell population is the usage of pure starting populations. Using the postnatal generation of olfactory bulb interneurons as a model system, it was possible to isolate all required cell types at high purities. The established purification strategy combined a selective magnetic cell sorting based approach for known surface markers with a prior reduction of the starting tissue complexity (see 2.8.4 and Fig. 3.17).
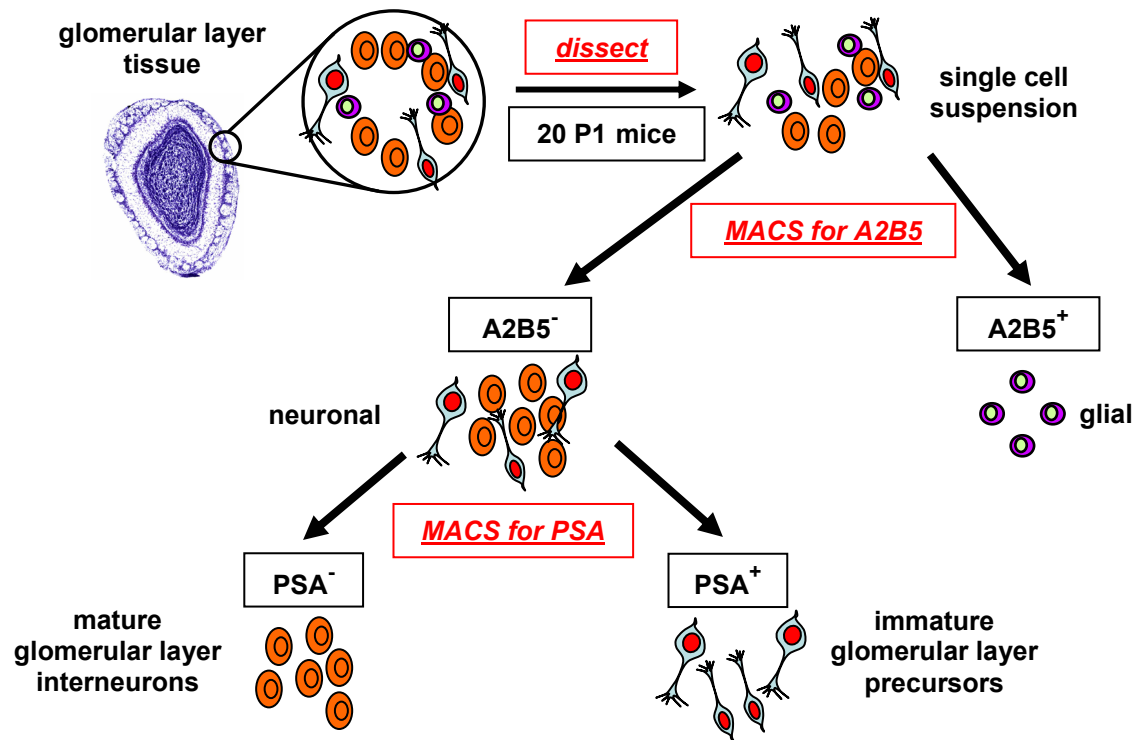
Figure 3.17: Scheme for purification of glomerular layer interneurons and their precursors
Glomerular layer interneurons and their progenitors were purified using a two step MACS$^{®}$ strategy. The glomerular layer of olfactory bulbs from 20 postnatal day 1 mice was dissected and dissociated to a single cell suspension. Subsequently, A2B5^{+} glial cells (violet) were depleted by using magnetic antibodies specific for A2B5. In the remaining neuronal fraction, magnetic antibodies specific for PSA were used to separate PSA^{+} late precursor cells (light blue) from PSA^{-} mature interneurons (orange). The nissl stained olfactory bulb was adopted from the Allan Reference Atlas (Lein *et al.*, 2007). Abbreviations: PSA = polysialic acid; P1 = postnatal day 1

The reduction of the starting material complexity prior to magnetic cell sorting was done by microdissection of the periglomerular layer. This step was crucial to deplete tissue containing cell types that could not be selectively sorted by MACS$^{®}$. Subsequently, the periglomerular layer tissue was dissociated to a single cell suspension and sorted using a two step magnetic cell sorting strategy. In the first step, magnetic antibodies specific for A2B5 were used to deplete A2B5^{+} glial cells yielding a population of mature interneurons and late precursor cells. In the second step, magnetic antibodies specific for PSA were used to separate PSA^{+} late precursor cells from PSA^{-} mature interneurons. Dissection and sorting of 20 mouse olfactory bulbs yielded 1.1×10^{5} PSA^{+} precursor cells and 1.4×10^{5} PSA^{-} interneurons with good purities (Fig. 3.18). In the PSA^{+} enriched fraction, 94% of all cells showed immunoreactivity for PSA. 71% were double positive for PSA and GAD65 and 8% were still

positive for A2B5. In the PSA$^-$ fraction, 72% were positive for GAD65, 10% for A2B5 and 2% were still PSA$^+$.

The PSA$^+$ Type A early precursor cells were purified using an equal approach, but with dissected SVZ- instead of periglomerular layer tissue as starting population. Subsequent immunolabeling of isolated cells indicated purities above 95% (data not shown).
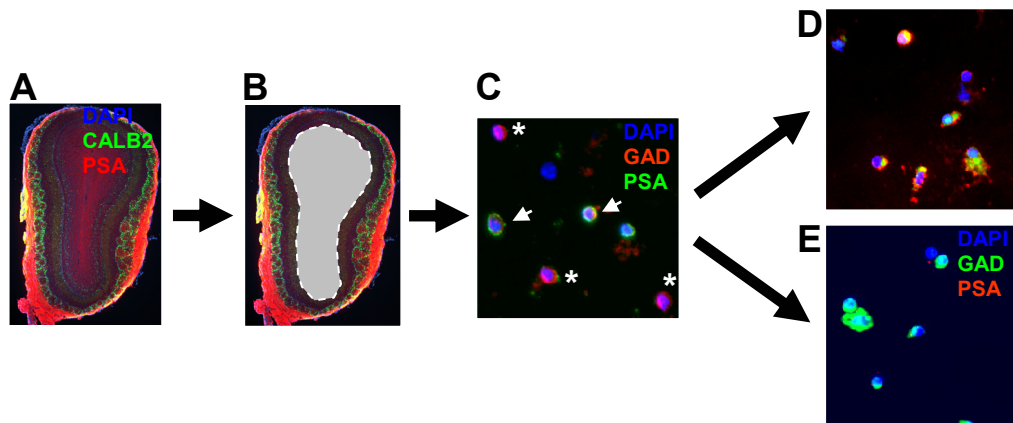
Figure 3.18: Purification of glomerular layer interneurons and their precursors

Immunostainings for the precursor marker PSA (red) and the interneuron marker CALB2 (green) in the olfactory bulb are shown (A and B). Cell nuclei were stained with DAPI (blue, A to E). In addition, immunostainings for the precursor marker PSA (green) and the interneuron marker GAD65/67 (red) after dissociation (C) and MACS$^®$ purification are shown (D and E). The dissociation of periglomerular layer tissue from the olfactory bulb is indicated by the grey area (A and B). Subsequent to dissociation (C), the single cell mixture contained PSA$^+$/GAD65/67$^+$ late precursor cells (arrows) and mature PSA$^-$/GAD65/67$^+$ interneurons (stars). The two step MACS$^®$ separation yields purified populations of PSA$^+$/GAD65/67$^+$ periglomerular layer precursor cells (D) and mature PSA$^-$/GAD65/67$^+$ interneurons (E).

3.6 Molecular analysis of olfactory bulb interneurons and their precursors

As mentioned above, dissection and sorting of periglomerular layer tissue from 20 mouse olfactory bulbs yielded 1.1×10^5 PSA$^+$ precursor cells and 1.4×10^5 PSA$^-$ interneurons. The yield of Type A precursor cells, isolated from SVZ tissue, was in the same range. As this cell numbers did not allow for standard gene expression profiling, all experiments were carried out using SuperAmp amplification of mRNA. For each experiment, 7000-10000 cells were directly lysed in lysis buffer after MACS$^®$ sorting and stored at -20°C until further processing. RNA amplification, cDNA labeling and microarray processing of Agilent whole mouse

genome 44k microarrays were carried out as described for the FACS purified cells (see 2.6.10). RNA, isolated from postnatal day 1 old wild type mice brains (n = 4), was amplified in the same way and served as a common reference for all hybridizations. Olfactory bulbs of 20 mice were pooled and used in each experiment. Two replicate hybridizations including a dye-swap were done for each of the 3 cell types, namely the Type A early precursors, the periglomerular late precursors and the mature periglomerular interneurons. Merged dye-swap data were used for further analysis. Correlation coefficients within replicates ranged from 0.92 to 0.98, demonstrating a good reproducibility.

3.6.1 Global changes during differentiation

In a first step, the general relationship among the 3 cell types was analyzed. Therefore, the gene expression profiles of the Type A early neuronal precursors, the periglomerular late precursors and the mature periglomerular interneurons were compared by calculating Pearson correlation coefficients of pairwise comparisons. Unsupervised hierarchical clustering of correlation coefficients grouped both cell types isolated from the periglomerular layer together and separated them from the Type A cells (Fig. 3.19 A). The correlation coefficients between Type A cells and periglomerular layer cells were 0.64 in comparison to PSA$^+$ cells and 0.60 in comparison to PSA$^-$ cells. This result is in agreement with the model that PSA$^+$ periglomerular layer precursors represent an intermediate state between SVZ precursors and PSA$^-$ periglomerular layer interneurons. Furthermore, the high similarity between the two periglomerular layer cell types (correlation coefficient of 0.97) indicates that the major changes during the development of olfactory bulb GABAergic interneurons occur during the migration of Type A precursor cells from the SVZ to the olfactory bulb, whereas only minor changes occur during the late step of differentiation in the periglomerular layer.

In addition, a multiclass SAM analysis was computed. Using this approach, the significant enrichment of genes showing a similar expression pattern is calculated. Enrichment for three groups of patterns was identified (Fig 3.19 B to D): first, genes which are downregulated during the migration of Type A precursor cells from the SVZ to the olfactory bulb that stay downregulated; second, genes which are upregulated during the migration of Type A precursor cells from the SVZ to the olfactory bulb that stay upregulated; third, genes which are upregulated during the last step of differentiation in the periglomerular layer. No significant enrichment of genes that are upregulated first and subsequently downregulated again or vice versa was observed. This result is again in good agreement with the proposed model.

A Type A precursor / PGL precursor / PGL interneuron
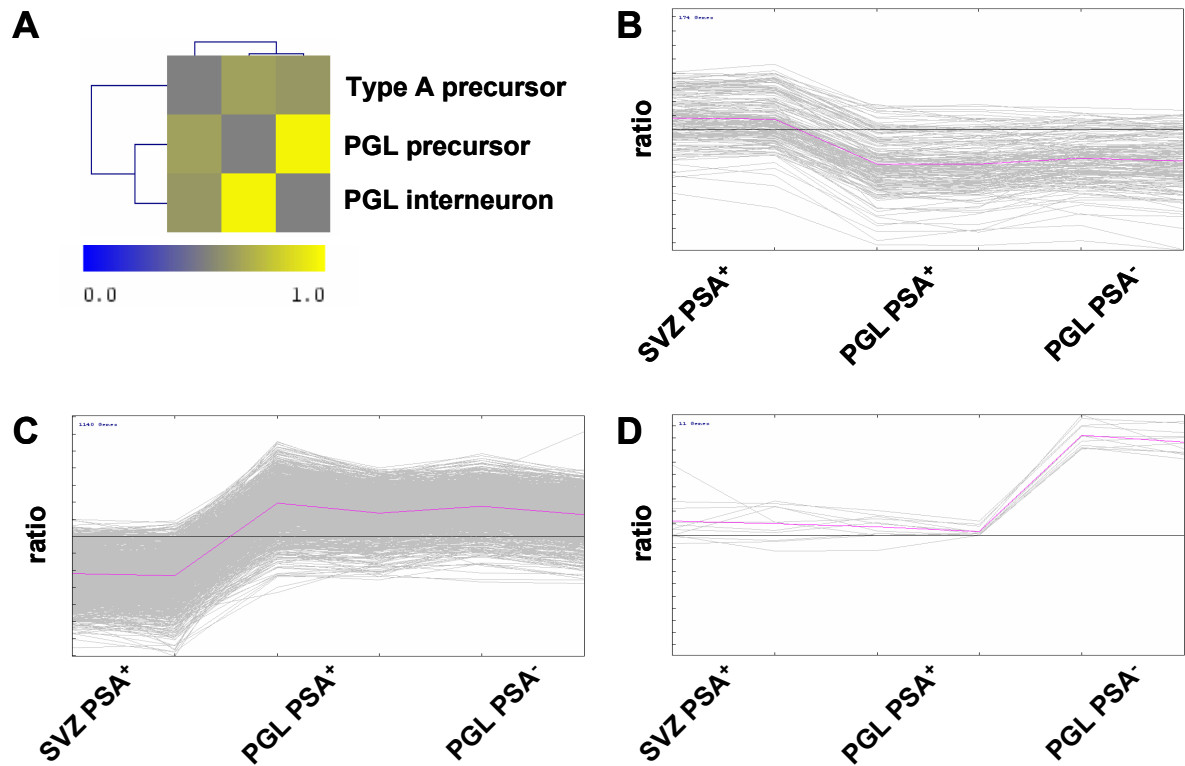
Figure 3.19: Correlation and multiclass SAM analysis

(A) Correlation matrix showing the relationship of gene expression profiles in all experiments. The matrix was generated by unsupervised hierarchical clustering of global expression data. Correlation coefficients are indicated by their color from blue (0.0) to yellow (1.0). The correlation coefficients between Type A cells and periglomerular layer cells were 0.64 when compared to PSA^+ cells and 0.60 when compared to PSA^- cells. In combination with the high similarity between the two periglomerular layer cell types (correlation coefficient of 0.97), this correlates to the model that PSA^+ periglomerular layer precursors represent an intermediate state between SVZ precursors and PSA^- periglomerular layer interneurons. (B to D) A multiclass SAM analysis to calculate significant enrichment of genes showing similar expression patterns is shown. The relative change of expression ratios for each analyzed cell type compared to the common reference is depicted. Groups of genes which are downregulated during the migration of Type A precursor cells from the SVZ to the olfactory bulb that stay downregulated (B), which are upregulated during the migration of Type A precursor cells from the SVZ to the olfactory bulb that stay upregulated (C) and which are upregulated during the last step of differentiation in the periglomerular layer were significantly enriched. Abbreviations: SVZ = subventricular zone; PSA = polysialic acid; PGL = periglomerular layer

3.6.2 Changes in gene expression during the migration of Type A precursor cells from the SVZ to the olfactory bulb

To obtain further information about the molecular changes which occur during the migration of Type A early neuronal precursor cells from the SVZ into the olfactory bulb and their differentiation to periglomerular cells, genes were analyzed that altered the expression patterns during these stages. As expected from the rather low correlation coefficients between Type A cells and olfactory bulb cells of 0.64 (compared to PSA$^+$ cells) and 0.60 (compared to PSA$^-$ cells), many genes were found to be significantly regulated. The 110 strongest upregulated as well as the 110 strongest downregulated genes are listed in supplementary tables 1 and 2 (see Tab. 6.1 and 6.2). Selected candidates are described below.

Many genes showed strong enrichment in both periglomerular cell types compared to their SVZ progenitors and may therefore represent candidates important for the differentiation of GABAergic interneurons. The enrichment of NeuropeptideY, which has signal modulating function and may be involved in many diseases, in these later stages of differentiation, is in concordance to its expression in mature subtypes of GABAergic interneurons (Kanatani *et al.*, 2000; Rohner-Jeanrenaud *et al.*, 1996). A huge number of genes was identified which are involved in synaptogenesis and synaptic plasticity. Examples are PTN, VTN, APOE, APOD, FBLN2, S100A1 and S100A13, NRXN1 and NLGN2 (Comoletti *et al.*, 2003; Hartmann *et al.*, 1994; Missler *et al.*, 2003; Okazaki *et al.*, 2002). Furthermore, NLGN2 is specific for inhibitory synapses (Varoqueaux *et al.*, 2004), which correlates with the observation that it is upregulated during differentiation. All these genes may play important roles during the synaptogenesis of olfactory bulb interneurons.

In addition, genes like EphrinA5, Semaphorin4A, Vimentin and CSPG3 act as axon guidance and cell motility factors (Lampa *et al.*, 2004; Li *et al.*, 2005; Menet *et al.*, 2003; Moretti *et al.*, 2006). Even more enriched genes, which were shown to be functional in mature neurons, like the glutamate receptors GRIK1 and GRINL1A, CALB1, CALR, GLUD, SLC13A3, MT2 and DBI correlate with an increased state of differentiation in periglomerular layer cells (Pajor *et al.*, 2001; Stankovic, 2005). As an example, mice deficient for TNC have a delayed onset of odor detection, again showing that genes identified in this screen have important functions during olfactory bulb neurogenesis (de Chevigny *et al.*, 2006). Upregulation of extracellular matrix components like MATN2, FBLN2, TNC, PTN, VTN and CSPG3 by periglomerular layer precursors and interneurons suggests also an active role of these cells in building up the neurogenic environment of the olfactory bulb (Mates *et al.*, 2002). A number of transcription factors, upregulated in periglomerular cells compared to SVZ precursors, indicate a function

of these molecules in the late phase of interneuron differentiation. Examples are OLIG1, XBP1, NFI/A, ZFP277, ZMYND11, GTF2B and E4F1. Several of them, like Nuclear Factor I/A, are already known to be involved in neuronal development but not linked to the olfactory bulb (Shu *et al.*, 2003; Wang *et al.*, 2004).

3.6.3 Genes differentially expressed during the maturation from periglomerular layer precursors to interneurons

After identifying candidates that may be involved in early stages of differentiation, genes which were differently regulated among the 2 periglomerular layer cell types were further analyzed. These genes may be important for late differentiation steps. Although a high correlation coefficient of 0.97 between PSA$^+$ periglomerular layer precursors and PSA$^-$ periglomerular layer interneurons indicated a high similarity of these cell types, several interesting genes with strong expression differences were found. The >5-fold upregulated as well as the >5-fold downregulated genes are listed in supplementary tables 3 and 4 (see Tab. 6.3 and 6.4).

Comparable to the results for periglomerular layer- against Type A cells, genes with functions in mature neurons were identified to be enriched in the PSA$^-$ fraction showing their advanced differentiation status. Examples of these genes were GAD2, SST, NEFL, NRXN, HTR3B, SLC1A1, CALB1 and CALR. Additionally, markers of neuronal progenitor cells, like TUBB3, Nestin and DCX were downregulated. Some of them, for example DCX and Nestin, had already been downregulated in late PSA$^+$ periglomerular layer precursors compared to early Type A precursors and than even more in mature PSA$^-$ periglomerular layer interneurons. Enriched expression of several OLFR- and other rhodopsin like receptors in mature olfactory bulb interneurons was consistent to results from the expression profiling of GABAergic neurons.

Several upregulated genes, like STX3, STX6, SYT4 and SLC1A1, are important for vesicular- and neurotransmitter transport (Ferguson *et al.*, 2004a). Many genes with functions in the regulation of the cytoskeleton, especially involved in axon outgrowth and guidance, like KTN1, NTRK3, NTRK3, C130076O07Rik, TBCE, BC050903 (DCAMKL1) and Ablim1 were identified (Bommel *et al.*, 2002; Deuel *et al.*, 2006; Erkman *et al.*, 2000; Martin *et al.*, 2002; Stenqvist *et al.*, 2005). But also in the fraction of downregulated transcripts, many genes connected to the cytoskeleton, like CRMP1, MAPT, KIF5A, TUBB3 and EPB4.2 were found (Bretin *et al.*, 2005; Kanai *et al.*, 2000; Yamashita *et al.*, 2006). The interaction of these

genes probably regulates the final positioning, morphological changes and axonal innervations during the final differentiation of olfactory bulb interneurons.

As before, a number of transcription factors with expression differences among the 2 periglomerular populations were found that may be important for the regulation of this differentiation step. The transcription factors BHLHB9, PAX6 and PAX8, OBOX2 and 3, PMS1, SFPI1, GABPB1, MTF1, ZHX3 and ISL2 were enriched in PSA⁻ cells. For example, ISL2 specifies RGC laterality by repressing an ipsilateral pathfinding program (Pak *et al.*, 2004). In contrast, the transcription factors PNMA1, SOX30, ZFP219 and NFKBIE were downregulated in PSA⁻ interneurons. Interestingly, an oppositional regulation of DLX1 and DLX2 was found. DLX2 was upregulated in PSA⁻ interneurons, whereas DLX1 was downregulated. In contrast, DLX5 and 6 were already downregulated in periglomerular layer cells compared to Type A precursors, suggesting that DLX genes are important for the early and late differentiation of olfactory bulb interneurons.

In addition, also oppositional regulation of the basic helix-loop-helix transcription factors NeuroD1 (ND1) and NeuroD2 (ND2) was found. Whereas NeuroD1 became highly upregulated in mature interneurons, NeuroD2 was downregulated during this step. Both genes are already known as important factors for the development of the nervous system (Cho and Tsai, 2004; Noda *et al.*, 2006). The PAX6 gene, which was also enriched in mature interneurons, is activated by NeuroD1 (Marsich *et al.*, 2003). PAX6 plays a role in the establishment of a postmitotic phenotype and periglomerular differentiation, but not in olfactory granule cell differentiation (Cartier *et al.*, 2006; Hack *et al.*, 2005). This data represents the first evidence for an involvement of NeuroD1 and NeuroD2 in olfactory bulb interneuron differentiation, which may be partially mediated by PAX6.

In conclusion, many genes were identified to be differently expressed during early or late stages of periglomerular interneuron differentiation. Several of them, especially the transcription factors, may play important roles in the control of differentiation. Others, like the cytoskeletal proteins and regulators, probably represent essential downstream effectors.

3.6.4 Independent validation of gene expression

To validate the microarray hybridization results, the expression data were compared to already published expression patterns for several marker genes. Expression patterns of the genes CALB1, CALR, TUBB3 and DCX in the analyzed cell populations matched with published data (Lledo *et al.*, 2006). Furthermore, expression of known marker genes like TH, GAD65, SST and Nestin was nicely reproduced by the microarray results and the differential

expression of CRMP1 among the periglomerular layer cell types also matches with published data (Veyrac *et al.*, 2005).

As adult neurogenesis takes place throughout live in mice, the results should match with expression patterns observed in the SVZ/RMS/olfactory bulb-system of adult mice. Therefore, the microarray results were compared with *in situ* hybridization data obtained from the Allan Brain Atlas (Lein *et al.*, 2007). The expression signals of *in situ* hybridizations for a number of genes (NPY, GRIK1, VTN, APOD, APOE, FBLN2, S100A1, NRXN1, GLUD, FABP7, DBI, SEPT4, SLC13A3, SCD2, IGF1 and PEA15), found to be enriched in periglomerular layer cells compared to Type A precursors, were checked and showed the expected patterns. In addition, *in situ* hybridizations for KIF5A and TUBB3 showed high expression in the SVZ and RMS but no signals in the glomerular layer, also in concordance to the microarray data. Furthermore, the differential expression of several genes (GAD2, NEFL, NeuroD1, NeuroD2, CRMP1, GPR103, NTRK3, STX3, KTN1, C130076O07Rik, NFKBIE, GREM1, PAX6, SFPI1, GABPB1 and MTF1) in PSA$^+$ late precursors and PSA$^-$ mature interneurons could be reproduced by *in situ* data (Lein *et al.*, 2007). As an example, the *in situ* signal for NeuroD1 was only detectable in the periglomerular layer. In contrast, the signal for NeuroD2 was also abundant in the centre of the olfactory bulb. This pattern would also be expected from the microarray results, which showed that NeuroD1 became highly upregulated in mature interneurons, whereas NeuroD2 was enriched in the progenitor population. In addition, the number of positive cells for NeuroD1 observed in the *in situ* hybridization suggests that this gene is highly expressed in only a subpopulation of periglomerular interneurons rather than all of these cells (Fig. 3.20). The specific expression of NeuroD1 was also validated by the observation of an equal expression pattern in the NeuroD1-GFP mouse strain (strain Tg(Neurod1-EGFP)1Gsat/Mmcd, http://gensat.org/).

The results of this screen yielded many interesting candidates for an involvement in olfactory bulb interneuron differentiation. Two particularly interesting genes were further analyzed for their functional relevance *in vivo*.
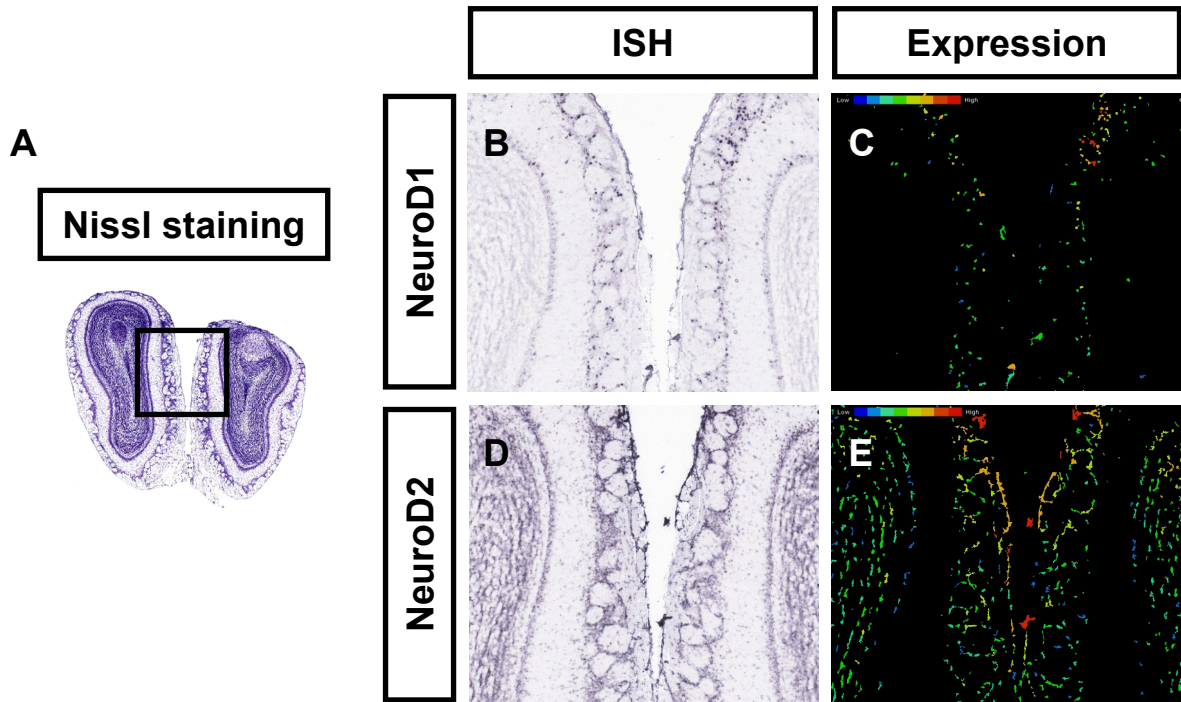
Figure 3.20: *In situ* hybridization for NeuroD1 and NeuroD2

Expression patterns of NeuroD1 and NeuroD2 from *in situ* hybridizations in adult mice were analyzed (Lein *et al.*, 2007). The square in the nissl stained olfactory bulb (A) indicates the region depicted in B to D. The *in situ* hybridization signals (B and D) were automatically quantified and plotted as expression strength (C and E) from low (blue) to high (red). A specific signal for NeuroD1 was only detectable in the periglomerular layer, where the mature interneurons are localized (B and C). In contrast, the signal for NeuroD2 was also abundant in the centre of the olfactory bulb, where the precursors arrive (D and E). Abbreviations: ISH = *in situ* hybridization

3.7 Functional *in vivo* analysis of NeuroD1 and NeuroD2

As mentioned above, an oppositional regulation of the basic helix-loop-helix transcription factors NeuroD1 and NeuroD2 was found. Whereas NeuroD1 was upregulated in mature PSA$^-$ periglomerular layer interneurons, NeuroD2 was downregulated at the same time. These two genes were selected for functional analysis, as both are involved in several differentiation processes during the development of the central nervous system. This was also true for DLX1 and DLX2, but in contrast to genes of the DLX-family, no impact on inhibitory interneuron differentiation was known so far for NeuroD1 and NeuroD2. To address the question, if these genes function as key regulators in the control of interneuron development, or if they are only downstream markers correlating with the stage of differentiation, the functional relevance of NeuroD1 and NeuroD2 expression *in vivo* was analyzed.

3.7.1 *In vivo* electroporation

A novel method, allowing the targeted transfection of adult neuronal stem cells in the SVZ (see 2.8.6), was established by Camille Boutin (Boutin *et al.*, 2008) Expression vectors are injected into the lateral ventricle of early postnatal mice. Subsequently, a series of defined electrical currents causes transfer of the plasmid DNA into radial glia cells, the stem cells in the SVZ/RMS/olfactory bulb system of adult neurogenesis. Therefore, transfection induces strong expression of transgenes in radial glia, neuronal precursors and mature neurons of the olfactory system. Using this method, the effects upon expression of specific genes during adult neurogenesis can be analyzed *in vivo*.

In this study, postnatal day 1 mice were used for *in vivo* electroporation. For each transgene and time point, always 10 biological replicates were analyzed. Electroporation of empty expression vector (pCX-MCS2, see 2.6.9) served as control. Control electroporations were carried out at the same day and as for the transgene, always 10 replicates were analyzed. To visualize transfected cells, transgenes and controls were co-electroporated with either GFP (pCX-GFP) or RFP (pCX-RFP, both gifts from Camille Boutin). The efficiency of co-electroporation was always higher than 95% (Boutin *et al.*, 2008).

Between 6 and 8 hours after electroporation, only radial glia cells expressed the transgene (Fig. 3.21 B). After 1 to 2 days, many Type A neuronal precursor cells (Fig. 3.21 C) were labeled in the SVZ. After 4 days, most of these cells were localized in the RMS or already arrived in the olfactory bulb. Differentiated granule neurons (Fig. 3.21 D) and periglomerular interneurons (Fig. 3.21 E) were found in the olfactory bulb 15 days post electroporation. As the cells only proliferate during the first days, the expression of transgenes is stable for more than 30 days (data not shown).
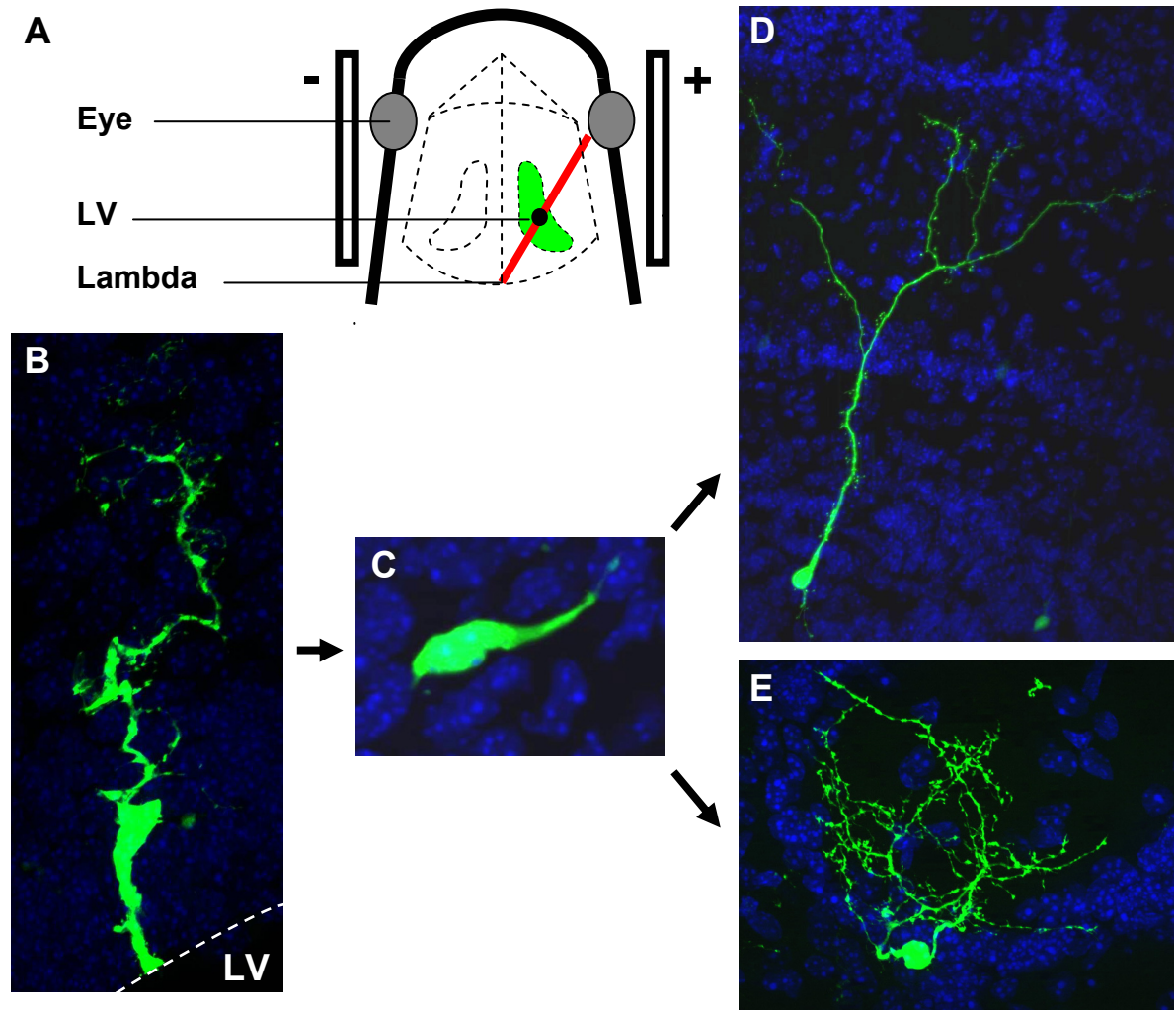
Figure 3.21: *In vivo* electroporation of a GFP expression construct

(A) Scheme of the injection and electroporation process. A virtual line (red), connecting the right eye to the craniometrical landmark lambda, served as positional marker for DNA injection. The incision point is indicated as a dot. Lateral bars indicate the position of the electrodes. Between 6 and 8 hours after electroporation, only radial glia cells expressed GFP (B). After 1 to 2 days, many Type A neuronal precursor cells (C) were labeled in the SVZ. After 4 days, most of these cells were localized in the RMS or already arrived in the olfactory bulb. Differentiated granule neurons (D) and periglomerular interneurons (E) were found in the olfactory bulb 15 days post electroporation. Abbreviations: LV = lateral ventricle

3.7.2 Overexpression of NeuroD1 and NeuroD2

To analyze the effects of an ectopic and strong expression of either NeuroD1 or NeuroD2 by *in vivo* electroporation, constructs for overexpression of both genes were generated (see 2.6.9). To test the functionality of the resulting constructs, pCX-ND1 and pCX-ND2, the 1881 cell line was transfected with the respective vector by electroporation (see 2.8.3). One day

after transfection, the cells were lysed and protein expression was analyzed by Western Blot (see 2.7.1 to 2.7.4). Both constructs showed strong expression of either NeuroD1 in the case of pCX-ND1 or NeuroD2 in the case of pCX-ND2 (Fig. 3.22).
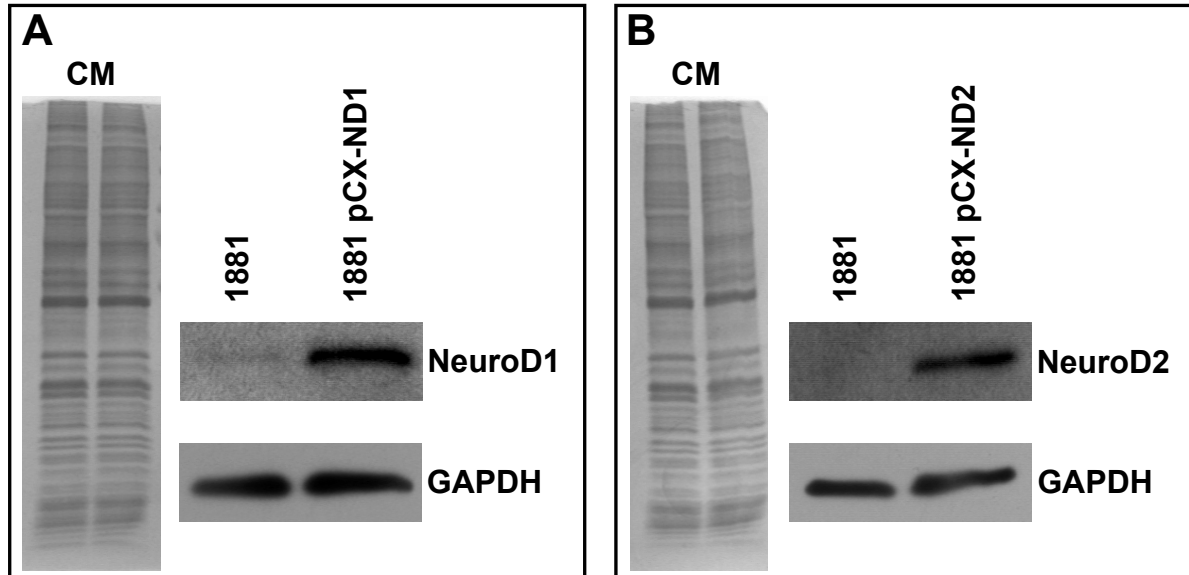
Figure 3.22: Validation of the expression constructs

The 1881 cell line was transfected with an overexpression plasmid containing the cDNA of either NeuroD1 (A) or NeuroD2 (B). After 24 h, the cells were lysed and protein expression analyzed by Western blot. Both constructs showed strong expression of either NeuroD1 in the case of pCX-ND1 (A) or NeuroD2 in the case of pCX-ND2 (B). A coomassie staining of the gel and expression of the housekeeper gene GAPDH served as loading controls. Abbreviations: CM = coomassie staining

3.7.3 Effects of NeuroD2 overexpression 2 days post electroporation

NeuroD2 was found to be downregulated during differentiation of periglomerular interneurons. This suggests an early role of this transcription factor during the development of olfactory bulb interneurons. However, it had to be examined, if the downregulation of NeuroD2 is a result of increasing differentiation, or if it is necessary to allow differentiation.

To check the effect of an early NeuroD2 overexpression, radial glia were transfected with pCX-ND2 *in vivo*. After 2 days, the mice were perfused with 4% PFA, the brains removed and cut at 50 μm on a vibratome (see 2.9.1). Fluorescence microscopy did not reveal any obvious morphological differences of transfected cells between NeuroD2 (n = 10) and control (n = 10) electroporations. Furthermore, also quantification of identified cell types did not reveal significant differences (Fig 3.23).

In conclusion, overexpression of NeuroD2 neither led to a morphological nor to a quantitative alteration of transfected cells after short time periods.
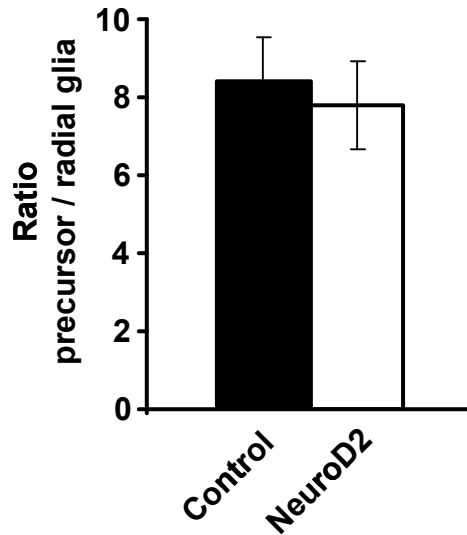
Figure 3.23: Quantification of cell types after NeuroD2 expression for 2 days
Radial glia cells were electroporated with pCX-ND2 *in vivo*. After 2 days, GFP[+] transfected precursor- and radial glia cells were quantified. The ratio of both cell types is depicted. No significant difference between NeuroD2 (n = 997 cells from 10 mice) and control (n = 1360 cells from 10 mice) electroporations was observed.

3.7.4 Effects of NeuroD2 overexpression 4 days post electroporation

After this short time period, the same experiment was carried out with a survival time of 4 days after electroporation to check for effects of NeuroD2 overexpression at this time point. A very strong difference between the NeuroD2 and control electroporation was observed (n = 10 mice for NeuroD2 and 10 mice for control electroporation). In the control electroporation, the majority of GFP^{+} cells were found to be Type A neuronal precursors. These cells were mainly localized in the anterior part of the RMS or already in the core of the olfactory bulb, whereas some radial glia cells remained in the SVZ (Fig. 3.24 A). In contrast, cells overexpressing NeuroD2 showed normal morphology but were localized in much more caudal parts, especially the posterior SVZ (Fig. 3.24 A). Quantification of transfected cells along the anterior-posterior axis of the brain revealed significant differences in their distribution (Fig. 3.24 B; n = 2168 cells from 6 mice for the control; n = 2022 cells from 6 mice for NeuroD2). In the control, most of the cells already reached the anterior- (21.3%,

$\Delta = 1.5\%$) or posterior core (37.5%, $\Delta = 2.8\%$) of the olfactory bulb, whereas only few cells remained in the anterior- (18.7%, $\Delta = 3.1\%$) or posterior SVZ (8.4%, $\Delta = 1.4\%$). Upon overexpression of NeuroD2 for 4 days, few cells were localized in the anterior- (1.4%, $\Delta = 0.8\%$) and only a small percentage in the posterior olfactory bulb (2.8%, $\Delta = 0.8\%$). In contrast, most of the Type A precursors were found in the anterior- (29.6%, $\Delta = 3.1\%$) or posterior SVZ (57.6%, $\Delta = 2.7\%$).

All together, strong expression of NeuroD2 for 4 days *in vivo* decelerates or even impairs the migration of Type A precursor cells from the SVZ to the olfactory bulb. In addition, neither the morphology nor the overall number of transfected cells seemed to be affected.

A

B
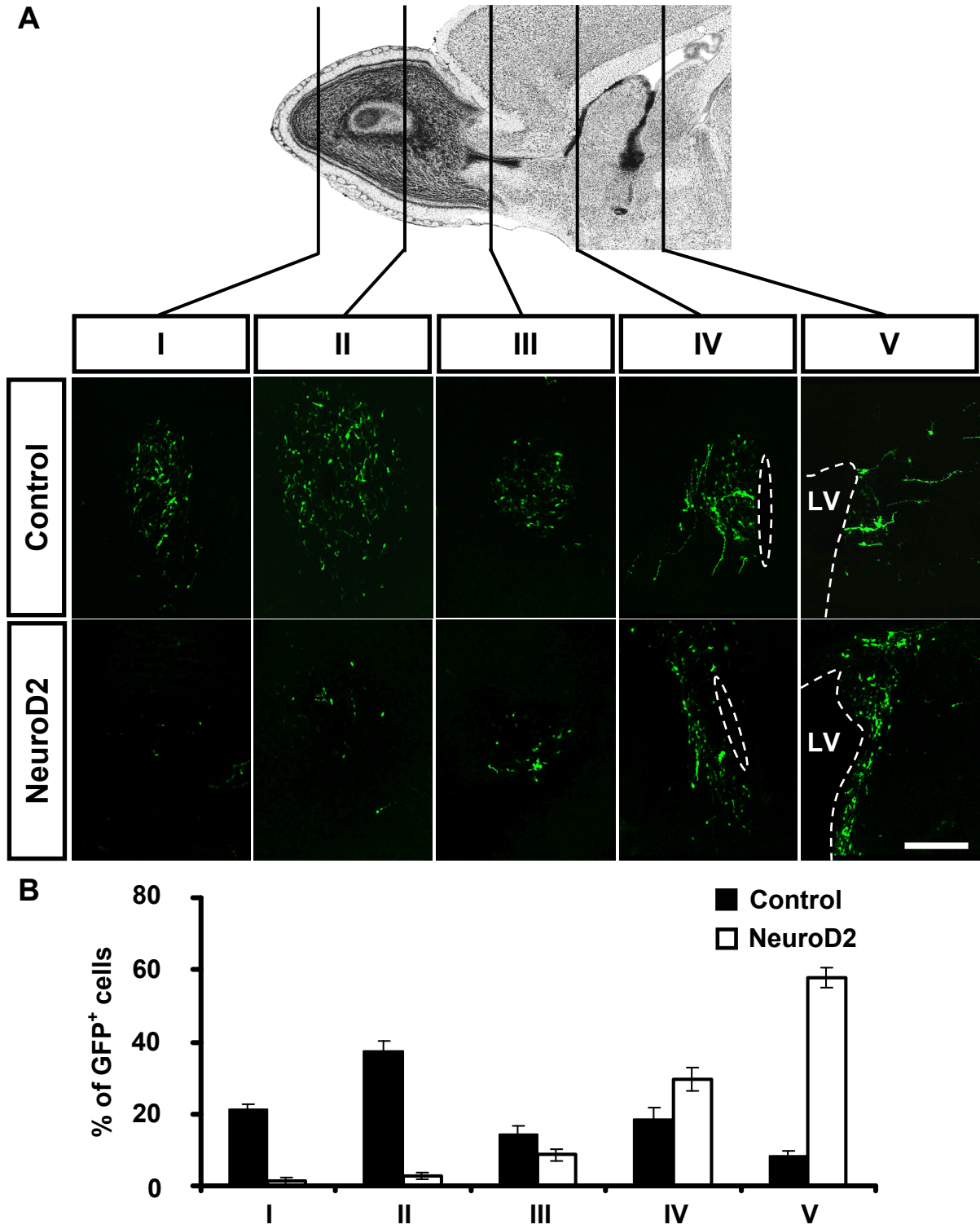
Figure 3.24: Analysis NeuroD2 transfected cells after 4 days *in vivo*

Figure legend on the next page

Figure 3.24: Analysis NeuroD2 transfected cells after 4 days *in vivo*

The localizations of respective coronal sections I to V are indicated by the black lines crossing the sagittal overview of a brain (A). In the control electroporation, the majority of GFP$^+$ cells were Type A neuronal precursors, localized mainly in the anterior part of the RMS or already in the core of the olfactory bulb, whereas only several radial glia cells remained in the SVZ. In contrast, cells overexpressing NeuroD2 showed normal morphology but were localized to much more caudal parts, especially the posterior SVZ. Subsequently, the transfected cells of control (n = 2168 cells from 6 mice) and NeuroD2 (n = 2022 cells from 6 mice) electroporations were quantified and displayed with their relative abundance in each slice (B). In the control, most of the cells were found in the anterior- (21.3%, Δ = 1.5%) or posterior core (37.5%, Δ = 2.8%) of the olfactory bulb, whereas only few cells remained in the anterior- (18.7%, Δ = 3.1%) or posterior SVZ (8.4%, Δ = 1.4%). Upon overexpression of NeuroD2 for 4 days, nearly no cells were localized in the anterior- (1.4%, Δ = 0.8%) and only a small percentage in the posterior olfactory bulb (2.8%, Δ = 0.8%). In contrast, most of the Type A precursors were found in the anterior- (29.6%, Δ = 3.1%) or posterior SVZ (57.6%, Δ = 2.7%), indicating decelerated or impaired migration upon NeuroD2 overexpression. Scale bar = 200 μm

3.7.5 Effects of NeuroD2 overexpression 15 days post electroporation

Considering the strong phenotype after 4 days of NeuroD2 overexpression, the influence of the observed differences on the further fate of transfected cells was investigated. To distinguish, if the onset of migration was completely blocked, or if the defect was rescued after a certain time, a time point 15 days after the initiation of NeuroD2 overexpression was analyzed. In the control condition, nearly all GFP$^+$ cells had reached the olfactory bulb and were differentiated in the granule- or the periglomerular layer (Fig. 3.25 A). In contrast, after NeuroD2 overexpression many of the cells still showed a bipolar, precursor like morphology and were localized in the center of the olfactory bulb (Fig. 3.25 B). Relative quantification of the specific cell types, namely the precursor like cells, the granular neurons and the periglomerular neurons, yielded significant variation with and without NeuroD2 overexpression (Fig. 3.25 C; n = 1184 cells from 8 mice for the control; n = 645 cells from 10 mice for NeuroD2). Most of the transfected cells were differentiated into granule cells or periglomerular interneurons in the control (77.8%, Δ = 2.9% for granule cells; 9.9%, Δ = 1.2% for periglomerular interneurons), whereas about 12.4% (Δ = 2.5%) still had a precursor like morphology. In the NeuroD2 electroporated mice, the portion of differentiated granule neurons but more strikingly that of periglomerular neurons was reduced (53.7%, Δ = 4.1% for granule cells; 2.0%, Δ = 1.0% for periglomerular interneurons), whereas the number of precursor like cells was significantly increased (44.3%, Δ = 4.8%). Indeed, the

final differentiation of periglomerular layer interneurons was affected most drastically with a reduction of about 80% in this subpopulation.
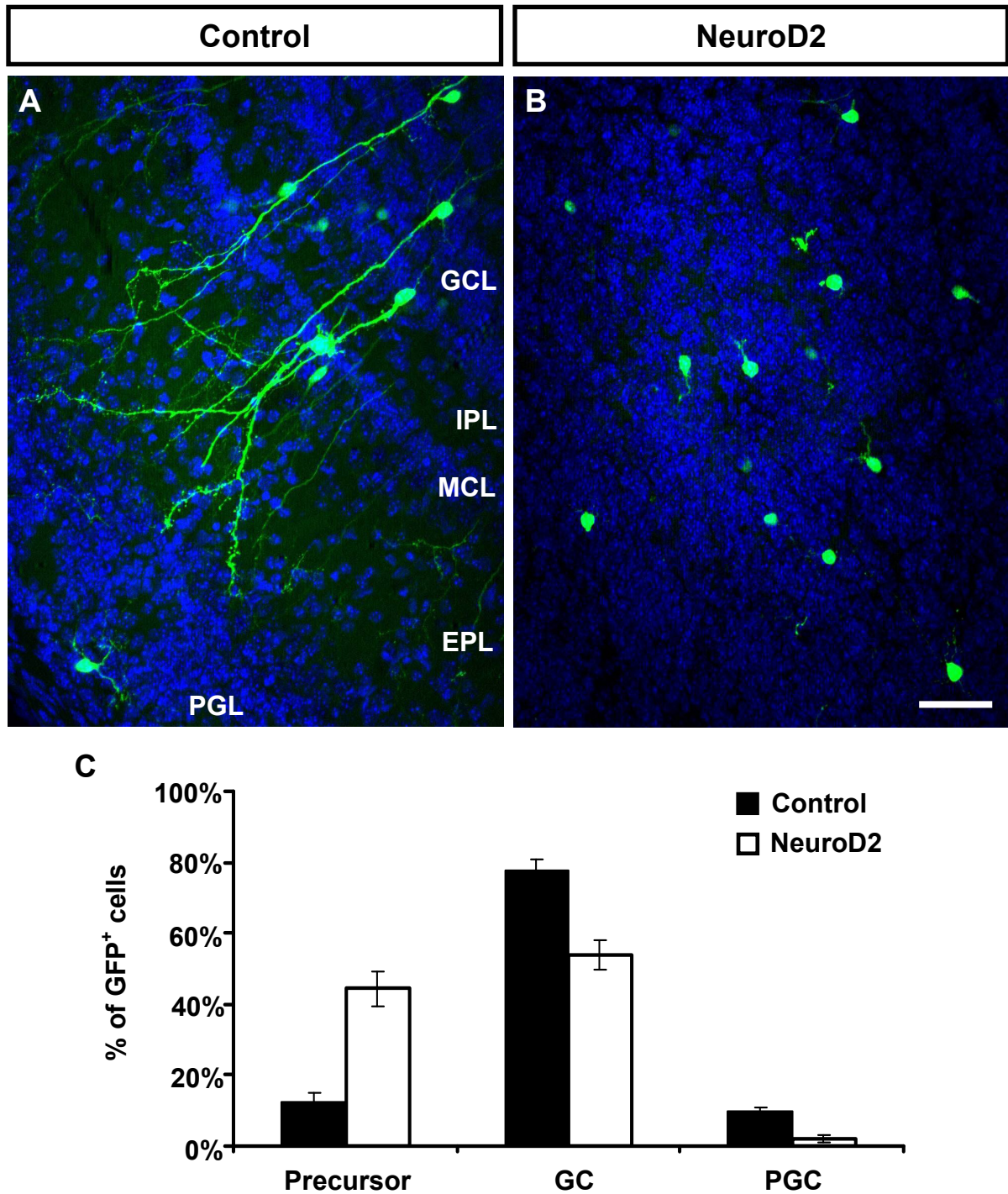
Figure 3.25: Analysis NeuroD2 transfected cells after 15 days *in vivo*

Figure legend on the next page

Figure 3.25: Analysis NeuroD2 transfected cells after 15 days *in vivo*

Coronal sections from the olfactory bulb of control (A) or NeuroD2 (B) electroporated mice showed differing distributions of transfected cells. Whereas in the control condition, nearly all GFP$^+$ cells had reached the olfactory bulb and were differentiated in the granule- or the periglomerular layer, after NeuroD2 overexpression many of the cells still showed a bipolar, precursor like morphology and were localized in the center of the olfactory bulb. The relative abundance of a specific cell types is indicated in C (n = 1184 cells from 8 mice for the control; n = 645 cells from 10 mice for NeuroD2). Most of the transfected cells differentiated into granule cells (77.8%, Δ = 2.9%) or periglomerular interneurons (9.9%, Δ = 1.2%) in the control, whereas about 12.4% (Δ = 2.5%) still had a precursor like morphology. In the NeuroD2 electroporated mice, the portion of differentiated granule neurons (53.7%, Δ = 4.1%) but more strikingly that of periglomerular neurons (2.0%, Δ = 1.0%) was reduced, whereas the number of precursor like cells (44.3%, Δ = 4.8%) was significantly increased. Scale bar = 50 μm; Abbreviations: GCL = granule cell layer; IPL = internal plexiform layer; MCL = mitral cell layer; EPL = external plexiform layer; PGL = periglomerular layer; GC = granule cell; PGC = periglomerular layer cell

The morphological analysis revealed that not only the ratio between differentiated and non-differentiated cells was shifted but that the morphology of the cells, especially that of periglomerular interneurons, was affected. In the control, GFP$^+$ cells that were localized in the periglomerular layer showed a differentiated morphology with multiple neurite branches innervating the glomeruli (Fig. 3.26 A). Upon NeuroD2 overexpression, cells in this area still showed a more precursor like morphology, as they had only few branches (Fig. 3.26 B). Several cells showed bipolar morphology, which was never observed in the control periglomerular layer after 15 days. Quantification of neurite branches revealed a significant reduction in case of NeuroD2- (8.7, Δ = 5.6; n = 52 cells from 10 mice) compared to control electroporated (52.8, Δ = 13.6; n = 52 cells from 8 mice) cells (Fig. 3.26 C).

To summarize these results, NeuroD2 overexpression decelerated the migration and changed the final differentiation of Type A neuronal precursor cells. This was particularly evident for the differentiation of periglomerular interneurons.
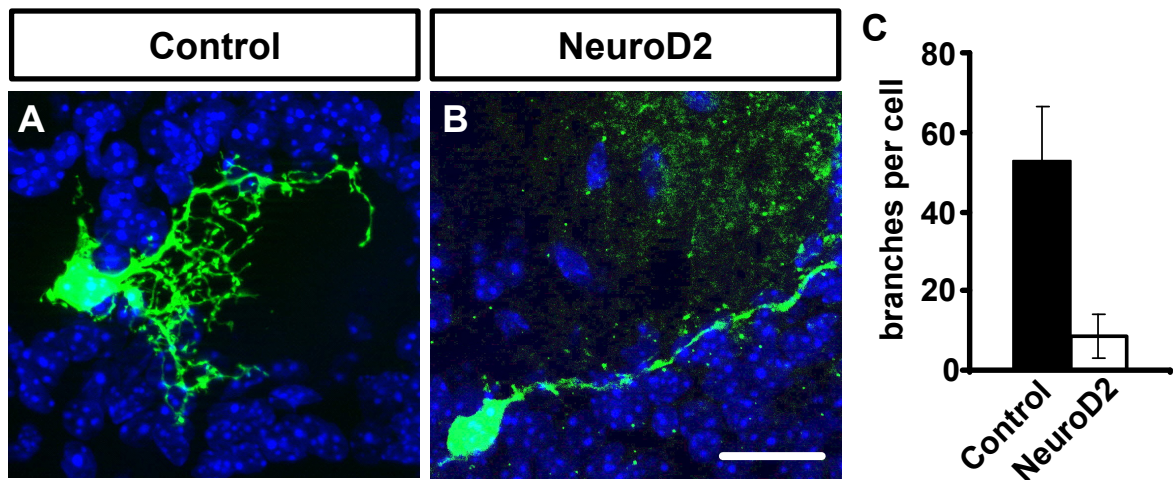
Figure 3.26: Analysis of periglomerular layer interneurons upon NeuroD2 overexpression

In the control, GFP$^+$ cells that were localized in the periglomerular layer 15 days post electroporation showed a differentiated morphology with multiple neurite branches innervating the glomeruli (A). Upon NeuroD2 overexpression, cells in this area still showed a more precursor like morphology with only few branches (B). Quantification of neurite branches revealed a significant reduction in NeuroD2- (8.7, Δ = 5.6; n = 52 cells from 10 mice) compared to control electroporated (52.8, Δ = 13.6; n = 52 cells from 8 mice) cells (C). Scale bar = 20 µm

3.7.6 Effects of NeuroD1 overexpression 2 days post electroporation

The transcription factor NeuroD1 was found to be upregulated during the final differentiation of periglomerular precursors to mature interneurons, indicating the involvement of NeuroD1 in the late stage of olfactory bulb interneuron differentiation. However, it had to be examined, if the increased expression was only a marker of differentiation, or if NeuroD1 is involved in the regulation of this final transition step.

As for NeuroD2, radial glia were transfected with the NeuroD1 expression vector pCX-ND1. The SVZ of electroporated mice was analyzed after 2 days (n = 10 mice for the control and 10 mice for NeuroD1). In the control, the morphology showed radial glia stem cells in the ventricular zone (VZ) and neuronal precursor cells in the SVZ (Fig. 3.27 A). In contrast, a dramatic reduction of radial glia cells was observed upon overexpression of NeuroD1 for 2 days (Fig. 3.27 B). No morphological differences were observed in the SVZ.

In conclusion, the expression of NeuroD1 is not compatible with radial glia identity.
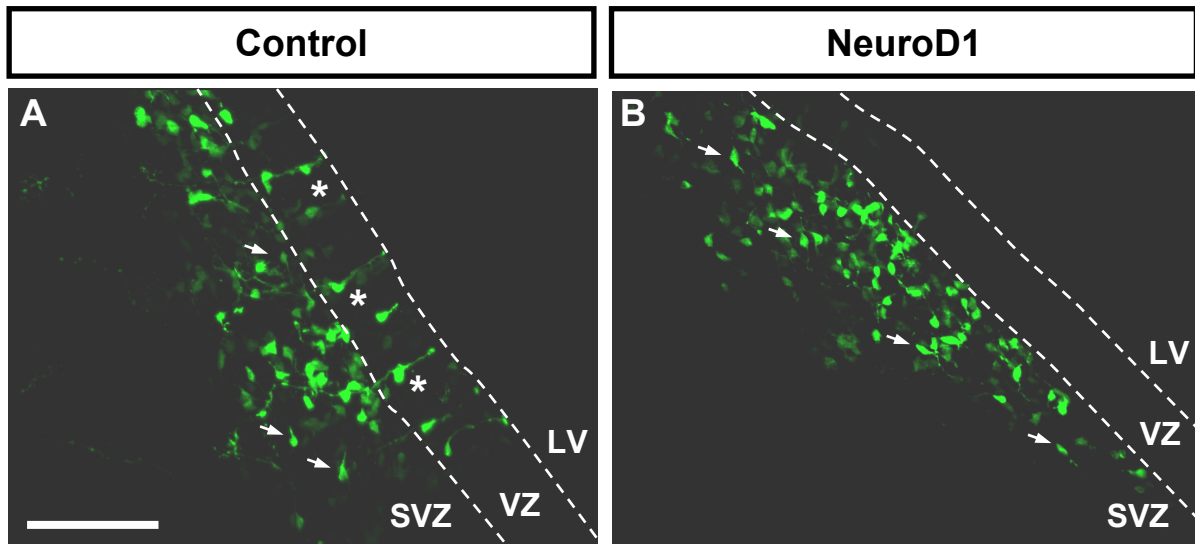
Figure 3.27: Analysis of NeuroD1 overexpression *in vivo* after 2 days

Two days after electroporation of either a control- or a NeuroD1 expression vector, the brains were sectioned coronally (n = 10 mice for the control and 10 mice for NeuroD1). The area between the lateral ventricle and the striatum is depicted. In the control, radial glia stem cells (stars) in the VZ as well as neuronal precursor cells (arrows) in the SVZ could be identified according to their morphology (A). Upon overexpression of NeuroD1, a dramatic reduction of radial glia cells was observed (B). No morphological differences were observed in the SVZ. Scale bar = 100 µm; Abbreviations: SVZ = subventricular zone; VZ = ventricular zone; LV = lateral ventricle

3.7.7 Effects of NeuroD1 overexpression 4 days post electroporation

Subsequently, the effect of NeuroD1 expression after an extended time period was examined. Sagittal and coronal sections of control- (n = 9 mice) and NeuroD1 (n = 10 mice) transfected brains were analyzed 4 days post electroporation. As already shown before, control electroporated cells at this time point were Type A neuronal precursors showing a bipolar, migratory phenotype (Fig. 3.28 A and B). These cells were mainly localized in the RMS or already in the core of the olfactory bulb. In contrast, a population of NeuroD1 expressing cells had left the RMS and was found inside the striatum (Fig. 3.28 C). In addition to their ectopic localization, also the morphology of these cells was different. Instead of the bipolar Type A cell phenotype, a multipolar, differentiated morphology was observed (Fig. 3.29 A and B). Furthermore, also cells inside the RMS (Fig. 3.28 D) or the olfactory bulb (Fig. 3.29 C) showed a multipolar phenotype which was similar to that of interneurons. Interestingly, there was a correlation between the expression level of GFP, and therefore NeuroD1, and the degree of altered morphology. Whereas the majority of cells with strong expression displayed

a differentiated morphology, cells with only weak expression showed a nearly normal phenotype, indicating a dose dependency.
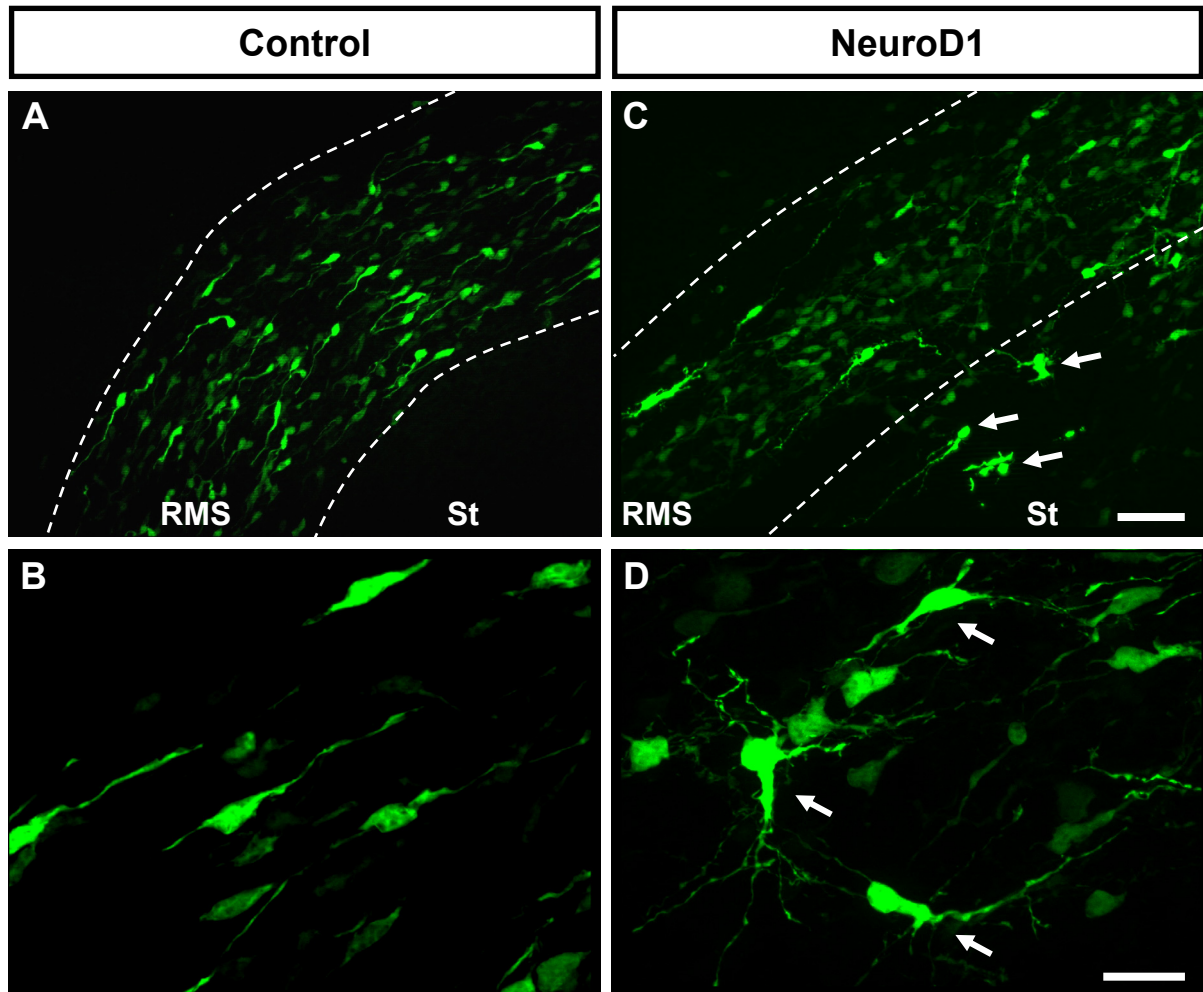
Figure 3.28: Analysis of precursor cells after NeuroD1 overexpression *in vivo* for 4 days

Sagittal sections of control (A and B) and NeuroD1 (C and D) transfected mice are shown. In the control (n = 9 mice), the majority of GFP^{+} cells were Type A neuronal precursors showing a bipolar, migratory phenotype (A and B). The cells in this region were exclusively localized in the RMS. Contrarily, a population of NeuroD1 expressing cells (n = 10 mice) had left the RMS and was found inside the striatum (C, arrows). This was observed in particular for the cells with highest transgene expression. In addition to their ectopic localization, also the morphology of these cells was different. Instead of a bipolar phenotype, a multipolar, differentiated morphology was observed (C). Furthermore, also cells inside the RMS (D, arrows) showed a multipolar phenotype which was similar to that of interneurons. Scale bar = 50 µm for A and C; 20 µm for B and D; Abbreviations: RMS = rostral migratory stream; ST = striatum
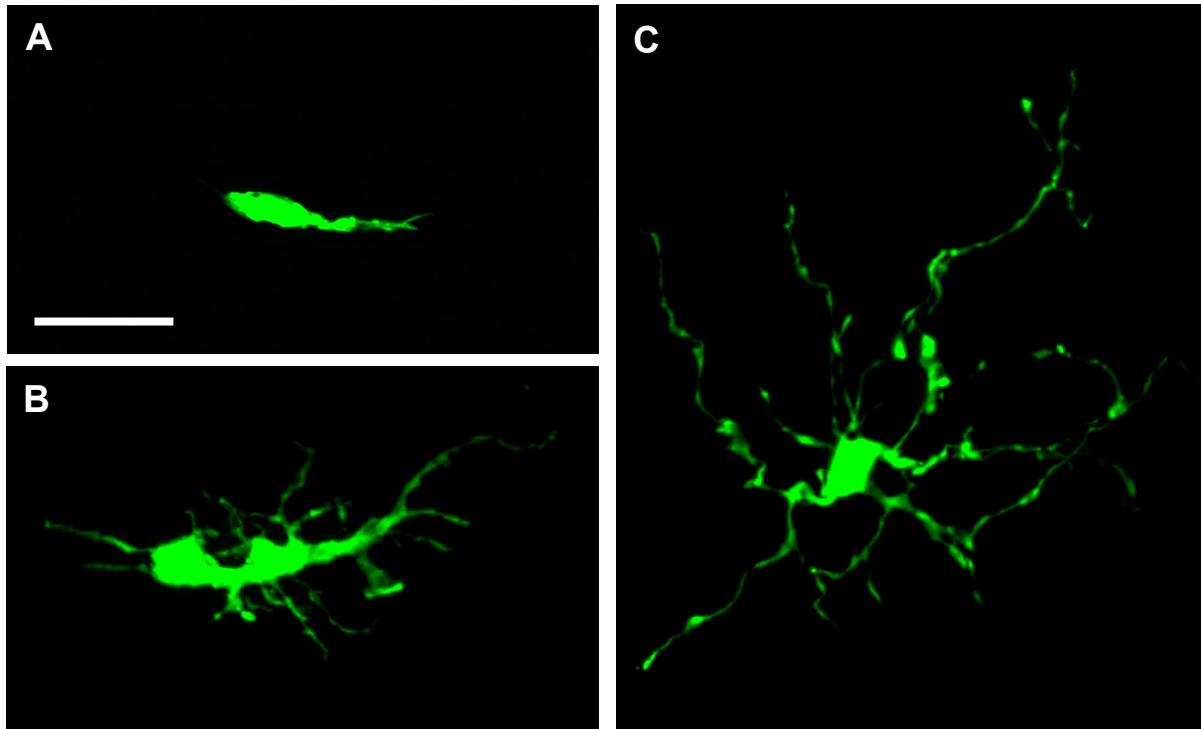
Figure 3.29: Cellular morphology upon NeuroD1 overexpression *in vivo* for 4 days
After 4 days of NeuroD1 overexpression, the cellular morphology changed dramatically. In the control, the majority of GFP⁺ cells were Type A neuronal precursors showing a bipolar, migratory phenotype (A). In contrast, a population of NeuroD1 expressing cells showed a multipolar, differentiated morphology. Some of these cells were found in the striatum (B) or the olfactory bulb (C) and had a phenotype which was similar to that of interneurons. Scale bar = 20 µm

As the cellular morphology upon NeuroD1 expression changed to a differentiated phenotype, the question was, if these transformations were accompanied with a characteristic change in the expression of known marker genes that indicate the differentiation status of the cell. To address this question, immunohistochemical stainings for the progenitor cell markers doublecortin (DCX) and PSA-NCAM were done (n = 4 mice for the control and 4 mice for NeuroD1). In the analyzed region of the anterior forebrain, all control transfected cells were localized inside the RMS and expressed the characteristic precursor markers DCX and PSA-NCAM (Fig. 3.30 A to D). In contrast, the differentiated cells transfected with NeuroD1 showed indeed no expression of these marker genes indicating an advanced state of differentiation (Fig. 3.30 E to H).
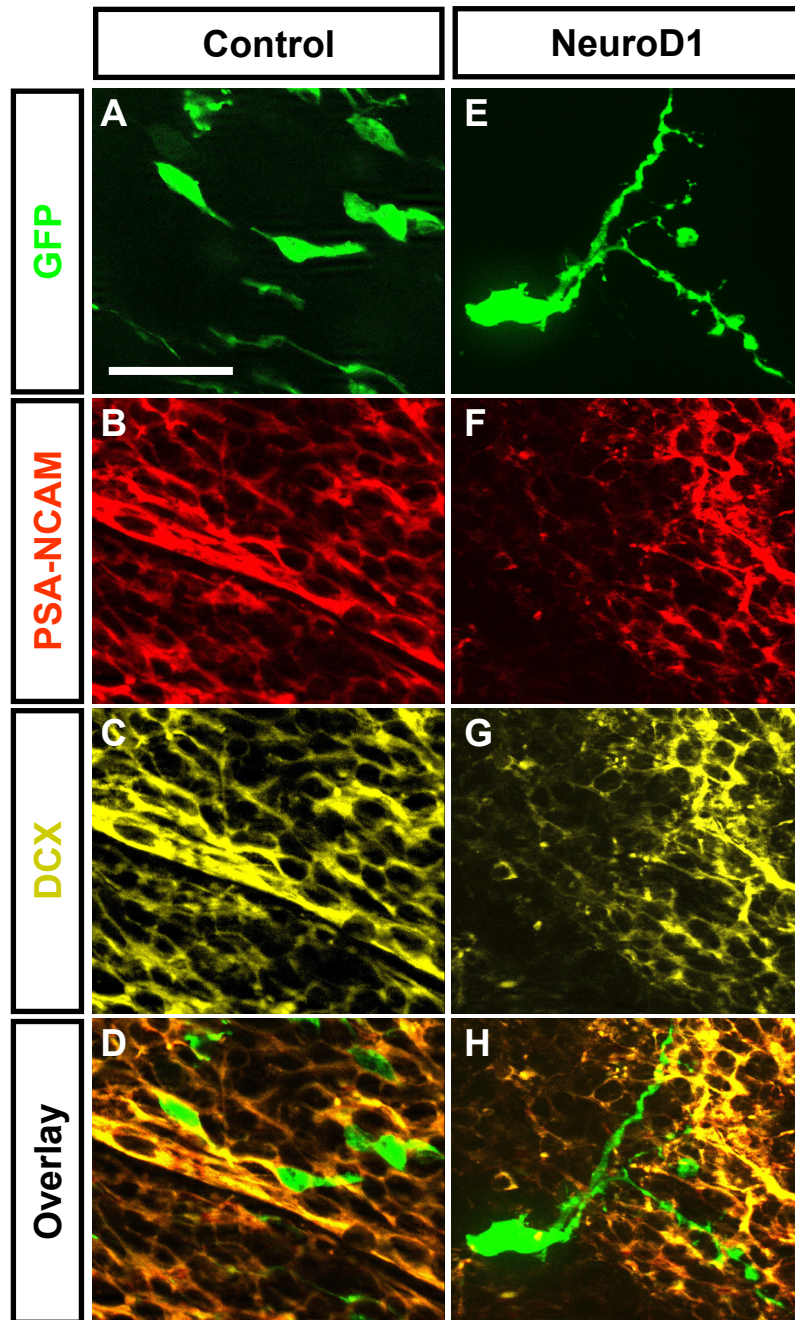
Figure 3.30: Immunohistochemical analysis for the expression of precursor markers

An immunohistochemical analysis of PSA-NCAM (red) and DCX (yellow) expression was done on sections from either control (A to D) of NeuroD1 (E to H) transfected brains after 4 days *in vivo* (n = 5 mice for the control and 5 mice for NeuroD1). In the anterior forebrain, all control transfected cells were localized inside the RMS and expressed the characteristic precursor markers DCX and PSA-NCAM (A to D). In contrast, the morphologically differentiated cells upon transfection with NeuroD1 showed no expression of these marker genes (E to H). Scale bar = 20 µm; Abbreviations: DCX = doublecortin; PSA = polysialic acid

The observation of an advanced differentiation state was further confirmed by the expression of NeuN, a frequently used marker specifically expressed in differentiated neuronal cells. As NeuN is upregulated upon differentiation of neurons, it is absent in all types of progenitor cells. Therefore, usually no expression of NeuN is found in the SVZ or the RMS. As expected, no specific staining was observed to colocalize with control transfected cells 4 days after electroporation (Fig. 3.31 A to C). In the SVZ and RMS of NeuroD1 electroporated mice however, NeuN was expressed and colocalized with transfected cells that showed a differentiated morphology (Fig. 3.31 D to F).
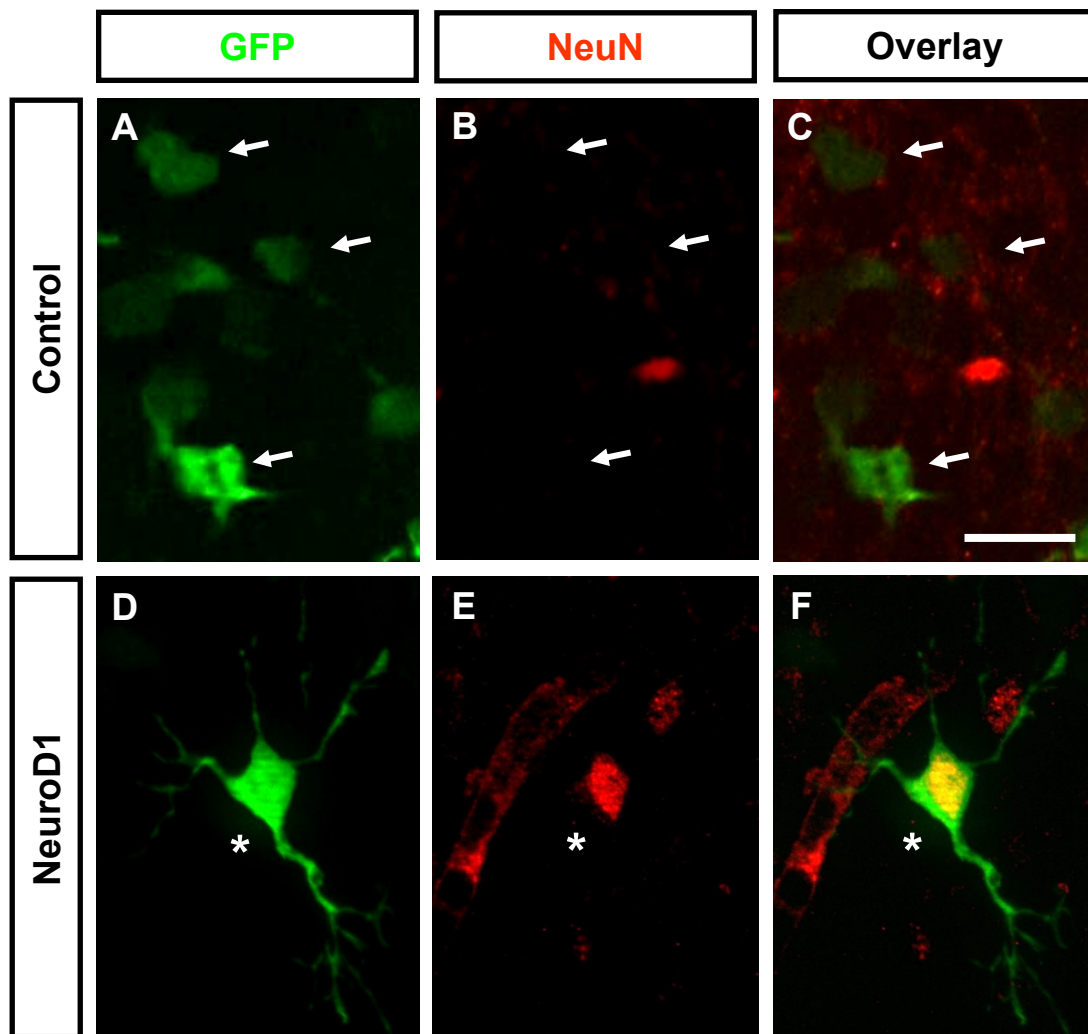
Figure 3.31: Immunohistochemical analysis for the expression of NeuN
An immunohistochemical analysis of NeuN (red) expression was done on sections from either control (A to C) of NeuroD1 (D to F) transfected brains after 4 days *in vivo*. No specific staining was observed to colocalize with control transfected cells (A to C, arrows). In the SVZ and RMS of NeuroD1 electroporated mice, NeuN was expressed and colocalized with transfected cells displaying a differentiated morphology (D to F, star). Scale bar = 10 µm

As suggested from the *in situ* hybridization (see Fig. 3.20), NeuroD1 seemed to be highly expressed only in a subpopulation of olfactory bulb interneurons. The aim was to determine, if cells expressing this transcription factor differentiate into a specific subpopulation of periglomerular interneurons. As already mentioned, one of these subpopulations localized in the olfactory bulb shows a bifunctional dopaminergic and GABAergic neurotransmitter phenotype. It was shown that the transcription factor PAX6 is necessary for the differentiation of these cells (Hack *et al.*, 2005). As PAX6 is activated by NeuroD1 (Marsich *et al.*, 2003), it was possible that also NeuroD1 is involved in this system. To test this hypothesis, TH-GFP mice were transfected with the NeuroD1 expression vector and mice analyzed after 4 days (n = 6 mice). TH-GFP mice express GFP under the control of the tyrosine hydroxylase promotor which becomes active exclusively in dopaminergic neurons (Sawamoto *et al.*, 2001). During postnatal neurogenesis, the TH promotor activity is restricted to the anterior RMS and the olfactory bulb (Saino-Saito *et al.*, 2004). To identify transfected cells, NeuroD1 was coelectroporated with a RFP expression vector, since GFP was already used as readout of TH promotor activity.

As expected, SVZ tissue not transfected with NeuroD1 showed no GFP$^+$ cells (Fig. 3.32 A to C), whereas upon NeuroD1 expression, GFP fluorescence was observed in this region. Colocalization analysis showed that only transfected cells became GFP$^+$ (Fig. 3.32 D to F). In addition, quantification of labeled cells in the SVZ (n = 298 cells from 6 mice, Fig. 3.32 G) showed that the vast majority of cells were GFP/RFP double positive (96.0%, Δ = 2.1% GFP/RFP double positive; 0.7%, Δ = 0.9% only GFP$^+$; 3.3%, Δ = 1.8% only RFP$^+$). Therefore, expression of NeuroD1 seemed to induce a differentiation towards a dopaminergic fate at ectopical localizations even after 4 days.
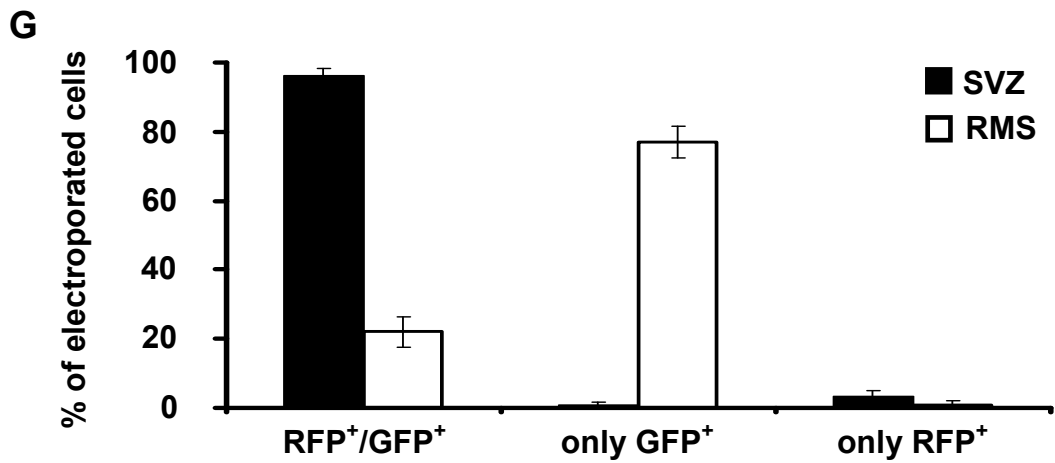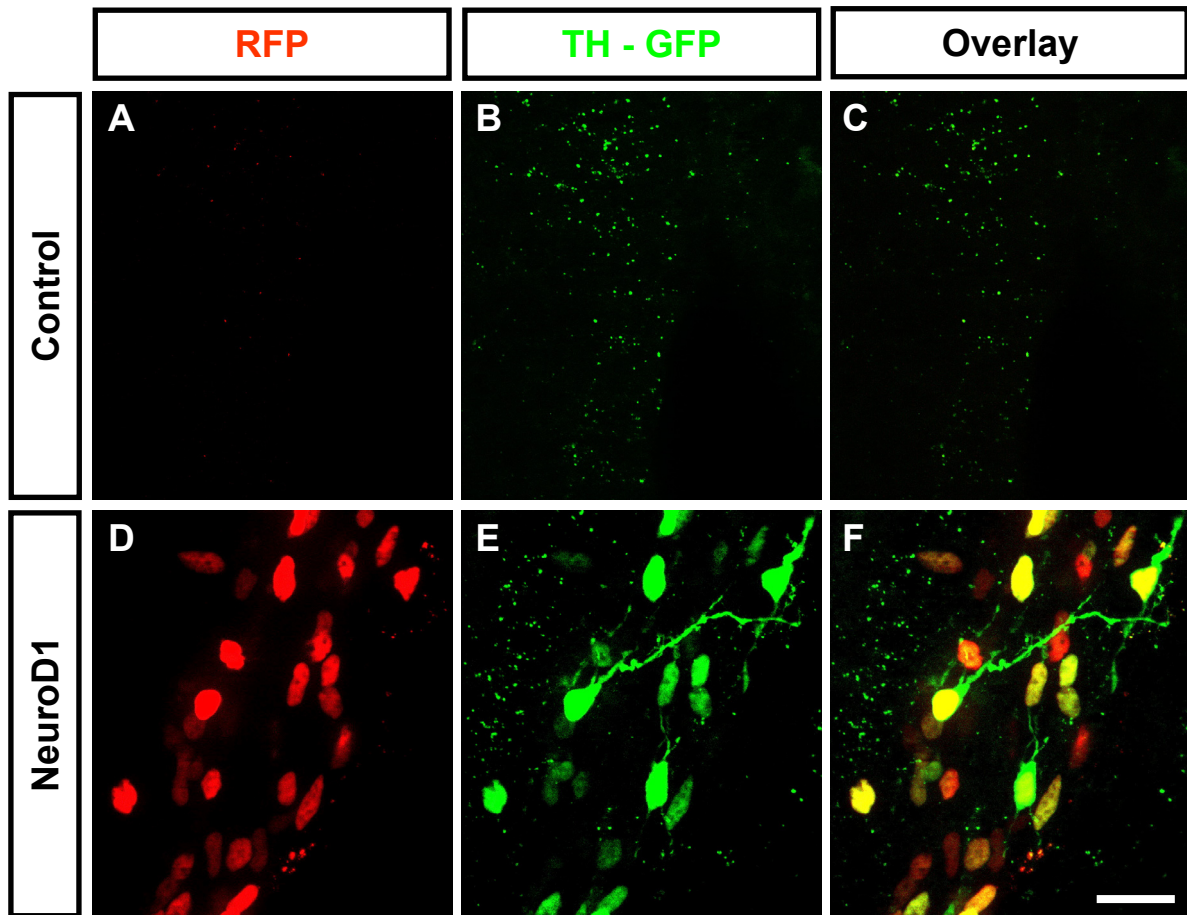
Figure 3.32: Analysis of effects on dopaminergic differentiation upon NeuroD1 expression

Figure legend on the next page

Figure 3.32: Analysis of effects on dopaminergic differentiation upon NeuroD1 expression

TH-GFP mice, expressing GFP specifically in dopaminergic neurons, were transfected with a NeuroD1 expression vector and analyzed after 4 days *in vivo* (n = 6 mice). Transfected cells were visualized by coexpression of RFP. SVZ tissue not transfected with NeuroD1 showed no GFP$^+$ cells (A to C). Upon NeuroD1 expression, GFP fluorescence was observed in the SVZ (E). Colocalization analysis showed that only cells expressing NeuroD1 became GFP$^+$ (D to F). Quantification of fluorescent cells in the SVZ (n = 298 cells from 6 mice) resulted in 96.0% (Δ = 2.1%) GFP/RFP double positive, 0.7% (Δ = 0.9%) only GFP$^+$ and 3.3% (Δ = 1.8%) only RFP$^+$ cells (G). Quantification of fluorescent cells in the RMS (n = 147 cells from 6 mice) resulted in 77.0% (Δ = 4.6%) only GFP$^+$ cells, reflecting the normal activation of the TH promoter in this region. In contrast, only 1.0% (Δ = 1.6%) of the cells were only RFP$^+$, whereas 22.3% (Δ = 4.3%) were GFP/RFP double positive, indicating that again nearly all transfected cells expressing NeuroD1 induced the TH-promotor. Scale bar = 20 µm; Abbreviations: RMS = rostral migratory stream; SVZ = subventricular zone

In addition to the TH promotor activation inside the SVZ, nearly all NeuroD1 transfected cells in the RMS (Fig. 3.33 A to C) and the striatum (Fig. 3.33 D to F) became GFP positive. However, as the TH promotor is naturally activated in the anterior part of the RMS (Saino-Saito *et al.*, 2004), many not transfected GFP$^+$ cells were found (Fig. 3.33 A to C). Quantification of fluorescent cells in the RMS (Fig. 3.32 G, n = 147 cells from 6 mice) resulted in 77.0% (Δ = 4.6%) GFP$^+$ only cells. In contrast, only 1.0% (Δ = 1.6%) of the cells were only RFP$^+$, whereas 22.3% (Δ = 4.3%) were GFP/RFP double positive, indicating that again nearly all transfected cells became dopaminergic. In addition, the GFP fluorescence was stronger in double positive cells, probably because the promotor was activated earlier and the GFP protein was already accumulated at this time.

To summarize these results, overexpression of NeuroD1 in neuronal progenitor cells induced a premature differentiation into an interneuron like phenotype at ectopic localizations. These cells adopted a multipolar morphology, downregulated the expression of precursor markers and induced the expression of markers specific for maturated neurons. In addition, nearly all NeuroD1 transfected cells induced a differentiation towards a dopaminergic fate.
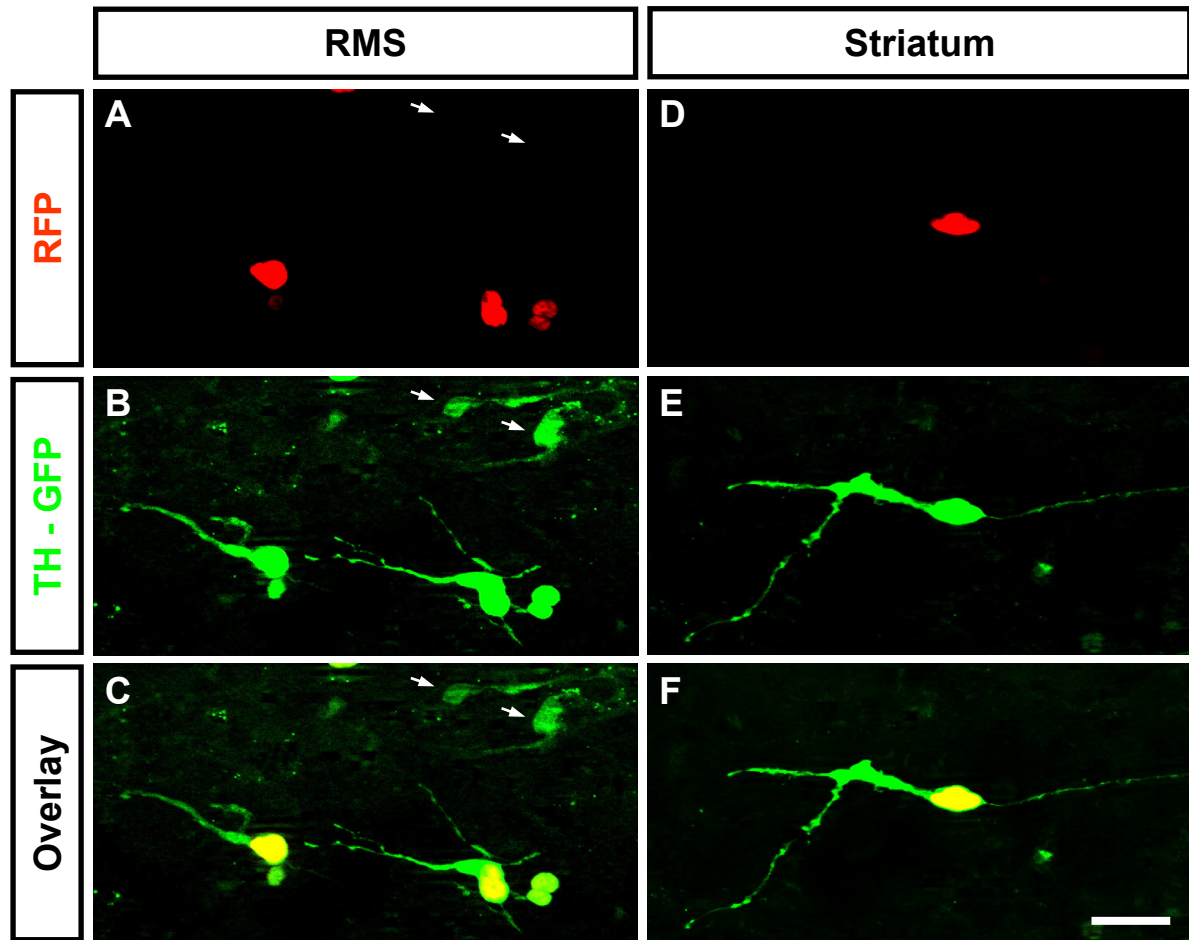
Figure 3.33: Analysis of effects on dopaminergic differentiation upon NeuroD1 expression

TH-GFP mice, expressing GFP specifically in dopaminergic neurons, were transfected with a NeuroD1 expression vector and analyzed after 4 days *in vivo* (n = 6 mice). Transfected cells were visualized by coexpression of RFP. Nearly all transfected cells in the RMS (A to C) and the striatum (D to F) became GFP positive. As the TH promotor is naturally activated in the anterior part of the RMS, many not transfected GFP^{+} cells were found (A to C, arrows). Scale bar = 20 µm; Abbreviations: RMS = rostral migratory stream

3.7.8 Effects of NeuroD1 overexpression at later time points

As already shown, NeuroD1 induced the differentiation of Type A neuronal precursor cells already after 4 days and at localizations which naturally do not show neuronal differentiation. To investigate the further fate of these cells, it was analyzed if they were able to survive and further differentiate in these regions.

Again, NeuroD1 was electroporated *in vivo* and the brains were removed and analyzed after 8 days (n = 10 mice for NeuroD1- and 10 mice for control electroporations). In the control, nearly all transfected cells had reached the olfactory bulb and started their final

differentiation. Most of them were localized in the granule cell layer and already extended a long primary dendrite in lateral direction (Fig. 3.34 A). Upon NeuroD1 transfection, the number of cells localized inside the olfactory bulb was strongly reduced (80% reduction compared to the control, Fig. 3.34 B). Furthermore, the morphology of cells that reached their correct position was different as again an increased number of processes was observed (Fig. 3.34 C). In contrast to the control, where no cells remained in the RMS, many NeuroD1 transfected cells were still found in this region (Fig. 3.34 D and E). In addition, the differentiated cells inside the striatum were still present; however, their number was reduced compared to the experiment at day 4 (Fig. 3.34 D and E).
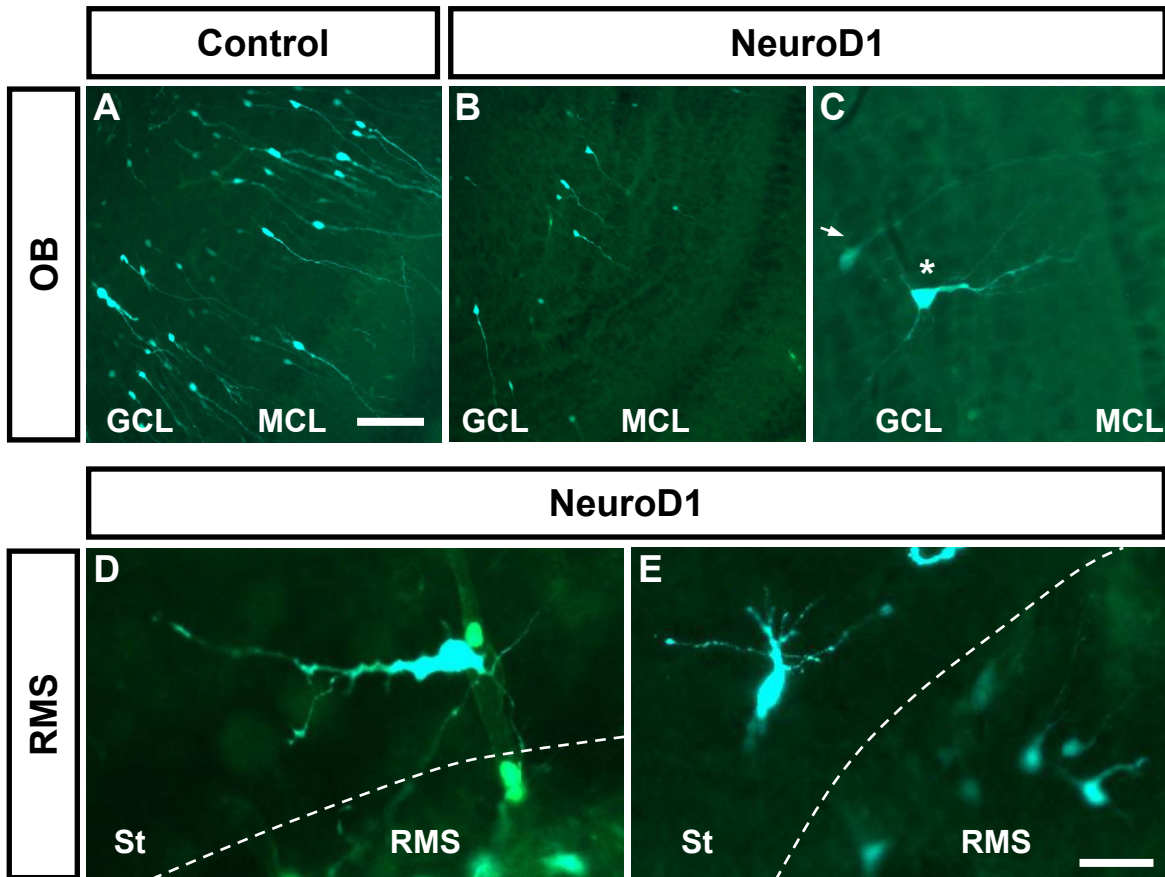
Figure 3.34: Analysis NeuroD1 transfected cells after 8 days *in vivo*

Eight days after electroporation of either a control- or a NeuroD1 expression vector, brains were removed and sectioned coronally (n = 10 mice for the control and 10 mice for NeuroD1). In the control, nearly all of the transfected cells reached the olfactory bulb and started their differentiation. Most of them were localized in the GCL and already extended a long primary dendrite in lateral direction (A). Upon NeuroD1 transfection, the number of cells localized inside the olfactory bulb was strongly reduced (>80% less cells compared to the control, B). The morphology of some cells that reached their correct position was different from the one found also mainly in the control (C, arrow), as again multiple processes were observed (C, star). In contrast to the control, where no cells remained in the RMS, many NeuroD1 transfected cells were still found in this region (D and E). Also the differentiated cells inside the striatum were still present (D and E). Scale bar = 50 µm for A and B, 20 µm for D and E; Abbreviations: RMS = rostral migratory stream; ST = striatum; GCL = granule cell layer; MCL = mitral cell layer; OB = olfactory bulb

The dramatic loss of NeuroD1 transfected cells was even more obvious after 15 days (n = 10 mice for NeuroD1- and 10 mice for control electroporations). Comparable to the control electroporation of the NeuroD2 experiment, most of the GFP only transfected cells were differentiated into granule- or periglomerular neurons after 15 days (Fig. 3.35 A). In contrast, nearly no GFP$^+$ cells were found anymore in NeuroD1 transfected brains (Fig. 3.34 B). The small amount of cells that were still present, expressed GFP only very

weak. In addition, GFP$^+$ cells in the SVZ of control mice were differentiated into ependymocytes or Type B neurogenic astrocytes, whereas only ependymocytes were found in the respective tissue upon NeuroD1 transfection (data not shown).

In conclusion, the number of neuronal precursors that reached their final positions in the olfactory bulb and differentiated into granule- or periglomerular layer neurons was strongly reduced upon expression of NeuroD1. Whereas after 8 days *in vivo* many of the cells were still present, all of them disappeared after 15 days indicating that massive apoptosis occurred in this fraction of prematurely and ectopically differentiated cells.
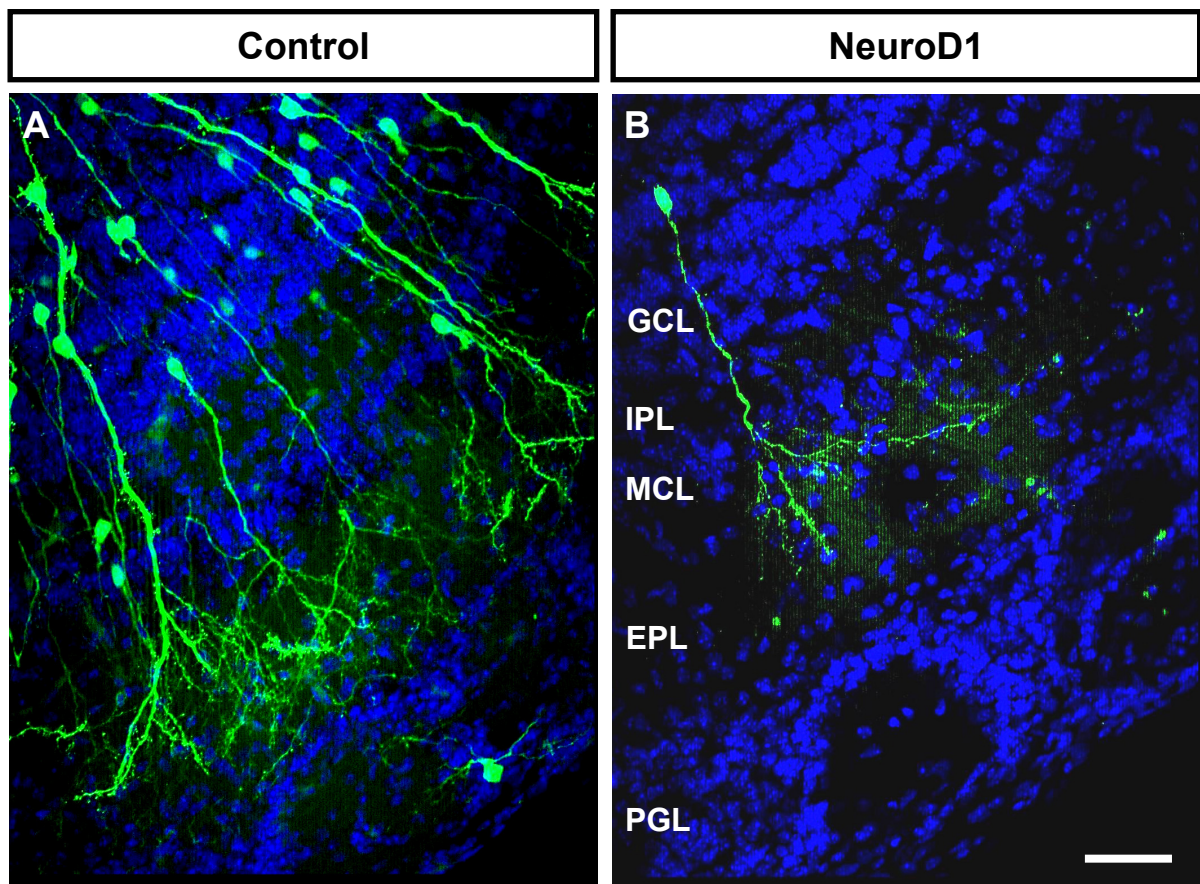
Figure 3.35: Analysis NeuroD1 transfected cells after 15 days *in vivo*

Fifteen days after electroporation of either a control- or a NeuroD1 expression vector, brains were removed and sectioned coronally (n = 10 mice for the control and 10 mice for NeuroD1). Most of the only GFP transfected cells were differentiated into granule- or periglomerular neurons after 15 days (A). In contrast, nearly no cells were found anymore in NeuroD1 transfected brains (B). The few cells that were still present in the olfactory bulb, expressed GFP only very weakly. Scale bar = 50 µm; Abbreviations: GCL = granule cell layer; IPL = internal plexiform layer; MCL = mitral cell layer; EPL = external plexiform layer; PGL = periglomerular layer

4 Discussion

4.1 The distribution of GABAergic neurons among different brain areas

As a first step towards the molecular analysis of GABAergic neurons, a new method for the isolation of these cells was established. The gentle dissociation in combination with the use of fluorescently labeled GABAergic neurons derived from the GAD67-GFP mouse strain (Tamamaki *et al.*, 2003) allowed for the quantification as well as the isolation of these cells by flow cytometry. The quantification of GABAergic neurons resulted mainly in two observations. First, the dynamic range of the cell numbers was very high, with about 3% of the total cells in the cerebellum and a 20-fold higher number in the olfactory bulb. Second, the number of GABAergic neurons in the olfactory bulb was considerably higher than previously reported. Kosaka *et al.* (Kosaka and Kosaka, 2005) concluded from immunohistochemical analyses that only 50% of glomerular neurons in the olfactory bulb are GABAergic, pointing to an overall lower number of this cell type than observed in the flow cytometric analysis. This may be due to the higher sensitivity of FACS in combination with the enrichment of GABA at synapses in the cell periphery, leading to low signal intensities of immunohistochemical staining in the cell soma. However, the higher number of GABAergic neurons that was found here is in agreement with recent data, claiming that almost all periglomerular cells are GABAergic (Panzanelli *et al.*, 2007) and do not represent a mixed population of either dopaminergic or GABAergic neurons. In addition, also developmental differences between neonatal and adult mice should be considered.

The dynamic range of GABAergic neuron numbers probably reflects the high degree of specialization for different brain regions, especially regarding information processing. For instance, while the olfactory bulb is mainly responsible for modulation of incoming sensory stimuli and replacement of interneurons might be one way to adapt to a continuously changing environment, the cerebellum coordinates motor output which depends on a high degree of recurring activity patterns.

4.2 The general gene expression signature of GABAergic neurons

Isolation of GABAergic neurons from whole brain tissue as well as distinct brain areas allowed molecular analysis of these populations by gene expression profiling. Combination of the transcriptomes of GABAergic neurons from whole brain, cortex, olfactory bulb, striatum and cerebellum led to the identification of genes that were expressed in all of these populations and may therefore represent genes important for GABAergic cell functionality in general. Furthermore, some of these candidates may serve as novel marker genes in addition to GAD1, GAD2 and VIAAT.

The transcriptome signature of general GABAergic neurons assembled, as expected, groups of over represented genes acting in GABA metabolism and groups of underrepresented genes related to non-GABAergic neurons and glia. Among the genes not described so far to be overexpressed in GABAergic neurons were mainly RNA processing enzymes, transcription factors and genes coding for cytoskeletal proteins. RNA processing enzymes like ADARB1 and DRADA have been shown to broaden the repertoire of electrophysiological properties by editing the mRNA coding for glutamate receptor subunits (Melcher *et al.*, 1996; Mittaz *et al.*, 1997). It is tempting to speculate that the closely related homologs ADARB2 and TRSPAP1, which were overexpressed in GABAergic neurons, fulfill similar functions to yet unknown targets, thereby adding a further level of regulation to input signal modulation. Furthermore, RNA editing mechanisms have been linked to different neurological diseases including Alzheimer's disease, Huntington's disease and schizophrenia (Akbarian *et al.*, 1995) and it would be interesting to address their roles in GABA related dysfunctions.

An interesting observation was the strong expression of genes that are linked to developmental processes in GABAergic neurons. For example, the strong presence of SOX7 and HOXA1, both genes that have multiple functions in brain development, point to a general delayed differentiation of GABAergic neurons. Furthermore, MYST4 (Qkf, Querkopf) plays a major role in the development of cortical interneurons and adult neurogenesis in the olfactory bulb (Merson *et al.*, 2006; Thomas and Voss, 2004). Although there was a peak of expression in the olfactory bulb, a universal and strong expression of MYST4 in interneurons from all brain areas was observed, suggesting that this gene might be a general marker for developing GABAergic neurons. Due to these observations, it might be interesting to test whether transgenic expression of MYST4 in embryonic stem- or adult progenitor cells is sufficient to drive GABAergic differentiation. This would allow generating a broader spectrum of

GABAergic neurons than it has been shown for DLX, which has a restricted expression in the developing mouse forebrain.

4.3 The genomic relationship among GABAergic neurons from different brain regions

In addition to the general genomic signature of GABAergic neurons, differences among GABAergic neuron subpopulations from distinct brain regions were defined.

Unsupervised hierarchical clustering of correlation coefficients pointed to a general genomic relationship between regionally defined interneurons. Whereas GABAergic neurons from all forebrain regions showed a high degree of similarity, major changes were observed when comparing forebrain to hindbrain populations. The major differences among fore- and hindbrain populations probably reflect their distinct origins that separate these subpopulations early during development. Whereas GABAergic neurons of the forebrain are generated mainly in the medial and caudal ganglionic eminences, those of the cerebellum originate from the ventricular neuroepithelium (Leto *et al.*, 2006; Xu *et al.*, 2004).

Nevertheless, a subgrouping among the forebrain populations was found, showing more differences between olfactory bulb cells to those of the striatum and cortex. This may be due to the general aspect that GABAergic neurons in the striatum and cortex are in late or even terminal differentiation stages, whereas in the olfactory bulb, the differentiation of these cell types from neuronal Type A precursor cells continues throughout live (Lledo *et al.*, 2006).

4.4 Differential gene expression reflected distinct functions of GABAergic neurons in specific forebrain regions

Unsupervised hierarchical clustering of correlation coefficients pointed to a general genomic relationship between regionally defined interneurons of the forebrain. However, differences between distinct forebrain populations were also evident. As mentioned above, olfactory bulb GABAergic neurons were clearly distinct from those of the striatum and cortex, probably because the olfactory bulb contains a considerable amount of type A interneuron precursors (Lois *et al.*, 1996). Previous studies showed that these precursors already express the here used selection marker GAD67 and would therefore be represented in the olfactory bulb samples. This immature cell population shows a particular gene expression profile in which, for example, gene clusters involved in cell cycle, apoptosis, axon outgrowth or chemotaxis are

highly represented (Pennartz *et al.*, 2004). Thus, the obvious differences might be partially due to a high degree of immature precursors in the olfactory bulb.

This view was exemplified by several factors specifically expressed in the olfactory bulb fraction. For example, FGF2 plays an important role in maintaining neural stem cells in the subventricular zone where the new interneurons destined for the olfactory bulb are generated. As a result of decreased neurogenesis in knockout animals, FGF2$^{-/-}$ mice have smaller olfactory bulbs (Zheng *et al.*, 2004). Furthermore, the phosphatidylinositol 3-kinase regulatory subunit gene PIK3R1 is crucial for neuronal cell proliferation and survival and a role of this isoform in neuronal signaling has been suggested (Horsch and Kahn, 1999).

Concerning recognition cues defining functional differences, strong expression of SLIT1/2 and ROBO1/2 in the olfactory bulb GABAergic neuron fraction was found. The Slits and ROBO1 have been directly implicated in the migration of precursors in the olfactory bulb (Chen *et al.*, 2001; Nguyen-Ba-Charvet *et al.*, 2004) as well as in cortical interneuron migration (Andrews *et al.*, 2007). The finding of additional strong ROBO2 expression in GABAergic neurons suggests that this receptor might also be involved in the guidance of postnatally generated interneurons in the forebrain.

In contrast to other forebrain interneurons, striatal GABAergic neurons are projection neurons. This was reflected by the finding that a variety of genes that were linked to cellular processes like axonogenesis and cytoskeleton control were differentially expressed compared to the other brain areas. Genes like CSF1, LAMA1, EDG1, BCL11B, FOXJ1 and TITF1 might represent regulators important to distinguish between interneuron and projection neuron morphologies. Furthermore, the two genes ACE and NOS were found to be enriched, whose expression lead to decreased reactivity of GABAergic neurotransmission, thereby modulating also specifically the electrophysiological properties of this subpopulation (Frisch *et al.*, 2000; Li and Pan, 2005).

Interestingly, Insulin-like growth factors and interacting partners were found to be over represented in the striatum. During brain development, IGFs act as tropic factors and are important for development of the nervous system (Naeve *et al.*, 2000). Although IGF2, IGF-receptors and binding proteins are expressed in the adult CNS, their role in the adult brain is less well understood (Dikkes *et al.*, 2007). Notably, while IGF1 is neuroprotective in mouse models of Huntington's disease, several reports have shown that IGF2 may antagonizes neuroprotective effects, possibly by displacing it from IGF-binding proteins (Alexi *et al.*, 1999; Dikkes *et al.*, 2007; Guan *et al.*, 1996). One important yet not fully understood feature

of Huntington's disease is the early loss of GABAergic neurons in the striatum prior to cell death in other brain areas. High expression of IGF2 and IGFBP3 especially in striatal GABAergic neurons - as observed in this study - may contribute to an increased sensitivity of these cells.

4.5 Forebrain and hindbrain GABAergic neurons are generated by different transcriptional mechanisms

Despite the fact that differences between the different forebrain populations could be clearly established, GABAergic neurons from these areas were strongly related concerning the transcription factors that regulate their generation and identity. This was particularly obvious when comparing forebrain interneurons to such isolated from the cerebellum.

Forebrain GABAergic neuron specific transcription factor families could be arranged in three groups, one connected to the Distal-less-family (DLX), a second to POU-transcription factors and a third linking ETS and FOX family members. DLX-genes are well known regulators of GABAergic differentiation with DLX1 and DLX2 in earlier and DLX5 and DLX6 in later stages (He *et al.*, 2001). Ectopic expression of DLX2 and DLX5 is sufficient to induce GAD1 expression and mice lacking DLX1 show subtype specific loss of interneurons, reduced inhibition and epilepsy (Cobos *et al.*, 2005b; Stuhmer *et al.*, 2002a; Stuhmer *et al.*, 2002b). In addition, transcription of ARX, the vertebrate homolog of *aristaless*, is regulated by DLX (Cobos *et al.*, 2005a) and essential for the correct formation of interneurons in the olfactory system (Yoshihara *et al.*, 2005). Finally, mutations of VAX1, as for other DLX family members, have been reported to impair forebrain interneuron generation (Taglialatela *et al.*, 2004). Also members of the other two families are linked to the development of the central nervous system (Hoekman *et al.*, 2006; McEvilly *et al.*, 2002; Shah *et al.*, 2006; Wijchers *et al.*, 2006). These transcription factor families may therefore regulate the identity and differentiation of forebrain specific GABAergic neurons.

In contrast, cerebellar interneuron identity and function appears to be regulated by fundamentally different factors. This was exemplified by the observation that none of the above forebrain specific factors was expressed or has been shown to be important for the generation of hindbrain GABAergic neurons. Instead, Zinc-finger transcription factors like ZIC1, ZIC2 and ZIC5 were found to be cerebellum specific. Furthermore, Engrailed2, LHX1

and LHX5 were highly over-represented in this brain region. For all of these genes, striking and specific cerebellar phenotypes have been observed in the corresponding murine knockout models. Mutations in ZIC1 and ZIC2 are responsible for abnormal cerebellar development and a targeted deletion of the Engrailed2 gene leads to an altered cerebellar foliation pattern (Titomanlio *et al.*, 2005; Wurst *et al.*, 1994). Besides these general cerebellar defects, mice lacking the function of LHX1 and LHX5 show a severe and specific reduction in the number of Purkinje cells (Zhao *et al.*, 2007). These genes may extend the knowledge about candidates important for differentiation of cerebellar GABAergic neurons, which is very limited so far to a few genes like PTF1A. PTF1A is highly expressed in a subpopulation of cerebellar ventricular zone precursors at embryonic stages E12 to E14 and specifically drives GABAergic over glutamatergic granule cell differentiation in the cerebellum (Hoshino *et al.*, 2005; Pascual *et al.*, 2007).

Also differences in the physiological function of GABAergic neurons among fore- and hindbrain populations were defined by several enriched candidates. One example was the strong presence of factors associated with the SST pathway. SST modulates GABA-signaling and a differential expression of its receptors during cerebellar development has been reported in rats (Bossy-Wetzel *et al.*, 2004b; Viollet *et al.*, 1997). Furthermore, differential expression of the potassium inwardly-rectifying channel KCNJ6 might characterize the specific electrophysiological features of these cells.

4.6 Candidates that may serve as surface markers for GABAergic neurons

To overcome the need of mouse strains with genetically labeled GABAergic neurons and maybe allow the purification of further subpopulations of these cells, new surface markers have to be identified. This would enable direct labeling of intact GABAergic neurons followed by magnetic or flow cytometric isolation protocols.

Many genes had been identified to be highly and specifically expressed in GABAergic neurons by gene expression profiling. However, only very few of these candidates were localized in the plasma membrane and could serve as cell surface markers for the isolation of GABAergic neurons. Only one of these, CD72, was identified for which an antibody specific for an extracellular epitope was available. The strong and specific expression of CD72 in GABAergic neurons, as identified by microarrays, was validated by *in situ* hybridization using postnatal day 1 as well as adult mice. Subsequently, a monoclonal antibody was used to

stain cells dissociated from GAD67-GFP mice to check for protein expression on GABAergic neurons. Unfortunately, no staining was observed on any brain cell (data not shown). There are several possible reasons for this observation. First, the protein can be sensitive to protease digestion. However, even with very low protease concentrations (either 10 min incubation in 0.5 U/ml Papain or 0.1% Trypsin), no staining was observed. Second, post-translational protein modifications, like glycosylations, may differ among distinct tissues. As the antibody was generated to recognize the CD72 protein on hematopoietic cells, it may not bind differently modified forms in the brain. And third, due to post-transcriptional regulation, the protein level may be too low for an antibody staining, although the mRNA level was rather high.

A parallel approach to the molecular identification of novel markers was to use purified GABAergic neurons directly as immunogenic material in order to generate antibodies specific for so far unknown surface markers of these cells. Unfortunately, ten different immunization approaches did not lead to the generation of a single specific antibody. One reason could be that GABAergic neurons do not express surface proteins which are exclusively expressed by these cells but also on other populations of brain cells. To overcome this problem, recombinant GFP protein was used as decoy instead of GFP$^-$ cells in several approaches, so that only the anti-GFP reactivity but not that for other proteins was directed to the contralateral lymph node. However, by using this strategy, again no specific antibody was identified. Furthermore, even the use of PHA-L as adjuvant did not result in a larger size of the target lymph nodes that were very small compared to the decoy lymph nodes. Therefore, the most likely explanation is that GABAergic neurons do not express highly immunogenic epitopes on their surface, or at least that these targets are highly sensitive to the obligatory protease treatment. The use of CpG as a more potent adjuvant increased the general efficiency but not the specificity of the immune response.

As an alternative to this approach, a newly established protocol for the direct identification of cell surface glycoproteins by tandem mass spectrometry was used (Zhang *et al.*, 2003). Thereby, novel surface markers can be identified directly on the protein level and therefore also overcome the mentioned problem of post-transcriptional regulation. A group of proteins was identified in the GFP$^+$ but not the GFP$^-$ fraction of cells isolated from GAD67-GFP mice. Most of these candidates were indeed known to be localized in the membrane fraction. Several identified proteins were also enriched in GABAergic neurons on the transcriptome level as found by the gene expression analysis. Other candidates, as expected, did not correlate with the transcriptome data. This can be explained by post-transcriptional regulation

and protein stability. In conclusion, several proteins were identified that are probably expressed on the surface of GABAergic neurons and can serve as targets for a directed generation of monoclonal antibodies. Furthermore, an analysis of the specific function for these candidates on GABAergic neurons may provide new insights for the understanding of this cell population. In addition, the proteins which were found only in the GFP$^-$ fraction might represent novel surface markers specific for other populations of brain cells. Therefore, they may be used either for the purification or the depletion of the respective cells.

4.7 Isolation and molecular analysis of olfactory bulb interneurons and their progenitors

In an additional approach, the differentiation of periglomerular layer interneurons was analyzed as it represents an appropriate and accessible model system for the generation of GABAergic as well as dopaminergic neurons. Like for the analysis of GABAergic neuron subtypes from distinct brain regions, a method for the isolation of the respective cell populations was established. In this case, the use of GFP-fluorescence in cells from the GAD67-GFP mouse strain as a marker was not possible, because GFP is also expressed in progenitor cells and distinct differentiation states can not be distinguished. However, the combination of reducing the starting population complexity by microdissection and a two step magnetic cell sorting approach based on the surface markers A2B5 and PSA-NCAM, allowed for the purification of early Type A neuronal precursors from the SVZ as well as late precursors and mature interneurons from the periglomerular layer. The purified populations were analyzed by whole genome gene expression profiling.

Unsupervised hierarchical clustering of correlation coefficients was used again to define a general genomic relationship between the respective cell populations. Both cell types isolated from the periglomerular layer grouped closely together but displayed major differences compared to early Type A neuronal precursors. This indicates that the major changes during the development of olfactory bulb GABAergic interneurons occur during the migration of Type A precursor cells from the SVZ to the olfactory bulb, whereas only minor changes occur during the late step of differentiation in the periglomerular layer. In addition, the genomic relationship as well as a multiclass SAM analysis resulted in a molecular validation of the proposed model in which PSA$^+$ periglomerular layer precursors represent an intermediate state between SVZ Type A precursors and PSA$^-$ periglomerular layer interneurons.

4.8 Genes important for early differentiation states of olfactory bulb interneurons

Several genes were found to be strongly upregulated in both periglomerular cell types compared to their SVZ progenitors and may therefore represent candidates important for early steps during the generation GABAergic interneurons.

Whereas known marker genes of neuronal precursors, like DCX and TUBB3 were downregulated, genes that were known before to be expressed in mature GABAergic neurons, like CALB1, CALR and NPY were upregulated (Kanatani *et al.*, 2000; Rohner-Jeanrenaud *et al.*, 1996). Also the upregulated gene PTN is linked to neuronal differentiation and neurite outgrowth (Carvalho, 2003). Furthermore, PTN as well as APOE, APOD, FBLN2, S100A1 and S100A13 have important functions in neuronal synaptic plasticity, calcium signaling and calcium homeostasis (Hartmann *et al.*, 1994; Okazaki *et al.*, 2002). In addition, NRXN1, which interacts with the also enriched NLGN2, influences synaptic transmission by regulating calcium channels (Comoletti *et al.*, 2003; Missler *et al.*, 2003), whereas VTN can selectively regulate the inactivating potassium current (Vasilyev and Barish, 2003). Interestingly, NLGN2 was shown to be specific for inhibitory synapses (Varoqueaux *et al.*, 2004), which matches with the observation that it is upregulated during differentiation. The enriched gene NOTCH1 is also involved in synaptogenesis by decreasing the number of dendrites but increasing the number of inhibitory synapses (Salama-Cohen *et al.*, 2006). FABP7, a Notch target gene in the central nervous system, was also upregulated (Anthony *et al.*, 2005). In summary, many candidates were identified that may play important roles during the regulation of synaptic plasticity in olfactory bulb interneurons.

In addition, an enrichment of further genes connected to neuronal differentiation was observed. EphrinA5, Semaphorin4A, Vimentin and CSPG3 act as axon guidance and cell motility factors (Lampa *et al.*, 2004; Li *et al.*, 2005; Menet *et al.*, 2003; Moretti *et al.*, 2006). Interestingly, it was shown that EphrinA5 expression is modulated by expression of different odorant receptors (Cutforth *et al.*, 2003). For SEPT4, a gene of the cytoskeleton, a role in the development of neurons was already published (Takahashi *et al.*, 2003). However, it was not connected to this system so far, whereas the enriched prion protein was already suggested to act during adult neurogenesis (Steele *et al.*, 2006). The glutamate receptors GRIK1 and GRINL1A, CALB1, CALR, GLUD, SLC13A3, MT2 and DBI correlated with an increased state of differentiation in periglomerular layer cells (Pajor *et al.*, 2001; Stankovic, 2005). Mice deficient for TNC show a delayed onset of odor detection, showing that a functional relevance for at least several of the identified candidates can be expected (de Chevigny *et al.*, 2006).

The upregulation of extracellular matrix components like MATN2, FBLN2, TNC, PTN, VTN and CSPG3 by periglomerular layer precursors and interneurons suggests an intrinsic role of these cells in building up the neurogenic environment of the olfactory bulb (Mates *et al.*, 2002). Furthermore, the high expression of APOE may be involved directly in the change from tangential chain- to radial individual migration of neuronal precursors upon arrival in the olfactory bulb. The apolipoprotein-E receptor 2 as well as its downstream signaling target, the adaptor protein disabled-1 is present in the migrating cells and Reelin acts as a detachment signal by activating this cascade (Ghashghaei *et al.*, 2007; Hack *et al.*, 2002). It is possible, that the high expression of APOE acts as an autocrine signal to enhance this process.

As shown for GABAergic neurons from other brain areas, also targets of the WNT signaling pathway, like APCDD1 (Jukkola *et al.*, 2004) as well as IGF1 were enriched. A number of transcription factors like OLIG1, XBP1, NFI/A, ZFP277, ZMYND11, GTF2B and E4F1 were strongly upregulated. Several of them, like Nuclear Factor I/A, are already known to be involved in neuronal development (Shu *et al.*, 2003; Wang *et al.*, 2004). However, the specific role of these genes during adult neurogenesis still has to be investigated.

4.9 Genes important for late differentiation states of olfactory bulb interneurons

Although a high correlation coefficient of 0.97 between periglomerular layer precursors and interneurons indicated a high similarity of these cell types, several candidates were identified that were significantly regulated and may therefore be important for this final step of differentiation. About three times more genes were strongly upregulated than downregulated, indicating that this step is mainly controlled by increasing gene expression of differentiation correlated genes.

Like for the results concerning periglomerular layer- against Type A cells, genes with functions in mature neurons, like GAD2, SST and NRXN, were identified to be upregulated in the PSA$^-$ fraction, whereas markers of neuronal progenitor cells, like TUBB3, Nestin and DCX, were further downregulated, correlating with an increased degree of differentiation.

An upregulation of NPY during the migration of Type A neuronal precursors from the SVZ to the olfactory bulb was described above. In the downstream transition from PSA$^+$ to PSA$^-$ periglomerular layer cells, upregulation of GPR103, an NPY receptor connected to the metabolic syndrome (Takayasu *et al.*, 2006), was found. This indicates the existence of an autocrine NPY signaling pathway in these cells.

Several genes that are important for vesicular and neurotransmitter transport, like STX3, STX6, SYT4 and SLC1A1 (Ferguson *et al.*, 2004a; Ferguson *et al.*, 2004b), became upregulated in mature interneurons. SLC1A1 is known to be expressed on GABAergic neurons, where it provides glutamate as a precursor for GABA synthesis (Palmada and Centelles, 1998).

A large group of genes connected to the cytoskeleton, important for neurite outgrowth, morphology and positioning, was differently expressed. Regulators of the cytoskeleton like KTN1 as well as NTRK3, C130076O07Rik, TBCE, BC050903 (DCAMKL1) and Ablim1 were upregulated, which are known to be involved in axon outgrowth and guidance (Bommel *et al.*, 2002; Deuel *et al.*, 2006; Erkman *et al.*, 2000; Martin *et al.*, 2002). Also the neurotrophic tyrosine kinase NTRK3, which plays a role in axon extension (Stenqvist *et al.*, 2005), was enriched, as was the receptor tyrosine kinase substrate SPRED1, of which a function in the brain was suggested (Engelhardt *et al.*, 2004). In contrast, CRMP1, MAPT, KIF5A, TUBB3 and EPB4.2 were examples of downregulated genes connected to the cytoskeletal control (Bretin *et al.*, 2005; Kanai *et al.*, 2000; Yamashita *et al.*, 2006). Many of the upregulated genes in this group are involved in neurite outgrowth, which is important for new interneurons finding their neuronal circuit. In contrast, the downregulated genes mainly function in the general migration of cells, important during earlier steps. Together, the regulation and interaction of these genes may regulate the final positioning, morphological changes and axonal innervations during the differentiation of periglomerular layer interneurons.

Furthermore, a number of transcription factors with expression differences among these populations were identified. Transcription factors like BHLHB9, PAX6 and PAX8, OBOX2 and 3, PMS1, SFPI1, GABPB1, MTF1, ZHX3, and ISL2, were enriched in mature interneurons. In contrast, transcription factors like PNMA1, SOX30, ZFP219, and NFKBIE were downregulated in PSA$^-$ interneurons. These genes are therefore likely to be involved in the specification of inhibitory interneurons. Interestingly, an oppositional regulation of the homeobox transcription factors DLX1 and DLX2 was observed. Whereas DLX2 was enriched in PSA$^-$ interneurons, DLX1 was enriched in PSA$^+$ precursors. In contrast, DLX5 and 6 were already downregulated in both periglomerular layer populations compared to Type A precursors. This suggests that DLX genes are important for the early as well as the late differentiation of olfactory bulb interneurons. In combination with the results that members of the DLX family were enriched in all GABAergic neuron populations of the forebrain, a general function of these genes for GABAergic differentiation from embryonic to adult stages

can be suggested, which is in concordance to published data (Brill *et al.*, 2008; He *et al.*, 2001). In addition, an oppositional regulation of the basic helix-loop-helix transcription factors ND1 (NeuroD1) and ND2 (NeuroD2) was observed. Whereas NeuroD1 became highly upregulated in mature interneurons, NeuroD2 was downregulated. In addition, also PAX6, a target gene of NeuroD1 (Marsich *et al.*, 2003) was upregulated upon differentiation. NeuroD1 as well as NeuroD2 are already known to be important factors in the development of the nervous system, but in contrast to the DLX genes, nothing was known about their function during the generation of inhibitory interneurons so far (Cho and Tsai, 2004; Noda *et al.*, 2006). As the regulation of these two candidates suggests a function during the differentiation of olfactory bulb interneurons, they were chosen for a further analysis in order to test their functional relevance *in vivo*.

4.10 Overexpression of NeuroD2 interfered with the migration and differentiation of neuronal precursors *in vivo*

The NeuroD2 expression was downregulated during differentiation of periglomerular interneurons. This suggested the importance of this transcription factor during an early state in the development of olfactory bulb interneurons. Also previous published results concerning NeuroD2 indicate an early function of this transcription factor during neurogenesis, important especially for an initial neurogenic fate decision (Lin *et al.*, 2004). In concordance, after overexpression of NeuroD2 in mouse embryonic stem cells, N1E-115 neuroblastoma cells, or P19 embryonal carcinoma cells, neuronal differentiation is observed (Farah *et al.*, 2000; Kanda *et al.*, 2004; Mie *et al.*, 2003). Furthermore, as a lack of NeuroD2 expression results in Congenital hypothyroidism (cretinism) in mice (Lin *et al.*, 2006), the understanding of its function during neurogenesis is of broad interest for the development of novel therapies. The question was, if NeuroD2 is downregulated only as a downstream result of an increasing differentiation state, or if this downregulation is necessary to allow further differentiation. To address this question, NeuroD2 overexpression was induced in radial glia, neuronal precursors and mature neurons of the olfactory system by *in vivo* electroporation.

After overexpression of NeuroD2 for 2 days *in vivo*, no significant different phenotype compared to the control condition was observed. In conclusion, a strong expression of this gene neither affects the stem cell properties of radial glia, nor impairs the behavior of Type C or early Type A progenitors regarding their cell morphology or division rate.

In contrast, 4 days after electroporation, a strongly altered phenotype was observed. Whereas in the control most of the electroporated cells were Type A neuronal precursors localized in anterior parts of the RMS or even arrived in the olfactory bulb, NeuroD2 overexpressing cells showed an overall more caudal localization. The majority of cells were still localized in the SVZ but showed normal bipolar morphology. This indicates that an expression of NeuroD2 above normal wild type levels decelerates or even impairs the migration of Type A neuronal precursor cells from the SVZ to the olfactory bulb. However, it has to be shown if the time the cells need to change from a non-migratory phenotype inside the SVZ into a migratory phenotype and enter the RMS is prolonged, or if the general speed of migration inside the RMS is altered. The first hypothesis seems to be more probable from the overall distribution of the cells as well as their intact morphology and orientation. However, an overall decreased migratory speed should be visible by *in vitro* migration assays.

In addition, the molecular mechanisms underlying this phenotype still have to be evaluated. The mechanisms allowing high migration speeds of up to 120 µm/h, as observed in wild type Type A cells, are poorly understood (Alvarez-Buylla and Garcia-Verdugo, 2002; Wichterle *et al.*, 1997). One possibility is that NeuroD2 directly or indirectly interferes with the expression of genes important for correct migration. Possible targets would be genes regulating microtubule polymerization and depolymerization, like the microtubule associated protein Doublecortin (Gleeson *et al.*, 1999). Doublecortin mutations do not affect the direction of migration but can reduce its velocity (Kappeler *et al.*, 2006; Koizumi *et al.*, 2006a; Koizumi *et al.*, 2006b). Other targets could be related cell surface adhesion- and chemotaxis signaling molecules. Besides PSA-NCAM (Cremer *et al.*, 1994), further candidates are α6β1 integrin that appears to be necessary for chain migration of Type A cells (Jacques *et al.*, 1998) or the Eph tyrosine kinase receptors EPHA4 and EPHB1-3, which are important for neuroblast migration (Conover *et al.*, 2000). On the other hand, NeuroD2 overexpression may result in a negative regulation of genes important for the onset of migration. This initiation is regulated by chemoattractive as well as chemorepulsive signals (Ghashghaei *et al.*, 2007). However, as the existence of an olfactory bulb is not essential for correct migration of Type A precursors (Kirschenbaum *et al.*, 1999), it seems that chemorepulsion is the main force to direct migration. Chemorepulsion mediated by Slit-Robo signaling may be involved in the migration of young neurons in the RMS (Hu, 1999; Wu *et al.*, 1999) and an overexpression of NeuroD2 probably extends the time until this pathway is activated. Additionally, interfering with chemoattraction signals mediated by DCC/Netrin signaling (Mason *et al.*, 2001; Murase and

Horwitz, 2002) may lead to comparable results. The interaction of NeuroD2 with these candidates will be analyzed in further studies.

A deceleration instead of a complete migratory block is also in agreement with the observation that after 15 days the precursors finally arrived in the olfactory bulb. In the control condition, most electroporated cells were differentiated into granule- or periglomerular layer interneurons after this time period. In contrast, a significantly higher amount of cells overexpressing NeuroD2 were still localized in the core of the olfactory bulb and showed a bipolar precursor like morphology. The most prominent effect was observed for periglomerular layer interneurons. Besides the strongly decreased amount of this cell type, their morphology was altered in the way that the number of neurite branches and synaptic connections was significantly reduced suggesting an immature state. Similar effects were observed during cortical development, where NeuroD2 was shown to regulate synaptic maturation of thalamocortical connections (Ince-Dunn *et al.*, 2006). Experiments with extended time periods are required to show if these effects originate from decelerated migration inducing prolonged differentiation, or if the maintained expression of NeuroD2 completely inhibits this process. This may be the case if NeuroD2 is a repressor of factors essential for final differentiation, like proteins involved in the regulation of the cytoskeleton, cell-cell contacts or synaptic maturation. A further goal would be the identification of the downstream target genes mediating these effects.

In conclusion, NeuroD2 represents a novel key regulator involved in the control of olfactory bulb interneuron generation and its downregulation is essential for normal differentiation.

4.11 Overexpression of NeuroD1 induced highly specific a premature and ectopic dopaminergic differentiation *in vivo*

In contrast to NeuroD2, the expression of NeuroD1 was upregulated during the final differentiation of periglomerular layer precursors into mature interneurons. This suggested an importance of this transcription factor during the late state of olfactory bulb interneuron development, which is in agreement with published data from other systems. Mice lacking NeuroD1 show a malformation of the dentate gyrus, the cerebellum and develop epilepsy (Liu *et al.*, 2000b; Miyata *et al.*, 1999). Interestingly, the granule cells of the dentate gyrus in these mice are normally generated but fail to mature (Schwab *et al.*, 2000). The function of NeuroD1 for the final step of differentiation in this system is supported by the here presented observation of an upregulation in a late state of development. Notably, granule cells of the

dentate gyrus and cerebellum are, like periglomerular interneurons, postnatally generated microneurons, suggesting a general role for NeuroD1 during postnatal differentiation. In addition, NeuroD1 mutant mice show a severe reduction of sensory neurons in the cochlear-vestibular ganglion important for vestibular and auditory systems (Kim *et al.*, 2001; Liu *et al.*, 2000a) and also the terminal differentiation of photoreceptors is dependent on its expression (Pennesi *et al.*, 2003). The consequential question was again, if the upregulation of NeuroD1 is only a marker of an increasing differentiation state, or if this upregulation is essential or even sufficient to drive final differentiation. Therefore, the effects upon ectopic expression of NeuroD1 were analyzed by *in vivo* electroporation.

Overexpression of NeuroD1 for two days resulted in an efficient and specific depletion of radial glia. This indicates that an expression of NeuroD1 is not consistent with stem cell maintenance. A possible explanation is that NeuroD1 either activates genes responsible for the transition of radial glia into progenitor cells or represses factors important for a stem cell status. Usually, radial glia undergo asymmetrical divisions resulting in one precursor and one radial glia cell (Merkle and Alvarez-Buylla, 2006). Perhaps a NeuroD1 mediated impairment of initiating the correct asymmetry results in a prematurely conversion of radial glia into precursor cells. Further studies will focus on the identification of target genes mediating this phenotype.

A dramatic phenotype appeared upon overexpression of NeuroD1 for 4 days. In the control condition, the majority of cells were bipolar Type A neuronal precursors in the RMS at this time point. In contrast, cells expressing NeuroD1, especially the cells with high electroporation efficiencies, were localized at ectopic positions and showed a multipolar, interneuron-like morphology. Comparable morphologies were found in the control first after approximately 15 days. This indicates a dose dependent effect of NeuroD1 for the regulation of the cellular differentiation state. Besides the induced morphological differentiation, also the expression of known differentiation marker genes was altered. Cells expressing NeuroD1 downregulated the expression of precursor markers like DCX and PSA-NCAM. As PSA-NCAM is important for the regulation of cell adhesion in the RMS (Chazal *et al.*, 2000; Ono *et al.*, 1994), its downregulation may represent an initial reason for the ectopic localization of many cells. Probably, after downregulation of PSA-NCAM the cells are displaced by the migratory population. A possible changed expression of other cell adhesion- and chemotaxis signaling molecules towards a more mature composition could also lead to an active innervation of the striatum as it represents the nearest niche for mature neurons. In concordance to the downregulation of progenitor marker genes, expression of NeuN, a

frequently used marker of differentiated neurons, was induced. As the morphology of ectopically localized cells inside the striatum was still interneuron-like, a significant part of the final cellular morphology seems to be regulated intrinsically rather than dependent on extracellular cues. Strikingly, an examination of the neurotransmitter phenotype resulted in the observation of a highly specific differentiation towards a dopaminergic fate. In the control condition, expression from the TH-promotor, a specific marker for dopaminergic cells, is activated only in the anterior RMS and mature dopaminergic neurons are exclusively found in the granule and periglomerular layers of the olfactory bulb (Saino-Saito *et al.*, 2004; Sawamoto *et al.*, 2001). The observation of an ectopic and premature differentiation towards a dopaminergic fate inside the striatum, SVZ and RMS suggests that NeuroD1 is a key regulator for the specification of this olfactory bulb interneuron subtype. Interestingly, the PAX6 gene, which was also found to be enriched in mature interneurons, is activated by NeuroD1 (Marsich *et al.*, 2003). It was shown that precursors deficient for PAX6 can not differentiate into dopaminergic neurons anymore (Hack *et al.*, 2005; Kohwi *et al.*, 2005). This suggests that NeuroD1 is a novel regulator for dopaminergic differentiation which is mediated by the activation of PAX6. In addition, as PAX6 was shown to be essential for this step, it is likely that also the expression of NeuroD1 is not only sufficient but furthermore essential for a dopaminergic fate decision. However, an inhibition of NeuroD1 expression is necessary to finally proof this hypothesis. A recent study claims further that a direct interaction between DLX2 and PAX6 is important for dopaminergic differentiation (Brill *et al.*, 2008). The overexpression of PAX6 and DLX2 by *in vivo* electroporation may answer the question, if there are additional genes involved in this cascade and if their expression is also sufficient to induce ectopic and premature dopaminergic differentiation.

After an extended period of time, the cells that were electroporated with NeuroD1 disappeared. Whereas after 8 days cells with neuronal morphology inside the striatum and the RMS were still visible, none of these cells were found after 15 days, indicating that this population was removed, most probably by apoptosis. About 50% of the newly generated cells, especially those which do not differentiate properly, are removed by programmed cell death also under wild type condition (Kim *et al.*, 2007; Lemasson *et al.*, 2005). It is widely accepted that neuronal survival is strictly dependent on extracellular signals, like neurotrophin signaling and correct synaptical activity (Lipsky and Marini, 2007). The premature and ectopic differentiation of neuronal precursors upon NeuroD1 expression impairs their correct positioning as well as circuit establishment. This probably results in the displacement from

correct survival factors resulting in extensive anoikis. Further experiments will define the exact time window and perhaps the involved signaling cascades of induced cell death.

The observed effects seem to be specific for this system, as preliminary experiments showed no effect of NeuroD1 overexpression in cortical projection neuron precursors (data not shown). This may be due to an already fixed developmental fate of these cells. However, it was shown that PAX6 is essential for the generation of glutamatergic neurons during cortical development (Heins *et al.*, 2002; Kroll and O'Leary, 2005; Nikoletopoulou *et al.*, 2007; Stoykova *et al.*, 1996). As NeuroD1 activates PAX6 (Marsich *et al.*, 2003), its role may be changed in this system because of altered functions for such downstream effectors. Another point could be that the progenitor population is not competent to respond to NeuroD1 expression in this case, for example due to missing additional cofactors which still have to be identified.

In summary, an early overexpression of NeuroD1 is not compatible with the stem cell status of radial glia cells. Furthermore, NeuroD1 can induce the premature and ectopic differentiation of neuronal precursors in the striatum, RMS and SVZ towards a dopaminergic neurotransmitter phenotype. This effect seems to be dose dependent.

5 Conclusion and Outlook

In the first part of this work, a molecular analysis of regionally defined GABAergic neurons was carried out. This analysis was based on the establishment of a protocol for the isolation of highly pure GABAergic neuron populations from distinct brain areas. Potential new marker genes for GABAergic neurons and factors probably important for their differentiation and general functionality were determined. Furthermore, genes characteristic for regionally defined populations of GABAergic neurons were identified, reflecting region specific functionality and pointing to different developmental pathways generating fore- and hindbrain subpopulations. These genes build a molecular basis for a detailed understanding of morphological, physiological and developmental differences among these cells and can be used, for example, to generate region-specific knockout mice using the Cre/loxP-system.

Furthermore, putative cell surface markers specific for GABAergic neurons were identified by defining the cell surface proteome. These candidates allow for the targeted generation of antibodies that would enable new possibilities to purify GABAergic neurons or even subpopulations of these cells.

In summary, this study led to the identification of new candidate genes that will be characterized in future analysis to increase our understanding of the genesis and function of GABAergic neurons and associated diseases.

In the second part of this work, a specific molecular analysis of interneuron differentiation was carried out. The isolation and characterization of mature olfactory bulb interneurons as well as their progenitor cells allowed for the identification of genes involved in the regulation of this differentiation process. Two of these candidates, NeuroD1 and NeuroD2, were analyzed for their functional relevance *in vivo*.

The overexpression of NeuroD2 decelerated or even impaired the migration and differentiation of neuronal precursor cells. Therefore, NeuroD2 represents a novel key regulator involved in the control of olfactory bulb interneuron generation probably via maintaining the precursor state. Further experiments have to identify target genes of NeuroD2 and clarify the basal mechanisms underlying these effects. Migration assays after the overexpression or knock down of NeuroD2 *in vitro* and *in vivo*, for example by shRNA, probably will increase our understanding concerning these points.

In contrast, the overexpression of NeuroD1 is sufficient to induce the premature and ectopic differentiation of neuronal precursors in the striatum, RMS and SVZ towards a dopaminergic

neurotransmitter phenotype. Subsequent experiments will show, if NeuroD1 is also essential or if there is a redundancy in this system. Therefore, the knockdown of NeuroD1 expression by shRNA or the complete knock out by electroporation of a Cre-expression construct in conditionally targeted mice will be done in the near future. It would be also interesting to investigate a possible interaction between NeuroD1 and NeuroD2, for example a dependent cross regulation and to identify novel target genes as well as interacting partners of NeuroD1. As the SVZ represents a major source for adult stem cells in the brain, its targeted modulation has a huge potential for intrinsic repair approaches upon neurodegeneration. In addition, it will be addressed, if the expression of NeuroD1 alone or in combination with additional factors can induce dopaminergic differentiation in embryonic stem- or induced pluripotent stem cells. Grafting of such cells into the striatum of Parkinson's disease model mice would represent the first step towards a therapeutic application. However, further molecular and electrophysiological characterization of these cells need to be done prior to downstream applications.

This study yielded new insights on the regulation of adult neurogenesis. As the SVZ is affected by multiple neurodegenerative diseases, like Huntington's-, Parkinson's- and Alzheimer's disease, understanding the underlying mechanisms is essential for the development of novel cell- or drug based therapeutic approaches.

6 Appendix

6.1 Sequences of NeuroD1 and NeuroD2

Protein Sequence of NeuroD1 (single letter amino acid code):

```
        10         20         30         40         50         60
MTKSYSESGL MGEPQPQGPP SWTDECLSSQ DEEHEADKKE DELEAMNAEE DSLRNGGEEE

        70         80         90        100        110        120
EEDEDLEEEE EEEEEEEDQK PKRRGPKKKK MTKARLERFK LRRMKANARE RNRMHGLNAA

       130        140        150        160        170        180
LDNLRKVVPC YSKTQKLSKI ETLRLAKNYI WALSEILRSG KSPDLVSFVQ TLCKGLSQPT

       190        200        210        220        230        240
TNLVAGCLQL NPRTFLPEQN PDMPPHLPTA SASFPVHPYS YQSPGLPSPP YGTMDSSHVF

       250        260        270        280        290        300
HVKPPPHAYS AALEPFFESP LTDCTSPSFD GPLSPPLSIN GNFSFKHEPS AEFEKNYAFT

       310        320        330        340        350
MHYPAATLAG PQSHGSIFSS GAAAPRCEIP IDNIMSFDSH SHHERVMSAQ LNAIFHD
```

Protein Sequence of NeuroD2 (single letter amino acid code):

```
        10         20         30         40         50         60
MLTRLFSEPG LLSDVPKFAS WGDGDDDEPR SDKGDAPPQP PPAPGSGAPG PARAAKPVSL

        70         80         90        100        110        120
RGGEEIPEPT LAEVKEEGEL GGEEEEEEEE EEGLDEAEGE RPKKRGPKKR KMTKARLERS

       130        140        150        160        170        180
KLRRQKANAR ERNRMHDLNA ALDNLRKVVP CYSKTQKLSK IETLRLAKNY IWALSEILRS

       190        200        210        220        230        240
GKRPDLVSYV QTLCKGLSQP TTNLVAGCLQ LNSRNFLTEQ GADGAGRFHG SGGPFAMHPY

       250        260        270        280        290        300
PYPCSRLAGA QCQAAGGLGG GAAHALRTHG YCAAYETLYA AAGGGGASPD YNSSEYEGPL

       310        320        330        340        350        360
SPPLCLNGNF SLKQDSSPDH EKSYHYSMHY SALPGSRPTG HGLVFGSSAV RGGVHSENLL

       370        380
SYDMHLHHDR GPMYEELNAF FHN
```

6.2 Tables of genes strongly regulated during olfactory bulb interneuron differentiation

Table 6.1: Genes upregulated during the differentiation of Type A progenitor cells into periglomerular layer precursors and interneurons

Symbol	Gene Name	GeneBank	Ratio	p-Value
Slc1a3	solute carrier family 1, member 3	NM_148938	**159,9**	0
X66118	glutamate receptor subunit GluR5-2c	X66118	**155,3**	0
Fabp7	fatty acid binding protein 7, brain	NM_021272	**153,2**	0
AK122233	mRNA for mKIAA0275 protein	AK122233	**150,9**	0
1810029G24Rik	RIKEN cDNA 1810029G24 gene	NM_025468	**150,8**	0
Aqp1	aquaporin 1	NM_007472	**134,5**	9,49675E-24
Phlda1	pleckstrin homology-like domain, family A, member 1	NM_009344	**127,7**	0
Sep15	selenoprotein 15	NM_053102	**118,1**	0
M10466	mouse alpha-globin mRNA	M10466	**116,8**	0
Nr2f1	nuclear receptor subfamily 2, group F, member 1	NM_010151	**115,0**	0
Hba-a1	hemoglobin alpha, adult chain 1	NM_008218	**111,3**	0
D12Ertd553e	DNA segment, Chr 12, ERATO Doi 553	NM_029758	**109,9**	0
2610205H19Rik	RIKEN cDNA 2610205H19 gene	NM_027430	**98,3**	0
Sepp1	selenoprotein P, plasma, 1	NM_009155	**92,3**	0
Olfr807	olfactory receptor 807	NM_146929	**90,6**	9E-05
mt-Cytb	subunit I of cytochrome c oxidase	X57780	**87,8**	0
Fmo1	flavin containing monooxygenase 1	NM_010231	**85,9**	1,58318E-15
Zcchc2	zinc finger, CCHC domain containing 2	BC055760	**81,4**	0
Tm4sf2	transmembrane 4 superfamily member 2	NM_019634	**79,6**	0
Srcasm	similar to adaptor molecule srcasm	AK033712	**78,8**	0
Vtn	vitronectin	NM_011707	**75,7**	3,65607E-36
Prkar1a	protein kinase, cAMP dependent regulatory, type I, alpha	NM_021880	**74,2**	0
Scrn1	mRNA for mKIAA0193 protein	AK129084	**73,8**	4,47174E-30
BF142805	601790552F1 NCI_CGAP_Lu30 cDNA clone IMAGE:4021285 5'	BF142805	**73,1**	0
Grik1	glutamate receptor, ionotropic, kainate 1	NM_146072	**72,8**	3,05391E-26
AF378830	cytochrome c oxidase subunit II	AF378830	**69,9**	0
Npy	neuropeptide Y	NM_023456	**69,8**	0
Tkt	transketolase	NM_009388	**67,5**	0
Eps15	epidermal growth factor receptor pathway substrate 15	BC048783	**66,0**	0
2010012C16Rik	RIKEN cDNA 2010012C16 gene	NM_025564	**64,1**	1,96883E-43
BY592157	BY592157 RIKEN full-length enriched	BY592157	**63,8**	3,62395E-18
TC1323472	Q86ZH4 probable centromere/microtubule binding protein CBF5	TC1323472	**62,4**	2,48733E-07
Ctsl	cathepsin L	NM_009984	**62,3**	0
TC1367583	Cytochrome b (Fragment)	TC1367583	**62,1**	0
BC055791	cDNA clone MGC:67622 IMAGE:6410794	BC055791	**61,9**	0
Rpl26	ribosomal protein L26	NM_009080	**58,2**	0
Ptn	pleiotrophin	NM_008973	**58,1**	0
Slc16a6	similar to monocarboxylate transporter 7	AK032026	**57,0**	0
1700019B16Rik	RIKEN cDNA 1700019B16 gene	NM_028829	**56,4**	0
Rps26	ribosomal protein S26	NM_013765	**55,9**	0
Sc4mol	sterol-C4-methyl oxidase-like	NM_025436	**54,6**	0
Atp6ap2	ATPase, H+ transporting, lysosomal accessory protein 2	NM_027439	**52,1**	0
Hs3st1	heparan sulfate (glucosamine) 3-O-sulfotransferase 1	NM_010474	**51,7**	0
Txn1	thioredoxin 1	NM_011660	**51,4**	1,89141E-41
BC020382	Mus musculus, clone IMAGE:3582855	BC020382	**50,9**	0
6530401D17Rik	RIKEN cDNA 6530401D17 gene	NM_029823	**50,4**	0
Dbi	diazepam binding inhibitor	NM_007830	**50,0**	0
Lrp4	low density lipoprotein receptor-related protein 4	NM_172668	**48,0**	1,05803E-36
8030451F13Rik	RIKEN cDNA 8030451F13 gene	NM_175418	**45,7**	0
Grp58	glucose regulated protein	NM_007952	**44,8**	1,4013E-45
Mbnl1	muscleblind-like 1	NM_020007	**44,6**	8,55629E-14
TC1294250	T-cell immunomodulatory protein precursor	TC1294250	**44,5**	0
Sec6l1	mRNA for mFLJ00157 protein	AK131141	**43,2**	0,000100646
AB023957	EIG 180 mRNA for ethanol induced gene product	AB023957	**43,0**	7,471E-42
D130058I21Rik	RIKEN cDNA D130058I21 gene	NM_177776	**43,0**	0
Aprin	mRNA for mKIAA0979 protein	AK122414	**42,7**	0
Acadl	acetyl-Coenzyme A dehydrogenase, long-chain	NM_007381	**42,2**	3,53248E-22
TC1243572	RL35_RAT (P17078) 60S ribosomal protein L35	TC1243572	**42,0**	0
BI646741	BI646741 603279769F1 NCI_CGAP_Mam3 cDNA clone	BI646741	**41,5**	1,34595E-09
Gas5	growth arrest specific 5	NM_013525	**41,4**	0
C1qbp	complement component 1, q subcomponent binding protein	NM_007573	**41,2**	0

Table 6.1: continued

Symbol	Gene Name	GeneBank	Ratio	p-Value
Rps24	ribosomal protein S24	NM_207634	**40,7**	0
Slc13a3	solute carrier family 13, member 3	NM_054055	**40,6**	0
Slco2b1	solute carrier organic anion transporter family, member 2b1	NM_175316	**40,6**	0
Atp5h	ATP synthase, H transporting, mitochondrial F0 complex, subunit d	NM_027862	**40,1**	0
Nrxn1	neurexin I	NM_020252	**39,8**	4,07897E-27
Olig1	oligodendrocyte transcription factor 1	NM_016968	**39,0**	9,26293E-21
1700010A06Rik	RIKEN cDNA 1700010A06 gene	NM_027044	**38,3**	0
Rpl35	ribosomal protein L35	NM_025592	**38,0**	1,74462E-43
Pgk1	phosphoglycerate kinase 1	NM_008828	**37,7**	0
Pea15	phosphoprotein enriched in astrocytes 15	NM_008556	**37,5**	0
Tnc	tenascin C	NM_011607	**37,2**	2,69162E-29
Psma5	proteasome subunit, alpha type 5	NM_011967	**36,3**	0
Cd81	CD 81 antigen	NM_133655	**35,9**	2,30283E-33
Mest	mesoderm specific transcript	NM_008590	**35,8**	0
BE985144	UI-M-CG0p-bdi-a-04-0-UI.s1 NIH_BMAP_Ret4_S2 cDNA clone	BE985144	**35,8**	0
Tmsb10	thymosin, beta 10	NM_025284	**35,3**	0
Apod	apolipoprotein D	NM_007470	**35,3**	7,08905E-24
Slc30a4	solute carrier family 30, member 4	NM_011774	**34,6**	0
1110019J04Rik	UI-M-FZ0-ccu-c-05-0-UI.r1 NIH_BMAP_FZ0 cDNA clone	CA326234	**34,6**	1,77225E-29
Oat	ornithine aminotransferase	NM_016978	**34,4**	0
Stard13	serologically defined colon cancer antigen 13	NM_146258	**34,0**	7,20275E-08
Cct5	chaperonin subunit 5	NM_007637	**33,9**	0
D6Wsu176e	DNA segment, Chr 6, Wayne State University 176	NM_138587	**33,6**	4,12227E-20
Ppp4r1	protein phosphatase 4, regulatory subunit 1	NM_146081	**33,5**	1,88191E-39
2700060E02Rik	RIKEN cDNA 2700060E02 gene	NM_026528	**33,0**	0
BC016624	similar to actin, beta, clone IMAGE:4501052	BC016624	**33,0**	1,26035E-30
Atp11a	potential phospholipid-transporting ATPase IH (EC 3.6.3.13)	AK028779	**32,9**	4,78914E-34
D130038B21Rik	RIKEN cDNA D130038B21 gene	NM_178644	**32,8**	3,74793E-21
Mtdh	LYRIC like (Rattus norvegicus)	AK035302	**32,6**	1,4013E-45
Rps21	ribosomal protein S21	NM_025587	**32,6**	1,03183E-17
BC016267	clone IMAGE:4924122	BC016267	**31,3**	1,982E-41
Aatk	apoptosis-associated tyrosine kinase	NM_007377	**31,0**	0
Glud	glutamate dehydrogenase	NM_008133	**30,9**	0
Gpd2	glycerol phosphate dehydrogenase 1, mitochondrial	AK079336	**30,8**	0
Kctd12	potassium channel tetramerisation domain containing 12	NM_177715	**30,8**	0
Maged1	melanoma antigen, family D, 1	NM_019791	**30,8**	0
Nab1	Ngfi-A binding protein 1	NM_008667	**30,7**	2,27299E-31
Rps21	40S ribosomal protein S21 homolog	AK010610	**30,6**	0
Il18	interleukin 18	NM_008360	**30,5**	0
Rpl9	ribosomal protein L9	NM_011292	**30,0**	4,89701E-29
Scd2	stearoyl-Coenzyme A desaturase 2	NM_009128	**29,9**	9,67975E-27
Psat1	phosphoserine aminotransferase 1	NM_177420	**29,6**	0
Rpl18a	Ribosomal protein L18A	NM_029751	**29,3**	0
Hadhb	hydroxyacyl-Coenzyme A dehydrogenase, beta subunit	NM_145558	**29,0**	2,72763E-42
Plp1	proteolipid protein (myelin) 1	NM_011123	**28,6**	3,44929E-40
Sorcs3	sortilin-related VPS10 domain containing receptor 3	NM_025696	**28,6**	1,77848E-10
AU022870	expressed sequence AU022870	NM_177682	**28,5**	0
6430556C10Rik	RIKEN cDNA 6430556C10 gene	NM_178725	**27,5**	1,87298E-26
AK042850	similar to serine threonine kinase 32 homolog	AK042850	**26,9**	0,004605
Igfbp3	insulin-like growth factor binding protein 3	AK077477	**26,7**	3,29854E-08
1200015A19Rik	RIKEN cDNA 1200015A19 gene	NM_026388	**26,2**	3,69912E-25

List of genes that showed the strongest upregulation during the differentiation of Type A progenitor cells into periglomerular layer precursors and interneurons. The ratio indicates the mean fold upregulation in periglomerular cells compared to Type A progenitor cells. The p-Value indicates the significance level (two-tailed *t* test) of a differential regulation.

Table 6.2: Genes downregulated during the differentiation of Type A progenitor cells into periglomerular layer precursors and interneurons

Symbol	Gene Name	GeneBank	Ratio	p-Value
AK122256	mRNA for mKIAA0357 protein	AK122256	**37,0**	0,0042
D130016K21Rik	RIKEN cDNA D130016K21 gene	NM_177145	**32,0**	0,00006
TC1322692	A33283 ADP-ribosylation factor 1 - human homolog	TC1322692	**29,9**	0
4932432K03Rik	putative HIV-1 infection related protein homolog	AK036465	**28,9**	0,02307
9430029A11	RIKEN cDNA 9430029A11 gene	NM_177881	**28,0**	1,86789E-16
A930011O12Rik	RIKEN cDNA A930011O12 gene	BC030402	**27,7**	3,44569E-08
ENSMUST000075701	Q7PI85 (Q7PI85) ENSANGP00000022586	ENSMUST000075701	**20,4**	6,9735E-28
Dspg3	dermatan sulphate proteoglycan 3	NM_007884	**19,9**	2,53065E-40
E030034C22Rik	RIKEN cDNA E030034C22 gene	NM_144840	**19,6**	6,0032E-05
AV280394	cDNA clone 4933414A22 3'	AV280394	**19,3**	0,032945438
BM934588	UI-M-BH3-aqq-h-06-0-UI.r1 NIH_BMAP_M_S4 cDNA clone	BM934588	**18,7**	3,80591E-18
Hipk1	homeodomain interacting protein kinase 1	NM_010432	**18,0**	1,2872E-17
ORF28	open reading frame 28	NM_138664	**17,1**	3,94017E-09
Sema3e	sema domain, short basic domain, secreted, 3E	AK049580	**16,7**	0,073725
AY255623	secretin receptor	AY255623	**16,3**	0,008225
Plxna4	plexin A4	NM_175750	**16,1**	1,14243E-11
BC059864	cDNA clone MGC:69721 IMAGE:6417471	BC059864	**15,5**	2,83408E-06
1700122C07Rik	serine/threonine kinase 33	AK020360	**14,7**	0,00277
Cpz	carboxypeptidase Z	NM_153107	**14,6**	1,54633E-13
AF543214	strain C57BL/6 CD72 variant	AF543214	**14,6**	0
1700067I02Rik	RIKEN cDNA 1700067I02 gene	NM_178387	**14,1**	1,96672E-38
Kirl2	killer immunoglobulin-like receptor-like 2	NM_177748	**14,0**	7,8656E-27
Mc5r	melanocortin 5 receptor	NM_013596	**13,5**	1,37067E-15
D330023I21Rik	BB383K5.1 homolog [Homo sapiens]	AK077972	**13,2**	0,04569
A630050E13Rik	RIKEN cDNA A630050E13 gene	NM_176982	**12,9**	0,05395
Fpr-rs4	formyl peptide receptor, related sequence 4	NM_008041	**12,9**	5,86865E-42
Dcdc2	doublecortin domain containing 2	NM_177577	**12,9**	9,9154E-32
4930548H24Rik	RIKEN cDNA 4930548H24 gene	NM_026296	**12,5**	3,74042E-29
4931407G18Rik	RIKEN cDNA 4931407G18 gene	NM_027631	**12,1**	7,68195E-07
Nap1l2	nucleosome assembly protein 1-like 2	NM_008671	**12,1**	0,0001
6820408C15	RIKEN cDNA 6820408C15 gene	NM_177656	**12,0**	2,74265E-07
Epb4.9	erythrocyte protein band 4.9	AK048309	**11,7**	2,9181E-13
AK019935	serine protease inhibitor 2-1	AK019935	**11,6**	3,35383E-36
TC1312776	TGF-beta receptor type I precursor, partial (17%)	TC1312776	**11,1**	1,06042E-08
AY236491	transmembrane channel-like protein 3	AY236491	**11,0**	1,00453E-10
Loxl3	lysyl oxidase-like 3	NM_013586	**11,0**	6,89564E-21
Cyp11b2	cytochrome P450, family 11, subfamily b, polypeptide 2	NM_009991	**11,0**	6,43055E-26
Z83815	axonemal dynein heavy chain (partial, ID mdhc7)	Z83815	**10,8**	6,31685E-07
AK040722	GA repeat binding protein, beta 1	AK040722	**10,7**	0,042985
D32072	mRNA for TGF-b type II receptor isoform	D32072	**10,6**	0,001975
Scn3a	sodium channel 21	L42337	**10,5**	1,1122E-06
AW544865	expressed sequence AW544865	NM_178918	**10,5**	1,10326E-10
NAP042698-1	cDNA clone E030012C13 3'	NAP042698-1	**10,4**	1,32003E-25
2310045A20Rik	RIKEN cDNA 2310045A20 gene	NM_172710	**10,3**	1,1391E-18
Ar	androgen receptor	NM_013476	**10,1**	1,27715E-20
Dnase2a	deoxyribonuclease II alpha	NM_010062	**10,0**	3,2938E-34
4930429J24Rik	RIKEN cDNA 4930429J24 gene	NM_026132	**9,9**	2,81371E-21
1110030H18Rik	SV2 related protein homolog	AK082744	**9,8**	0
Grik2	glutamate receptor, ionotropic, kainate 2 (beta 2)	NM_010349	**9,7**	0,00004
AK047503	DGCRK6 protein homolog [Homo sapiens]	AK047503	**9,6**	0,002185
Insm1	insulinoma-associated 1	NM_016889	**9,6**	2,50185E-20
NAP013333-001	RIKEN cDNA 4930526H21 gene	NAP013333-001	**9,4**	3,00959E-07
Rab3b	RAB3B, member RAS oncogene family	NM_023537	**9,2**	0,001160223
TC1282921	Q9NS72 (Q9NS72) Leucine-zipper-like protein 1	TC1282921	**9,2**	2E-05
AK037161	calcium binding protein P22	AK037161	**9,2**	0,014075
AW554518	cDNA clone 4921522H04 3'	AV255740	**9,1**	1,33413E-11
Akr1b7	aldo-keto reductase family 1, member B7	NM_009731	**9,1**	7,84803E-11
AK122557	mRNA for mKIAA1809 protein	AK122557	**9,1**	4,95811E-07
Cacna2d1	calcium channel, voltage-dependent, alpha2/delta subunit 1	NM_009784	**9,0**	3,73469E-08
A430083B19	RIKEN cDNA A430083B19 gene	NM_177624	**9,0**	0,001955
Kcnd1	potassium voltage-gated channel, Shal-related family, member 1	NM_008423	**8,9**	4,37471E-20

Table 6.2: continued

Symbol	Gene Name	GeneBank	Ratio	p-Value
BC055738	cDNA clone MGC:67028 IMAGE:6413697	BC055738	**8,8**	0
H2-M10.5	histocompatibility 2, M region locus 10.5	NM_177637	**8,8**	1,05415E-08
AI313915	expressed sequence AI313915	NM_144845	**8,8**	4,00227E-23
C030030A07Rik	RIKEN cDNA C030030A07 gene	NM_178776	**8,7**	0,01702
Prelp	proline arginine-rich end leucine-rich repeat	NM_054077	**8,7**	1,7016E-09
Nalp9c	NACHT, LRR and PYD containing protein 9c	NM_194062	**8,6**	2,79524E-30
Scnn1a	sodium channel, nonvoltage-gated, type I, alpha polypeptide	NM_011324	**8,6**	5,51302E-26
NAP022882-001	similar to putative protein (80.3 kD) (5T676) (LOC382989)	NAP022882-001	**8,5**	0,013345
AK083596	ischemia related factor NYW-1 homolog	AK083596	**8,5**	0
Golga4	golgi autoantigen, golgin subfamily a, 4	NM_018748	**8,5**	0,00086
X65157	desmoyokin, partial	X65157	**8,5**	6,7321E-07
Shprh	SNF2 histone linker PHD RING helicase	NM_172937	**8,5**	0,00531
Xlr5	X-linked lymphocyte-regulated 5	NM_031493	**8,4**	1,75296E-21
AK040212	cDNA FLJ10893 fis, clone NT2RP4002791 homolog	AK040212	**8,4**	0,043185
AK090281	ELAV (embryonic lethal, abnormal vision, Drosophila)-like 3	AK090281	**8,3**	4,66087E-29
5430404L10Rik	RIKEN cDNA 5430404L10 gene	NM_025769	**8,3**	0,001575001
ENSMUST000024744	ORF 2. [Source:SPTREMBL;Acc:Q62295]	ENSMUST000024744	**8,3**	6,77082E-09
NAP018455-001	similar to KIAA1529 protein	NAP018455-001	**8,2**	0,023271167
AY364010	NALP12	AY364010	**8,1**	9,47896E-19
1700028O09Rik	RIKEN cDNA 1700028O09 gene	NM_029381	**8,1**	3,21073E-10
Star	steroidogenic acute regulatory protein	NM_011485	**8,1**	0,00337
Frmd3	FERM domain containing 3	NM_172869	**8,0**	2,96379E-33
AK076605	BM259 homolog [Rattus norvegicus]	AK076605	**8,0**	0,121375
Dcx	doublecortin	NM_010025	**8,0**	0,00098
Nos1	nitric oxide synthase 1, neuronal	NM_008712	**8,0**	1,03225E-09
Il2ra	interleukin 2 receptor, alpha chain	NM_008367	**7,8**	0,000860928
1700027M21Rik	RIKEN cDNA 1700027M21 gene	NM_025499	**7,8**	5,6981E-26
Cox5a	cytochrome c oxidase, subunit Va	AK046580	**7,7**	2,78609E-12
Olfr993	olfactory receptor 993	NM_146435	**7,7**	0,00001
AY255593	G protein-coupled receptor PGR23	AY255593	**7,7**	7,7912E-43
6430571L13Rik	RIKEN cDNA 6430571L13 gene	NM_175486	**7,7**	1,79133E-17
Myh3	Mouse embryonic/foetal skeletal myosin heavy chain	M11154	**7,6**	4,51187E-15
Slco6c1	solute carrier organic anion transporter family, member 6c1	NM_028942	**7,6**	8,7273E-24
Olfr352	olfactory receptor 352	NM_146940	**7,5**	0,01954
Kcnq2	potassium voltage-gated channel, subfamily Q, member 2	NM_010611	**7,5**	0,000415641
Ms4a1	Mouse CD20 cell surface protein	M62541	**7,4**	1,41442E-22
Msx2	homeo box, msh-like 2	NM_013601	**7,4**	5,1206E-15
AK051460	adenosine deaminase 3	AK051460	**7,4**	0,005465005
Cnnm1	cyclin M1	NM_031396	**7,4**	5,1701E-34
Lenep	lens epithelial protein	NM_020517	**7,4**	2,66703E-20
NAP039752-1	Makorin 1	NAP039752-1	**7,4**	1,68156E-44
Lpin3	lipin 3	NM_022883	**7,4**	3,8046E-15
AK082644	Zinc finger protein 68	AK082644	**7,3**	0,000245001
Cd3z	CD3 antigen, zeta polypeptide	NM_031162	**7,2**	0,004165
B830013J05Rik	RIKEN cDNA B830013J05 gene	NM_178722	**7,2**	6,0264E-17
5330420D20Rik	similar to D-aspartate oxidase (EC 1.4.3.1) (DASOX)	AK017475	**7,2**	0,072755
3830417A13Rik	RIKEN cDNA 3830417A13 gene	NM_027512	**7,2**	1,70399E-16
Lgr8	similar to G protein coupled receptor affecting testicular descent	AK039086	**7,2**	4,96148E-08
Glt8d2	RIKEN cDNA 1110021D20 gene	NM_029102	**7,1**	0,00137
AB081756	brain chitinase like protein 2	AB081756	**7,0**	0,006055017
Zfa	zinc finger protein, autosomal	NM_009540	**6,9**	3,61342E-11

List of genes that showed the strongest downregulation during the differentiation of Type A progenitor cells into periglomerular layer precursors and interneurons. The ratio indicates the mean fold downregulation in periglomerular cells compared to Type A progenitor cells. The p-Value indicates the significance level (two-tailed *t* test) of a differential regulation.

Table 6.3: Genes upregulated during the differentiation of periglomerular layer precursors into mature interneurons

Symbol	Gene Name	GeneBank	Ratio	p-Value
Grap2	RIKEN monocytic adaptor	AK030809	**694,4**	2,11E-28
Olfr1204	olfactory receptor 1204	NM_146463	**478,5**	2,34E-22
BF021831	uy58f06.y1 McCarrey Eddy round spermatid cDNA clone	BF021831	**478,5**	2,74E-15
Nfat5	nuclear factor of activated T-cells 5	AK045123	**381,7**	4,83E-18
Mak10	corneal wound healing related protein	AK050805	**378,8**	1,61E-18
AK041673	proton myo-inositol transporter homolog	AK041673	**363,6**	8,65E-22
4833418A01Rik	RIKEN cDNA 4833418A01 gene	NM_198005	**359,7**	3,53E-21
Hpse	heparanase	NM_152803	**344,8**	6,54E-22
Trpv3	transient receptor potential cation channel, subfamily V, member 3	NM_145099	**321,5**	2,62E-18
AI592258	mt14e07.y1 Soares mouse 3NbMS cDNA clone	AI592258	**316,5**	4,00E-21
Obox2	oocyte specific homeobox 2	NM_145708	**298,5**	4,92E-15
Trim21	tripartite motif protein 21	NM_009277	**293,3**	1,60E-15
Prlpe	prolactin-like protein E	NM_008930	**276,2**	5,67E-21
Gpr103	G protein-coupled receptor 103	NM_198192	**273,2**	2,57E-11
Vipr2	vasoactive intestinal peptide receptor 2	NM_009511	**267,4**	2,97E-14
BC020388	ATP-binding cassette, sub-family D (ALD), member 2	BC020388	**257,1**	1,83E-15
TC1253808	L1 element insertion in intron 3 of Mitf gene	TC1253808	**251,3**	1,46E-20
AK042696	NMDA receptor-regulated gene 1	AK042696	**247,5**	1,70E-21
Edn1	endothelin 1	NM_010104	**247,5**	4,48E-17
9230117E20Rik	RIKEN cDNA 9230117E20 gene	NM_030061	**238,7**	1,45E-13
Pi4k2b	phosphatidylinositol 4-kinase type 2 beta	NM_028744	**235,3**	4,92E-15
1700012M14Rik	RIKEN cDNA 1700012M14 gene	NM_023816	**234,2**	2,27E-12
AK173321	mKIAA1993 protein	AK173321	**230,9**	9,76E-14
Nin	ninein	NM_008697	**211,9**	3,14E-18
4931414P19Rik	RIKEN cDNA 4931414P19 gene	NM_028890	**211,4**	5,26E-12
BC058796	cDNA clone MGC:67967 IMAGE:6486091	BC058796	**207,5**	3,47E-21
BC056221	cDNA clone IMAGE:5253487	BC056221	**204,5**	1,29E-13
AB049605	caveolin-2 isoform	AB049605	**189,8**	1,65E-13
AK011813	TAT1protein homolog	AK011813	**184,8**	1,20E-12
AK017788	small nuclear ribonucleoprotein D1	AK017788	**183,8**	9,54E-18
BI732528	603355435F1 NIH_MGC_94 cDNA clone IMAGE:5362568	BI732528	**183,8**	0,00003
Olfr908	olfactory receptor 908	NM_146872	**180,8**	6,02E-12
Ntng1	netrin G1	AK048796	**180,2**	8,19E-15
2600011C06Rik	RIKEN cDNA 2600011C06 gene	BC067400	**179,2**	6,81E-12
Pcdhb11	protocadherin beta 11	NM_053136	**178,9**	0,0049
BC022150	cDNA clone IMAGE:5102760	BC022150	**170,1**	5,48E-08
Pms1	postmeiotic segregation increased 1	NM_153556	**167,5**	2,34E-11
Ndrg3	N-myc downstream regulated 3	AK029378	**155,5**	3,15E-10
BC021897	mRNA similar to RIKEN cDNA 2900042B11 gene	BC021897	**154,1**	4,92E-11
2010002A20Rik	RIKEN cDNA 2010002A20 gene	NM_025655	**145,3**	3,83E-09
AK051306	cAMP responsive element binding protein, delta chain homolog	AK051306	**144,1**	1,76E-10
V1re2	vomeronasal 1 receptor, E2	NM_134191	**142,5**	1,81E-12
AK129034	mRNA for mKIAA0013 protein	AK129034	**141,2**	9,06E-12
Fgg	fibrinogen, gamma polypeptide	NM_133862	**139,9**	6,20E-10
Htr3b	5-hydroxytryptamine (serotonin) receptor 3B	NM_020274	**139,7**	2,49E-08
Slco5a1	solute carrier organic anion transporter family, member 5A1	NM_172841	**134,8**	1,85E-09
Olfr244	olfactory receptor 244	NM_001005520	**132,5**	2,62E-08
AK041992	KPL2 homolog	AK041992	**131,6**	1,81E-11
Dedd2	similar to death effector domain-containing / DNA-binding protein 2	AK043908	**130,9**	9,38E-14
AK053176	interleukin 18 receptor accessory protein	AK053176	**129,0**	3,25E-09
G630039H03Rik	RIKEN cDNA G630039H03 gene	BC031204	**124,7**	5,75E-09
AY263157	Tmc3 protein	AY263157	**123,3**	3,83E-10
BC056494	cDNA clone IMAGE:5707460	BC056494	**117,0**	1,41E-08
Olfr676	olfactory receptor 676	NM_147095	**105,0**	8,59E-10
Mmp20	matrix metalloproteinase 20 (enamelysin)	NM_013903	**104,4**	7,78E-11
AK035678	programmed cell death 1 ligand 1	AK035678	**104,1**	2,10E-08
Cts8	cathepsin 8	NM_019541	**103,8**	1,11E-10
AK041814	signal transducer and activator of transcription 1	AK041814	**102,6**	4,67E-11
Rgmb	RGM domain family, member B	NM_178615	**101,5**	2,25E-09
G431001I09Rik	D123 homolog	AK047302	**101,1**	3,54E-07
NAP020528-001	similar to MrgA6 G protein-coupled receptor	NAP020528-001	**96,2**	0,00012

Table 6.3: continued

Symbol	Gene Name	GeneBank	Ratio	p-Value
AK036217	F-box protein FBL2 homolog	AK036217	**95,4**	9,50E-10
Olfr107	olfactory receptor 107	NM_146511	**89,6**	0,00003
BC048502	cDNA sequence BC048502	NM_177631	**89,0**	2,04E-06
Tnfrsf21	death receptor 6	AK036984	**88,4**	4,47E-07
Olfr142	olfactory receptor 142	NM_146984	**87,1**	2,08E-06
Ube2l3	ubiquitin-conjugating enzyme E2L 3	AK032396	**85,0**	1,10E-09
AK087984	Pinch protein (particulary interesting new cys-his protein) homolog	AK087984	**82,8**	1,81E-08
ENSMUST000009521	interferon-induced protein with tetratricopeptide repeats 1	ENSMUST000009521	**82,0**	0,00013
Pftk1	PFTAIRE protein kinase 1	AK087398	**81,0**	4,71E-08
AK018271	requiem	AK018271	**78,2**	1,98E-06
4922502D21Rik	RIKEN cDNA 4922502D21 gene	NM_199034	**77,5**	0,00002
Ube1y1	ubiquitin-activating enzyme E1, Chr Y 1	NM_011667	**74,5**	0,00001
Dhfr	dihydrofolate reductase	NM_010049	**73,6**	0,00003
AK042238	nuclear receptor coactivator 6 interacting protein	AK042238	**71,3**	2,94E-07
Rapgef6	rap guanine nucleotide exchange factor homolog	AK038235	**69,8**	0,00007
Stxbp4	syntaxin binding protein 4	AK012293	**64,7**	2,51E-06
Tshb	thyroid stimulating hormone	AK036251	**61,9**	0,00136
Grb14	growth factor receptor bound protein 14	AK034134	**61,3**	0,00058
Astn2	astrotactin 2	AK047058	**61,1**	1,70E-06
Bcl2l10	Bcl2-like 10	NM_013479	**60,3**	0,00007
Srpk2	serine/arginine-rich protein specific kinase 2	AK014004	**60,0**	0,00004
Ndufab1	acyl carrier protein (ACP)	AK003696	**59,6**	2,95E-07
Areg	amphiregulin	NM_009704	**59,3**	0,00064
Cd209a	CD209a antigen	NM_133238	**55,6**	0,00061
Neurod1	neurogenic differentiation 1	NM_010894	**54,5**	0,00063
Lmo6	LIM domain only 6	NM_175097	**53,7**	2,15E-07
Rrm2b	ribonucleotide reductase M2 B (TP53 inducible)	NM_199476	**49,4**	4,27E-06
Kng1	kininogen 1	NM_023125	**42,2**	0,00523
Edaradd	EDAR (ectodysplasin-A receptor)-associated death domain	NM_133643	**36,3**	0,00019
Ell3	elongation factor RNA polymerase II-like 3	NM_145973	**36,1**	0,00314
V1rb1	vomeronasal 1 receptor, B1	NM_053225	**21,4**	0,00003
Klrk1	killer cell lectin-like receptor subfamily K, member 1	NM_033078	**21,1**	0,00363
AB093209	mRNA for mKIAA0054 protein	AB093209	**17,2**	1,87E-07
Creb3l4	cAMP responsive element binding protein 3-like 4	NM_030080	**15,5**	0,00279
Eraf	erythroid associated factor	NM_133245	**15,3**	0
2310075A12Rik	RIKEN cDNA 2310075A12 gene	NM_178027	**10,1**	6,81E-09
Tes	testis derived transcript	NM_207176	**10,0**	0,00801
AK048143	SRY-box containing gene 6	AK048143	**10,0**	0,00367
Hbb-b1	hemoglobin, beta adult major chain	NM_008220	**9,0**	7,97E-13
Olfr998	olfactory receptor 998	NM_146436	**8,5**	0,00059
C230012O17Rik	RIKEN cDNA C230012O17 gene	NM_176944	**8,2**	0,00406
2010321J07Rik	RIKEN cDNA 2010321J07 gene	NM_028094	**7,7**	0
Clra	C lectin-related protein A	NM_153506	**7,7**	0,0031
Sfpi1	SFFV proviral integration 1	NM_011355	**7,4**	5,18E-06
Brd7	bromodomain containing 7	NM_012047	**7,3**	0,00911
Olfr805	olfactory receptor 805	NM_146555	**7,1**	9,36E-29
Slc4a1	solute carrier family 4 (anion exchanger), member 1	NM_011403	**7,1**	0
Zwint	ZW10 interactor	NM_025635	**7,1**	3,46E-08
Ktn1	kinectin 1	NM_008477	**6,9**	8,48E-15
BC038279	RIKEN cDNA C130052G03 gene	BC038279	**6,5**	0,00553
TC1334041	Q7PJ14 (Q7PJ14) ENSANGP00000025094 (Fragment)	TC1334041	**6,1**	0
Srp54	signal recognition particle 54	NM_011899	**5,5**	0,00016
M10466	Mouse alpha-globin	M10466	**5,3**	0
TC1343649	COAT_FMVD (P09519) Probable coat protein	TC1343649	**5,2**	0,00002
1100001I19Rik	RIKEN cDNA 1100001I19 gene	NM_172920	**5,1**	0,00349
AA674270	mouse major urinary protein IV	AA674270	**5,0**	1,71E-06

List of genes that showed >5-fold upregulation during the differentiation of periglomerular layer precursors into mature periglomerular interneurons. The ratio indicates the mean fold upregulation in periglomerular layer interneurons compared to periglomerular precursors. The p-Value indicates the significance level (two-tailed *t* test) of a differential regulation.

Table 6.4: Genes downregulated during the differentiation of periglomerular layer precursors into mature interneurons

Symbol	Gene Name	GeneBank	Ratio	p-Value
AK051785	12 days embryo spinal ganglion cDNA	AK051785	**143,6**	0,00004
MOR135-11	olfactory receptor MOR135-11	NM_146923	**130,2**	3,21E-06
AK042378	3 days neonate thymus cDNA	AK042378	**130,1**	0,00332
Pnma1	paraneoplastic antigen MA1	NM_027438	**118,5**	4,79E-08
Lrba	adult male urinary bladder cDNA	AK035483	**110,3**	1,25E-06
Bmp15	bone morphogenetic protein 15	NM_009757	**106,6**	1,53E-08
Smc2l1	fibroblast growth factor inducible gene 16	U42385	**81,7**	0,00063
Adarb2	adenosine deaminase, RNA-specific, B2	NM_052977	**77,3**	0,00003
V1rb6	vomeronasal 1 receptor, B6	NM_020522	**75,9**	0,00023
Cbfa2t2h	core-binding factor, runt domain, alpha subunit 2	AK030597	**71,3**	0,00002
Sox30	SRY-box containing gene 30	NM_173384	**69,8**	0,00005
Nlgn1	neuroligin 1 homolog	AK083116	**69,2**	0,00029
Hist1h3a	histone 1, H3a	NM_013550	**64,3**	0,00069
Sdfr2	stromal cell derived factor receptor 2	NM_009146	**63,8**	0,00058
2610524B01Rik	RIKEN cDNA 2610524B01 gene	NM_028150	**60,2**	0,00013
AK086594	stromal interaction molecule 1	AK086594	**59,2**	0,00373
Sh3d1B	SH3 domain protein 1B	AK050865	**57,9**	0,00005
Prpf39	PRP39 pre-mRNA processing factor 39 homolog	BC033575	**57,0**	0,00017
Ngfb	nerve growth factor, beta	NM_013609	**51,5**	0,00022
Ptpn13	protein-tyrosine phosphatase nonreceptor-type 13	AK084198	**47,6**	1,93E-07
Pla2g4c	phospholipase A2, group IVC (cytosolic, calcium-independent)	NM_001004762	**47,1**	0,00041
Ikbkg	inhibitor of kappaB kinase gamma	NM_178590	**46,4**	0,00016
Armc8	armadillo repeat containing 8	BC030311	**45,8**	0,00066
AK031304	eukaryotic translation initiation factor 2, subunit 3	AK031304	**43,3**	0,00297
Mum1l1	melanoma associated antigen (mutated) 1-like 1	NM_175541	**40,9**	0,00039
Sytl2	synaptotagmin-like 2	NM_031394	**40,6**	0,00124
Clca1	chloride channel calcium activated 1	NM_009899	**37,7**	0,0021
AK042419	asporin	AK042419	**35,5**	0,00495
AK016178	histone 4 protein	AK016178	**35,1**	0,00155
AK030290	sex comb on midleg-like 1	AK030290	**33,8**	0,00038
Lipl2	lipase-like, ab-hydrolase domain containing 2	NM_172837	**33,4**	0,00817
2810034D10Rik	zinc finger protein 54 homolog	AK012854	**33,1**	0,00153
1700083M11Rik	RIKEN cDNA 1700083M11 gene	NM_029674	**31,8**	0,00185
Ndufab1	acyl carrier protein	AK008788	**31,0**	0,00131
AF222442	Nkx-1.2 gene, 3' untranslated region	AF222442	**30,5**	0,00109
Vim	vimentin	AK033175	**30,3**	0,00686
AK009272	flavohemoprotein B5/B5RR	AK009272	**29,7**	0,00878
1500019C06Rik	RIKEN cDNA 1500019C06 gene	AK005284	**29,4**	0,00136
AK044643	myocyte enhancer factor 2C	AK044643	**28,0**	0,00531
4931409K22	RIKEN cDNA 4931409K22 gene	NM_177676	**27,9**	0,00824
AK046777	Cdk5 and Abl enzyme substrate	AK046777	**23,2**	0,00317
TC1349965	Q8BUJ7	TC1349965	**19,7**	0,00721
BE981005	UI-M-CG0-bct-c-04-0-UI.s1 NIH_BMAP_Ret4_S1 cDNA clone	BE981005	**18,2**	0,00876
BC055056	cDNA clone MGC:62829 IMAGE:6492855	BC055056	**17,7**	0,00113
BC055295	dedicator of cytokinesis 8	BC055295	**17,3**	0,00652
Lyzs	lysozyme	NM_017372	**16,5**	0,00132
AK049000	mitochondrial intermediate peptidase homolog	AK049000	**15,5**	0,00841
Prkcn	PKC MU protein homolog	AK050059	**15,3**	0,00726
Igfbpl1	insulin-like growth factor binding protein-like 1	NM_018741	**14,3**	3,49E-12
BC054851	cDNA clone IMAGE:6528953	BC054851	**13,6**	0,00205
Kif5a	kinesin family member 5A	NM_008447	**10,3**	2,53E-10
Neurod2	neurogenic differentiation 2	NM_010895	**9,1**	5,80E-08
S100a5	S100 calcium binding protein A5	NM_011312	**8,5**	2,81E-41
1200007B05Rik	RIKEN cDNA 1200007B05 gene	NM_026165	**7,0**	0,00239
Nfkb1	NFkB p105 subunit	AK036827	**7,0**	6,61E-07
BB254136	BB254136 RIKEN full-length enriched	BB254136	**6,4**	0,00238
0610030H11Rik	RIKEN cDNA 0610030H11 gene	NM_026712	**6,2**	3,06E-13
D130060C09Rik	RIKEN cDNA D130060C09 gene	NM_177054	**6,0**	0,00451
Gng13	guanine nucleotide binding protein 13, gamma	NM_022422	**5,6**	1,42E-17
BC055811	cDNA sequence BC055811	NM_198610	**5,0**	0,00007
Cadps2	cerebellum postnatal development associated protein 2	AK042634	**5,0**	0,0001

List of genes that showed >5-fold downregulation during the differentiation of periglomerular layer precursors into mature periglomerular interneurons. The ratio indicates the mean fold downregulation in periglomerular layer interneurons compared to periglomerular precursors. The p-Value indicates the significance level (two-tailed *t* test) of a differential regulation.

7 References

Abts, H., Emmerich, M., Miltenyi, S., Radbruch, A., Tesch, H., 1989. **CD20 positive human B lymphocytes separated with the magnetic cell sorter (MACS) can be induced to proliferation and antibody secretion in vitro.** J Immunol Methods 125, 19-28.

Ache, B.W., Young, J.M., 2005. **Olfaction: diverse species, conserved principles.** Neuron 48, 417-430.

Akbarian, S., Smith, M.A., Jones, E.G., 1995. **Editing for an AMPA receptor subunit RNA in prefrontal cortex and striatum in Alzheimer's disease, Huntington's disease and schizophrenia.** Brain Res 699, 297-304.

Alexi, T., Hughes, P.E., van Roon-Mom, W.M., Faull, R.L., Williams, C.E., Clark, R.G., Gluckman, P.D., 1999. **The IGF-I amino-terminal tripeptide glycine-proline-glutamate (GPE) is neuroprotective to striatum in the quinolinic acid lesion animal model of Huntington's disease.** Exp Neurol 159, 84-97.

Alonso, M., Viollet, C., Gabellec, M.M., Meas-Yedid, V., Olivo-Marin, J.C., Lledo, P.M., 2006. **Olfactory discrimination learning increases the survival of adult-born neurons in the olfactory bulb.** J Neurosci 26, 10508-10513.

Alvarez-Buylla, A., Garcia-Verdugo, J.M., 2002. **Neurogenesis in adult subventricular zone.** J Neurosci 22, 629-634.

Anderson, S.A., Eisenstat, D.D., Shi, L., Rubenstein, J.L., 1997. **Interneuron migration from basal forebrain to neocortex: dependence on Dlx genes.** Science 278, 474-476.

Andrews, W., Barber, M., Hernadez-Miranda, L.R., Xian, J., Rakic, S., Sundaresan, V., Rabbitts, T.H., Pannell, R., Rabbitts, P., Thompson, H., Erskine, L., Murakami, F., Parnavelas, J.G., 2007. **The role of Slit-Robo signaling in the generation, migration and morphological differentiation of cortical interneurons.** Dev Biol.

Anthony, T.E., Mason, H.A., Gridley, T., Fishell, G., Heintz, N., 2005. **Brain lipid-binding protein is a direct target of Notch signaling in radial glial cells.** Genes Dev 19, 1028-1033.

Anton, E.S., Ghashghaei, H.T., Weber, J.L., McCann, C., Fischer, T.M., Cheung, I.D., Gassmann, M., Messing, A., Klein, R., Schwab, M.H., Lloyd, K.C., Lai, C., 2004. **Receptor tyrosine kinase ErbB4 modulates neuroblast migration and placement in the adult forebrain.** Nat Neurosci 7, 1319-1328.

Appay, V., Bosio, A., Lokan, S., Wiencek, Y., Biervert, C., Kusters, D., Devevre, E., Speiser, D., Romero, P., Rufer, N., Leyvraz, S., 2007. **Sensitive Gene Expression Profiling of Human T Cell Subsets Reveals Parallel Post-Thymic Differentiation for CD4+ and CD8+ Lineages.** J Immunol 179, 7406-7414.

Arevian, A.C., Kapoor, V., Urban, N.N., 2008. **Activity-dependent gating of lateral inhibition in the mouse olfactory bulb.** Nat Neurosci 11, 80-87.

Arlotta, P., Molyneaux, B.J., Chen, J., Inoue, J., Kominami, R., Macklis, J.D., 2005. **Neuronal subtype-specific genes that control corticospinal motor neuron development in vivo.** Neuron 45, 207-221.

Auffray, C., Fogg, D., Garfa, M., Elain, G., Join-Lambert, O., Kayal, S., Sarnacki, S., Cumano, A., Lauvau, G., Geissmann, F., 2007. **Monitoring of blood vessels and tissues by a population of monocytes with patrolling behavior.** Science 317, 666-670.

Awapara, J., Landua, A.J., Fuerst, R., Seale, B., 1950. **Free gamma-aminobutyric acid in brain.** J Biol Chem 187, 35-39.

Beal, M.F., Ferrante, R.J., 2004. **Experimental therapeutics in transgenic mouse models of Huntington's disease.** Nat Rev Neurosci 5, 373-384.

Becker, M., Lavie, V., Solomon, B., 2007. **Stimulation of endogenous neurogenesis by anti-EFRH immunization in a transgenic mouse model of Alzheimer's disease.** Proc Natl Acad Sci U S A 104, 1691-1696.

Belluzzi, O., Benedusi, M., Ackman, J., LoTurco, J.J., 2003. **Electrophysiological differentiation of new neurons in the olfactory bulb.** J Neurosci 23, 10411-10418.

Ben-Ari, Y., Cherubini, E., Corradetti, R., Gaiarsa, J.L., 1989. **Giant synaptic potentials in immature rat CA3 hippocampal neurones.** J Physiol 416, 303-325.

Birnboim, H.C., Doly, J., 1979. **A rapid alkaline extraction procedure for screening recombinant plasmid DNA.** Nucleic Acids Res 7, 1513-1523.

Blatow, M., Caputi, A., Monyer, H., 2005. **Molecular diversity of neocortical GABAergic interneurones.** J Physiol 562, 99-105. Epub 2004 Nov 2011.

Bommel, H., Xie, G., Rossoll, W., Wiese, S., Jablonka, S., Boehm, T., Sendtner, M., 2002. **Missense mutation in the tubulin-specific chaperone E (Tbce) gene in the mouse mutant progressive motor neuronopathy, a model of human motoneuron disease.** J Cell Biol 159, 563-569.

Bormann, J., 1988. **Electrophysiology of GABAA and GABAB receptor subtypes.** Trends Neurosci 11, 112-116.

Bormann, J., 2000. **The 'ABC' of GABA receptors.** Trends Pharmacol Sci 21, 16-19.

Bormann, J., Feigenspan, A., 1995. **GABAC receptors.** Trends Neurosci 18, 515-519.

Bosch, M., Pineda, J.R., Sunol, C., Petriz, J., Cattaneo, E., Alberch, J., Canals, J.M., 2004. **Induction of GABAergic phenotype in a neural stem cell line for transplantation in an excitotoxic model of Huntington's disease.** Exp Neurol 190, 42-58.

Bossy-Wetzel, E., Schwarzenbacher, R., Lipton, S.A., 2004a. **Molecular pathways to neurodegeneration.** Nat Med 10 Suppl, S2-9.

Bossy-Wetzel, E., Talantova, M.V., Lee, W.D., Scholzke, M.N., Harrop, A., Mathews, E., Gotz, T., Han, J., Ellisman, M.H., Perkins, G.A., Lipton, S.A., 2004b. **Crosstalk between nitric oxide and zinc pathways to neuronal cell death involving mitochondrial dysfunction and p38-activated K+ channels.** Neuron 41, 351-365.

Boutin, C., Diestel, S., Desoeuvre, A., Tiveron, M.C., Cremer, H., 2008. **Efficient in vivo electroporation of the postnatal rodent forebrain.** PLoS ONE 3, e1883.

Bradford, D.S., Foster, R.R., Nossel, H.L., 1970. **Coagulation alterations, hypoxemia, and fat embolism in fracture patients.** J Trauma 10, 307-321.

Bretin, S., Reibel, S., Charrier, E., Maus-Moatti, M., Auvergnon, N., Thevenoux, A., Glowinski, J., Rogemond, V., Premont, J., Honnorat, J., Gauchy, C., 2005. **Differential expression of CRMP1, CRMP2A, CRMP2B, and CRMP5 in axons or dendrites of distinct neurons in the mouse brain.** J Comp Neurol 486, 1-17.

Brill, M.S., Snapyan, M., Wohlfrom, H., Ninkovic, J., Jawerka, M., Mastick, G.S., Ashery-Padan, R., Saghatelyan, A., Berninger, B., Gotz, M., 2008. **A dlx2- and pax6-dependent transcriptional code for periglomerular neuron specification in the adult olfactory bulb.** J Neurosci 28, 6439-6452.

Brooks, P.C., Lin, J.M., French, D.L., Quigley, J.P., 1993. **Subtractive immunization yields monoclonal antibodies that specifically inhibit metastasis.** J Cell Biol 122, 1351-1359.

Cantor, H., Simpson, E., Sato, V.L., Fathman, C.G., Herzenberg, L.A., 1975. **Characterization of subpopulations of T lymphocytes. I. Separation and functional studies of peripheral T-cells binding different amounts of fluorescent anti-Thy 1.2 (theta) antibody using a fluorescence-activated cell sorter (FACS).** Cell Immunol 15, 180-196.

Carleton, A., Petreanu, L.T., Lansford, R., Alvarez-Buylla, A., Lledo, P.M., 2003. **Becoming a new neuron in the adult olfactory bulb.** Nat Neurosci 6, 507-518.

Carothers, A.M., Urlaub, G., Mucha, J., Grunberger, D., Chasin, L.A., 1989. **Point mutation analysis in a mammalian gene: rapid preparation of total RNA, PCR amplification of cDNA, and Taq sequencing by a novel method.** Biotechniques 7, 494-496, 498-499.

Cartier, L., Laforge, T., Feki, A., Arnaudeau, S., Dubois-Dauphin, M., Krause, K.H., 2006. **Pax6-induced alteration of cell fate: shape changes, expression of neuronal alpha tubulin, postmitotic phenotype, and cell migration.** J Neurobiol 66, 421-436.

Carvalho, D.P., 2003. **Modulation of uterine iodothyronine deiodinases--a critical event for fetal development?** Endocrinology 144, 4250-4252.

Chazal, G., Durbec, P., Jankovski, A., Rougon, G., Cremer, H., 2000. **Consequences of neural cell adhesion molecule deficiency on cell migration in the rostral migratory stream of the mouse.** J Neurosci 20, 1446-1457.

Chen, G., Trombley, P.Q., van den Pol, A.N., 1996. **Excitatory actions of GABA in developing rat hypothalamic neurones.** J Physiol 494 (Pt 2), 451-464.

Chen, J.H., Wen, L., Dupuis, S., Wu, J.Y., Rao, Y., 2001. **The N-terminal leucine-rich regions in Slit are sufficient to repel olfactory bulb axons and subventricular zone neurons.** J Neurosci 21, 1548-1556.

Chen, K., Ochalski, P.G., Tran, T.S., Sahir, N., Schubert, M., Pramatarova, A., Howell, B.W., 2004. **Interaction between Dab1 and CrkII is promoted by Reelin signaling.** J Cell Sci 117, 4527-4536.

Cherubini, E., Conti, F., 2001. **Generating diversity at GABAergic synapses.** Trends Neurosci 24, 155-162.

Cho, J.H., Tsai, M.J., 2004. **The role of BETA2/NeuroD1 in the development of the nervous system.** Mol Neurobiol 30, 35-47.

Cobos, I., Broccoli, V., Rubenstein, J.L., 2005a. **The vertebrate ortholog of Aristaless is regulated by Dlx genes in the developing forebrain.** J Comp Neurol 483, 292-303.

Cobos, I., Calcagnotto, M.E., Vilaythong, A.J., Thwin, M.T., Noebels, J.L., Baraban, S.C., Rubenstein, J.L., 2005b. **Mice lacking Dlx1 show subtype-specific loss of interneurons, reduced inhibition and epilepsy.** Nat Neurosci 8, 1059-1068.

Comoletti, D., Flynn, R., Jennings, L.L., Chubykin, A., Matsumura, T., Hasegawa, H., Sudhof, T.C., Taylor, P., 2003. **Characterization of the interaction of a recombinant soluble neuroligin-1 with neurexin-1beta.** J Biol Chem 278, 50497-50505.

Conover, J.C., Doetsch, F., Garcia-Verdugo, J.M., Gale, N.W., Yancopoulos, G.D., Alvarez-Buylla, A., 2000. **Disruption of Eph/ephrin signaling affects migration and proliferation in the adult subventricular zone.** Nat Neurosci 3, 1091-1097.

Coskun, V., Wu, H., Blanchi, B., Tsao, S., Kim, K., Zhao, J., Biancotti, J.C., Hutnick, L., Krueger, R.C., Jr., Fan, G., de Vellis, J., Sun, Y.E., 2008. **CD133+ neural stem cells in the ependyma of mammalian postnatal forebrain.** Proc Natl Acad Sci U S A 105, 1026-1031.

Cotton, R.G., Milstein, C., 1973. **Letter: Fusion of two immunoglobulin-producing myeloma cells.** Nature 244, 42-43.

Cremer, H., Lange, R., Christoph, A., Plomann, M., Vopper, G., Roes, J., Brown, R., Baldwin, S., Kraemer, P., Scheff, S., et al., 1994. **Inactivation of the N-CAM gene in mice results in size reduction of the olfactory bulb and deficits in spatial learning.** Nature 367, 455-459.

Curtis, M.A., Faull, R.L., Eriksson, P.S., 2007a. **The effect of neurodegenerative diseases on the subventricular zone.** Nat Rev Neurosci 8, 712-723.

Curtis, M.A., Kam, M., Nannmark, U., Anderson, M.F., Axell, M.Z., Wikkelso, C., Holtas, S., van Roon-Mom, W.M., Bjork-Eriksson, T., Nordborg, C., Frisen, J., Dragunow, M., Faull, R.L., Eriksson, P.S., 2007b. **Human neuroblasts migrate to the olfactory bulb via a lateral ventricular extension.** Science 315, 1243-1249.

Cutforth, T., Moring, L., Mendelsohn, M., Nemes, A., Shah, N.M., Kim, M.M., Frisen, J., Axel, R., 2003. **Axonal ephrin-As and odorant receptors: coordinate determination of the olfactory sensory map.** Cell 114, 311-322.

de Chevigny, A., Lemasson, M., Saghatelyan, A., Sibbe, M., Schachner, M., Lledo, P.M., 2006. **Delayed onset of odor detection in neonatal mice lacking tenascin-C.** Mol Cell Neurosci 32, 174-186.

Deacon, T.W., Pakzaban, P., Isacson, O., 1994. **The lateral ganglionic eminence is the origin of cells committed to striatal phenotypes: neural transplantation and developmental evidence.** Brain Res 668, 211-219.

DeFelipe, J., 1997. **Types of neurons, synaptic connections and chemical characteristics of cells immunoreactive for calbindin-D28K, parvalbumin and calretinin in the neocortex.** J Chem Neuroanat 14, 1-19.

DeLong, M.R., 1990. **Primate models of movement disorders of basal ganglia origin.** Trends Neurosci 13, 281-285.

Deuel, T.A., Liu, J.S., Corbo, J.C., Yoo, S.Y., Rorke-Adams, L.B., Walsh, C.A., 2006. **Genetic interactions between doublecortin and doublecortin-like kinase in neuronal migration and axon outgrowth.** Neuron 49, 41-53.

Dikkes, P., D, B.J., Guo, W.H., Chao, C., Hemond, P., Yoon, K., Zurakowski, D., Lopez, M.F., 2007. **IGF2 knockout mice are resistant to kainic acid-induced seizures and neurodegeneration.** Brain Res 1175, 85-95.

Donovan, M.H., Yazdani, U., Norris, R.D., Games, D., German, D.C., Eisch, A.J., 2006. **Decreased adult hippocampal neurogenesis in the PDAPP mouse model of Alzheimer's disease.** J Comp Neurol 495, 70-83.

Durbec, P., Cremer, H., 2001. **Revisiting the function of PSA-NCAM in the nervous system.** Mol Neurobiol 24, 53-64.

Eccles, J.C., Llinas, R., Sasaki, K., 1966. **The mossy fibre-granule cell relay of the cerebellum and its inhibitory control by Golgi cells.** Exp Brain Res 1, 82-101.

Eisen, M.B., Spellman, P.T., Brown, P.O., Botstein, D., 1998. **Cluster analysis and display of genome-wide expression patterns.** Proc Natl Acad Sci U S A 95, 14863-14868.

Elliott, K.A., Hobbiger, F., 1959. **gamma Aminobutyric acid; circulatory and respiratory effects in different species; re-investigation of the anti-strychnine action in mice.** J Physiol 146, 70-84.

Emsley, J.G., Hagg, T., 2003. **alpha6beta1 integrin directs migration of neuronal precursors in adult mouse forebrain.** Exp Neurol 183, 273-285.

Engelhardt, C.M., Bundschu, K., Messerschmitt, M., Renne, T., Walter, U., Reinhard, M., Schuh, K., 2004. **Expression and subcellular localization of Spred proteins in mouse and human tissues.** Histochem Cell Biol 122, 527-538.

Erkman, L., Yates, P.A., McLaughlin, T., McEvilly, R.J., Whisenhunt, T., O'Connell, S.M., Krones, A.I., Kirby, M.A., Rapaport, D.H., Bermingham, J.R., O'Leary, D.D., Rosenfeld, M.G., 2000. **A POU domain transcription factor-dependent program regulates axon pathfinding in the vertebrate visual system.** Neuron 28, 779-792.

Erlander, M.G., Tillakaratne, N.J., Feldblum, S., Patel, N., Tobin, A.J., 1991. **Two genes encode distinct glutamate decarboxylases.** Neuron 7, 91-100.

Erlander, M.G., Tobin, A.J., 1991. **The structural and functional heterogeneity of glutamic acid decarboxylase: a review.** Neurochem Res 16, 215-226.

Farah, M.H., Olson, J.M., Sucic, H.B., Hume, R.I., Tapscott, S.J., Turner, D.L., 2000. **Generation of neurons by transient expression of neural bHLH proteins in mammalian cells.** Development 127, 693-702.

Feldblum, S., Erlander, M.G., Tobin, A.J., 1993. **Different distributions of GAD65 and GAD67 mRNAs suggest that the two glutamate decarboxylases play distinctive functional roles.** J Neurosci Res 34, 689-706.

Ferguson, G.D., Herschman, H.R., Storm, D.R., 2004a. **Reduced anxiety and depression-like behavior in synaptotagmin IV (-/-) mice.** Neuropharmacology 47, 604-611.

Ferguson, G.D., Wang, H., Herschman, H.R., Storm, D.R., 2004b. **Altered hippocampal short-term plasticity and associative memory in synaptotagmin IV (-/-) mice.** Hippocampus 14, 964-974.

Fine, E.J., Ionita, C.C., Lohr, L., 2002. **The history of the development of the cerebellar examination.** Semin Neurol 22, 375-384.

Flames, N., Marin, O., 2005. **Developmental mechanisms underlying the generation of cortical interneuron diversity.** Neuron 46, 377-381.

Fon, E.A., Edwards, R.H., 2001. **Molecular mechanisms of neurotransmitter release.** Muscle Nerve 24, 581-601.

Frielingsdorf, H., Schwarz, K., Brundin, P., Mohapel, P., 2004. **No evidence for new dopaminergic neurons in the adult mammalian substantia nigra.** Proc Natl Acad Sci U S A 101, 10177-10182.

Frisch, C., Dere, E., Silva, M.A., Godecke, A., Schrader, J., Huston, J.P., 2000. **Superior water maze performance and increase in fear-related behavior in the endothelial nitric oxide synthase-deficient mouse together with monoamine changes in cerebellum and ventral striatum.** J Neurosci 20, 6694-6700.

Gerfen, C.R., 1992. **The neostriatal mosaic: multiple levels of compartmental organization in the basal ganglia.** Annu Rev Neurosci 15, 285-320.

Ghashghaei, H.T., Lai, C., Anton, E.S., 2007. **Neuronal migration in the adult brain: are we there yet?** Nat Rev Neurosci 8, 141-151.

Ghashghaei, H.T., Weber, J., Pevny, L., Schmid, R., Schwab, M.H., Lloyd, K.C., Eisenstat, D.D., Lai, C., Anton, E.S., 2006. **The role of neuregulin-ErbB4 interactions on the proliferation and organization of cells in the subventricular zone.** Proc Natl Acad Sci U S A 103, 1930-1935.

Gheusi, G., Cremer, H., McLean, H., Chazal, G., Vincent, J.D., Lledo, P.M., 2000. **Importance of newly generated neurons in the adult olfactory bulb for odor discrimination.** Proc Natl Acad Sci U S A 97, 1823-1828.

Gleeson, J.G., Minnerath, S.R., Fox, J.W., Allen, K.M., Luo, R.F., Hong, S.E., Berg, M.J., Kuzniecky, R., Reitnauer, P.J., Borgatti, R., Mira, A.P., Guerrini, R., Holmes, G.L., Rooney, C.M., Berkovic, S., Scheffer, I., Cooper, E.C., Ricci, S., Cusmai, R., Crawford, T.O., Leroy, R., Andermann, E., Wheless, J.W., Dobyns, W.B., Walsh, C.A., et al., 1999. **Characterization of mutations in the gene doublecortin in patients with double cortex syndrome.** Ann Neurol 45, 146-153.

Gomperts, B.N., Gong-Cooper, X., Hackett, B.P., 2004. **Foxj1 regulates basal body anchoring to the cytoskeleton of ciliated pulmonary epithelial cells.** J Cell Sci 117, 1329-1337.

Gotz, M., Barde, Y.A., 2005. **Radial glial cells defined and major intermediates between embryonic stem cells and CNS neurons.** Neuron 46, 369-372.

Gotz, M., Huttner, W.B., 2005. **The cell biology of neurogenesis.** Nat Rev Mol Cell Biol 6, 777-788.

Graybiel, A.M., 2000. **The basal ganglia.** Curr Biol 10, R509-511.

Guan, J., Williams, C.E., Skinner, S.J., Mallard, E.C., Gluckman, P.D., 1996. **The effects of insulin-like growth factor (IGF)-1, IGF-2, and des-IGF-1 on neuronal loss after hypoxic-ischemic brain injury in adult rats: evidence for a role for IGF binding proteins.** Endocrinology 137, 893-898.

Hack, I., Bancila, M., Loulier, K., Carroll, P., Cremer, H., 2002. **Reelin is a detachment signal in tangential chain-migration during postnatal neurogenesis.** Nat Neurosci 5, 939-945.

Hack, M.A., Saghatelyan, A., de Chevigny, A., Pfeifer, A., Ashery-Padan, R., Lledo, P.M., Gotz, M., 2005. **Neuronal fate determinants of adult olfactory bulb neurogenesis.** Nat Neurosci 8, 865-872.

Hansel, D.E., Eipper, B.A., Ronnett, G.V., 2001. **Neuropeptide Y functions as a neuroproliferative factor.** Nature 410, 940-944.

Hartmann, H., Eckert, A., Muller, W.E., 1994. **Apolipoprotein E and cholesterol affect neuronal calcium signalling: the possible relationship to beta-amyloid neurotoxicity.** Biochem Biophys Res Commun 200, 1185-1192.

Hashimoto, T., Volk, D.W., Eggan, S.M., Mirnics, K., Pierri, J.N., Sun, Z., Sampson, A.R., Lewis, D.A., 2003. **Gene expression deficits in a subclass of GABA neurons in the prefrontal cortex of subjects with schizophrenia.** J Neurosci 23, 6315-6326.

Haughey, N.J., Liu, D., Nath, A., Borchard, A.C., Mattson, M.P., 2002a. **Disruption of neurogenesis in the subventricular zone of adult mice, and in human cortical neuronal precursor cells in culture, by amyloid beta-peptide: implications for the pathogenesis of Alzheimer's disease.** Neuromolecular Med 1, 125-135.

Haughey, N.J., Nath, A., Chan, S.L., Borchard, A.C., Rao, M.S., Mattson, M.P., 2002b. **Disruption of neurogenesis by amyloid beta-peptide, and perturbed neural progenitor cell homeostasis, in models of Alzheimer's disease.** J Neurochem 83, 1509-1524.

He, W., Ingraham, C., Rising, L., Goderie, S., Temple, S., 2001. **Multipotent stem cells from the mouse basal forebrain contribute GABAergic neurons and oligodendrocytes to the cerebral cortex during embryogenesis.** J Neurosci 21, 8854-8862.

Heins, N., Malatesta, P., Cecconi, F., Nakafuku, M., Tucker, K.L., Hack, M.A., Chapouton, P., Barde, Y.A., Gotz, M., 2002. **Glial cells generate neurons: the role of the transcription factor Pax6.** Nat Neurosci 5, 308-315.

Higginbotham, H., Tanaka, T., Brinkman, B.C., Gleeson, J.G., 2006. **GSK3beta and PKCzeta function in centrosome localization and process stabilization during Slit-mediated neuronal repolarization.** Mol Cell Neurosci 32, 118-132.

Hirsch, J.A., Gilbert, C.D., 1991. **Synaptic physiology of horizontal connections in the cat's visual cortex.** J Neurosci 11, 1800-1809.

Hoekman, M.F., Jacobs, F.M., Smidt, M.P., Burbach, J.P., 2006. **Spatial and temporal expression of FoxO transcription factors in the developing and adult murine brain.** Gene Expr Patterns 6, 134-140.

Hoglinger, G.U., Rizk, P., Muriel, M.P., Duyckaerts, C., Oertel, W.H., Caille, I., Hirsch, E.C., 2004. **Dopamine depletion impairs precursor cell proliferation in Parkinson disease.** Nat Neurosci 7, 726-735.

Horsch, D., Kahn, C.R., 1999. **Region-specific mRNA expression of phosphatidylinositol 3-kinase regulatory isoforms in the central nervous system of C57BL/6J mice.** J Comp Neurol 415, 105-120.

Hoshino, M., Nakamura, S., Mori, K., Kawauchi, T., Terao, M., Nishimura, Y.V., Fukuda, A., Fuse, T., Matsuo, N., Sone, M., Watanabe, M., Bito, H., Terashima, T., Wright, C.V., Kawaguchi, Y., Nakao, K., Nabeshima, Y., 2005. **Ptf1a, a bHLH transcriptional gene, defines GABAergic neuronal fates in cerebellum.** Neuron 47, 201-213.

Hu, H., 1999. **Chemorepulsion of neuronal migration by Slit2 in the developing mammalian forebrain.** Neuron 23, 703-711.

Huang, Z.J., Di Cristo, G., Ango, F., 2007. **Development of GABA innervation in the cerebral and cerebellar cortices.** Nat Rev Neurosci 8, 673-686.

Ince-Dunn, G., Hall, B.J., Hu, S.C., Ripley, B., Huganir, R.L., Olson, J.M., Tapscott, S.J., Ghosh, A., 2006. **Regulation of thalamocortical patterning and synaptic maturation by NeuroD2.** Neuron 49, 683-695.

Jacques, T.S., Relvas, J.B., Nishimura, S., Pytela, R., Edwards, G.M., Streuli, C.H., ffrench-Constant, C., 1998. **Neural precursor cell chain migration and division are regulated through different beta1 integrins.** Development 125, 3167-3177.

Jukkola, T., Sinjushina, N., Partanen, J., 2004. **Drapc1 expression during mouse embryonic development.** Gene Expr Patterns 4, 755-762.

Juliano, R.L., 2002. **Signal transduction by cell adhesion receptors and the cytoskeleton: functions of integrins, cadherins, selectins, and immunoglobulin-superfamily members.** Annu Rev Pharmacol Toxicol 42, 283-323.

Kanai, Y., Okada, Y., Tanaka, Y., Harada, A., Terada, S., Hirokawa, N., 2000. **KIF5C, a novel neuronal kinesin enriched in motor neurons.** J Neurosci 20, 6374-6384.

Kanatani, A., Mashiko, S., Murai, N., Sugimoto, N., Ito, J., Fukuroda, T., Fukami, T., Morin, N., MacNeil, D.J., Van der Ploeg, L.H., Saga, Y., Nishimura, S., Ihara, M., 2000. **Role of the Y1 receptor in the regulation of neuropeptide Y-mediated feeding: comparison of wild-type, Y1 receptor-deficient, and Y5 receptor-deficient mice.** Endocrinology 141, 1011-1016.

Kanda, S., Tamada, Y., Yoshidome, A., Hayashi, I., Nishiyama, T., 2004. **Over-expression of bHLH genes facilitate neural formation of mouse embryonic stem (ES) cells in vitro.** Int J Dev Neurosci 22, 149-156.

Kappeler, C., Saillour, Y., Baudoin, J.P., Tuy, F.P., Alvarez, C., Houbron, C., Gaspar, P., Hamard, G., Chelly, J., Metin, C., Francis, F., 2006. **Branching and nucleokinesis defects in migrating interneurons derived from doublecortin knockout mice.** Hum Mol Genet 15, 1387-1400.

Kempermann, G., Wiskott, L., Gage, F.H., 2004. **Functional significance of adult neurogenesis.** Curr Opin Neurobiol 14, 186-191.

Kim, W.R., Kim, Y., Eun, B., Park, O.H., Kim, H., Kim, K., Park, C.H., Vinsant, S., Oppenheim, R.W., Sun, W., 2007. **Impaired migration in the rostral migratory stream but spared olfactory function after the elimination of programmed cell death in Bax knock-out mice.** J Neurosci 27, 14392-14403.

Kim, W.Y., Fritzsch, B., Serls, A., Bakel, L.A., Huang, E.J., Reichardt, L.F., Barth, D.S., Lee, J.E., 2001. **NeuroD-null mice are deaf due to a severe loss of the inner ear sensory neurons during development.** Development 128, 417-426.

Kirschenbaum, B., Doetsch, F., Lois, C., Alvarez-Buylla, A., 1999. **Adult subventricular zone neuronal precursors continue to proliferate and migrate in the absence of the olfactory bulb.** J Neurosci 19, 2171-2180.

Kohler, G., Milstein, C., 1975. **Continuous cultures of fused cells secreting antibody of predefined specificity.** Nature 256, 495-497.

Kohwi, M., Osumi, N., Rubenstein, J.L., Alvarez-Buylla, A., 2005. **Pax6 is required for making specific subpopulations of granule and periglomerular neurons in the olfactory bulb.** J Neurosci 25, 6997-7003.

Koizumi, H., Higginbotham, H., Poon, T., Tanaka, T., Brinkman, B.C., Gleeson, J.G., 2006a. **Doublecortin maintains bipolar shape and nuclear translocation during migration in the adult forebrain.** Nat Neurosci 9, 779-786.

Koizumi, H., Tanaka, T., Gleeson, J.G., 2006b. **Doublecortin-like kinase functions with doublecortin to mediate fiber tract decussation and neuronal migration.** Neuron 49, 55-66.

Kosaka, K., Kosaka, T., 2005. **synaptic organization of the glomerulus in the main olfactory bulb: compartments of the glomerulus and heterogeneity of the periglomerular cells.** Anat Sci Int 80, 80-90.

Kroll, T.T., O'Leary, D.D., 2005. **Ventralized dorsal telencephalic progenitors in Pax6 mutant mice generate GABA interneurons of a lateral ganglionic eminence fate.** Proc Natl Acad Sci U S A 102, 7374-7379.

Laemmli, U.K., 1970. **Cleavage of structural proteins during the assembly of the head of bacteriophage T4.** Nature 227, 680-685.

Lampa, S.J., Potluri, S., Norton, A.S., Fusco, W., Laskowski, M.B., 2004. **Ephrin-A5 overexpression degrades topographic specificity in the mouse gluteus maximus muscle.** Brain Res Dev Brain Res 153, 271-274.

Lein, E.S., Hawrylycz, M.J., Ao, N., Ayres, M., Bensinger, A., Bernard, A., Boe, A.F., Boguski, M.S., Brockway, K.S., Byrnes, E.J., Chen, L., Chen, L., Chen, T.M., Chin, M.C., Chong, J., Crook, B.E., Czaplinska, A., Dang, C.N., Datta, S., Dee, N.R., Desaki, A.L., Desta, T., Diep, E., Dolbeare, T.A., Donelan, M.J., Dong, H.W., Dougherty, J.G., Duncan, B.J., Ebbert, A.J., Eichele, G., Estin, L.K., Faber, C., Facer, B.A., Fields, R., Fischer, S.R., Fliss, T.P., Frensley, C., Gates, S.N., Glattfelder, K.J., Halverson, K.R., Hart, M.R., Hohmann, J.G., Howell, M.P., Jeung, D.P., Johnson, R.A., Karr, P.T., Kawal, R., Kidney, J.M., Knapik, R.H., Kuan, C.L., Lake, J.H., Laramee, A.R., Larsen, K.D., Lau, C., Lemon, T.A., Liang, A.J., Liu, Y., Luong, L.T., Michaels, J., Morgan, J.J., Morgan, R.J., Mortrud, M.T., Mosqueda, N.F., Ng, L.L., Ng, R., Orta, G.J., Overly, C.C., Pak, T.H., Parry, S.E., Pathak, S.D., Pearson, O.C., Puchalski, R.B., Riley, Z.L., Rockett, H.R., Rowland, S.A., Royall, J.J., Ruiz, M.J., Sarno, N.R., Schaffnit, K., Shapovalova, N.V., Sivisay, T., Slaughterbeck, C.R., Smith, S.C., Smith, K.A., Smith, B.I., Sodt, A.J., Stewart, N.N., Stumpf, K.R., Sunkin, S.M., Sutram, M., Tam, A., Teemer, C.D., Thaller, C., Thompson, C.L., Varnam, L.R., Visel, A., Whitlock, R.M., Wohnoutka, P.E., Wolkey, C.K., Wong, V.Y., Wood, M., Yaylaoglu, M.B., Young, R.C., Youngstrom, B.L., Yuan, X.F., Zhang, B., Zwingman, T.A., Jones, A.R., 2007. **Genome-wide atlas of gene expression in the adult mouse brain.** Nature 445, 168-176.

Lemasson, M., Saghatelyan, A., Olivo-Marin, J.C., Lledo, P.M., 2005. **Neonatal and adult neurogenesis provide two distinct populations of newborn neurons to the mouse olfactory bulb.** J Neurosci 25, 6816-6825.

Leto, K., Carletti, B., Williams, I.M., Magrassi, L., Rossi, F., 2006. **Different types of cerebellar GABAergic interneurons originate from a common pool of multipotent progenitor cells.** J Neurosci 26, 11682-11694.

Li, D.P., Pan, H.L., 2005. **Angiotensin II attenuates synaptic GABA release and excites paraventricular-rostral ventrolateral medulla output neurons.** J Pharmacol Exp Ther 313, 1035-1045.

Li, H.P., Oohira, A., Ogawa, M., Kawamura, K., Kawano, H., 2005. **Aberrant trajectory of thalamocortical axons associated with abnormal localization of neurocan immunoreactivity in the cerebral neocortex of reeler mutant mice.** Eur J Neurosci 22, 2689-2696.

Lin, C.H., Stoeck, J., Ravanpay, A.C., Guillemot, F., Tapscott, S.J., Olson, J.M., 2004. **Regulation of neuroD2 expression in mouse brain.** Dev Biol 265, 234-245.

Lin, C.H., Tapscott, S.J., Olson, J.M., 2006. **Congenital hypothyroidism (cretinism) in neuroD2-deficient mice.** Mol Cell Biol 26, 4311-4315.

Lipsky, R.H., Marini, A.M., 2007. **Brain-derived neurotrophic factor in neuronal survival and behavior-related plasticity.** Ann N Y Acad Sci 1122, 130-143.

Liu, M., Pereira, F.A., Price, S.D., Chu, M.J., Shope, C., Himes, D., Eatock, R.A., Brownell, W.E., Lysakowski, A., Tsai, M.J., 2000a. **Essential role of BETA2/NeuroD1 in development of the vestibular and auditory systems.** Genes Dev 14, 2839-2854.

Liu, M., Pleasure, S.J., Collins, A.E., Noebels, J.L., Naya, F.J., Tsai, M.J., Lowenstein, D.H., 2000b. **Loss of BETA2/NeuroD leads to malformation of the dentate gyrus and epilepsy.** Proc Natl Acad Sci U S A 97, 865-870.

Liu, X., Wang, Q., Haydar, T.F., Bordey, A., 2005. **Nonsynaptic GABA signaling in postnatal subventricular zone controls proliferation of GFAP-expressing progenitors.** Nat Neurosci 8, 1179-1187.

Lledo, P.M., Alonso, M., Grubb, M.S., 2006. **Adult neurogenesis and functional plasticity in neuronal circuits.** Nat Rev Neurosci 7, 179-193.

Lledo, P.M., Gheusi, G., Vincent, J.D., 2005. **Information processing in the mammalian olfactory system.** Physiol Rev 85, 281-317.

Lledo, P.M., Saghatelyan, A., 2005. **Integrating new neurons into the adult olfactory bulb: joining the network, life-death decisions, and the effects of sensory experience.** Trends Neurosci 28, 248-254.

Lledo, P.M., Saghatelyan, A., Lemasson, M., 2004. **Inhibitory interneurons in the olfactory bulb: from development to function.** Neuroscientist 10, 292-303.

Lobo, M.K., Karsten, S.L., Gray, M., Geschwind, D.H., Yang, X.W., 2006. **FACS-array profiling of striatal projection neuron subtypes in juvenile and adult mouse brains.** Nat Neurosci 9, 443-452.

Loeb, J.E., Chauveau, J., 1969. **[Preparation of DNA by filtration on agarose gel].** Biochim Biophys Acta 182, 225-234.

Lois, C., Alvarez-Buylla, A., 1994. **Long-distance neuronal migration in the adult mammalian brain.** Science 264, 1145-1148.

Lois, C., Garcia-Verdugo, J.M., Alvarez-Buylla, A., 1996. **Chain migration of neuronal precursors.** Science 271, 978-981.

Madsen, K.K., Larsson, O.M., Schousboe, A., 2008. **Regulation of excitation by GABA neurotransmission: focus on metabolism and transport.** Results Probl Cell Differ 44, 201-221.

Marin, O., Anderson, S.A., Rubenstein, J.L., 2000. **Origin and molecular specification of striatal interneurons.** J Neurosci 20, 6063-6076.

Markram, H., Toledo-Rodriguez, M., Wang, Y., Gupta, A., Silberberg, G., Wu, C., 2004. **Interneurons of the neocortical inhibitory system.** Nat Rev Neurosci 5, 793-807.

Marshall, C.A., Novitch, B.G., Goldman, J.E., 2005. **Olig2 directs astrocyte and oligodendrocyte formation in postnatal subventricular zone cells.** J Neurosci 25, 7289-7298.

Marsich, E., Vetere, A., Di Piazza, M., Tell, G., Paoletti, S., 2003. **The PAX6 gene is activated by the basic helix-loop-helix transcription factor NeuroD/BETA2.** Biochem J 376, 707-715.

Martin, N., Jaubert, J., Gounon, P., Salido, E., Haase, G., Szatanik, M., Guenet, J.L., 2002. **A missense mutation in Tbce causes progressive motor neuronopathy in mice.** Nat Genet 32, 443-447.

Mason, H.A., Ito, S., Corfas, G., 2001. **Extracellular signals that regulate the tangential migration of olfactory bulb neuronal precursors: inducers, inhibitors, and repellents.** J Neurosci 21, 7654-7663.

Mates, L., Korpos, E., Deak, F., Liu, Z., Beier, D.R., Aszodi, A., Kiss, I., 2002. **Comparative analysis of the mouse and human genes (Matn2 and MATN2) for matrilin-2, a filament-forming protein widely distributed in extracellular matrices.** Matrix Biol 21, 163-174.

Matter, M.L., Laurie, G.W., 1994. **A novel laminin E8 cell adhesion site required for lung alveolar formation in vitro.** J Cell Biol 124, 1083-1090.

Mattson, M.P., 2000. **Apoptosis in neurodegenerative disorders.** Nat Rev Mol Cell Biol 1, 120-129.

McEvilly, R.J., de Diaz, M.O., Schonemann, M.D., Hooshmand, F., Rosenfeld, M.G., 2002. **Transcriptional regulation of cortical neuron migration by POU domain factors.** Science 295, 1528-1532.

Melcher, T., Maas, S., Herb, A., Sprengel, R., Higuchi, M., Seeburg, P.H., 1996. **RED2, a brain-specific member of the RNA-specific adenosine deaminase family.** J Biol Chem 271, 31795-31798.

Menet, V., Prieto, M., Privat, A., Gimenez y Ribotta, M., 2003. **Axonal plasticity and functional recovery after spinal cord injury in mice deficient in both glial fibrillary acidic protein and vimentin genes.** Proc Natl Acad Sci U S A 100, 8999-9004.

Merkle, F.T., Alvarez-Buylla, A., 2006. **Neural stem cells in mammalian development.** Curr Opin Cell Biol 18, 704-709.

Merkle, F.T., Mirzadeh, Z., Alvarez-Buylla, A., 2007. **Mosaic organization of neural stem cells in the adult brain.** Science 317, 381-384.

Merkle, F.T., Tramontin, A.D., Garcia-Verdugo, J.M., Alvarez-Buylla, A., 2004. **Radial glia give rise to adult neural stem cells in the subventricular zone.** Proc Natl Acad Sci U S A 101, 17528-17532.

Merson, T.D., Dixon, M.P., Collin, C., Rietze, R.L., Bartlett, P.F., Thomas, T., Voss, A.K., 2006. **The transcriptional coactivator Querkopf controls adult neurogenesis.** J Neurosci 26, 11359-11370.

Mie, M., Endoh, T., Yanagida, Y., Kobatake, E., Aizawa, M., 2003. **Induction of neural differentiation by electrically stimulated gene expression of NeuroD2.** J Biotechnol 100, 231-238.

Miltenyi, S., Muller, W., Weichel, W., Radbruch, A., 1990. **High gradient magnetic cell separation with MACS.** Cytometry 11, 231-238.

Ming, G.L., Song, H., 2005. **Adult neurogenesis in the mammalian central nervous system.** Annu Rev Neurosci 28, 223-250.

Missler, M., Zhang, W., Rohlmann, A., Kattenstroth, G., Hammer, R.E., Gottmann, K., Sudhof, T.C., 2003. **Alpha-neurexins couple Ca2+ channels to synaptic vesicle exocytosis.** Nature 423, 939-948.

Mittaz, L., Antonarakis, S.E., Higuchi, M., Scott, H.S., 1997. **Localization of a novel human RNA-editing deaminase (hRED2 or ADARB2) to chromosome 10p15.** Hum Genet 100, 398-400.

Miyata, T., Maeda, T., Lee, J.E., 1999. **NeuroD is required for differentiation of the granule cells in the cerebellum and hippocampus.** Genes Dev 13, 1647-1652.

Mizrahi, A., 2007. **Dendritic development and plasticity of adult-born neurons in the mouse olfactory bulb.** Nat Neurosci 10, 444-452.

Monyer, H., Markram, H., 2004. **Interneuron Diversity series: Molecular and genetic tools to study GABAergic interneuron diversity and function.** Trends Neurosci 27, 90-97.

Moretti, P., Levenson, J.M., Battaglia, F., Atkinson, R., Teague, R., Antalffy, B., Armstrong, D., Arancio, O., Sweatt, J.D., Zoghbi, H.Y., 2006. **Learning and memory and synaptic plasticity are impaired in a mouse model of Rett syndrome.** J Neurosci 26, 319-327.

Morin, X., Jaouen, F., Durbec, P., 2007. **Control of planar divisions by the G-protein regulator LGN maintains progenitors in the chick neuroepithelium.** Nat Neurosci 10, 1440-1448.

Morse, D.E., Duncan, H., Hooker, N., Baloun, A., Young, G., 1980. **GABA induces behavioral and developmental metamorphosis in planktonic molluscan larvae.** Fed Proc 39, 3237-3241.

Mullis, K., Faloona, F., Scharf, S., Saiki, R., Horn, G., Erlich, H., 1986. **Specific enzymatic amplification of DNA in vitro: the polymerase chain reaction.** Cold Spring Harb Symp Quant Biol 51 Pt 1, 263-273.

Murase, S., Horwitz, A.F., 2002. **Deleted in colorectal carcinoma and differentially expressed integrins mediate the directional migration of neural precursors in the rostral migratory stream.** J Neurosci 22, 3568-3579.

Murray, V., 1989. **Improved double-stranded DNA sequencing using the linear polymerase chain reaction.** Nucleic Acids Res 17, 8889.

Naeve, G.S., Vana, A.M., Eggold, J.R., Verge, G., Ling, N., Foster, A.C., 2000. **Expression of rat insulin-like growth factor binding protein-6 in the brain, spinal cord, and sensory ganglia.** Brain Res Mol Brain Res 75, 185-197.

Nguyen-Ba-Charvet, K.T., Picard-Riera, N., Tessier-Lavigne, M., Baron-Van Evercooren, A., Sotelo, C., Chedotal, A., 2004. **Multiple roles for slits in the control of cell migration in the rostral migratory stream.** J Neurosci 24, 1497-1506.

Nikoletopoulou, V., Plachta, N., Allen, N.D., Pinto, L., Gotz, M., Barde, Y.A., 2007. **Neurotrophin Receptor-Mediated Death of Misspecified Neurons Generated from Embryonic Stem Cells Lacking Pax6.** Cell Stem Cell 1, 529-540.

Noctor, S.C., Martinez-Cerdeno, V., Ivic, L., Kriegstein, A.R., 2004. **Cortical neurons arise in symmetric and asymmetric division zones and migrate through specific phases.** Nat Neurosci 7, 136-144.

Noda, T., Kawamura, R., Funabashi, H., Mie, M., Kobatake, E., 2006. **Transduction of NeuroD2 protein induced neural cell differentiation.** J Biotechnol 126, 230-236.

Okazaki, Y., Furuno, M., Kasukawa, T., Adachi, J., Bono, H., Kondo, S., Nikaido, I., Osato, N., Saito, R., Suzuki, H., Yamanaka, I., Kiyosawa, H., Yagi, K., Tomaru, Y., Hasegawa, Y., Nogami, A., Schonbach, C., Gojobori, T., Baldarelli, R., Hill, D.P., Bult, C., Hume, D.A., Quackenbush, J., Schriml, L.M., Kanapin, A., Matsuda, H., Batalov, S., Beisel, K.W., Blake, J.A., Bradt, D., Brusic, V., Chothia, C., Corbani, L.E., Cousins, S., Dalla, E., Dragani, T.A., Fletcher, C.F., Forrest, A., Frazer, K.S., Gaasterland, T., Gariboldi, M., Gissi, C., Godzik, A., Gough, J., Grimmond, S., Gustincich, S., Hirokawa, N., Jackson, I.J., Jarvis, E.D., Kanai, A., Kawaji, H., Kawasawa, Y., Kedzierski, R.M., King, B.L., Konagaya, A., Kurochkin, I.V., Lee, Y., Lenhard, B., Lyons, P.A., Maglott, D.R., Maltais, L., Marchionni, L., McKenzie, L., Miki, H., Nagashima, T., Numata, K., Okido, T., Pavan, W.J., Pertea, G., Pesole, G., Petrovsky, N., Pillai, R., Pontius, J.U., Qi, D., Ramachandran, S., Ravasi, T., Reed, J.C., Reed, D.J., Reid, J., Ring, B.Z., Ringwald, M., Sandelin, A., Schneider, C., Semple, C.A., Setou, M., Shimada, K., Sultana, R., Takenaka, Y., Taylor, M.S., Teasdale, R.D., Tomita, M.,

Verardo, R., Wagner, L., Wahlestedt, C., Wang, Y., Watanabe, Y., Wells, C., Wilming, L.G., Wynshaw-Boris, A., Yanagisawa, M., Yang, I., Yang, L., Yuan, Z., Zavolan, M., Zhu, Y., Zimmer, A., Carninci, P., Hayatsu, N., Hirozane-Kishikawa, T., Konno, H., Nakamura, M., Sakazume, N., Sato, K., Shiraki, T., Waki, K., Kawai, J., Aizawa, K., Arakawa, T., Fukuda, S., Hara, A., Hashizume, W., Imotani, K., Ishii, Y., Itoh, M., Kagawa, I., Miyazaki, A., Sakai, K., Sasaki, D., Shibata, K., Shinagawa, A., Yasunishi, A., Yoshino, M., Waterston, R., Lander, E.S., Rogers, J., Birney, E., Hayashizaki, Y., 2002. **Analysis of the mouse transcriptome based on functional annotation of 60,770 full-length cDNAs.** Nature 420, 563-573.

Ono, K., Tomasiewicz, H., Magnuson, T., Rutishauser, U., 1994. **N-CAM mutation inhibits tangential neuronal migration and is phenocopied by enzymatic removal of polysialic acid.** Neuron 13, 595-609.

Owens, D.F., Kriegstein, A.R., 2002a. **Developmental neurotransmitters?** Neuron 36, 989-991.

Owens, D.F., Kriegstein, A.R., 2002b. **Is there more to GABA than synaptic inhibition?** Nat Rev Neurosci 3, 715-727.

Paik, J.H., Skoura, A., Chae, S.S., Cowan, A.E., Han, D.K., Proia, R.L., Hla, T., 2004. **Sphingosine 1-phosphate receptor regulation of N-cadherin mediates vascular stabilization.** Genes Dev 18, 2392-2403.

Pajor, A.M., Gangula, R., Yao, X., 2001. **Cloning and functional characterization of a high-affinity Na(+)/dicarboxylate cotransporter from mouse brain.** Am J Physiol Cell Physiol 280, C1215-1223.

Pak, W., Hindges, R., Lim, Y.S., Pfaff, S.L., O'Leary, D.D., 2004. **Magnitude of binocular vision controlled by islet-2 repression of a genetic program that specifies laterality of retinal axon pathfinding.** Cell 119, 567-578.

Palmada, M., Centelles, J.J., 1998. **Excitatory amino acid neurotransmission. Pathways for metabolism, storage and reuptake of glutamate in brain.** Front Biosci 3, d701-718.

Pan, J., You, Y., Huang, T., Brody, S.L., 2007. **RhoA-mediated apical actin enrichment is required for ciliogenesis and promoted by Foxj1.** J Cell Sci 120, 1868-1876.

Panzanelli, P., Fritschy, J.M., Yanagawa, Y., Obata, K., Sassoe-Pognetto, M., 2007. **GABAergic phenotype of periglomerular cells in the rodent olfactory bulb.** J Comp Neurol 502, 990-1002.

Parnavelas, J.G., Alifragis, P., Nadarajah, B., 2002. **The origin and migration of cortical neurons.** Prog Brain Res 136, 73-80.

Parnavelas, J.G., Anderson, S.A., Lavdas, A.A., Grigoriou, M., Pachnis, V., Rubenstein, J.L., 2000. **The contribution of the ganglionic eminence to the neuronal cell types of the cerebral cortex.** Novartis Found Symp 228, 129-139; discussion 139-147.

Parrish-Aungst, S., Shipley, M.T., Erdelyi, F., Szabo, G., Puche, A.C., 2007. **Quantitative analysis of neuronal diversity in the mouse olfactory bulb.** J Comp Neurol 501, 825-836.

Pascual, M., Abasolo, I., Mingorance-Le Meur, A., Martinez, A., Del Rio, J.A., Wright, C.V., Real, F.X., Soriano, E., 2007. **Cerebellar GABAergic progenitors adopt an external granule cell-like phenotype in the absence of Ptf1a transcription factor expression.** Proc Natl Acad Sci U S A 104, 5193-5198.

Pennartz, S., Belvindrah, R., Tomiuk, S., Zimmer, C., Hofmann, K., Conradt, M., Bosio, A., Cremer, H., 2004. **Purification of neuronal precursors from the adult mouse brain: comprehensive gene expression analysis provides new insights into the control of cell migration, differentiation, and homeostasis.** Mol Cell Neurosci 25, 692-706.

Pennesi, M.E., Cho, J.H., Yang, Z., Wu, S.H., Zhang, J., Wu, S.M., Tsai, M.J., 2003. **BETA2/NeuroD1 null mice: a new model for transcription factor-dependent photoreceptor degeneration.** J Neurosci 23, 453-461.

Peters, A., Kara, D.A., Harriman, K.M., 1985. **The neuronal composition of area 17 of rat visual cortex. III. Numerical considerations.** J Comp Neurol 238, 263-274.

Phillips, W., Morton, A.J., Barker, R.A., 2005. **Abnormalities of neurogenesis in the R6/2 mouse model of Huntington's disease are attributable to the in vivo microenvironment.** J Neurosci 25, 11564-11576.

Radbruch, A., Mechtold, B., Thiel, A., Miltenyi, S., Pfluger, E., 1994. **High-gradient magnetic cell sorting.** Methods Cell Biol 42 Pt B, 387-403.

Ramon, Y.C.S., 1952. **Structure and connections of neurons.** Bull Los Angel Neuro Soc 17, 5-46.

Reif, A., Schmitt, A., Fritzen, S., Chourbaji, S., Bartsch, C., Urani, A., Wycislo, M., Mossner, R., Sommer, C., Gass, P., Lesch, K.P., 2004. **Differential effect of endothelial nitric oxide synthase (NOS-III) on the regulation of adult neurogenesis and behaviour.** Eur J Neurosci 20, 885-895.

Roberts, E., Frankel, S., 1950. **gamma-Aminobutyric acid in brain: its formation from glutamic acid.** J Biol Chem 187, 55-63.

Rohner-Jeanrenaud, F., Cusin, I., Sainsbury, A., Zakrzewska, K.E., Jeanrenaud, B., 1996. **The loop system between neuropeptide Y and leptin in normal and obese rodents.** Horm Metab Res 28, 642-648.

Rutishauser, U., 1996. **Polysialic acid and the regulation of cell interactions.** Curr Opin Cell Biol 8, 679-684.

Saeed, A.I., Sharov, V., White, J., Li, J., Liang, W., Bhagabati, N., Braisted, J., Klapa, M., Currier, T., Thiagarajan, M., Sturn, A., Snuffin, M., Rezantsev, A., Popov, D., Ryltsov, A., Kostukovich, E., Borisovsky, I., Liu, Z., Vinsavich, A., Trush, V., Quackenbush, J., 2003. **TM4: a free, open-source system for microarray data management and analysis.** Biotechniques 34, 374-378.

Saghatelyan, A., de Chevigny, A., Schachner, M., Lledo, P.M., 2004. **Tenascin-R mediates activity-dependent recruitment of neuroblasts in the adult mouse forebrain.** Nat Neurosci 7, 347-356.

Saghatelyan, A., Roux, P., Migliore, M., Rochefort, C., Desmaisons, D., Charneau, P., Shepherd, G.M., Lledo, P.M., 2005. **Activity-dependent adjustments of the inhibitory network in the olfactory bulb following early postnatal deprivation.** Neuron 46, 103-116.

Saiki, R.K., Gelfand, D.H., Stoffel, S., Scharf, S.J., Higuchi, R., Horn, G.T., Mullis, K.B., Erlich, H.A., 1988. **Primer-directed enzymatic amplification of DNA with a thermostable DNA polymerase.** Science 239, 487-491.

Saino-Saito, S., Sasaki, H., Volpe, B.T., Kobayashi, K., Berlin, R., Baker, H., 2004. **Differentiation of the dopaminergic phenotype in the olfactory system of neonatal and adult mice.** J Comp Neurol 479, 389-398.

Saito, T., Nakatsuji, N., 2001. **Efficient gene transfer into the embryonic mouse brain using in vivo electroporation.** Dev Biol 240, 237-246.

Salama-Cohen, P., Arevalo, M.A., Grantyn, R., Rodriguez-Tebar, A., 2006. **Notch and NGF/p75NTR control dendrite morphology and the balance of excitatory/inhibitory synaptic input to hippocampal neurones through Neurogenin 3.** J Neurochem 97, 1269-1278.

Sambrook, J., Russell, D.W., 2001. **Molecular cloning: a laboratory manual.** Cold Spring Harbor Laboratory Press, Cold Spring Harbor, New York.

Sanai, N., Tramontin, A.D., Quinones-Hinojosa, A., Barbaro, N.M., Gupta, N., Kunwar, S., Lawton, M.T., McDermott, M.W., Parsa, A.T., Manuel-Garcia Verdugo, J., Berger, M.S., Alvarez-Buylla, A., 2004. **Unique astrocyte ribbon in adult human brain contains neural stem cells but lacks chain migration.** Nature 427, 740-744.

Sanger, F., Nicklen, S., Coulson, A.R., 1977. **DNA sequencing with chain-terminating inhibitors.** Proc Natl Acad Sci U S A 74, 5463-5467.

Sawamoto, K., Nakao, N., Kobayashi, K., Matsushita, N., Takahashi, H., Kakishita, K., Yamamoto, A., Yoshizaki, T., Terashima, T., Murakami, F., Itakura, T., Okano, H., 2001. **Visualization, direct isolation, and transplantation of midbrain dopaminergic neurons.** Proc Natl Acad Sci U S A 98, 6423-6428. Epub 2001 May 6415.

Schmid, R.S., Jo, R., Shelton, S., Kreidberg, J.A., Anton, E.S., 2005. **Reelin, integrin and DAB1 interactions during embryonic cerebral cortical development.** Cereb Cortex 15, 1632-1636.

Schoppa, N.E., Urban, N.N., 2003. **Dendritic processing within olfactory bulb circuits.** Trends Neurosci 26, 501-506.

Schulman, J.A., Bloom, F.E., 1981. **Golgi cells of the cerebellum are inhibited by inferior olive activity.** Brain Res 210, 350-355.

Schwab, M.H., Bartholomae, A., Heimrich, B., Feldmeyer, D., Druffel-Augustin, S., Goebbels, S., Naya, F.J., Zhao, S., Frotscher, M., Tsai, M.J., Nave, K.A., 2000. **Neuronal basic helix-loop-helix proteins (NEX and BETA2/Neuro D) regulate terminal granule cell differentiation in the hippocampus.** J Neurosci 20, 3714-3724.

Shah, R., Medina-Martinez, O., Chu, L.F., Samaco, R.C., Jamrich, M., 2006. **Expression of FoxP2 during zebrafish development and in the adult brain.** Int J Dev Biol 50, 435-438.

Shimogori, T., Ogawa, M., 2008. **Gene application with in utero electroporation in mouse embryonic brain.** Dev Growth Differ.

Shu, T., Butz, K.G., Plachez, C., Gronostajski, R.M., Richards, L.J., 2003. **Abnormal development of forebrain midline glia and commissural projections in Nfia knock-out mice.** J Neurosci 23, 203-212.

Silberberg, G., Wu, C., Markram, H., 2004. **Synaptic dynamics control the timing of neuronal excitation in the activated neocortical microcircuit.** J Physiol 556, 19-27.

Snyder, J.S., Kee, N., Wojtowicz, J.M., 2001. **Effects of adult neurogenesis on synaptic plasticity in the rat dentate gyrus.** J Neurophysiol 85, 2423-2431.

Sotelo, C., 1990. **Cerebellar synaptogenesis: what we can learn from mutant mice.** J Exp Biol 153, 225-249.

Stankovic, R.K., 2005. **Atrophy of large myelinated axons in metallothionein-I, II knockout mice.** Cell Mol Neurobiol 25, 943-953.

Steele, A.D., Emsley, J.G., Ozdinler, P.H., Lindquist, S., Macklis, J.D., 2006. **Prion protein (PrPc) positively regulates neural precursor proliferation during developmental and adult mammalian neurogenesis.** Proc Natl Acad Sci U S A 103, 3416-3421.

Stenqvist, A., Agerman, K., Marmigere, F., Minichiello, L., Ernfors, P., 2005. **Genetic evidence for selective neurotrophin 3 signalling through TrkC but not TrkB in vivo.** EMBO Rep 6, 973-978.

Stoykova, A., Fritsch, R., Walther, C., Gruss, P., 1996. **Forebrain patterning defects in Small eye mutant mice.** Development 122, 3453-3465.

Stuhmer, T., Anderson, S.A., Ekker, M., Rubenstein, J.L., 2002a. **Ectopic expression of the Dlx genes induces glutamic acid decarboxylase and Dlx expression.** Development 129, 245-252.

Stuhmer, T., Puelles, L., Ekker, M., Rubenstein, J.L., 2002b. **Expression from a Dlx gene enhancer marks adult mouse cortical GABAergic neurons.** Cereb Cortex 12, 75-85.

Taglialatela, P., Soria, J.M., Caironi, V., Moiana, A., Bertuzzi, S., 2004. **Compromised generation of GABAergic interneurons in the brains of Vax1-/- mice.** Development 131, 4239-4249.

Takahashi, M., Ogino, T., Baba, K., 1969. **Estimation of relative molecular length of DNA by electrophoresis in agarose gel.** Biochim Biophys Acta 174, 183-187.

Takahashi, S., Inatome, R., Yamamura, H., Yanagi, S., 2003. **Isolation and expression of a novel mitochondrial septin that interacts with CRMP/CRAM in the developing neurones.** Genes Cells 8, 81-93.

Takash, W., Canizares, J., Bonneaud, N., Poulat, F., Mattei, M.G., Jay, P., Berta, P., 2001. **SOX7 transcription factor: sequence, chromosomal localisation, expression, transactivation and interference with Wnt signalling.** Nucleic Acids Res 29, 4274-4283.

Takayasu, S., Sakurai, T., Iwasaki, S., Teranishi, H., Yamanaka, A., Williams, S.C., Iguchi, H., Kawasawa, Y.I., Ikeda, Y., Sakakibara, I., Ohno, K., Ioka, R.X., Murakami, S., Dohmae, N., Xie, J., Suda, T., Motoike, T., Ohuchi, T., Yanagisawa, M., Sakai, J., 2006. **A neuropeptide ligand of the G protein-coupled receptor GPR103 regulates feeding, behavioral arousal, and blood pressure in mice.** Proc Natl Acad Sci U S A 103, 7438-7443.

Tamamaki, N., Yanagawa, Y., Tomioka, R., Miyazaki, J., Obata, K., Kaneko, T., 2003. **Green fluorescent protein expression and colocalization with calretinin, parvalbumin, and somatostatin in the GAD67-GFP knock-in mouse.** J Comp Neurol 467, 60-79.

Tao, W.A., Wollscheid, B., O'Brien, R., Eng, J.K., Li, X.J., Bodenmiller, B., Watts, J.D., Hood, L., Aebersold, R., 2005. **Quantitative phosphoproteome analysis using a dendrimer conjugation chemistry and tandem mass spectrometry.** Nat Methods 2, 591-598.

Thomas, T., Voss, A.K., 2004. **Querkopf, a histone acetyltransferase, is essential for embryonic neurogenesis.** Front Biosci 9, 24-31.

Thomas, T., Voss, A.K., Chowdhury, K., Gruss, P., 2000. **Querkopf, a MYST family histone acetyltransferase, is required for normal cerebral cortex development.** Development 127, 2537-2548.

Titomanlio, L., Pierri, N.B., Romano, A., Imperati, F., Borrelli, M., Barletta, V., Diano, A.A., Castaldo, I., Santoro, L., Del Giudice, E., 2005. **Cerebellar vermis aplasia: patient report and exclusion of the candidate genes EN2 and ZIC1.** Am J Med Genet A 136, 198-200.

Tomasiewicz, H., Ono, K., Yee, D., Thompson, C., Goridis, C., Rutishauser, U., Magnuson, T., 1993. **Genetic deletion of a neural cell adhesion molecule variant (N-CAM-180) produces distinct defects in the central nervous system.** Neuron 11, 1163-1174.

Treloar, H.B., Feinstein, P., Mombaerts, P., Greer, C.A., 2002. **Specificity of glomerular targeting by olfactory sensory axons.** J Neurosci 22, 2469-2477.

Tusher, V.G., Tibshirani, R., Chu, G., 2001. **Significance analysis of microarrays applied to the ionizing radiation response.** Proc Natl Acad Sci U S A 98, 5116-5121.

Urban, N.N., 2002. **Lateral inhibition in the olfactory bulb and in olfaction.** Physiol Behav 77, 607-612.

Varoqueaux, F., Jamain, S., Brose, N., 2004. **Neuroligin 2 is exclusively localized to inhibitory synapses.** Eur J Cell Biol 83, 449-456.

Vasilyev, D.V., Barish, M.E., 2003. **Regulation of an inactivating potassium current (IA) by the extracellular matrix protein vitronectin in embryonic mouse hippocampal neurones.** J Physiol 547, 859-871.

Veyrac, A., Giannetti, N., Charrier, E., Reymond-Marron, I., Aguera, M., Rogemond, V., Honnorat, J., Jourdan, F., 2005. **Expression of collapsin response mediator proteins 1, 2 and 5 is differentially regulated in newly generated and mature neurons of the adult olfactory system.** Eur J Neurosci 21, 2635-2648.

Viollet, C., Bodenant, C., Prunotto, C., Roosterman, D., Schaefer, J., Meyerhof, W., Epelbaum, J., Vaudry, H., Leroux, P., 1997. **Differential expression of multiple somatostatin receptors in the rat cerebellum during development.** J Neurochem 68, 2263-2272.

Vonsattel, J.P., Myers, R.H., Stevens, T.J., Ferrante, R.J., Bird, E.D., Richardson, E.P., Jr., 1985. **Neuropathological classification of Huntington's disease.** J Neuropathol Exp Neurol 44, 559-577.

Waclaw, R.R., Allen, Z.J., 2nd, Bell, S.M., Erdelyi, F., Szabo, G., Potter, S.S., Campbell, K., 2006. **The zinc finger transcription factor Sp8 regulates the generation and diversity of olfactory bulb interneurons.** Neuron 49, 503-516.

Wang, W., Stock, R.E., Gronostajski, R.M., Wong, Y.W., Schachner, M., Kilpatrick, D.L., 2004. **A role for nuclear factor I in the intrinsic control of cerebellar granule neuron gene expression.** J Biol Chem 279, 53491-53497.

Wichterle, H., Garcia-Verdugo, J.M., Alvarez-Buylla, A., 1997. **Direct evidence for homotypic, glia-independent neuronal migration.** Neuron 18, 779-791.

Wijchers, P.J., Hoekman, M.F., Burbach, J.P., Smidt, M.P., 2006. **Identification of forkhead transcription factors in cortical and dopaminergic areas of the adult murine brain.** Brain Res 1068, 23-33.

Wonders, C., Anderson, S.A., 2005. **Cortical interneurons and their origins.** Neuroscientist 11, 199-205.

Wonders, C.P., Anderson, S.A., 2006. **The origin and specification of cortical interneurons.** Nat Rev Neurosci 7, 687-696.

Wright, C.V., Cho, K.W., Oliver, G., De Robertis, E.M., 1989. **Vertebrate homeodomain proteins: families of region-specific transcription factors.** Trends Biochem Sci 14, 52-56.

Wu, W., Wong, K., Chen, J., Jiang, Z., Dupuis, S., Wu, J.Y., Rao, Y., 1999. **Directional guidance of neuronal migration in the olfactory system by the protein Slit.** Nature 400, 331-336.

Wurst, W., Auerbach, A.B., Joyner, A.L., 1994. **Multiple developmental defects in Engrailed-1 mutant mice: an early mid-hindbrain deletion and patterning defects in forelimbs and sternum.** Development 120, 2065-2075.

Xu, Q., Cobos, I., De La Cruz, E., Rubenstein, J.L., Anderson, S.A., 2004. **Origins of cortical interneuron subtypes.** J Neurosci 24, 2612-2622.

Yamashita, N., Uchida, Y., Ohshima, T., Hirai, S., Nakamura, F., Taniguchi, M., Mikoshiba, K., Honnorat, J., Kolattukudy, P., Thomasset, N., Takei, K., Takahashi, T., Goshima, Y., 2006. **Collapsin response mediator protein 1 mediates reelin signaling in cortical neuronal migration.** J Neurosci 26, 13357-13362.

Yang, F.C., Chen, S., Robling, A.G., Yu, X., Nebesio, T.D., Yan, J., Morgan, T., Li, X., Yuan, J., Hock, J., Ingram, D.A., Clapp, D.W., 2006. **Hyperactivation of p21ras and PI3K cooperate to alter murine and human neurofibromatosis type 1-haploinsufficient osteoclast functions.** J Clin Invest 116, 2880-2891.

Yin, A.H., Miraglia, S., Zanjani, E.D., Almeida-Porada, G., Ogawa, M., Leary, A.G., Olweus, J., Kearney, J., Buck, D.W., 1997. **AC133, a novel marker for human hematopoietic stem and progenitor cells.** Blood 90, 5002-5012.

Yoshihara, S., Omichi, K., Yanazawa, M., Kitamura, K., Yoshihara, Y., 2005. **Arx homeobox gene is essential for development of mouse olfactory system.** Development 132, 751-762.

Young, K.M., Fogarty, M., Kessaris, N., Richardson, W.D., 2007. **Subventricular zone stem cells are heterogeneous with respect to their embryonic origins and neurogenic fates in the adult olfactory bulb.** J Neurosci 27, 8286-8296.

Zhang, H., Li, X.J., Martin, D.B., Aebersold, R., 2003. **Identification and quantification of N-linked glycoproteins using hydrazide chemistry, stable isotope labeling and mass spectrometry.** Nat Biotechnol 21, 660-666.

Zhao, M., Momma, S., Delfani, K., Carlen, M., Cassidy, R.M., Johansson, C.B., Brismar, H., Shupliakov, O., Frisen, J., Janson, A.M., 2003. **Evidence for neurogenesis in the adult mammalian substantia nigra.** Proc Natl Acad Sci U S A 100, 7925-7930.

Zhao, Y., Kwan, K.M., Mailloux, C.M., Lee, W.K., Grinberg, A., Wurst, W., Behringer, R.R., Westphal, H., 2007. **LIM-homeodomain proteins Lhx1 and Lhx5, and their cofactor Ldb1, control Purkinje cell differentiation in the developing cerebellum.** Proc Natl Acad Sci U S A 104, 13182-13186.

Zheng, W., Nowakowski, R.S., Vaccarino, F.M., 2004. **Fibroblast growth factor 2 is required for maintaining the neural stem cell pool in the mouse brain subventricular zone.** Dev Neurosci 26, 181-196.

Acknowledgement

I am very grateful to Prof. Dr. Knebel-Mörsdorf, who supported this work by her supervision and her kind and helpful advice and Prof. Dr. Korsching for taking over the second review.

I am sincerely grateful to my supervisors at Miltenyi Biotec and the Developmental Biology Institute of Marseille (IBDML), Dr. Andreas Bosio and Dr. Harold Cremer, for initiation of this project, scientific and personal support, critical comments and useful advice throughout the whole time.

I would like to thank Stefan Miltenyi for providing me with the opportunity to perform this PhD-thesis at Miltenyi Biotec GmbH, Cologne. I thank the whole Miltenyi Biotec team for the great atmosphere and all the support. Many thanks to Dr. Hartmut Scheel, Dr. Stefan Tomiuk, Dr. Corinna Scholz and Dr. Kay Hofmann for bioinformatical support and nice hiking trips. I would like to thank Dr. Frank Single, Dr. Alena Bencsik and all further members of the "Transgenic" team for discussions and support concerning mouse techniques and breeding. I would like to thank Daniel Küsters and Dr. Sandra Pennartz for their support concerning the *in situ* hybridizations, tissue dissociation and further questions. Special thanks belong to Gerd Großhauser, Dirk Dietrich, Dr. Sebastian Knöbel and Dr. Bernhard Gerstmayer for enjoyable time-outs at lunch, jokes, discussions and advice. I am very grateful to Dr. Melanie Jungblut for helpful advice and critically reading of this manuscript.

I would like to thank Camille Boutin, Angelique Desoeuvre and Dr. Marie-Catherine Tiveron for the nice and familiar atmosphere and all the support during my time in Marseille. In particular, I thank Camille Boutin for teaching me the *in vivo* electroporation technique and lots of other techniques as well as for her great teamwork concerning our ongoing collaboration.

Thanks to Christoph Göttlinger and Birgit Mechthold from the Institute for Genetics of the University of Cologne for their assistance concerning the FACS experiments.

I thank Dr. Bernd Wollscheid and Damaris Bausch for all their support concerning the proteome analysis during our ongoing collaboration.

Of course, I would also like to thank my wife, my whole family and my friends for their support during all the time.

Erklärung

Ich versichere, dass ich die von mir vorgelegte Dissertation selbständig angefertigt, die benutzten Quellen und Hilfsmittel vollständig angegeben und die Stellen der Arbeit − einschließlich Tabellen, Karten und Abbildungen −, die anderen Werken im Wortlaut oder dem Sinn nach entnommen sind, in jedem Einzelfall als Entlehnung kenntlich gemacht habe; dass diese Dissertation noch keiner anderen Fakultät oder Universität zur Prüfung vorgelegen hat; dass sie − abgesehen von unten angegebenen Teilpublikationen − noch nicht veröffentlicht worden ist sowie, dass ich eine solche Veröffentlichung vor Abschluss des Promotionsverfahrens nicht vornehmen werde. Die Bestimmungen der Promotionsordnung sind mir bekannt. Die von mir vorgelegte Dissertation ist von Frau Prof. Dr. Knebel-Mörsdorf betreut worden.

Köln, 06. August 2008

Olaf Thorsten Hardt

Lebenslauf

<u>Persönliche Daten</u>

Name:	Olaf Thorsten Hardt
Geburtsdaten:	17. April 1980 in Köln
Familienstand:	verheiratet
Staatsangehörigkeit:	deutsch

<u>Schulbildung</u>

08/86-06/90	Carl-Orff Grundschule, Hürth
08/90-06/96	Elsa-Brändström Schule, Köln
08/96-06/99	Gymnasium Hürth, Hürth
06/99	Abitur, Hürth

<u>Grundwehrdienst</u>

07/99-04/00	Grundwehrdienst als Sanitätssoldat auf dem Luftwaffenstützpunkt in Roth und dem Bundessprachenamt in Hürth

<u>Hochschulausbildung</u>

10/00-03/05	Studium der Biologie mit den Schwerpunkten Genetik, Entwicklungsbiologie und Organische Chemie, Universität zu Köln
09/02	Vordiplom in Biologie
05/04-03/05	Diplomarbeit im Labor für genetische Biochemie am Institut für Genetik der Universität zu Köln, Betreuer: Prof. Dr. Langer
03/05	Abschluss als Diplom-Biologe
seit 05/05	Promotionsarbeit im Fach Genetik bei der Miltenyi Biotec GmbH in Köln in Kollaboration mit dem Developmental Biology Institute of Marseille (IBDML), Frankreich, Betreuerin an der Universität zu Köln: Prof. Dr. Knebel-Mörsdorf
10/08	Voraussichtlicher Abschluss der Promotion an der Universität zu Köln

<u>Praktika</u>

05/03-08/03 und 03/05-04/05	Praktika im Labor für genetische Biochemie am Institut für Genetik der Universität zu Köln
02/03-04/03	Praktikum an der University of British Columbia in Vancouver, Kanada
05/00-07/00, 02/01-04/01 und 08/01-09/01	Werkstudent in der biologischen Forschung für Pflanzenschutz bei der Bayer AG in Monheim

Köln, 06.August 2008